COMPARATIVE STUDY OF THE PELVIC GANGLION IN ADULT AND IN DEVELOPING, MALE AND FEMALE RATS.

Thesis submitted for the degree:

Doctor of Philosophy

by

EDWARD ROBERT CLEGG BLISS

DEPARTMENT OF ANATOMY AND DEVELOPMENTAL BIOLOGY

UNIVERSITY COLLEGE LONDON

JULY, 1997.

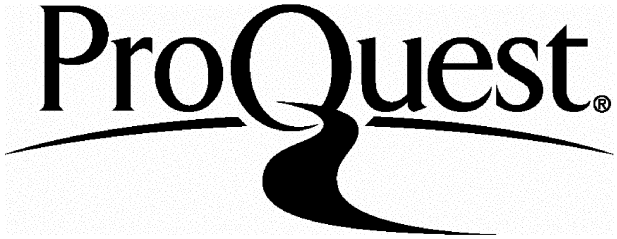

ABSTRACT

The development and comparison of structural features of the pelvic ganglion in male and female rats was investigated with morphometric and histochemical techniques in light and electron microscopes.

Pelvic ganglia from adult rats were sexually dimorphic in volume (approximately $0.3mm^3$ in the male and $0.18mm^3$ in the female), neuron number (12,506 ± 668 neurons in the male and 6,845 ± 717 in the female) and average neuron size.

At three weeks of age ganglion volume and neuron number were similar to the adult and were, therefore, already distinctly sexually dimorphic, although the smaller average neuron size showed no gender difference.

In contrast, at birth pelvic ganglia revealed no gender-related differences in either volume, neuron number or size. Whereas ganglion volume and neuronal size were less than in the older animal groups, neuron numbers in newborn ganglia from both sexes were similar to those in adult male rats. Ganglia from adult males that had been castrated before puberty, were similar in volume and neuron number to unoperated animals, although neuronal size was significantly reduced.

Neuronal death was observed in ganglia from newborn rats at similar extents in both sexes. Apoptotic neurons were also present in ganglia from 7-day old rats, when the extent of cell loss appeared greater in the female than in the male.

It is concluded that the main features of the sexual dimorphism in the pelvic ganglion become established after birth and before puberty. Increasing testosterone levels in the early post-natal period probably influence the ontogeny of the pelvic ganglion, acting either directly on the neurons, or indirectly via trophic factors released from developing pelvic organs. Evidence suggests that target-derived factors, effected by hormone or not, play a role in neuronal survival and neuronal growth in the pelvic ganglion.

TABLE OF CONTENTS

CHAPTER 1

GENERAL INTRODUCTION

1.1 Autonomic Nervous System

1.1.1 Organisation of the Autonomic Nervous System

The autonomic nervous system consists of nerves and ganglia that provide innervation of the heart and blood vessels, abdominal and thoracic viscera, glands, and smooth muscle of the eye and skin; nuclei and pathways in the hypothalamus, brain stem and spinal cord provide the input from the central nervous system. The peripheral autonomic nervous system is connected on one side to the central nervous system and to the visceral targets on the other. It consists of a wide spectrum of nerves and ganglia, within which the neuronal cell bodies are situated. This structural plan, common to all mammals, has been extensively studied in many species including man, and for experimental work mainly in the rat, which is the species of choice in this Thesis.

Classically the autonomic nervous system is described as efferent in function (Langley, 1921), thus ignoring the substantial numbers of sensory neurons contained in the dorsal root ganglia. It is divided into sympathetic, parasympathetic and enteric divisions depending on the anatomical location of ganglia and neural pathways, and the pharmacological characteristics of its neurons. Initially, autonomic ganglia were regarded as simple relay stations distributing nerve signals from the central nervous system to the peripheral organs. Much subsequent evidence has shown that these ganglia undertake more complex functions, enabling not only relay of nerve impulses but also filtering and integration of impulses originating from different sources. Afferent nerve fibres from sensory neurons in dorsal root

ganglia travel in autonomic trunks, and traverse through and synapse with autonomic ganglia (Matthews and Cuello, 1982).

1.1.2 Sympathetic Division

Sympathetic neurons are usually situated at some distance from the effector organs they innervate, in aggregations that form relatively large ganglia just visible to the naked eye. There are two anatomical sub-divisions, the paravertebral ganglia and the prevertebral ganglia. The paravertebral ganglia, as the name suggests, lie close to the vertebral column and extend continuously from the base of skull to the sacrum. Each ganglion is connected to the next to form a sympathetic chain, on either side of the spine. There are about 10 ganglia in the thorax and 5-6 ganglia in the abdomen, each connected to the thoracolumbar spinal cord via rami communicantes; some rami (white) mainly carry preganglionic fibres from the spinal cord, while others (grey) mainly carry post-ganglionic fibres which reach the periphery along somatic nerves. The thoracic and abdominal sympathetic chains issue the splanchnic nerves that travel to the abdominal plexus. At the rostral end of the chain is the superior cervical ganglion which supplies the head and neck, including the pupil, the lachrymal and salivary glands and cerebral blood vessels. Caudal to the superior cervical ganglion is the stellate ganglion which supplies the heart, and is formed from the amalgamation of the inferior cervical ganglion and the first two or three thoracic ganglia (Hedger and Webber, 1976). The other ganglia of the sympathetic chains issue nerves which supply the blood vessels of the body, and other small branches that reach the abdominal plexus (lumbar splanchnic nerves).

The prevertebral ganglia are found at the mid-line, ventral to the abdominal aorta. These ganglia are part of a complex mesh of nerves termed the abdominal plexus, the main ganglia of which are the celiac ganglion and the superior mesenteric ganglion. Of all the sympathetic ganglia, the superior cervical ganglion, due to its size, location and relative ease of removal, has been investigated the most (Hedger and Webber, 1976; Gabella, 1995). Most neurons in sympathetic ganglia are noradrenergic, the catecholamine being stored in the cell body, dendrites and axons; concentrations are highest in the terminal portion of the axon in the varicosities (swellings in the axon specialised for transmitter release). A small proportion of

sympathetic neurons express acetylcholine (Yamauchi and Lever, 1971) with many of these cholinergic neurons also containing vasoactive intestinal peptide (Landis and Fredieu, 1986); these cholinergic neurons innervate some blood vessels and the sweat glands (Langley, 1921; Wechsler and Fisher, 1968). Neuropeptides are present in sympathetic ganglia; positive staining to substance P and vasoactive intestinal polypeptide in present in incoming fibres (Hökfelt et al., 1977a, 1977b) but not ganglion neurons, and similarly enkephalin and somatostatin (Hökfelt, 1977c). Many sympathetic neurons stain for NADPH-diaphorase (an enzyme cofactor in the biosynthesis of the putative neurotransmitter nitric oxide) (Santer and Simmons, 1993) while others express ATP (Burnstock, 1990).

Sympathetic neurons are innervated by cholinergic fibres travelling in the white rami communicantes from neurons in the intermediolateral column of the thoracic and lumbar spinal cord. These preganglionic fibres of the rat, in contrast to other species (humans and cats) are mostly unmyelinated, with less than 1% of axons in the cervical sympathetic trunk displaying myelination (Hedger and Webber, 1976; Brooks-Fournier and Coggeshall, 1981). In the case of prevertebral ganglia the preganglionic fibres extend beyond the sympathetic chain. The superior cervical ganglion of the rat receives an input from 1600 preganglionic neurons (Rando et al., 1981), and itself contains somewhere between 20,000 and 45,000 neurons (for review see Gabella, 1995). These numbers indicate a divergence of the preganglionic input where preganglionic fibres must branch several times and make contact with many post-ganglionic neurons. Furthermore, electrophysiological evidence suggests convergence of the preganglionic input onto the neurons of the superior cervical ganglion (Purves and Lichtman, 1985a, b) where each post-ganglionic neuron receive synapses from several separate preganglionic fibres. Modest topographical representation of innervated target organs is noted in the ganglion (Bowers and Zigmond, 1979) where cells are clustered in the region of the point of exit of their respective post-ganglionic nerve. In addition to preganglionic fibres, paravertebral ganglia also contain post-ganglionic fibres, and both pre- and post-ganglionic fibres en passage. Afferent fibres, presumably also en passage, are present because some dorsal root neurons are labelled after the injection of tracers in the superior cervical ganglion (Yamamoto et al, 1989).

The vagus nerve (the tenth cranial nerve) emerges from the cranial cavity through the jugular foramen and swells forming the nodose ganglion, which issues smaller cranial (pharyngeal) and caudal (laryngeal) branches. The main vagal trunk runs caudal from the nodose ganglion into the neck (where it issues a cardiac branch and the inferior laryngeal nerve) and thorax, and continues into the abdominal cavity where it reaches the stomach providing innervation to the stomach, small intestine and part of the large intestine (see section 1.1.4).

1.1.3 Parasympathetic Division

Parasympathetic ganglia are small or even microscopic aggregations of parasympathetic neurons and are located closeby to their target organs. Several of these diminutive ganglia are found in the head; the sphenopalatine ganglion that innervates the glands and blood vessels of the nose, and hair follicles of the facial skin (Ehinger et al., 1983; Gibbins, 1990), the ciliary ganglion that innervates the ciliary muscle (Wigston, 1983) and iris of the eye, and the submandibular (Lichtman, 1977) and otic ganglia (Al-Hadithi and Mitchell, 1987) providing innervation to the submandibular gland and the parotid gland respectively. In addition to the above, the otic and sphenopalatine ganglia innervate the cerebral vasculature (Suzuki et al., 1988; Suzuki and Hardebo, 1991). Parasympathetic ganglia are also found close to the heart (cardiac ganglia, King and Coakley, 1958), respiratory tract (tracheal ganglia, Baluk and Gabella, 1989), and the urinary bladder and reproductive organs (pelvic plexus, Langworthy, 1965; Purinton, 1973). Parasympathetic post-ganglionic neurons express acetylcholine often in conjunction with other neuropeptides. The pelvic ganglion, the largest ganglion of the pelvic plexus, also contains adrenergic neurons and is thus described as a mixed parasympathetic and sympathetic ganglion.

Neurons in the brain stem and sacral spinal cord supply the preganglionic input to the neurons of parasympathetic ganglia. Parasympathetic neurons receive a single preganglionic fibre; the submandibular ganglion has been well studied in this aspect and 75% of its 250 neurons have only single connections (Lichtman, 1977; Snider, 1987). Initially each neuron is driven by several preganglionic fibres; during the early postnatal period the majority of incoming fibres are eliminated, until the neuron has a large number of synapses all of which originate from one preganglionic neuron (Lichtman, 1977). The mixed sympathetic and parasympathetic pelvic ganglion correspondingly receives preganglionic fibres from both autonomic branches, i.e. from the lumbar spinal cord (sympathetic outflow) and from the sacral spinal cord (parasympathetic outflow).

1.1.4 Enteric Division

The microscopic intramural ganglia of the gastrointestinal tract and biliary system are collectively termed the enteric nervous system (for reviews see Furness and Costa, 1987;

Gabella, 1987). This network of myriads of tiny ganglia containing enteric neurons cannot be regarded as either sympathetic or parasympathetic; although it does receive extrinsic input from both of these outflows (Langley, 1921) as denervation from this supply has little effect on most of the spontaneous and reflex activity of the gut. Although enteric ganglia and parasympathetic ganglia show some similarity, the numerous fundamental structural and functional differences render these enteric neurons to a class of their own (similarities have even been pointed out between the enteric ganglia and the tissue of the central nervous system). The enteric system is divided into two plexuses positioned at different levels in the gastrointestinal wall; the intramuscular myenteric plexus located between the circular and longitudinal muscle layers that extends continuously from the oesophagus to the anal canal, and the less extensive submucosal plexus found in the submucosa of the small and large intestines.

Parasympathetic input to both plexi is carried by efferent vagal fibres and fibres from the pelvic plexus (Keast et al., 1989). The rat vagus nerve emerging from the cranial cavity contains many thousands of fibres (Prechtl and Powley, 1990) and projects to the stomach and proximal small intestine (and possibly as far as the mid colon in some species) (Gabella, 1976); the great proportion are afferent axons terminating in various different areas of the tract (oesophagus, Neuhuber, 1987; stomach, Berthoud and Powley, 1992) but also a small percentage are parasympathetic efferent fibres (stomach and small intestine, Connors et al, 1983; Berthoud et al., 1991). The sympathetic input is carried in the mesenteric nerves issued by the prevertebral ganglia (outlined above). Estimations of the number of enteric neurons are in the order of millions (approximately 1.85 million in the rat myenteric plexus) (Gabella, 1971). Although there is no direct evidence of convergence or divergence of the preganglionic input, in light of the contrast in the numbers of preganglionic inputs and total enteric neurons, it appears that there is either a large divergence or that many enteric neurons are isolated from the central nervous system altogether. Furthermore, independent reflex activity reported in the enteric ganglia is suggested to originate from the well documented afferent, efferent and interneuronal components present.

1.2 Pelvic Ganglion

1.2.1 General

The pelvic ganglia are unique structures in the autonomic nervous system containing both sympathetic and parasympathetic neurons (for review see Gabella, 1995; Keast, 1995). This bilateral intricate network of interconnected ganglia located amongst the pelvic viscera, makes up what is collectively known as the pelvic plexus and supplies post-ganglionic axons to the reproductive organs, the bladder and the lower gastrointestinal tract. Despite providing neural co-ordination of important physiological processes of this region (such as micturition and penile erection), the precise nature of these reflex activities, and even the ganglionic structure itself, remains poorly defined. A confounding factor, hindering progress in the understanding of this part of the autonomic nervous system, is the anatomical complexity of the pelvic plexus, resulting in difficulty in regular access and dissection.

Langley and Anderson provided detailed accounts of the pelvic innervation of cats, rabbits and dogs (Langley and Anderson, 1895a, 1895b and 1896). The pelvic plexus and constituent ganglia display marked variation between species, with a complicated network of numerous ganglia in some species, and a more simple arrangement with fewer, larger ganglia in others (for review see Keast, 1995). Common to all species are the nerve trunks supplying the ganglia, namely the pelvic nerve and the hypogastric nerve, which branch at variable extents as they approach the pelvic ganglia. In addition to these larger ganglia, smaller ganglia are also microscopically visible lying along nerves, a few in the preganglionic nerves, the majority along the nerves projecting to the target organs. Some ganglion neurons are embedded in the muscle and serosal layers of the pelvic organs, the extent of which vary considerably between different species (rat, cat, rabbit, guinea pig and human) (Langworthy and Rosenberg, 1939; Wozniak and Skowronska, 1967; Kluck, 1980; Gilpin et al, 1983; Alian and Gabella, 1996).

1.2.2 Rat Pelvic Ganglion

1.2.2.1 Nomenclature

Throughout the many years that the pelvic innervation has been studied, investigators have used different terminology for the various anatomical structures; already in 1975, Dail and co-workers commented on the inconsistencies in the nomenclature. The largest autonomic ganglion in the pelvic cavity of the rat has been given different names- two of these are limited to one sex, the paracervical ganglion and Frankenhäuser ganglion of the female, with the male equivalent termed the (major) pelvic ganglion. The paracervical ganglion (term employed by Hervonen et al, 1972; Kanerva and Teräväinen 1972; Inyama et al., 1985; Papka et al. 1985) is so called due to its close proximity to the uterine/vaginal junction, while the term pelvic ganglion (Langworthy, 1965) has no sexual limitation to its application and has therefore been used by authors investigating ganglia in both male and female animals.

The term major pelvic ganglion (employed by Purinton et al 1973; Dail et al., 1975) is used to describe the largest of the neural masses in the pelvic plexus as opposed to the much smaller accessory or satellite ganglia that are present close by within the same plexus; these satellite ganglia are sometimes termed hypogastric ganglia (Melvin and Hamill, 1986). Other authors (Wang et al., 1990; Warburton and Santer, 1993) use the term hypogastric ganglion for the major pelvic ganglion. Confusion arises when the hypogastric ganglia, used to describe accessory ganglia, is reported to have no female analogue (Melvin and Hamill, 1986; Hamill and Schroeder, 1990) when it is known that accessory ganglia do exist in the pelvic plexus of the female rat. The term hypogastric ganglion is contentious when employed to describe a ganglion in the pelvic cavity and the term has also been used for the inferior mesenteric ganglion (Langworthy, 1965).

In the plexus some ganglia are located more peripherally than others while some are gathered in microscopic clusters within the nerves themselves. Therefore nerves are always 'mixed' i.e. contain pre- and post-ganglionic fibres, and usually contain afferent fibres as well (Hulsebosch and Coggeshall, 1982). Consequently it is important to make the distinction when using the terms preganglionic and post-ganglionic between those incidences

when describing anatomical positions relating to the main pelvic ganglion, as opposed to the regular use of the terms which refer to the two components of efferent autonomic innervation.

1.2.2.2 Organisation

In the rat, the pelvic ganglia and related nerve trunks are arranged in a comparatively simple configuration. There are no diffuse small ganglia as observed in some larger animals (rabbit, cat), but instead a single, bilateral ganglion, the aggregation of the smaller equivalents in other species (Langworthy, 1965, Foroglou and Winkler, 1973; Purinton et al., 1973; Baljet and Drukker, 1980). The predominance of this large ganglion has in some studies earned it the name the major pelvic ganglion (outlined above).

In the adult male rat, the pelvic ganglion is located at the edge of the posterior lobe of the prostate gland (Langworthy, 1965; Purinton et al, 1973; Dail et al, 1989a), while in the female it is located at the transition of uterine cervix to the vagina (Langworthy, 1965; Purinton et al, 1973; Baljet and Drukker, 1980).

This dominating ganglion is also accompanied by 2-4 smaller accessory (or satellite) ganglia that are positioned close to the seminal vesicles and vas deferens in the male, and near the neck of the bladder, at the ventrolateral wall of the vagina in the female rat (Purinton et al., 1973). The pelvic ganglia from both sexes exhibit elongations that extend toward the organs they innervate, these becoming the post-ganglionic nerves; neuronal cell bodies have also been reported in the cavernous (penile) nerve (Dail et al, 1989a; Keast et al, 1989).

The relative structural simplicity of the pelvic innervation of the rat has many advantages; it enables assured dissection of the ganglion (that contain the majority of the neuronal perikarya), and allows confident isolation and experimental manipulation of the pre- and post-ganglionic nerves.

1.2.2.3 Preganglionic Input

The nerves supplying the pelvic organs in the rat have been well documented (Langworthy, 1965) with clear distinction made between the constituent neuronal elements - namely sympathetic and parasympathetic inputs, and post-ganglionic nerves to the pelvic organs.

The hypogastric nerve emerges from the inferior mesenteric ganglion and enters the pelvic ganglion at its cranial pole. It is the main source of sympathetic input to the pelvic ganglion originating from neurons in the thoracolumbar spinal cord.

The main parasympathetic input to the ganglion is provided by the pelvic nerve. It originates from spinal segments, namely the last lumbar- L6 and the first sacral- S1 (Purinton et al., 1973); this differs from the situation in the human where the outflow is from (S1), S2, S3 and S4. The nerve is comprised of between 5 and 7 fairly well differentiated tracts and runs with the pelvic artery (Hulsebosch and Coggeshall, 1982) or the urogenital artery (Purinton et al. 1973). The pelvic nerve travels ventrally and then enters the ganglion at its dorsolateral aspect.

1.2.2.4 Ganglion Structure

The key structure in the pelvic ganglion is the ganglion neuron. These neurons vary from 15μm - 60μm in diameter, are ensheathed by glial cells (satellite cells) and enveloped by a basal lamina. Greenwood and colleagues (1985) reported that male rats have approximately twice as many pelvic ganglion neurons as female rats (approximately 15,000 in male and 6,000 in females); Hondeau and co-workers (1995) reported approximately 5,000 neurons in the female rat. Permeating between the neurons is an intraganglionic blood supply (small arterioles, venules and capillaries) and the entire ganglion is bounded by a capsule (Dail et al., 1975; Kanerva and Hervonen, 1976; Wang et al., 1990) that continues over the emergent nerves. These characteristics are very similar to those of other autonomic ganglia (and in particular mesenteric ganglia) except from ganglia of the enteric nervous system.

In contrast to other autonomic ganglia of the rat, the pelvic ganglion contains neurons with few or no dendrites (Foroglou and Winkler, 1973; Tabatabai et al., 1986; Keast et al., 1989); neurons in pelvic ganglia from other species (e.g. guinea pig) have many dendrites (Yokota and Burnstock, 1983).

A small proportion of neurons in the ganglion exhibit large vacuoles (vacuolated neurons). The vacuoles, which measure up to 20μm in diameter, greatly enlarge these cells while at the same time displacing their organelles The vacuolated neurons, in all other respects are similar in structure to the principal ganglion neurons. Vacuolated neurons are 0.2% of the pelvic ganglion neuronal population in female rats and 0.8% in pregnant animals

(Lehmann and Stange, 1953). The pelvic ganglia of male rats also exhibit vacuolated neurons (Dail et al., 1975) and in the proportion of 0.8-1.2% of the total population (Partanen et al., 1979). These vacuolated neurons make their appearance at around the seventh week of life, and disappear with castration (Partanen et al., 1979).

Another cell population are the small, intensely fluorescent (S.I.F.) cells (Kanerva and Teräväinen, 1972) which are also found in other autonomic ganglia and are the main components of paraganglia. In the pelvic ganglia these are usually present in large numbers; two estimates in the superior cervical ganglion number these cells at 370 (Williams et al., 1977) to nearly 1000 (Santer et al., 1975). They can be identified by their small size of 10-15μm in diameter and their very intense fluorescence induced by formaldehyde. Under the electron microscope numbers of large, dense core vesicles can be seen in the cytoplasm (giving rise to the term small granule containing cells- Matthews and Raisman, 1969). Taxi (1979) used the variation in core vesicle size to divide S.I.F. cells into two groups: type I S.I.F. cells that have vesicles measuring between 80-100nm, and type II SIF cells that have larger vesicles that measure between 150-300nm. Most S.I.F. cells in the pelvic ganglion are type II (Dail et al., 1975).

1.2.2.5 Adrenergic/Cholinergic Composition

The pharmacological efficacy of acetylcholine and noradrenaline in pelvic effector organs has been accepted for many years. This concept has arisen from experiments employing neurotransmitter antagonists where it was conclusively demonstrated that relaxation of the colon or sphincter contraction (activities evoked by the hypogastric nerve) was blocked by adrenoceptor blockers, while contraction of the bladder and colon (a response to pelvic nerve stimulation) was susceptible to muscarinic antagonists. The pelvic ganglion accordingly contains both cholinergic and adrenergic neurons. The adrenergic neurons (identified by formaldehyde induced fluorescence and more recently by immunostaining for tyrosine hydroxylase) are some of the larger neurons (40-60μm in diameter) and, while constituting the majority in the male, (Dail et al., 1975), are reported to be only one third (Kanerva et al., 1972) or as little as 9% (Rousseau et al., 1995) of the total neuron population in the pelvic ganglion of the female. Cholinergic neurons are about one fifth of all the ganglion neurons, although the identification of cholinergic neurons is less certain as it is based upon an intense

reaction for acetylcholinesterase, an enzyme which is sometimes also present outside cholinergic neurons. Cholinergic activity from the pelvic ganglion has also been identified, more specifically, by biochemical measurement of the enzyme choline acetyltransferase (Dail and Hamill, 1989). Differences in cholinergic neurons between the sexes appear to exist, namely that in the male they are of small size (15-25μm) (Dail et al., 1975) while in the female are reported to be amongst some of the largest cells in the ganglion (Kanerva et al., 1972).

1.2.2.6 Non-Adrenergic, Non-Cholinergic Expression

Experiments have also demonstrated certain activities in the pelvic viscera that are resistant to the use of cholinergic and adrenergic antagonists. As with other visceral effectors these activities have been termed 'non-adrenergic, non-cholinergic' (NANC) responses. Investigation employing histochemical and pharmacological techniques has lead to the identification of many substances that may be the neurotransmitters responsible. Sub-populations of neurons expressing different peptides and thus displaying immunoreactivity to these substances, have been located in the pelvic ganglion. Vasoactive intestinal peptide (Dail et al., 1983; Gu et al., 1984; Keast and de Groat, 1989), neuropeptide Y (Papka et al, 1985; Morris and Gibbins, 1987; Keast and de Groat, 1989; Keast, 1991), enkephalin, substance P, and galanin, have all been reported in the neuronal somata (for review see Keast 1995). Often these peptides are restricted to either cholinergic or adrenergic neurons, although there are instances where the peptides are co-localised with both the classical transmitters (acetylcholine and noradrenalin) or neither of them. Nicotinamide adenine dinucleotide phosphate-diaphorase (NADPH-d), a cofactor of the biosynthesis of nitric oxide (Dawson et al., 1991; Hope et al., 1991) is present in the pelvic ganglion, and nitric oxide is believed to act as a NANC transmitter (Rand, 1992). Neurons containing nitric oxide in the female rat project to the uterus (Papka et al, 1995), while positive neurons in the male project to the penis (Keast, 1992).

1.2.2.7 Preganglionic Connections

Preganglionic fibres give cholinergic synapses to most of the ganglion neurons (including the vacuolated neurons). Whereas in other autonomic ganglia the incoming fibres synapse mainly on dendrites, in the pelvic ganglion they mainly make contact directly with the soma

or somatic spines (Kanerva and Teräväinen, 1972). Many of these terminals stain for a range peptides (somatostatin, substance P, enkephalin and calcitonin gene related polypeptide) (Dail and Dziurzynski, 1985; Keast 1991; Papka and McNeill, 1993; Keast and Chiam, 1994). There is also evidence of adrenergic terminals, thought to be collaterals of adrenergic neurons in the same ganglion, that surround some cholinergic neurons (Dail et al., 1975).

Purinton and co-workers (1971) suggested that the pelvic ganglion could mediate reflex activity without any relay to the dorsal root ganglia, and the presence of peripheral afferent neurons. Selective denervation experiments (Purinton et al., 1971) have concluded that these neurons are probably situated in the pelvic ganglion itself. Afferent fibres from the dorsal root ganglion that pass through the pelvic ganglion have been identified by anterograde filling; while many axons pass through the ganglion unbranched, others form varicosed clusters around certain neuronal perikarya and presumed to make synaptic contact with these cells (Dail and Dziurzynski, 1985; Papka 1990).

The pelvic ganglion receives two separate preganglionic inputs from parasympathetic cholinergic and sympathetic cholinergic fibres. Initially thought to enter separately via different nerves, electron microscopic study has shown the preganglionic input to be more complex. The hypogastric nerve contains 1600 axons comprised of 58% sympathetic post-ganglionic, 34% sympathetic preganglionic and 8% sensory axons (Hulsebosch and Coggeshall, 1982). Nearly 5,000 axons are present in the pelvic nerve, 34% of these are sensory, 49% parasympathetic preganglionic and the remaining 17% are sympathetic post-ganglionic axons. Of all the preganglionic fibres going to the pelvic ganglion only 12% are myelinated. A small number of myelinated axons are also present in the post-ganglionic fibres.

1.3 Neural Sexual Dimorphism

1.3.1 General

Numerous instances of morphological differences between analogous structures in males and females (known as sexual dimorphism) in the nervous system of vertebrates are known. Gonadal hormones play a crucial role in the sexual differentiation of the vertebrate periphery and thus also in this neural sexual dimorphism. The parental contribution of sex

chromosomes determines whether an individual will develop as a male or female (although in some vertebrates this control is via environmental stimuli such as incubation temperature). The result of this early divergence is that the embryonic gonads develop as either testes or ovaries. Whether the rest of the organism develops in a male or female fashion is as a direct result of the hormonal secretions of these sex glands. The testicular secretion testosterone induces masculinisation in all mammalian extragonadal tissues including the nervous system (although they may assist, ovarian secretions are not necessary for female development) (Wilson et al., 1981).

In advance of any direct evidence of sexual dimorphism in the central nervous system, predictions were made to its occurrence due to the effect that perinatal steroid exposure had on adult sexual behaviour. Phoenix and co-workers (1959) demonstrated that adult female guinea-pigs which had been treated with testosterone before birth displayed no sexual interest in the mounting attempts made by male guinea-pigs. It was suggested that the sex differences in adult behaviour were a reflection of the early organisation of the brain induced by androgenic steroids such as testosterone. Testosterone was thought to act as a pro-hormone for the masculinisation of adult copulatory behaviour and ovulatory functions in rats. It was later demonstrated that this androgen is converted via aromatisation into various oestrogens that induce masculinisation of the brain. Many other instances of sexually exclusive behaviour in adult animals were investigated and they were shown also to result from steroid exposure during a restricted sensitive period in development (for reviews Arnold and Breedlove, 1985; Kelley, 1988; Baum et al., 1990).

In the study of instances of sexual dimorphism the factors generally investigated are i) the actual steroid that drives the masculinisation (whether it is testosterone or one of its oestrogenic metabolites), ii) the sensitive period in development when the steroid induces masculinisation, iii) the cellular process that is altered by exposure to the steroid (e.g. cell division, migration, cell death), iv) the steroid stimulated cell population that initiates the masculinisation, v) the gene(s) in the cell population regulated by the steroid, vi) the connection between the altered gene expression and the altered cellular process, vii) the consequent behavioural changes due to the changed neural structure, and viii) whether there is any modulation of the effect of the steroid hormone due to environmental influences.

Much conclusive evidence relating to the first two criteria has been amassed in various different structures (see below). In some systems the third and fourth lines of enquiry have been partly answered, but in no system have the questions of gene expression been fully elucidated. In this thesis the first four characteristics: the masculinising steroid, the steroid sensitive period, the altered cellular process, and the affected cell population, will be investigated.

1.3.2 Central Nervous System

It has been well documented that the brain can develop either masculine or feminine behavioural characteristics depending on the presence or absence of gonadal hormone during the perinatal period. However, it is only recently that related morphological differences between the sexes have also been described.

Many investigations have been carried out in the central nervous system (CNS) (for reviews see MacLusky and Naftolin 1981; Arnold 1980; Breedlove 1992; Madeira and Lieberman 1995) where the songbird and frog vocal control regions have been studied in detail, along with the innervation (spinal nucleus of the bulbocavernosus -SNB) of the rat perineal muscles and preoptic area (POA) of the rat brain.

1.3.2.1 Songbird Vocal Control Region

Early investigations into the rat brain only reported subtle differences between male and female individuals (Pfaff, 1966; Raisman and Field, 1973). In contrast, it was reported (Nottebohm and Arnold, 1976) that parts of the songbird brain were five to six times greater in volume in the male than in the female, and that neurons in this region were larger, and had more dendrites in the male than in the female (DeVoogd and Nottebohm, 1981). This neural sexual dimorphism in a part of the brain that controls vocalisation in songbirds (canaries and zebra finches), was clearly related to behaviour as males sing more than females during courtship (Nottebohm et al., 1976), and because these vocal control regions (VCR) show no sex difference in bird species where both sexes sing (Brenowitz et al., 1985). Masculinisation of the VCR was induced as effectively by both testosterone and oestradiol (Gurney and Konishi, 1980; Gurney, 1981; Konishi, 1989). The testosterone was presumably derived from the gonads, while the oestradiol was produced as a result of the

well documented enzymatic action of aromatase on testosterone (for review see Naftolin and MacLusky, 1984) in the brain. In the canary there is some evidence that the behavioural ability of the bird to learn new seasonal song throughout adulthood is also accompanied by expansion of the VCR (Nottebohm, 1981; Nottebohm et al, 1990). Data suggests that the gender difference in the zebra finch is brought about by differing degrees of cell death in the VCR (specifically in the robust nucleus of the archistriatum) (Konishi and Akutagawa, 1985) between the two sexes, the reduced amount of cell death in the male finch being controlled by gonadal steroid and the extent of innervation from another VCR (the hyperstriatum ventrale caudale or higher vocal centre) (Konishi and Akutagawa, 1985; Herrmann and Arnold, 1991). At the same time limited observations of neurogenesis in the VCR of female canaries have also been made (Goldman and Nottebohm, 1984) and these lead to tentative conclusions being drawn between steroid control of this differentiation and the sex dimorphism (Nordeen and Nordeen, 1989) although much subsequent evidence lends little support to this mechanism.

1.3.2.2 Frog Vocalisation System

The larger larynx of the male African clawed frog (Xenopus laevis), due to the androgenic potentiation of myogenesis and chondrogenesis in the male larynx (Sassoon et al, 1986), results in courtship song not observed in the female. This distinct sexual behavioural, while initially appearing to be mediated in the periphery (musculature of the larynx), was also seen to manifest itself in the central nervous system, where there is a sex difference in the number of brainstem motoneurons that innervate the larynx (Kelley and Dennison, 1990).

1.3.2.3 Rat Spinal Nucleus of Bulbocavernosus

In both male and female newborn rats, the bulbocavernosus and levator ani muscles that are attached to the base of the penis and clitoris respectively, are innervated by cells in the spinal nucleus of the bulbocavernosus (SNB) (Sengelaub and Arnold, 1986; Rand and Breedlove, 1987). These perineal muscles undergo substantial atrophy in perinatal female rat (Hayes, 1965; Cihak et al, 1970; Tobin and Joubert, 1991) and this accompanied in the female animals by a greater loss of SNB cells than in the males (Nordeen et al., 1985; Breedlove, 1986) which results in a sexually dimorphic spinal nucleus of the

bulbocavernosus in adulthood (Breedlove and Arnold, 1980). Breedlove and Arnold (1983a, b) showed that testosterone maintained the perineal muscles in developing rats, and that both chemical and surgical castration induced their atrophy in perinatal males animals. It was shown that the androgen exerted its effect directly upon the bulbocavernosus and levator ani muscles, and that the sexual dimorphism in the innervating motoneurons was an indirect effect; Fishman and Breedlove (1988) produced evidence that the androgenic maintenance of these muscles was not dependent on the survival of SNB neurons, while other data showed that in the perinatal period while testosterone was bound in these muscles, it was not bound in the innervating motoneurons (Fishman at al., 1990; Jordan et al., 1991). Sensitivity to gonadal steroid in the levator ani muscle has been shown to persist into the prepubertal period, when the administering of testosterone (at post natal day 7 for 3 weeks) results in a reduction in the normal developmental elimination of multiple neuromuscular synapses (Jordan et al., 1989); accompanying changes in motor unit size indicates that it is intrinsic synapse elimination that is under androgen control (Jordan et al., 1992).

1.3.2.4 Rat Preoptic Area

The preoptic area of the rat brain has been strongly implicated in the sexual function of these animals; a nucleus in this region was reported to be five to six times larger in the male rat that in the female, and was subsequently named the sexually dimorphic nucleus of the preoptic area (SDN-POA) (Gorski et al., 1978). The volume of this nucleus is sensitive to androgen manipulation in the perinatal animal but not in the adult; Jacobson and Gorski (1981) demonstrated (with the use of tritiated thymidine) an increase in neurogenesis in the nucleus in the foetal period which coincides with testosterone secretion at that time (Warren et al., 1973). It is believed that oestrogenic metabolites of testosterone are more likely to exert sexual differentiation (Döhler et al., 1982); this is the case in the control of copulatory behaviour in the rat, and due to the reduction in this behaviour with lesion of the preoptic area, it is this activity that the preoptic area is thought to mediate (Hart and Leedy, 1985).

1.3.3 Peripheral Nervous System

Gender difference has also been observed in the peripheral nervous system (for review see Wright, 1995) although work in this part of the nervous system is still very much in its

infancy. Areas that have been specifically identified as exhibiting gender difference are the rat superior cervical ganglion (Wright and Smolen, 1983), the pelvic ganglia of the rat (Greenwood et al, 1985; Melvin and Hamill, 1989a) and the hypogastric ganglion of the mouse (Suzuki et al, 1983).

1.3.3.1 Superior Cervical Ganglion

The superior cervical ganglion is a prominent ganglion at the rostral end of the paravertebral sympathetic chain that supplies innervation to the pupil of the eye, and the tear and salivary glands. Much data has been gathered regarding the size of this ganglion, and substantial variation in estimated neuronal counts is seen in the literature with between 20,000 and 45,000 neurons present in the ganglion cited depending on the author (for review see Gabella, 1995).

1.3.3.2 Pelvic Ganglion

The autonomic innervation in the pelvic cavity seemed for a long time to have been overlooked in this matter. Bearing in mind the marked sex difference in anatomy in the pelvic region, with the specialisation that has evolved for reproduction, it would seem natural that differences also occur in the neuronal structures that innervate these organs.

However, no systematic comparison can be found in the literature. Most authors tend to work on ganglia from a single sex, the uniformity of tissue usually being the stated reason for this, which implies that sex differences may be present in the ganglion.

Another indication that sizeable differences occur between the pelvic ganglia of the two sexes is the conflicting nomenclature encountered in the literature. Many different terms (pelvic ganglion, major pelvic ganglion, hypogastric ganglion, paracervical ganglion, Frankenhäuser ganglion) are employed and sometimes interchanged, and although generally it can be understood what structure is being referred to, certain terms are sexually specific or pertain more obviously to one sex, and thus can lead to confusion.

From the literature it appears that the basic structure of the pelvic ganglion is the same in male and female rats i.e. a large, bilateral ganglion positioned in the pelvic plexus receiving preganglionic input from both the sympathetic and parasympathetic autonomic divisions. The only study to compare the pelvic ganglia from rats of both sex was that of Greenwood and colleagues (1985) who discovered that the numbers of neurons in the adult male rat are

approximately double that of the female (approximately 15,000 in male and 6,000 in females).

Other comparisons must be drawn from evidence gained from studies on only one or other sex. The average neuronal cross sectional area is larger in the male than in the female, and there also appears to be sex differences in the extent and distribution of certain non adrenergic, non-cholinergic transmitters. Further evidence (gained from castration experiments) has lead to the suggestion that the development of these sex differences are directly or indirectly due to the influence of testosterone (Melvin and Hamill, 1987 & 1989a; Partanen and Hervonen, 1979; Hamill and Schroeder, 1990).

The experiments carried out in this thesis were undertaken to investigate the development of the pelvic ganglion, and in particular the development of the sex related differences reported in its structure; morphometric and histochemical techniques were employed using light and electron microscopes. Additionally, an effort was made to determine the developmental mechanisms behind the sex differences of the mature ganglion; the factors studied included the actual steroid that induces the change (investigated by castration experiments), the sensitive period in development (adult, pre-pubertal and new-born rats were investigated) and the altered cellular process (incidence of cell death was investigated).

CHAPTER 2

METHODS

2.1 Dissection

2.1.1 Animals

Throughout this work male and female Sprague-Dawley rats were used. Adult rats weighed between 180g and 230g. The pre-pubertal rats were aged 21 days and weighed between 80g to 100g for either sex, while the newborn animals of both sexes weighed between 6g and 7g.

Rats were obtained from Biological Services (University College London) where they had been bred from a strain initially supplied by Charles River Ltd, UK. Adult animals were housed 4 to a cage, with free access to food and water. Cages were subjected to a 12 hour light/dark cycle, with one hour intervening periods of simulated dusk and dawn.

2.1.2 Anaesthesia

The rats were killed by an overdose of intra-peritoneally administered pentobarbitone (Sagatal™). The volume of pentobarbitone for irreversible over-anaesthesia used was approximately 15mg/100g rat body weight. Pentobarbitone was used because it induced a deep anaesthesia very quickly. After the animal displayed no cranial nerve reflex (corneal reflex, pain reflex from skin pinching), it was immobilised by pins through the carpals and tarsals and the perfusion process was carried out.

2.1.3 Perfusion

It was essential to complete the perfusion with minimal delay. For good perfusion the vasculature must be patent for the fixative fluid; if the perfusion was not carried out immediately, blood would coagulate in the vessels reducing the quality of tissue fixation. Exsanguination in animals of all age groups was carried out via the heart. On opening the thoracic cavity of adult and pre-pubertal rats, the tip of the heart was grasped with a "heart clip" and the left ventricle was cut. A bulb ended cannula was pushed up through this opening into the ascending aorta (coming to rest in the aortic arch) and isotonic Krebs solution (NaCl, 80%; KCl, 3.5%; $NaHCO_3$, 10%; $CaCl_2$, 2%; $MgCl_2.6H_2O$, 1%; $C_6H_{12}O_6$, 3.5%) was manually driven in from a 50ml syringe. The blood, and subsequently the perfusion fluids was drained through the right atrium, which was also cut open. Sodium nitrite (0.1%) and heparin (1%), was also present in the perfusing solution to induce vasodilation and to inhibit coagulation respectively. With respect to the pre-weaning specimens, particular care was taken not to rupture the less muscular, immature wall of the aortic arch. The perfusion of Krebs solution was stopped when clear solution could be seen effusing from the opened right atrium; usually between 100-200ml of Krebs solution was used, depending on the size of the animal. Next, fixative was perfused through the animal by the same route.

In the newborn animals a limited exsanguination was possible by using the same method as above except for using a syringe and needle only. The needle was entered into the intact left ventricle and first Krebs solution, then fixative (as above) driven manually into the animal. An incision in the right atrium no larger than a pin hole had been made prior in order to allow effusion.

2.2 Acetylcholinesterase

Extensive investigative dissection enabled accurate isolation and removal of the ganglia in all the animal groups used. To improve visualisation of the pelvic plexus a general neuronal stain, acetylcholinesterase, was used. This technique enabled the fine detail of the pelvic plexus to be studied, and afforded later ganglion dissection to be made with confidence due to the awareness of the topographical relations between the structures in the pelvic cavity.

2.2.1 Acetylcholinesterase Histochemistry.

Due to the translucent nature of fresh unfixed nervous tissue, the pelvic plexus is difficult to visualise in the animal and thus display its topographical visceral relations. In order to aid with observing the ganglion in situ, histochemical staining for the enzyme acetylcholinesterase (Karnovsky and Roots, 1964) was employed. This technique, however, has proved unreliable as a distinct marker for cholinergic neuron phenotype (as cholinesterase activity has been observed in non cholinergic sensory neurons (Cauna and Naik, 1963) and in most autonomic nerve terminals (Burnstock, 1970)) but provides general staining for nerve tissue. The method is based on thiocholine reducing ferricyanide to ferrocyanide. The latter combines with Cu^{2+} ions to form insoluble copper ferrocyanide (the reaction product - also known as Hatchett's Brown); the excess Cu^{2+} ions in the medium are complexed with citrate to prevent formation of copper ferricyanide.

The rats were killed with an overdose of pentobarbitone and perfused via the left ventricle with Krebs solution (as above). The lower abdomen was opened with a 4-5cm incision and the pelvic viscera deflected to one or other side depending on which side was to be stained. The entire pelvic viscera were removed from the animal fixed in cold, 10% buffered formalin and left in the refrigerator for one hour. Next the tissue was washed in Krebs solution and then left overnight in the refrigerator in a solution of Hyaluronidase (0.33mg/100ml; Sigma Ltd, UK) and tetraisopropylpyrophosphoramide (OMPA; final concentration of 10^{-4}M; Sigma). The solution was then changed to the acetyl cholinesterase incubating solution: 5mg acetylthiocholine iodide (Sigma), 6.5ml acetate buffer (0.1M), 0.5 ml sodium citrate (0.15M), 1ml copper sulphate (30mM), 1ml potassium ferric cyanide (5mM). The tissue was left in this solution for between 8-24 hours with the solution being changed every 2 hours for 8 hours and then every 8 hours. Specimens were regularly viewed (approximately once every hour) through a dissecting microscope during which adipose tissue was removed and unstained neuronal tissue exposed to the medium (it appears that the reaction product only develops on direct contact with the tissue); to aid the reaction, the capsule of the ganglion was scraped with forceps again in an effort to enhance penetration of the incubating medium. When an acceptable amount of stain had been picked up by the ganglion, the tissue was washed in water for 1 hour and then fixed again in buffered formalin.

2.2.2 Photography

2.2.2.1 In Situ Ganglion

The pelvic viscera together with the pelvic ganglion now stained a dark red, was photographed. The specimens were photographed through a stereo dissecting microscope using epi-illumination supplied by either a circular light source or twin fibre optic light sources. Various magnifications were employed and Nikon cameras used with Ilford black and white film of 400 ISO rating. The negatives once developed, were printed onto Ilford multigrade photographic paper typically at a 5x magnification.

2.2.2.2 Detached Ganglion

In order to identify the fine detail, ganglia from pre-pubertal and adult animals were carefully dissected away from the surrounding tissue. The ganglia were then placed onto glass slides and mounted in 70% glycerol. An attempt was made to display as many nerve structures as possible- this process may have inadvertently lead to a topographical representation slightly different to that in the intact animal. A second slide was placed on the specimen and any air bubbles removed. The isolated ganglia were photographed in the same manner as the whole mount preparations but this time trans illumination was also employed. Microscopic details of the preparations were photographed using a Zeiss™ light microscope employing bright field optics. The negatives obtained were again printed onto Ilford multigrade photographic paper at various magnifications.

2.3 Cytology

2.3.1 Fixation

Fixation was carried out via the same cannula as used for the exsanguination but this time the fluid was driven with gravitational pressure, the vessel of fixative positioned above the animal (the height varying from 1 metre for adult animals and 0.75 metre for pre-pubertal animals). The fixative used was 1% paraformaldehyde and 5% glutaraldehyde in 100mM sodium cacodylate at 7.4 pH. The perfusion usually lasted about 3 minutes, with 200 - 500ml of fixative being used. In newborn animals the fixative (between 75-100ml) was driven manually via a needle and syringe in the same manner as that used for the exsanguination.

The degree of success of the perfusion could be estimated by observing the rigidity of the hind limbs and tail- a good indicator of successful perfusion of the lower abdominal area, and therefore of the pelvic ganglion, was that these regions should be well perfused and therefore stiff. Next the abdominal cavity was opened and the gastro-intestinal viscera deflected to one side (or removed). The bladder was then used as a reference point from which the left and right pelvic ganglia could be found.

The ganglia together with their pre- and postganglionic nerves were then dissected out from both sides of the animal. The surrounding blood vessels were also dissected out with the ganglia and these together with the pre- and post-ganglionic nerves served well for orientation. The specimens were then placed in fresh fixative.

The ganglia were then pinned out on a Sylgard™ plate under a dissecting microscope. To reduce the size of the specimens and allow the cutting of sections of known orientation, some of the associated blood vessels and connective tissue were dissected away.

The ganglia were thoroughly washed in cacodylate buffer and then stained in 1% osmium tetroxide for 1 hour. After washing in buffer they were then further stained in an aqueous saturated solution of uranyl acetate for 1 hour. After a brief wash in distilled water the ganglia were dehydrated in graded alcohols ranging from 50% ethanol to absolute ethanol. When the specimens were in 70% alcohol, they were unpinned from the Sylgard™ plate so that they were not damaged as they contracted due to dehydration. The specimens were then ready for embedding.

2.3.2 Embedding

The resin used was an epoxy resin (Araldite™) and was prepared by mixing together 51g of CY212 polymer with 49g of DDSA polymer. The polymers were heated in an oven for twenty minutes reaching a temperature of about 65°C prior to mixing; at this temperature the two resins mixed much more completely than when they were at room temperature. Next 1ml of BDMA and 1.5ml of dibutyl-phthalate hardeners were added and all the elements mixed extremely thoroughly but taking care not to introduce air into the mixture. In preparation to the embedding in resin, the specimens were put into propylene oxide followed by a 50:50 resin/propylene oxide solution and finally infiltrated overnight in 100% resin.

The resin containing the specimens was then poured into to shallow foil dishes which were placed in an oven (70°C) to harden. The resin blocks took three days to harden after which the individual ganglia could be separated into smaller blocks by sawing, ready for sectioning.

2.3.3 Light Microscopy

For light microscopy, sections of between 0.5μm-2.5μm were cut with glass knives on a Reichert microtome. Ganglia were cut starting from the entry of the pelvic nerve, finishing at the emergence of the post ganglionic nerves. For the thinner of the sections, a wet knife was used, i.e. one with a boat constructed from tape on the knife edge, containing distilled water, onto which the sections float. These floating sections were then picked up with an eyelash supported in modelling wax attached to the end of a stick. The slightly thicker sections were cut with a dry knife as their increased rigidity enabled them to be picked up directly from the knife edge with fine forceps. All the sections for light microscopy were deposited onto to drops of distilled water on glass slides, which was then evaporated on a hot plate (at 50°C). In order to improve section adherence, the slides were also wafted once or twice through the flame of a butane gas burner. The sections were then stained for between 30-90 seconds (according to thickness) with 1% alcoholic toluidine blue. Excess stain was removed with 50% ethanol which also served to bring about staining contrast. The slides were again dried on the hot plate after which the sections were mounted with a drop of Araldite™ resin under a coverslip.

The slides prepared were viewed on two different Zeiss™ Axiophot light microscopes using phase contrast optics. Tissue that appeared to have been well fixed and in sharp outline was chosen for photography and this was carried out by the microscopes' in-built cameras. Ilford black and white 35mm film of ISO rating 50 was used for the exposures in conjunction with an orange filter. The negatives were developed and photographic prints produced (the final magnifications varying depending on the microscope, objective and darkroom enlargement selected) which were either viewed as individual images or assembled into small montages (again depending on the final magnification).

2.3.4 Transmission Electron Microscopy

The sections used for electron microscopy were thinner being between 0.1μm-0.2μm. These were cut with a wet glass knife and collected on copper grids. Further uranyl acetate was used along with lead citrate to give the sections increased contrast for the electron microscope.

The copper grids were floated section-side down on uranyl acetate for between 30 and 60 minutes. The uranyl acetate was 1% in 70% ethanol. The uranyl acetate was covered to avoid evaporation and a cardboard box was placed over the uranyl acetate to prevent the breakdown that is caused by exposure to light. A lamp was positioned about a foot away from the box to give warmth to the staining procedure as an increase of temperature has been seen to aid in the staining of certain tissue sections. After the staining period had elapsed, the grids were thoroughly washed in a stream of distilled water. Next, the grids were floated, again section-side down on a drop of lead citrate on dental wax. The lead citrate on the wax was surrounded by sodium hydroxide pellets and contained in a covered Petrie dish. The grids were left on the lead citrate drops for no longer than ten minutes, after which they were rinsed thoroughly in a stream of fresh, distilled water. Once the grids were dry, the sections were ready for viewing in the electron microscope.

2.3.5 Scanning Electron Microscopy

The aim of this work was to directly view the surface of the ganglion neurons contained within the pelvic ganglion. This would enable another 'dimension' of our understanding of the internal structure of the ganglion. It is clear that for the neurons to be viewed, the outer ganglion capsule would have to be removed or at least deflected. This could be done both by physical manipulation (partial cutting and tearing) and chemical removal. A combination of the two was used, although the physical manipulation was very limited in its extent (minimal efforts to lacerate the capsule, restricted in their extent due to the fragility of the structure). The main attempt at removing the capsule came from enzymatic digestion with trypsin and hydrolysis with hydrochloric acid.

2.3.5.1 Tissue Preparation and Digestion

Female pelvic ganglia were dissected (see section 3.1 above) by first removing the gross anatomical area (consisting of the pelvic viscera; uterus, vagina, bladder and rectum). From this, the pelvic ganglia were then isolated by fine dissection. Orientation of the ganglia was noted and the ganglia were pinned out onto Sylgard™ plates.

The process of digestion and dehydration was then carried following the methods used in the works by Baluk et al. (1985) and Baluk and Gabella (1989). While the ganglia were still pinned to the Sylgard™, they were placed in a solution of trypsin (Sigma type II, 2.5mg/ml in phosphate buffered saline) and placed in a 37°C water bath for 30 minutes. The ganglia were then removed from this digestion and rinsed thoroughly in phosphate buffered saline (PBS-Dulbecco 'A'; tablets from Oxoid, Unipath Ltd. UK). The ganglia were then fixed in 5% glutaraldehyde in cacodylate buffer for 2 hours. After further dissection to remove connective tissue, the ganglia were subjected to hydrolysis in 8M hydrochloric acid for 20-30 minutes at 60°C. Once rinsed with distilled water, the dehydration was then carried out by the use of graded alcohols starting with 50% ethanol and ending with 100% ethanol. The ganglia were finally placed in isoamyl acetate.

In preparation for the scanning electron microscope the ganglia were mounted onto a stub with either graphite paste or conductive coupling adhesive tape and then critical point dried with carbon dioxide. Once this was complete, the specimens were sputter coated with gold film and viewed using an Hitachi scanning electron microscope. Electron micrograph plates were exposed in this microscope and these negatives developed and then printed onto photographic paper.

2.4 Quantitative Morphometry

2.4.1 Ganglion Volume

To determine the ganglion volume in adult and pre-pubertal animals, the sectional area of the ganglion was measured every 100μm by tracing the outline of the capsule from light micrographs onto a digitising tablet connected to a personal computer. In newborn animals the gap between cross sectional areas traced was 50μm. In all animal groups the cross

sectional areas (in μm^2) were then averaged and the mean was multiplied by the length of the ganglion to calculate the overall ganglion volume (the Cavalieri method).

2.4.2 Three-Dimensional Graphic Representation.

The ganglion cross sections selected above (section 3.4.1) were again traced onto a digitising tablet connected to a personal computer. The use computer software (written by a laboratory colleague) then enabled these ganglion profiles to be separated at the correct morphometric distance (100μm in pre-pubertal and adult animals, and 50μm in newborn animals), and maintained and displayed at different perspectives in this spatial arrangement while still retaining the exact section to section relationship. Line drawings of these three dimensional representations were then printed onto to paper. This process allowed direct comparison of the relative size and shape of ganglia from different animal groups.

2.4.3 Neuron Populations

Accurate and consistent counts of neurons are very useful in neurobiology, but they are at a premium because of the difficulty, labour and uncertainty associated with the methods available. In principle it is always possible to determine the true number of neurons by collecting all the sections and then identifying and counting every single neuron, especially when the outline of the nervous structure in question is sharp, as is usually the case with a peripheral ganglion. In practise, this approach is of little use, because the vast amount of work involved appears unjustified. However, the approach is useful, even if applied to a very limited extent, to produce an absolute value against which the accuracy of methods based on sampling can be tested and it was for this reason that some full reconstructions were undertaken in conjunction with sampling work.

2.4.3.1 Total Neuronal Counts

Three pelvic ganglia from adult female rats were sectioned at a thickness of 1μm using a diamond knife. The ganglia were sectioned starting from the pelvic nerve and ending at the emergence of the post-ganglionic nerves, with ganglion sections containing not less than 10 neuronal profiles included in the reconstruction. Every 4th section was photographed in a Zeiss™ light microscope and printed onto photographic paper. Each and every neuron was labelled and numbered on all the photomicrographs on which it appeared, for identification

- Dehydration of specimens carried out during processing probably causes some tissue shrinkage which affects the ganglion volume and Nv data; when using larger tissue samples it may be possible to quantify the extent of this shrinkage but with an organ the size of the rat pelvic ganglion this would be very difficult; therefore, for these experiments no corrections of the values measured were carried out.

and counting. This process was carried out on every micrograph that was printed throughout the entire ganglion. The total neuronal count data was collected with collaboration with Dr. D. Kayanja (a fellow research student).

2.4.3.2 Disector Neuronal Estimation

An accurate method exists for estimating the number of cells present in a structure, thus removing the need to collect serial sections from the entire structure. The method is known as the Disector Method and is designed to produce an unbiased estimation of cell numbers. The basic principle of the disector method for particle (neuronal cell bodies in the case when sectioning a ganglion) number counting is to determine numbers per unit volume (Nv, numerical density). This numerical density is then multiplied by the total volume of the structure (Vref) giving the cell number estimation (N). This method was developed and first employed by Sterio (1984), was verified in accuracy in work on nervous tissue by Pover and Coggeshall (1991) and discussed in reviews by Gundersen et al (1988a and 1988b), Coggeshall (1992) and Mayhew (1992).

A disector is a short series of sections. The first section in the "mini-series" is termed the "reference" section. The last section in the "mini-series" is termed the "look-up" section. The number of sections in between the "reference" - "look-up" pair varies depending on the size of the particles being counted; there should be few enough sections so as not to miss any particles present, i.e. no neuronal cell body should be completely contained in the disector and therefore missed completely in counting estimates. The number of "tops" in each disector is counted; a "top" being a neuronal profile that is seen in the reference section but not in the look-up section. The volume of the disector is then calculated (area of the reference section multiplied by the height of the disector). The number of tops in each disector is then divided by the volume of each disector resulting in the average numerical density. As already described, the final estimation of ganglion cell number is obtained by multiplying the numerical density (Nv) by the total volume (Vref).

2.4.4 Neuronal Cell Size

To determine neuronal size (cross sectional area of the largest profile of a neuron), a region of the ganglion in sharp outline, was selected and photographed in serial section on

Ilford black and white 35mm film using an orange filter. All neurons that appeared in the series of micrographs were measured; approximately one hundred neurons were measured from each animal. The neurons were individually numbered on each micrograph and given a number that was used for all profiles of the same neuron. The largest profile of each neuron was identified and the section in which it appeared noted; this profile was then traced in pencil from the original negative, by use of a microfilm reader that projected the image onto drawing paper. Profile areas where measured with a digitising tablet connected to a personal computer. A graphical representation of the frequency and range of cross sectional areas was then produced.

2.5 Histochemistry and Immunohistochemistry

2.5.1 Ganglion Preparation

Pre- and post pubertal, male and female Sprague Dawley rats were used in this part of the work. The animals were terminally anaesthetised and perfused transcardially with 0.1M phosphate buffered saline (PBS- Dulbecco 'A'; tablets from Oxoid, Unipath Ltd. UK) (see above). PBS was infused via an opening in the left ventricle until the solution ran clear from the cut right atrium. After opening the abdominal cavity, the pelvic ganglia from the left side were removed and fixed in 10% neutral buffered formalin for one hour. The ganglia were then washed (3 x 30 minutes) in 0.1M PBS and immersed overnight in 0.1M PBS containing 7% sucrose and 0.1% sodium azide.

2.5.2 Cryosectioning

2.5.2.1 General

First a piece of cork was secured onto a cryostat cutting platform by tissue tec frozen isopentane that had been cooled in liquid nitrogen. A drop of tissue tec was then applied to this cork platform into which the ganglion to be sectioned was placed. The entire platform was again immersed in the cooled isopentane until the tissue tec was seen to be frozen. The platform and specimen were next placed in the chamber of the cryostat and allowed to acclimatise to the ambient chamber temperature (usually about -20°C); if this period of

acclimatisation was not allowed there was a great risk of the specimen fracturing during cutting.

Ganglia were cut at a thickness of 10μm. Resulting cryosections were individually thaw-mounted on coated slides, air dried and stored in a freezer prior to staining.

2.5.2.2 Ganglia for Quantitation

The ganglia used in the quantitative histochemical investigation were trimmed so that pre- and post ganglionic nerves were removed proximal to the ganglion body. These ganglia were then frozen in tissue tec and cryosectioned at 10μm with no topographical orientation known.

2.5.2.3 Ganglia for Topographical Work

The ganglia used in the topographical histochemical investigation retained their pre- and post-ganglionic nerves. The nerves were visualised through a dissecting microscope and spread in unfrozen tissue tec on a slide. This allowed good orientation to be retained as the viscosity of the unfrozen medium supported the ganglia prior to freezing. The ganglia were then frozen in isopentane that had been cooled in liquid nitrogen and sectioned longitudinally at 10μm on a cryostat.

2.5.3 NADPH-diaphorase Histochemistry

2.5.3.1 Staining

Sections were incubated in 0.1M PBS containing 1mg/ml βNADPH-diaphorase (reduced form), 1mg/ml nitroblue tetrazolium and 0.1% triton-X100 (all from Sigma) for between 30-60 minutes in the dark at room temperature. With the aid of a dissecting microscope the reaction was monitored; once adequate staining had been achieved, the sections were rinsed in 0.1M PBS and mounted in Citifluor mountant (City University, London, UK). Sections were viewed and photographed with bright field optics. In control experiments where the enzyme substrate βNADPH was omitted from the incubating medium, no staining product was produced.

2.5.3.2 Quantitative Investigation

Animals

3 male and 3 female adult rats, and 3 male and 3 female pre-pubertal (24 days) rats were used in this experiment. Ganglia from the left side of each of the animals were used. As described above (2.5.2.2) the ganglia were longitudinally cryosectioned with no preservation of orientation.

Sampling

Random sampling of ganglion sections was achieved by a similar method to that employed by Warburton and Santer (1994). A standard sized area (approx. 12,000μm^2) was randomly selected from every 4th cryosection. On approaching the section (while viewing through a Zeiss light microscope) the furthest left side of the section was selected as a reference point and the photographic field immediately to right of this edge was selected and photographed. As no orientation had been maintained while immersing and freezing the ganglia, this method would result in an unbiased selection of an area of section from which positively stained cells could be counted; this would also reduce bias in estimates due to counting in the area of ganglion close to the exit of the genital nerve known to be rich with NADPH-d positive neurons. This method produced a neuronal content per unit area of NADPH-d positive neurons.

2.5.4 Immunocytochemistry

2.5.4.1 Nitric Oxide Synthase Immunoreactivity

NOS expression was examined in frozen sections of pelvic ganglia using specific antisera raised against NOS purified from rat cerebellum (Ferring Diagnostica Ltd, Malmo, Sweden). Nitric oxide synthase immunoreactivity (NOS-I) was employed as a double label to calibrate neuronal NADPH-diaphorase positive cells from the range of histochemical staining intensities observed- histochemical labelling was carried out prior to immunolabelling. Sections were incubated in primary antisera at room temperature overnight (anti-NOS, 1:1000 , diluted in 0.1M PBS containing 0.1% triton-X100 and 0.1% sodium azide, both from Sigma). A biotinylated second layer (donkey anti-rabbit Ig, 1:250, Amersham) followed by streptavidin fluorescein (1:100, Amersham Ltd.) were used to visualise the

binding of the primary anti-sera. Areas of the ganglion demonstrating NOS-I were photographed onto 400 ISO black and white Ilford film in a Zeiss™ light microscope using a tungsten filament fluorescent light source. The negatives were then printed onto Ilford multigrade photographic paper.

2.5.4.2 Vasoactive Intestinal Polypeptide Immunoreactivity

VIP expression was examined in frozen sections of pelvic ganglia using specific antisera raised against VIP (Ferring Diagnostica Ltd, Malmo, Sweden). Sections were incubated in primary antisera at room temperature overnight (anti-VIP, 1:300 , diluted in 0.1M PBS containing 0.1% triton-X100 and 0.1% sodium azide, both from Sigma Ltd, UK.) in a humid chamber. A biotinylated second layer (donkey anti-rabbit Ig, 1:250, Amersham Ltd, UK.) followed by streptavidin fluorescein (1:100, Amersham) were used to visualise the binding of the primary anti-sera. Photography was as described above (section 2.5.4.1).

2.5.4.3 Neuropeptide Y Immunoreactivity

The presence of neuropeptide Y (NPY-I) was examined in frozen sections of pelvic ganglia using specific antisera raised against NPY (Sigma Ltd, UK). Sections were incubated in primary antisera at room temperature overnight (anti-NPY, 1:300, diluted in 0.1M PBS containing 0.1% triton-X100 and 0.1% sodium azide, both from Sigma) in a humid chamber. A biotinylated second layer (donkey anti-rabbit Ig, 1:250, Amersham) followed by streptavidin fluorescein (1:100, Amersham) were used to visualise the binding of the primary anti-sera. Photography was as described above (section 2.5.4.1).

2.5.4.4 Substance P Immunoreactivity

The presence of substance P (SP-I) was examined in frozen sections of pelvic ganglia using specific antisera raised against SP. Sections were incubated in primary antisera at room temperature overnight (anti-SP, 1:300, diluted in 0.1M PBS containing 0.1% triton-X100 and 0.1% sodium azide, both from Sigma) in a humid chamber. A biotinylated second layer followed by streptavidin fluorescein (concentrations as above) were used to visualise the binding of the primary anti-sera. Photography was as described above (section 2.5.4.1).

2.5.4.5 Tyrosine Hydroxylase Immunoreactivity

The presence of tyrosine hydroxylase (TH-I) was examined in frozen sections of pelvic ganglia using specific antisera raised against TH. Sections were incubated in primary

antisera at room temperature overnight (anti-TH, 1:300, diluted in 0.1M PBS containing 0.1% triton-X100 and 0.1% sodium azide, both from Sigma Ltd) in a humid chamber. A biotinylated second layer followed by streptavidin fluorescein (concentrations as above) were used to visualise the binding of the primary anti-sera. Photography was as described above (section 2.5.4.1).

2.5.5 Investigation of Apoptosis

2.5.5.1 Background

Apoptosis is investigated by several different methods and these include the analysis of the genomic DNA by agarose gel electrophoresis and DNA fragmentation assays based on H^3-thymidine and, alternatively, 5-bromo-2'-deoxy-uridine. The methods involve the separation of fragmented, low molecular weight DNA from unfragmented, high molecular weight DNA in a given cell population. Thus these methods do not provide information about the fate of an individual cell in a given cell population or, particularly in tissue sections. Alternatively, individual apoptotic cells may be recognised microscopically because of the characteristic appearance of nuclear chromatin condensation and fragmentation, but this method is subjective and limited to a relatively narrow time window when the morphological changes are at a maximum.

The hallmark of apoptosis is DNA degradation which in early stages is selective to the internucleosomal DNA linker regions. The DNA cleavage may yield double-stranded as well as single-stranded DNA breaks (nicks). Both types of breaks can be detected by labelling the free 3'-OH termini with modified nucleotides (e.g. biotin-dUTP, DIG-dUTP, fluorescein-dUTP) in an enzymatic reaction. The enzyme terminal deoxynucleotidyl transferase (TdT) catalyses the template independent polymerisation of deoxyribonucleotides to the 3'end of single- and double-stranded DNA . This method has been termed TUNEL (TdT-mediated dUTP-X nick end labelling) (Gavrielli et al., 1992).

2.5.5.2 TUNEL Staining

Sections of ganglia were prepared as for histo- and immunohistochemistry (2.5.1) and washed 3 times at 5 minutes each in 0.1M phosphate buffered saline (PBS- Dulbecco 'A'; tablets from Oxoid, Unipath). Next the sections were incubated in the 5 times diluted TdT

buffer (1.0M sodium cacodylate, 0.125M tris/HCl, 1.25mg/ml bovine serum albumin at pH6.6) for 15 minutes at room temperature. Next the enzymatic incubation was carried out for one hour at 37°c in an incubating chamber. The solution comprised 20μl of TdT buffer, 0.2μl terminal deoxynucleotidyl transferase (TdT) (Boehringer, Mannheim Ltd, UK.), 1μl biotin 16 dUTP (Boehringer, Mannheim), 5μl 25mm cobalt chloride and 74μl distilled water. After a subsequent rinse in distilled water and wash in PBS for five minutes the process of visualising of the reaction was undertaken.

This was achieved by use of diaminobenzidine staining that produces a dark brown permanent reaction product. Before this could be produced to satisfactory degree, the positive cytological reaction was amplified by use of avidinandbiotin. Firstly sections were pre-incubated in 10% normal goat serum (NGS) in PBS for 15 minutes. Next sections were incubated in avidin-biotin complex (ABC) kit (Vectorstain, Vector Inc., USA) diluted 1:100 in PBS with 0.1% NGS for 1.5 hours at room temperature. Finally the reaction was visualised with 0.05% diaminobenzidine (DAB Peroxidase Substrate Tablet Set; Sigma) in 0.1% tris buffer for 10-15 minutes, or until a satisfactory depth of stain was produced.

2.6 Surgical Orchidectomy

2.6.1 Operated Animals

Three groups (n=5) of littermate 21 day old male Sprague-Dawley rats were castrated. One group of littermate (n=5) 21 day old male Sprague-Dawley rats was used as a control.

2.6.2 Orchidectomy Procedure

Animals were operated upon with the assistance of staff from Biological Services (UCL). The nose of each animal to be castrated was placed in the anaesthetic gaseous mixture. An initial concentration of 4% halothane was used to induce anaesthesia. The halothane concentration was then reduced to 1.5% and mixed with 1.5% nitrous oxide in order to maintain a deep anaesthesia.

The animals were placed on a heat pad and their pedal reflex was tested by pinching. When seen to be deeply anaesthetised an incision of about 5mm was made along the scrotal midline towards the perineum. Next, a small incision was made in the tunica vaginalis and

pressure exerted onto the animals abdomen by the thumb and forefinger- this pressure caused a testis to be exposed. At a distance of about 1cm from the testis, the vas deferens and testicular artery was clamped tightly. A second clamp was then placed immediately distal to the first clamp. These two clamps were then twisted horizontally about each other until the testis was removed. The remainder of the vas deferens and arterial stump were replaced within the tunica vaginalis and then into the scrotum. The wound was wiped clean and the animals then placed in a warm recovery chamber. Once fully alert, the rats were returned to their cage. The position and size of the wound negated the need for suturing.

2.6.3 Tissue Preparation

Three weeks after castrating, the animals were killed (as described in section 2.1 above) and pelvic ganglia removed. Some animals were perfused with fixative and the ganglia resin embedded (as described in section 2.3 above). Other animals were perfused with phosphate buffered saline and the ganglia processed for cryosectioning (as described in section 3.5 above). In addition, the pelvic viscera (bladder, seminal vesicles, prostate gland and penis) were removed from each animal and weighed on a balance.

CHAPTER 3

RESULTS I: ADULT RATS

3.1 Anatomy of Pelvic Ganglion

Fresh dissections viewed through a dissecting microscope were used to study the pelvic plexus. A crucial enhancement helping identification was a whole-mount generic neuronal staining (acetylcholinesterase). The central element of the plexus in the female rat was a large ganglion (Fig. 1) located on the lateral aspect of the vaginal wall, in its most cranial portion near the uterine cervix. This structure, in accordance with the work of many authors (see Use of Nomenclature) was called the major pelvic ganglion. This ganglion was contained in parametrial tissue, and attached to the vaginal muscle coat; this close proximity to the reproductive organs lead to difficulty in its removal. The ganglion measured approximately 2 x 4 mm and was roughly triangular in shape, the ventral edge of the ganglion being the base of an isosceles triangle. On removal (Fig. 3B) it became apparent that the ganglion was flat and this was further demonstrated by the computer assisted reconstruction from serial sections (Fig. 5). At the dorsal end of the ganglion (the apex of the triangle) a nerve consisting of several trunks entered and this was identified as the pre-ganglionic pelvic nerve. A long slender nerve reached the cranial border of the ganglion identified as the pre-ganglionic hypogastric nerve, a sympathetic nerve issuing from the inferior mesenteric ganglion; a swelling in the hypogastric nerve was observed cranial to and a few millimetres away from the major pelvic ganglion, this termed the hypogastric ganglion. Numerous nerves left the pelvic ganglion from the ventral border and travelled to the pelvic organs; in many of them clusters of neuronal perikarya were in evidence (Fig. 4). A group of between

3 and 4 accessory ganglia (Fig. 4), variable in size, shape and position, were found ventral and cranial to the major ganglion, in proximity of the distal part of the ureter; sometimes these ganglia were amalgamated into 1 or 2 large accessory ganglia.

A prominent nerve from the caudal pole of the ganglion ran caudalwards to the pudendum and was called the genital nerve; from its proximal portion this nerve gave small branches to the rectum, which also received small nerves from the dorsal edge of the ganglion. From the ventrolateral aspect of the ganglion numerous nerves of various sizes ran to the vagina, the larger of which gave smaller branches which formed a plexus in the adventitia. From the ventral edge of the ganglion, nerves ran to the bladder; these numbered about eight, passed ventrally and caudally to the ureter and issued branches from their proximal segments that reached the urethra and cranial part of the vagina. Running from the craniolateral edge of the ganglion were nerves to the accessory ganglia; from the most caudal accessory ganglia emerged nerves that supplied the lateral and dorsal surface of the bladder, while more cranial accessory ganglia terminated at the ureter and in the uterine corpus and the plexus in the mesometrium of the uterine horns. The hypogastric nerve branched before it reached the pelvic ganglion forming the accessory hypogastric nerve which reached the accessory ganglia near the ureters.

In the male, the central element of the pelvic plexus similarly was a large ganglion (Fig. 2) positioned in the investing fascia of the posterior lobe of the prostate gland; the ganglion was hidden by the vas deferens, which was reflected ventrally and medially out of pelvic cavity during dissection, in order to expose it. Viewed from the side, the ganglion was crescent-shaped and measured approximately 2 x 3mm. In accordance with other authors (see Terminology and Nomenclature) this ganglion was called the major pelvic ganglion. The ganglion was easier to remove than in the female and was surrounded by a loose connective fascia (Fig. 3A); it was larger and more rounded than its female counterpart, a feature substantiated in the computer assisted reconstructions (Fig. 6). A multi-trunked nerve entered the ganglion (Fig. 4D & 10) at the dorsal edge and was identified as the pelvic nerve. A long thin nerve entered the ganglion midway along its cranial border, this was identified as the hypogastric nerve. Many nerves left the pelvic ganglion from the ventral border and travelled to the pelvic organs, and, as in the female, many of these contained neuronal

perikarya (Fig. 4B, C). Accompanying the main ganglion were accessory ganglia (Fig. 4E) positioned close to the ureter and vas deferens; these numbering between 2 and 4 were just visible through the dissecting microscope.

The most prominent postganglionic nerve ran from the caudal pole of the ganglion and terminated in the corpus cavernosum and was called the genital nerve. The dorsal convex edge of the ganglion gave rise to small nerves that terminated in the rectum, which also received branches from the proximal portion the genital nerve (Fig. 2). From the ventrolateral aspect of the ganglion (the surface comparable to the concave edge when using the crescent shape analogy) numerous nerves of various sizes ran to the anterior, lateral and posterior lobes of the prostate gland. The bladder received nerves from the most ventral edge of the ganglion; these numbered about eight and ran in front and behind the ureter, while additional branches reached the urethra. The accessory ganglia were connected by nerves running from the cranial edge of the ganglion. From the most caudal accessory ganglia emerged nerves that supplied the lateral and dorsal surface of the bladder, while more cranial accessory ganglia terminated at the ureter and in the seminal vesicles and in a plexus along the vas deferens. The preganglionic hypogastric nerve passed dorsal to the ureter and then separated, before it reached the pelvic ganglion, into two branches, the main and accessory hypogastric nerves; the accessory hypogastric nerve reached the accessory ganglia near the ureters. A ganglion along the main hypogastric nerve was less common in the male than in the female rat.

The major pelvic ganglion in rats of both sexes consisted of several thousand post-ganglionic neurons (Fig. 4A) many of which could be observed in the acetyl cholinesterase whole mount preparations. As already mentioned there were many ganglionic neurons that occurred in small aggregations outside the main ganglion. These ranged from small clusters of between 2-10 neurons or the larger groups termed accessory ganglia (Fig. 4E), that appear to contain in the order of a hundred neurons.

3.2 Histology of Pelvic Ganglion

3.2.1 General Histology

The pelvic ganglia were composed of neurons, connective tissue, small blood vessels and an extensive neuropil with predominantly unmyelinated, but also some myelinated, fibres (Fig. 7, 8 & 9). Almost all of the nerve fibres ran approximately dorsoventrally and were therefore in transverse section with the standard orientation used for cutting. Certain groups of fibres could be followed, in serial sections, for the entire length of the ganglion and were presumably fibres en passant. Ganglion neurons were not confined to the main body of the ganglion, but could also be seen within sections of the emerging nerve trunks (Fig. 23A). The proportion of neuropil varied considerably from one area of the ganglion to another in a manner which did not appear to be consistent in different ganglia. All these features were true of the ganglia in both sexes (Fig. 7, 8 & 9).

3.2.1.1 Capsule

A thin capsule of connective tissue sheathed the entire ganglion and extended into the perineurium of the emerging nerves (Fig. 10). The layers of the capsule consisted of a thin epineurium, a thick perineurium and a delicate endoneurium. The capsule sent connective tissue septa that partially separated groups of neurons within the ganglion, each septum eventually completely enclosing a portion of the ganglion leading into a post-ganglionic nerve (Fig. 9). The capsule was formed from concentric layers of closely united flattened cells assumed to be fibroblast processes; occasionally in the light microscope small swellings in these cell processes were observed and these contained the cells nucleus. Fine, wispy structures at the limit of resolution in the light microscope, interpreted as collagen fibres, interleaved the thicker layers. Despite the contrasting positions of the ganglia in male and female rats there appeared to be little sex-related difference in the structure of the capsules; there was no difference in the extent and thickness of the perineurial capsule (identifiable concentric layers as described), although in the female the extremities of capsule (epineurium) continued further and became diffuse, while in the male the capsule showed a more definite boundary.

3.2.1.2 Principal Neurons

Neuronal profiles from adult specimens were ovoid and smooth surfaced with the occasional large and straight process being observed, these interpreted as the emerging axons; dendritic processes were very rare, this observation concurring with the findings of Tabatabai et al. (1986) where electrophysiological and dye-filling techniques were employed. Many neuronal profiles exhibited a nuclear profile which was pale in appearance and generally centrally positioned; some of the larger neurons were binucleate. All neurons were individually sheathed by a capsule of glial cells. Generally only the nucleus of the associated glial cells were visible in the light microscope (Fig. 9) (with sometimes 2 or 3 associated with a single neuronal profile), although occasionally glial processes forming concentric layers around the neuron were also seen. The thin glial cell processes were in intimate contact with neurons and were difficult to differentiate from the neuronal cell membrane in the light microscope.

Vacuolated neurons were also observed but no accurate counts were performed on these cells. They contained large vacuoles that caused the other cytological components (typical of principal neurons) to be displaced; they were among the larger of the ganglion neurons and were sometimes binucleate (Fig. 11).

3.2.1.3 Cell Packing

Neurons of adult animals of both sexes were spread throughout the ganglion and showed no increased or decreased density either directly beneath the capsule or towards the centre of the ganglion (Fig. 9). Neurons most often appeared in large clusters that varied greatly in size (i.e. the numbers of neurons in the cluster) and each of these groups was surrounded by neuropil. The neurons in the clusters lay close to one another but still showed clear separation; although there was no distinct compartmentalisation in the ganglia of either sex, some of the clusters were grouped together by the dividing septa that extended from the capsule. Other neurons were more isolated and again these were surrounded by neuropil. All the neurons were clearly individual and encapsulated by glial cells but these clusters of neurons were never encapsulated by the same glial sheath.

3.2.1.4 Blood Vessels

An artery and vein, running in a ventro-dorsal direction, were often observed closely associated at the lateral edge of the pelvic ganglion (Fig. 7), although in some preparations this was removed during dissection. The artery supplying the ganglion arises from a branch of the obturator artery, which, in turn is a branch of the internal iliac artery (Greene, 1963). The obturator arterial branch and vein sometimes ran through the ganglion itself (these observations concurring with those of Keast et al., 1989) and this was the only artery vein pair observed in the ganglion. Other vascular profiles, presumably branches from the branch of the obturator artery, were usually individual, ranged greatly in diameter and were distributed throughout the ganglion (Fig. 8 & 9); profiles present in close proximity to the capsule were often observed to enter the ganglion when followed in serial sections. The larger profiles that had thicker walls were interpreted as arterioles while others of similar size but with thinner walls were interpreted as venules; the smallest profiles had the thinnest walls and were interpreted as capillaries. Many of the profiles showed swellings in their lumenal linings which were identified as endothelial cell nuclei. With the plane of sectioning employed (see section 2.3.3) generally the vessel profiles were circular or ovoid, indicating that the overall the passage of the vessels was also in the ventro-dorsal plane; however, longer, ellipsoid and irregularly shaped profiles were present and these were interpreted to result from vascular branching and looping (Fig. 8). The overall vascular appearance in the pelvic ganglia in rats of both sexes was similar to that described in other autonomic ganglia (Baker et al., 1989).

3.2.1.5 S.I.F. Cells and Other Cell Types

Numerous cells smaller than principal neurons were observed throughout the ganglia from rats of both sexes; these cells were also distinguishable due to their granular nuclei and relatively limited cytoplasm. They tended to occur in distinct clusters sometimes in close proximity to a blood vessel, although lone cells were not uncommon (Fig. 9). These cells were identified as small intensely fluorescent (S.I.F.) cells and resembled those described by Kanerva and Teräväinen, (1972) and Dail and co-workers (1975). No actual counts were made on their numbers, although no discernible difference was apparent between ganglia from either sex.

Other non-neuronal cells were seen in both sexes; these were mast cells, fibroblasts, Schwann cells and endothelial cells.

3.2.2 Ganglion Volume and Morphology

The ganglion volume, estimated morphometrically by the Cavalieri method, ranged between 278.6 $x10^6\mu m^3$ - 307.4 $x10^6\mu m^3$ in 3 male rats, with an average of 296 ± 15 $x10^6\mu m^3$ (296 million cubic microns or approximately $0.3mm^3$). In 3 female rats the range was between 161.3 $x10^6\mu m^3$ - 208.0 $x10^6\mu m^3$ with an average of 181± 24 $x10^6\mu m^3$ (181 million cubic microns or approximately $0.18mm^3$); values for male and female animals show a statistically significant difference ($P < 0.002$ with application of Student's t-test see Appendix 5).

Ganglia displayed a marked sex difference in their gross morphology; ganglia from rats of both sexes showed some degree of individual variability (in their fine structure) although the main morphological features were common to all specimens from the same group. Generally, ganglia from both genders were elongated in the ventro-dorsal plane. The three-dimensional shape of the female ganglion (Fig. 5), displayed graphically from the reconstruction of cross sectional areas, was markedly flat, its ventro-dorsal dimension roughly 9 times that of the medio-lateral, and it remained at a similar breadth from its dorsal to cranial extremity. Protrusions were present, the most dorsal of which corresponded to the point of entry of the hypogastric nerve. In contrast, the ganglion in the male rat (Fig. 6) was much rounder than that of the female, its bulbous shape manifested in its widest medio-lateral axis being approximately half the long, ventro-dorsal axis.

3.2.3 Nerve Cell Size

Neuron size (the area of the largest profile of a neuron identified from serial sections at 2μm intervals, see section 2.4.4) was measured in the ganglia of 3 adult male and 3 adult female rats; roughly one hundred neurons were measured in each animal. Neuronal profiles ranged in shape from roughly circular to oval; serial sections revealed that many neuronal perikarya extended in an ellipsoid fashion (long axis) in the ventro-dorsal axis, although due to the orientation of sectioning the profile from the short axis was measured. The largest sectional profile of a neuron almost invariably displayed the nucleus, however, since the

perikaryal border provided an equally sharp outline, the latter was preferred for size measurements. In all ganglia from both sexes the range of nerve cell sizes was wide (Graph. 1 & 2). In general the range of sizes was continuous; although some discontinuities were observed (particularly in the male animals), these gave no indication of sub-classes but appeared to result from individual variations (the profile of a histogram generated from the average of individual values was a smoother Gaussian curve). In male rats the neurons ranged in size from 121μm^2- 1155μm^2 and mean neuronal cell sizes from 3 animals ranged from 489μm^2 -513μm^2 and the average of the means was 501μm^2 ± 13. In female rats neurons ranged in size from 101μm^2 -964μm^2 and mean neuronal cell size from 3 animals ranged between 314μm^2 -346μm^2 and the average of the means was 328μm^2 ± 16. The data reveal some variability between neuron size ranges, but little between mean neuron sizes in ganglia of animals of the same age and sex. Generally, smaller neurons predominated in both sexes, but there was a wider range of neuronal sizes in ganglia of male rats (where the histogram is observed to be skewed to the right) with large neurons that are not present in histograms from female rats. There were larger average values in ganglia of male rats; the mean cross sectional area values for male and female animals showed a statistically significant difference ($P<0.01$ with application of t-test, see Appendix 5).

3.2.4 Neuron Number

3.2.4.1 Full Three-Dimensional Reconstruction

The total number of ganglion neurons identified and counted in serial resin sections (Fig. 8) in ganglia from three adult female rats were 10,332, 7,143 and 6,037. The number of binucleate neurons (Fig. 11) was 123, 178 and 118 respectively i.e. corresponding to 1.5 - 2.5% of the total neuronal population.

3.2.4.2 Disector Estimation

In three adult male and three adult female rats the total number of neurons in the major pelvic ganglion was estimated with the disector method (no estimations were made for the neuronal populations of the accessory ganglia). Numerical density (see section 2.4.3.2), calculated from the total number of 'tops' appearing in all the disector pairs (example in Fig. 12), was multiplied by the ganglion volume calculated by the Cavalieri method (section

2.4.1). For the complete table of disector calculations see *Appendix 1*. The number of neurons in the male pelvic ganglion ranged between 11,951- 13,247 with an average of 12,506 ± 668, while in the mature female the number ranged from 6,031 - 7,540 with an average of 6,845 ± 717. The difference in cell number between the sexes was statistically significant ($P < 0.001$ with application of Student's t-test, see Appendix 5).

3.2.5 Scanning Electron Microscopy

At lowest magnifications, scanning electron microscopy demonstrated the gross anatomy of the pelvic ganglion. The morphology of the ganglion body in conjunction with the pre- and post-ganglionic nerves was observed; the rough outer surface of a epineurium was seen to cover the associated nerves.

The capsule could be seen covering extensive portions of the ganglion (Fig. 13 & 14), while in other areas this structure was incomplete as a result of the enzymatic digestion and physical manipulation employed. In the areas of the ganglia where the outer capsule has been removed the ganglion contents could be observed (Fig. 13 & 14).

Rounded corpuscles were observed that represent neurons surrounded by a layer of glial cells. The surface of these neuron/glial complexes were mostly smooth, although there were lines of discontinuity (Fig. 14) which were interpreted as the boundaries of the separate glial cells' processes associated with each neuron. The neuron/glia associated units were grouped together although were distinct from one another with clear demarcation between them. Connective tissue components (presumably collagen fibrils and fibroblasts) could be seen both in the neuropil within the ganglion and in the partially digested areas of the ganglion capsule.

Blood vessels were observed; these often lay to the exterior of the perineurial capsule, but were also present in the interior of the ganglion. Clusters of smooth surfaced adipose droplets were identified loosely contained within connective tissue at the exterior of the ganglion.

3.3 Cytology of Pelvic Ganglion

3.3.1 Transmission Electron Microscopy

The morphology of pelvic ganglia and constituent neurons from adult animals of both sexes viewed through the electron microscope, had a general appearance similar to that observed in other autonomic ganglia (Elfvin, 1983; Gabella, 1976; Baluk, 1995) and concurred with previous descriptions (Kanerva and Teräväinen, 1972; Dail et al., 1975).

3.3.1.1 Neurons

Principal neurons were easily identified due to their large size and cytoplasm typical of autonomic ganglia (Fig. 15 & 16). The most prominent neuronal feature was the large electron lucent nucleus that contained between one and four dense nucleoli; close to the nuclear membrane other material of weaker density than nucleoli was observed forming smaller, rounded clumps. Rough endoplasmic reticulum was scattered throughout the cytosol and demonstrated cisternae roughly arranged in parallel. Occasional Golgi complexes were identified (Fig. 18A), usually positioned around the nucleus. Free ribosomes and polysomes were widely present. Many small mitochondria were observed and usually showed transverse cristae (Fig. 16 & 17B). Lysosomes were also occasionally seen, as were multivesicular bodies of various shapes and sizes that contained dense material. Structures identified as neurofilaments and microtubules were observed.

Processes were occasionally seen (Fig. 18A) but in general large dendrites were rare, whereas numerous short, intracapsular dendrites were common (Fig. 17B). Synaptic connections were observed between these intracapsular dendrites and presumably preganglionic fibres and nerve endings. Most of these nerve ending contained numerous small agranular vesicles (Fig. 17B) and sometimes larger dense core vesicles were also present; synaptic configurations of this type were interpreted as cholinergic (Gabella, 1976; Gordon-Weeks, 1988).

Vacuolated neurons were observed and contained large vacuoles that caused the other cytological components (typical of principal neurons) to be displaced and comprised of a fine, electron lucent substance. Other non-neuronal cells viewed in the ganglion had large

dark secretory vesicles and were identified as mast cells (Fig. 20B), while other cells located in the connective tissue forming the outer capsule were identified as fibroblasts (Fig. 17A).

3.3.1.2 Satellite Cells

Each neuron was wrapped by satellite cells (Fig. 15 & 16). The most prominent feature of these glial cells was an electron dense nucleus that dominated the limited cell body. The cytoplasm extended thin, laminar processes (often in the order of 1μm) that were very closely apposed and intricately associated with the neuronal surface. The glial wrappings were complete and were often of a concentric configuration, vaguely resembling the rings of an onion (Fig. 15), interleaved with collagen fibrils, all these components forming an encapsulating sheath.

3.3.1.3 Nerve Fibres in Transit

Some areas of the ganglion were dominated by numerous nerve processes (presumably axons) in cross section (Fig. 19), while these were less common in other areas that displayed neuronal perikarya. The fibres generally contained mitochondria, microtubules and neurofilaments. The fibres were of myelinated and unmyelinated type; myelinated fibres were sometimes heavily myelinated while others less so. Myelin being chiefly lipid (and therefore osmophilic) was highly electron-dense and consisted of thin lamellae, which formed a regular pattern of concentric thin and thick lines. Myelinated and unmyelinated fibres were often contained within processes emanating from Schwann cells; these had large, dense nuclei and while they enclosed several unmyelinated fibres at time (Fig. 19), only encapsulated a single myelinated fibre.

3.3.1.4 Collagen

The neuropil that surrounded all neurons contained extensive bundles of electron dense collagen fibrils (Fig. 19 & 20B). These collagen fibres projected in different directions but generally appeared as small round bodies as a result of transverse section. Often artefactual "cracks" were seen in the areas of neuropil produced by shrinkage resulting from the dehydration during embedding. These artefacts were generally found to run in parallel with collagen fibrils at what are paradoxically, structurally weak points.

3.3.1.5 Blood Vessels

The endothelial cells forming the blood vessels could also be viewed in detail (Fig. 18B). Endothelial nuclei were prominent, and were surrounded by a limited cytoplasm extensions of which formed the capillary walls; only unfenestrated capillary walls were observed.

3.3.1.6 S.I.F. Cells

Cells substantially smaller than principal neurons, containing nuclei with electron dense clumps close to the nuclear membrane, were regularly observed in ganglia from rats of both sexes (Fig. 20A). These cells exhibited dense core vesicles that were variable in size and distributed throughout the cytoplasm; these cells were identified as S.I.F. cells. Two types of S.I.F. cell were observed, distinguished by characteristic vesicles; one group had smaller dense core vesicles (approximately 150nm) and were distributed at the periphery of the cytoplasm, while the other group had larger vesicles (approximately 300nm) containing eccentrically positioned osmophilic material and were distributed throughout the cytoplasm (Fig. 20A). S.I.F. cells of both types showed synaptic contact (presumably afferent in nature) on their perikaryal surface. The pre-synaptic swelling sometimes caused grooves in the cell surface but more common was lesser indentation of the soma at the cites of synaptic contact. Numerous small clear vesicles were observed at all terminals of this type. This work did not study S.I.F. cell efferent synaptic contact.

3.4 Cytochemistry

3.4.1 NADPH-d / NOS-Immunoreactivity

Many neurons in the ganglia of both sexes demonstrated an intense blue-purple NADPH-diaphorase staining. The diaphorase stain was present throughout the cytoplasm but not in the cell nucleus. A range of NADPH-diaphorase staining intensities was observed (Fig. 21A, C & 22). Prominent processes emanated from many of the NADPH-diaphorase positive neurons, particularly those that were intensely stained (Fig. 21A).

Subsequent immunostaining for nitric oxide synthase (usually on the same cryosection) revealed an almost total coincidence between NOS immunofluorescence and neurons that were intensely stained for NADPH-diaphorase; a large proportion, but not all, moderately stained neurons were nitric oxide synthase immunoreactive (Fig. 21D). This extensive co-

localisation (Fig. 22) confirms that NADPH-diaphorase is a cofactor of nitric oxide synthase (NOS) (Dawson et al. 1991, Hope et al. 1991, Schmidt et al. 1992) and demonstrates that these neurons are able to synthesise the putative neurotransmitter nitric oxide.

NOS immunofluorescence showed the same cytological distribution as NADPH-diaphorase staining. NOS-immunoreactivity was spread over the cytoplasm and surrounded a dark (non-immunoreactive) nucleus. Axonal processes extended from the positive neuronal perikarya and ran between neighbouring cell bodies; these processes formed coarse NOS-immunoreactive trunks that travelled from the ganglia of both sexes.

3.4.1.1 NADPH-diaphorase Neurons Per Unit Area

The average number of NADPH-diaphorase positive neurons per unit area (approximately 12,000μm^2, randomly selected from every 4th cryosection) of pelvic ganglia in male animals ranged between 30±13 - 38±10 with a group average of 35±5. Average numbers of NADPH-diaphorase positive neurons per unit area in the female animals ranged between 12±3 - 20±4 with a group average of 17±4. ($P< 0.01$ with application of Student's t-test, see Appendix 5).

3.4.1.2 Distribution of NADPH-diaphorase

In the male pelvic ganglion, a large proportion of NADPH-diaphorase positive neurons were located in the dorsal region, close to the exit of the penile nerve (Fig. 23B & 24A) with many actually within this nerve (Fig. 23A); these findings concurred with those of Keast (1992). Other NADPH-diaphorase positive neurons were sparsely spread throughout the rest of the ganglion with some positive neurons in the adjacent accessory ganglia.

In contrast, neuronal somata in the female that stained positive to NADPH-diaphorase were sparsely spread throughout the ganglion as briefly described in work by Papka and co-workers (1995). There was no grouping at the exit of the genital or any other nerve and in general no particular grouping pattern seemed to exist.

3.4.2 Co-localisation of NADPH-diaphorase

3.4.2.1 VIP-Immunoreactivity

In the male pelvic ganglion a population of principal neurons contained immunoreactivity for VIP (Fig. 25D). The immunofluorescence was present throughout the perikaryon (areas

unlabelled corresponded to the cell nucleus). There was a high coincidence between VIP-immunoreactive structures and moderately and intensely dark blue NADPH-diaphorase positive cell bodies and nerve fibres (Fig. 25C), these findings in accord with those of Alm et al. (1995). The most intense NADPH-diaphorase staining was accompanied by a reduced, speckled VIP-immunofluorescence, while moderately NADPH-diaphorase stained perikarya exhibited a stronger fluorescent signal to VIP immunostaining; these observations strongly suggest a masking effect where the heavy formazan product in intensely stained nerve cells obstructs the fluorescent signal. The similar distribution of NOS-immunoreactivity and NADPH-diaphorase staining (see section 3.4.1 above) suggests a co-localisation of VIP and NOS in neuronal perikarya.

3.4.2.2 Tyrosine Hydroxylase

A positive immunohistochemical reaction to tyrosine hydroxylase (TH) was obtained in many neurons in the male pelvic ganglion (Fig. 26B). This stain was present in the neuronal perikarya and appeared more intense close to the cell membrane. TH-immunoreactive neurons were always separate to moderate and intense NADPH-diaphorase positive neurons. Some areas of the ganglion contained numerous TH-immunoreactive cells where there were less NADPH-diaphorase positive neurons, while other areas sparsely populated with TH-immunoreactive perikarya were more abundant with neurons positive to NADPH-diaphorase (Fig. 26A). In regions where the two populations of neurons were close together it was apparent that the TH-immunoreactive neuronal profiles were considerably larger than those positive for NADPH-diaphorase.

3.4.2.3 Neuropeptide Y

Many neurons in the pelvic ganglion from male rats displayed a positive immunocytochemical fluorescence to neuropeptide Y (Fig. 25B). The stain appeared as small clumps of fluorescence that generally was more intense close to the cell nucleus although was present throughout the perikaryon.

Neuronal perikarya that demonstrated moderate and intense NADPH-diaphorase formazan product did not show NPY-immunoreactivity with subsequent antibody exposure (Fig. 25A). Neurons that were NPY-immunoreactive were observed throughout the

ganglion and were less numerous than NADPH-diaphorase positive neurons. Occasionally neurons that appeared weakly stained for NADPH-diaphorase were also positive to NPY.

3.4.2.4 Substance P

Immunofluorescence to substance P was observed in nerve fibres that coursed in most regions of the male ganglion which ran close to the perikarya of many neurons (Fig. 25E) some of which were NADPH-diaphorase positive. Positive Substance P-immunoreactivity was sometimes in the form of fine non-varicose fibres that formed plexi resembling "baskets" that surrounded the neurons, while other reactivity was more varicose in nature and again abutted neuronal perikarya. Substance P-immunoreactivity was not viewed within neuronal perikarya or neuronal nucleus in the pelvic ganglion.

GRAPH 1

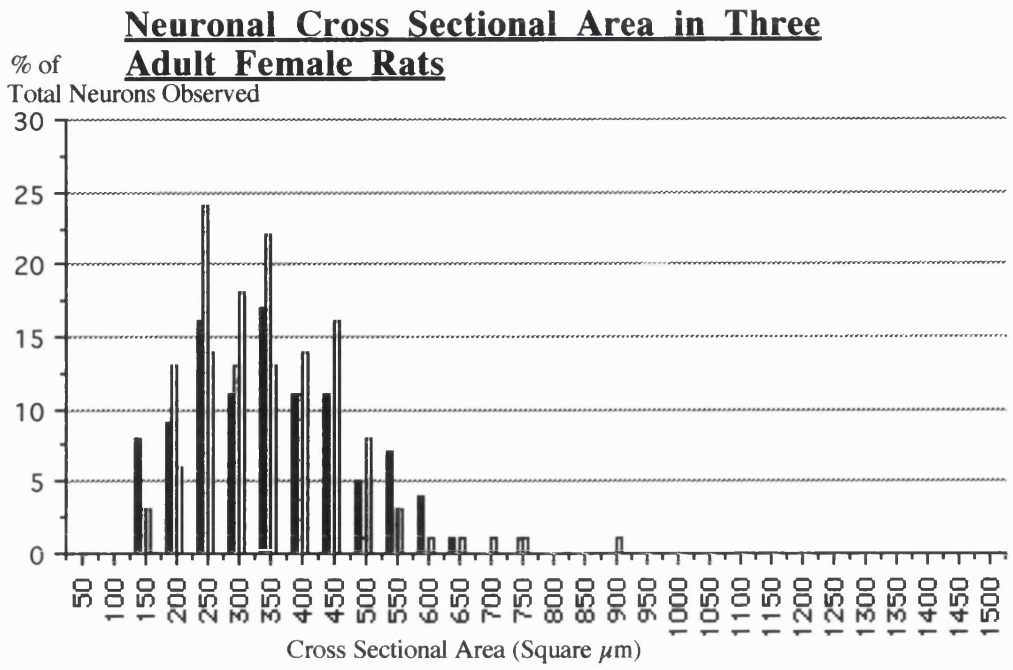

GRAPH 2

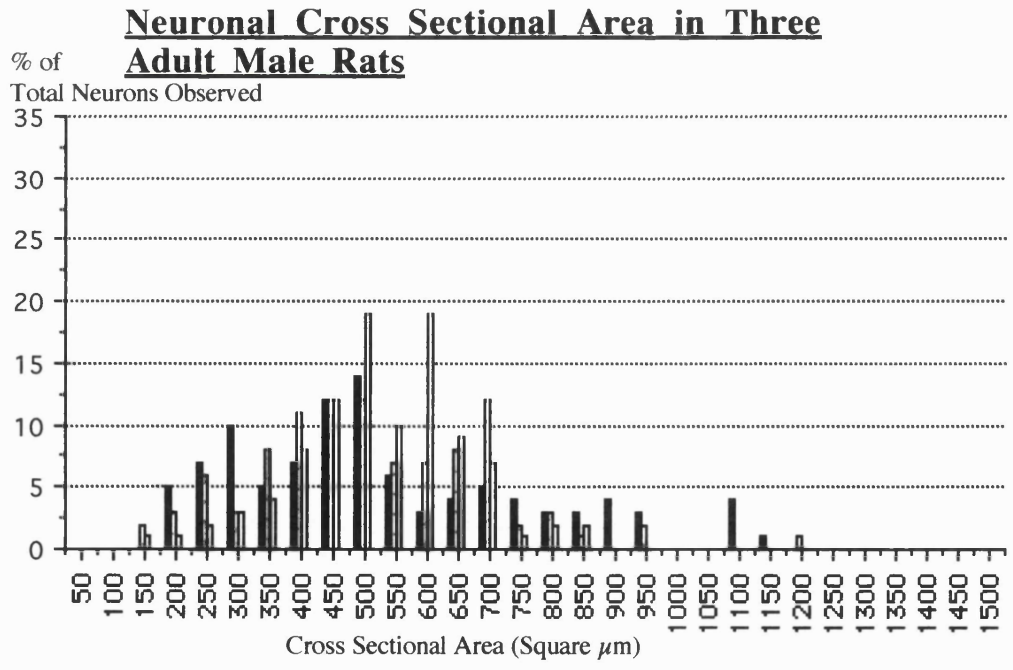

Figure 1

Side view of an acetyl cholinesterase stained preparation (Top) and diagrammatic representation (Bottom) of the left pelvic viscera and pelvic plexus of an adult female rat. In the diagram neural structures have been represented by filled black artwork. For clarity only two small portions of the enteric plexus has been shown.

(Scale Bar = 2.5mm)

ET	Enteric Plexus
GN	Genital Nerve
HN	Hypogastric Nerve
MPG	Major Pelvic Ganglion
PN	Pelvic Nerve
RT	Rectum
UA	Urethra
UR	Ureter
UT	Uterus
VA	Vagina

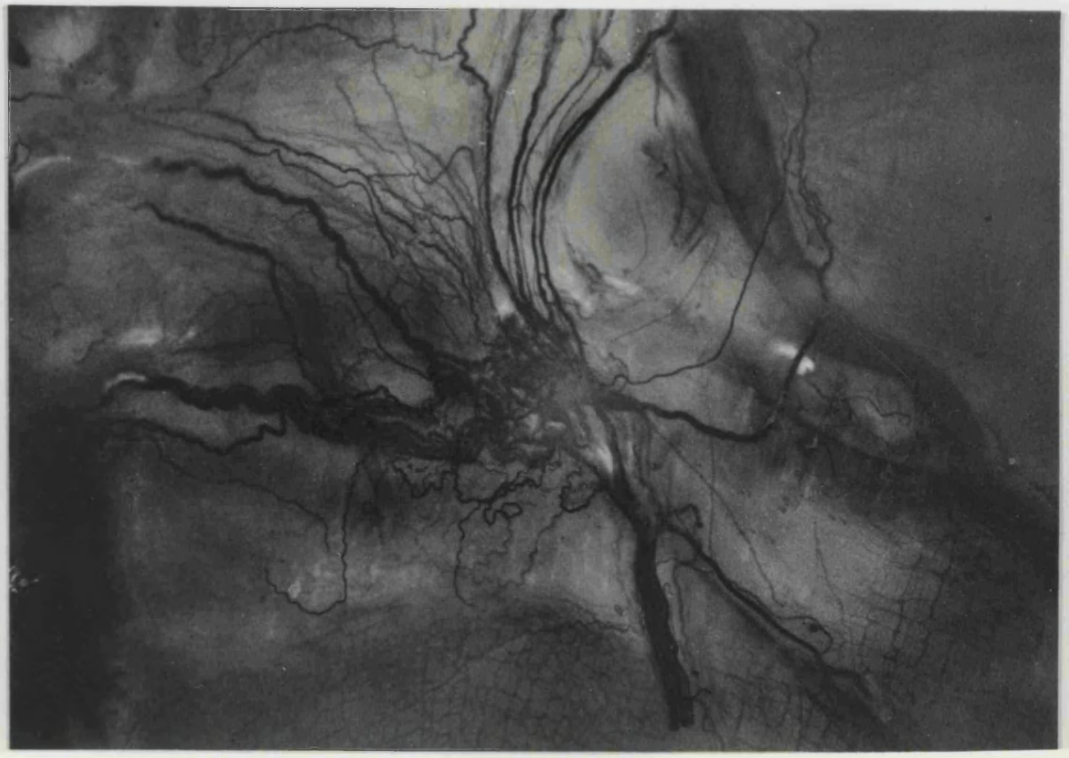

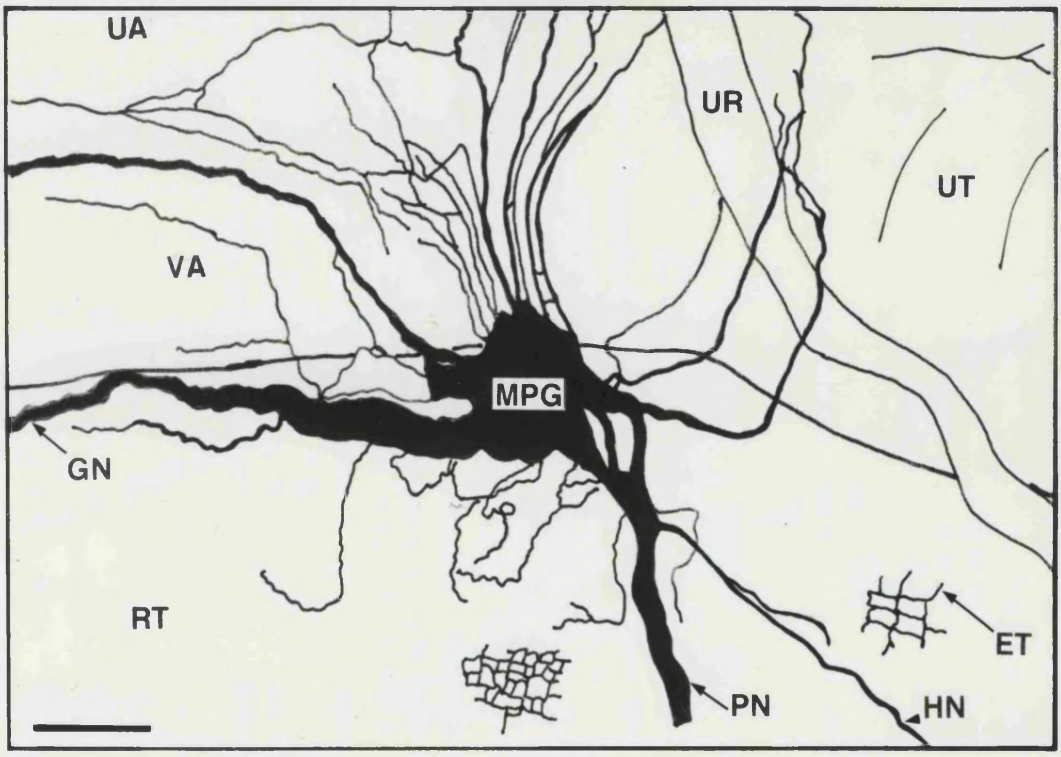
UA
UR
UT
VA
MPG
GN
RT
ET
PN
HN

Figure 2

Side view of an acetyl cholinesterase stained preparation (Top) and diagrammatic representation (Bottom) of the right pelvic viscera and pelvic plexus of an **adult male** rat. In the diagram neural structures have been represented by filled black artwork. For clarity only a small portion of the enteric plexus has been shown.

(Scale Bar = 2.5mm)

AG	Accessory Ganglion
GN	Genital Nerve
ET	Enteric Plexus
HN	Hypogastric Nerve
MPG	Major Pelvic Ganglion
PN	Pelvic Nerve
PR	Prostate Gland
RT	Rectum
SV	Seminal Vesicle
UR	Ureter

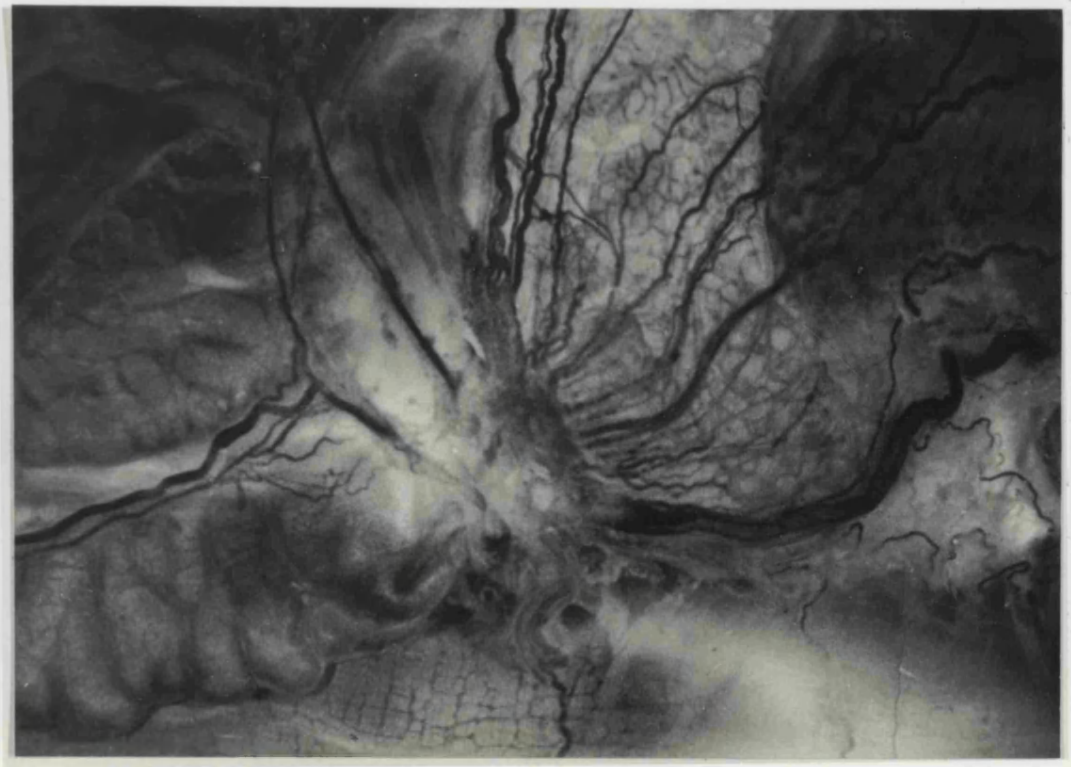

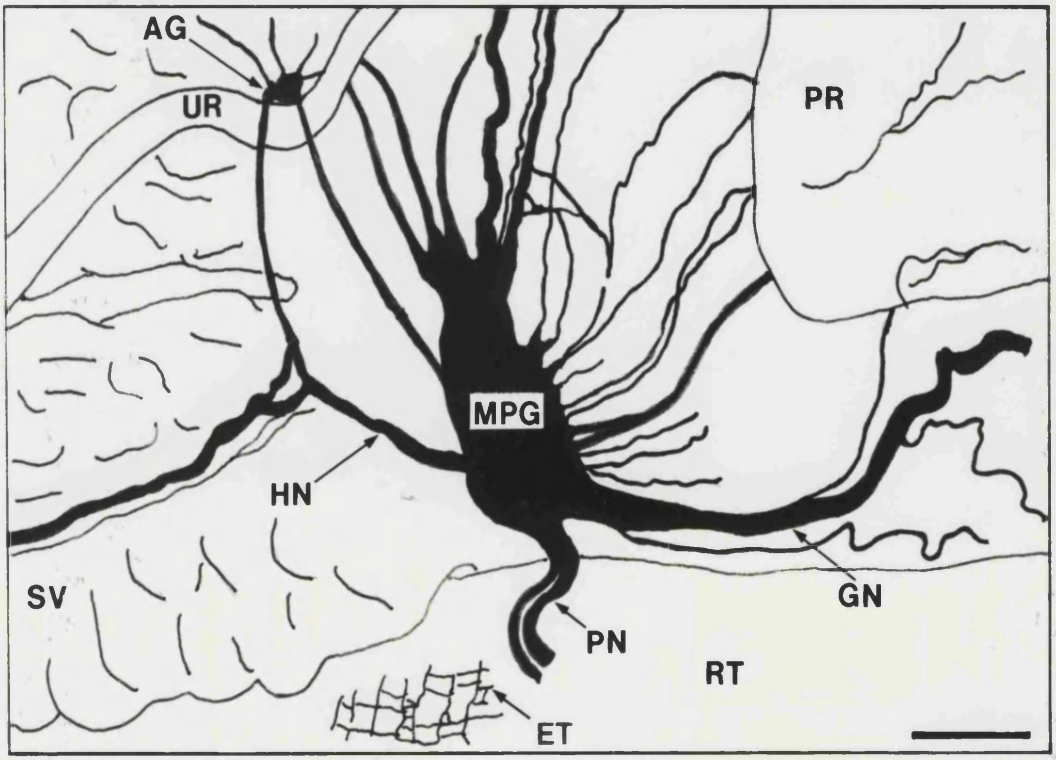
AG
UR
PR
MPG
HN
SV
GN
PN
RT
ET

Figure 3

A) Acetyl cholinesterase stained pelvic ganglion and associated nerves dissected from an **adult male rat** (Fig. 2).

(Scale Bar = 1.25mm applies to both).

B) Acetyl cholinesterase stained pelvic ganglion and associated nerves dissected from an **adult female rat** (Fig. 1).

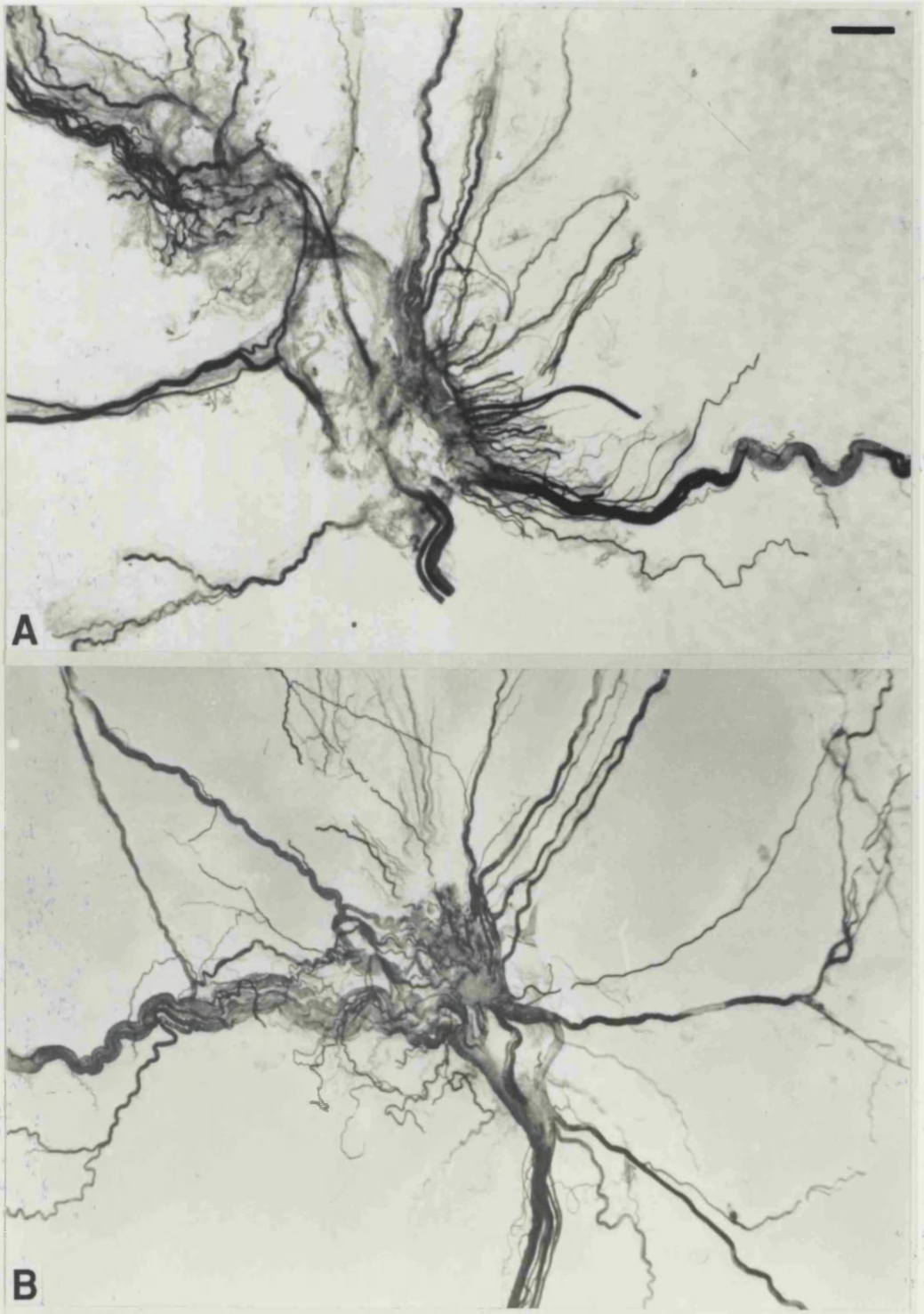
A
B

Figure 4

Anatomical details of a pelvic ganglion from an **adult male** rat stained using acetyl cholinesterase.

A) The surface of the ganglion with stained (dark) and unstained (light) neuronal somata is visible.

B) Small aggregations of ganglion neurons forming mini-accessory ganglia in post- ganglionic nerves supplying the prostate glands.

C) Aggregation of ganglion neurons forming a mini-accessory ganglion in post-ganglionic nerves supplying the bladder.

D) Separate trunks of the pelvic nerve demonstrating constituent nerve fibres.

E) Accessory ganglion in the proximity of the seminal vesicles that exhibits stained and unstained ganglion cells.

F) Ganglion neuronal cell body (arrowed) present in the post-ganglionic nerve that travels via the accessory ganglia.

(Scale Bar = 200μm - applies to all.)

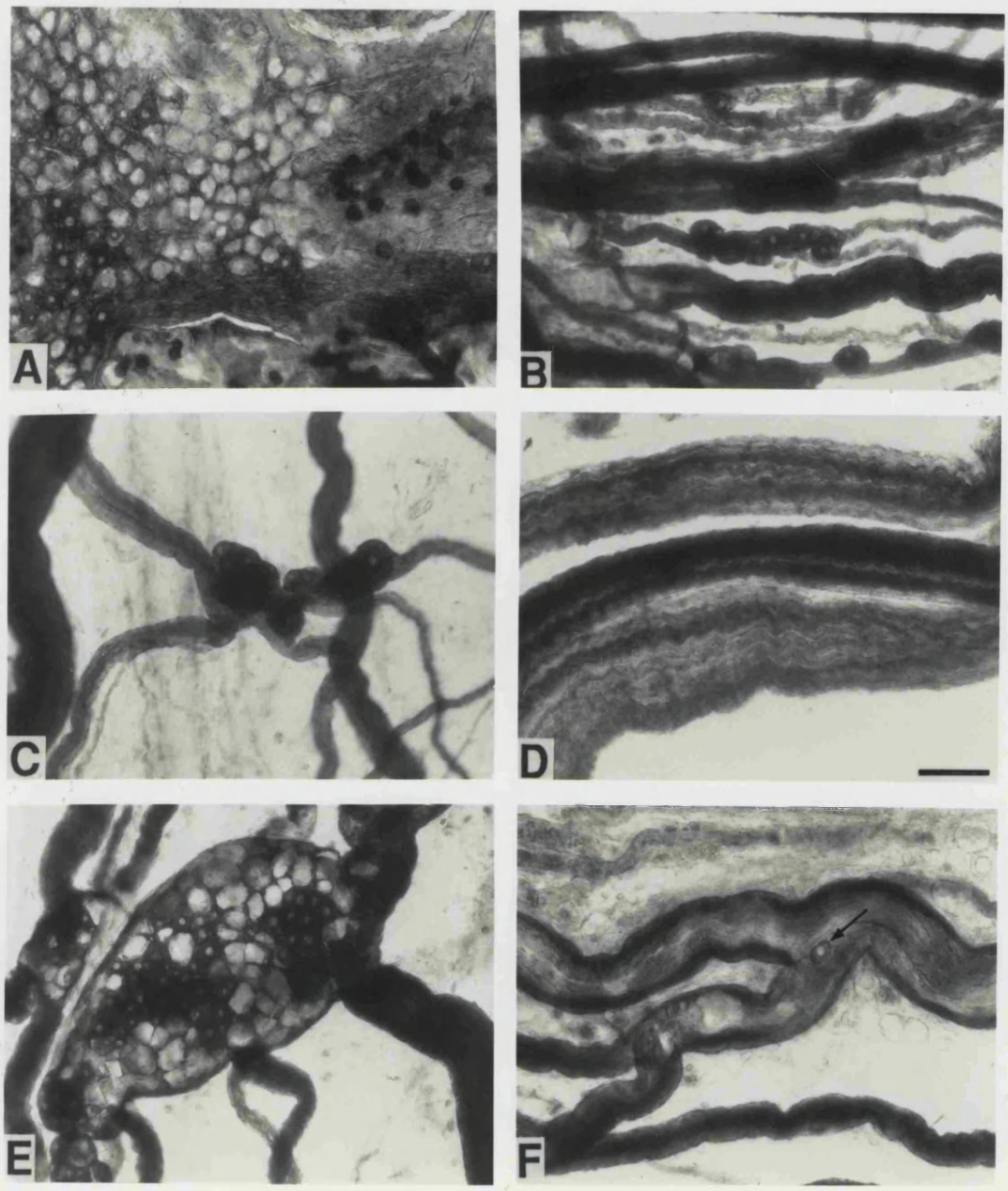
A
B
C
D
E
F

Figure 5

Line drawing representing the three dimensional outline of sections, 100μm apart, from a pelvic ganglion of an **adult female** rat. Note the flat shape of the ganglion demonstrating very little medial depth. Elongations from the dorsocranial edge represent the entrance of the pre-ganglionic hypogastric nerve.

(Axis bars: **V**, ventral; **M**, medial; **Cr**, cranial; **D**, dorsal; **L**, lateral; **Ca**, caudal).

(Scale Bar = 250μm)

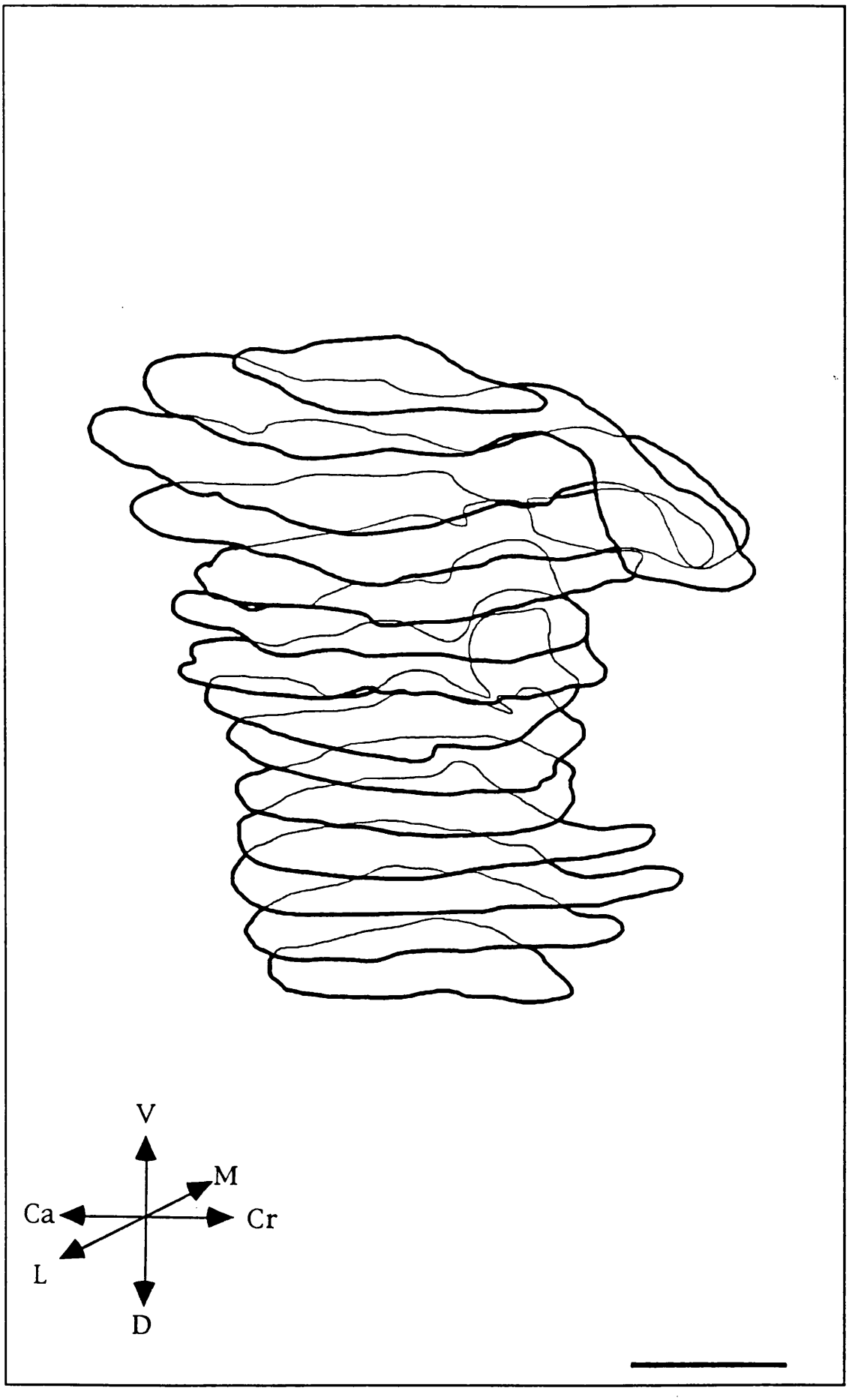
V
M
Ca
Cr
L
D

Figure 6

Line drawing representing the three dimensional outline of sections, 100μm apart, from a pelvic ganglion of an **adult male** rat. Note the marked barrel shape of the ganglion demonstrating extensive medial depth.

(Axis bars: **V**, ventral; **M**, medial; **Cr**, cranial; **D**, dorsal; **L**, lateral; **Ca**, caudal).

(Scale Bar = 250μm)

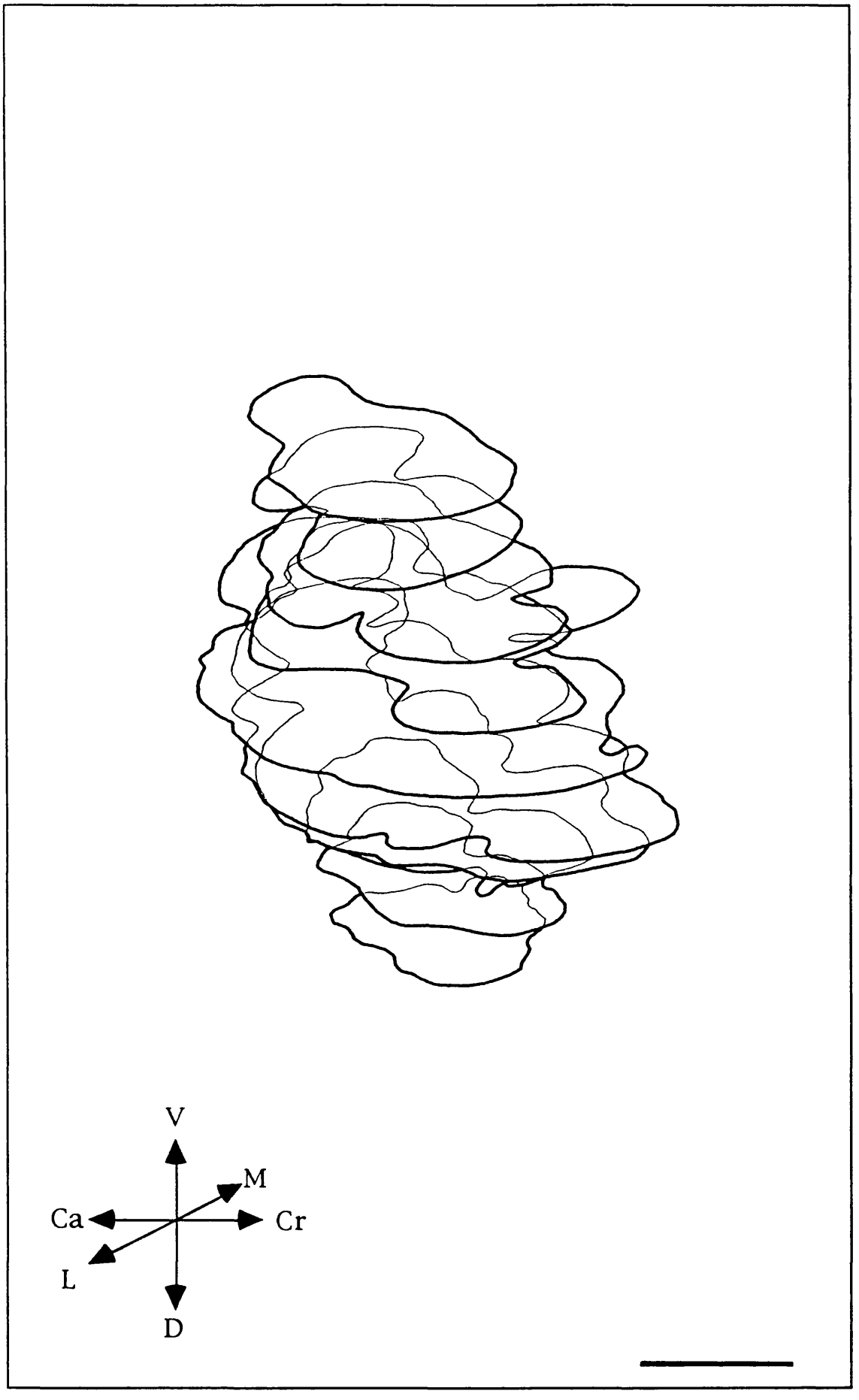
V
M
Ca
Cr
L
D

Figure 7

Light micrographs of major pelvic ganglia from adult rats.

A) Male. The ganglion is completely covered by an outer capsule (arrowhead) and has a large blood vessel (asterisk) passing through. The many neurons within the ganglion are evident.

B) Female. The ganglion is completely covered by an outer capsule (arrowhead) within the boundaries of which the many neurons are observed. (Scale Bar = 100μm applies to both).

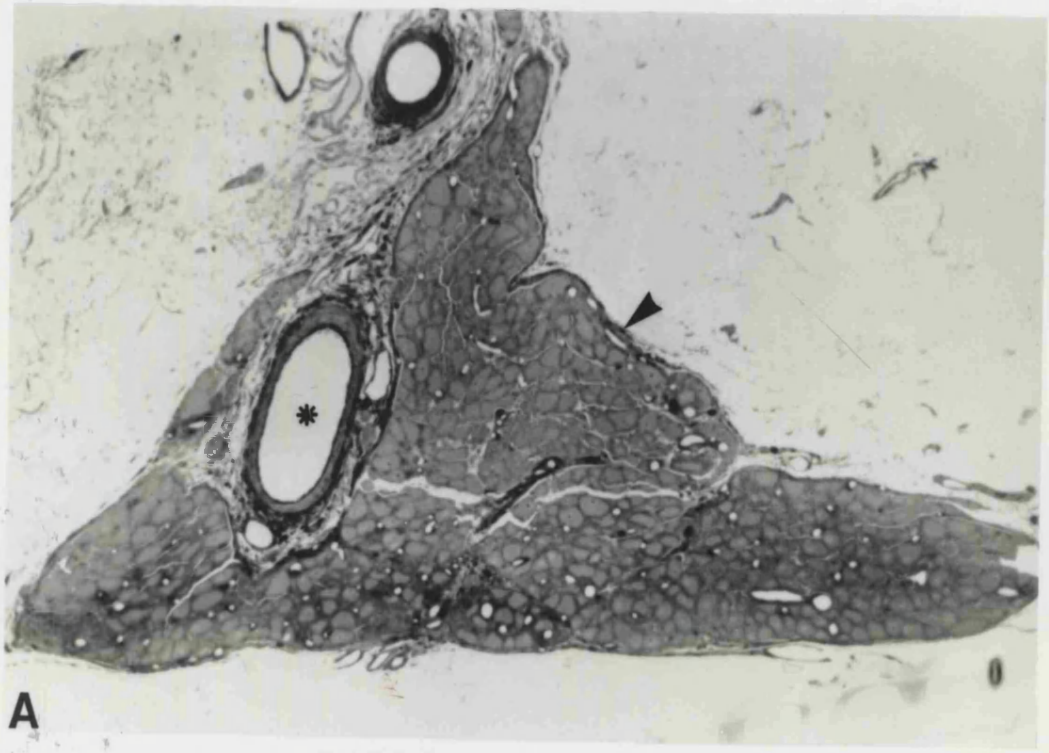
A


B

Figure 8

A series of 3 sections (**A-C**) of a pelvic ganglion from an adult female rat, each section being 1μm thick and 4μm apart .

The capsule (**c**) is clearly visible around the entire ganglion. Numerous distended blood vessels (**v**) are seen both fully within and at the periphery of the ganglion. Binucleate neurons (**b**) are observed, as are processes (**p**) in longitudinal section leaving certain neurons. Extensive areas occupied by nerve fibres (possibly axons, some of which are myelinated) en passage (**a**) in cross section can also be seen.

(Scale Bar = 50μm)

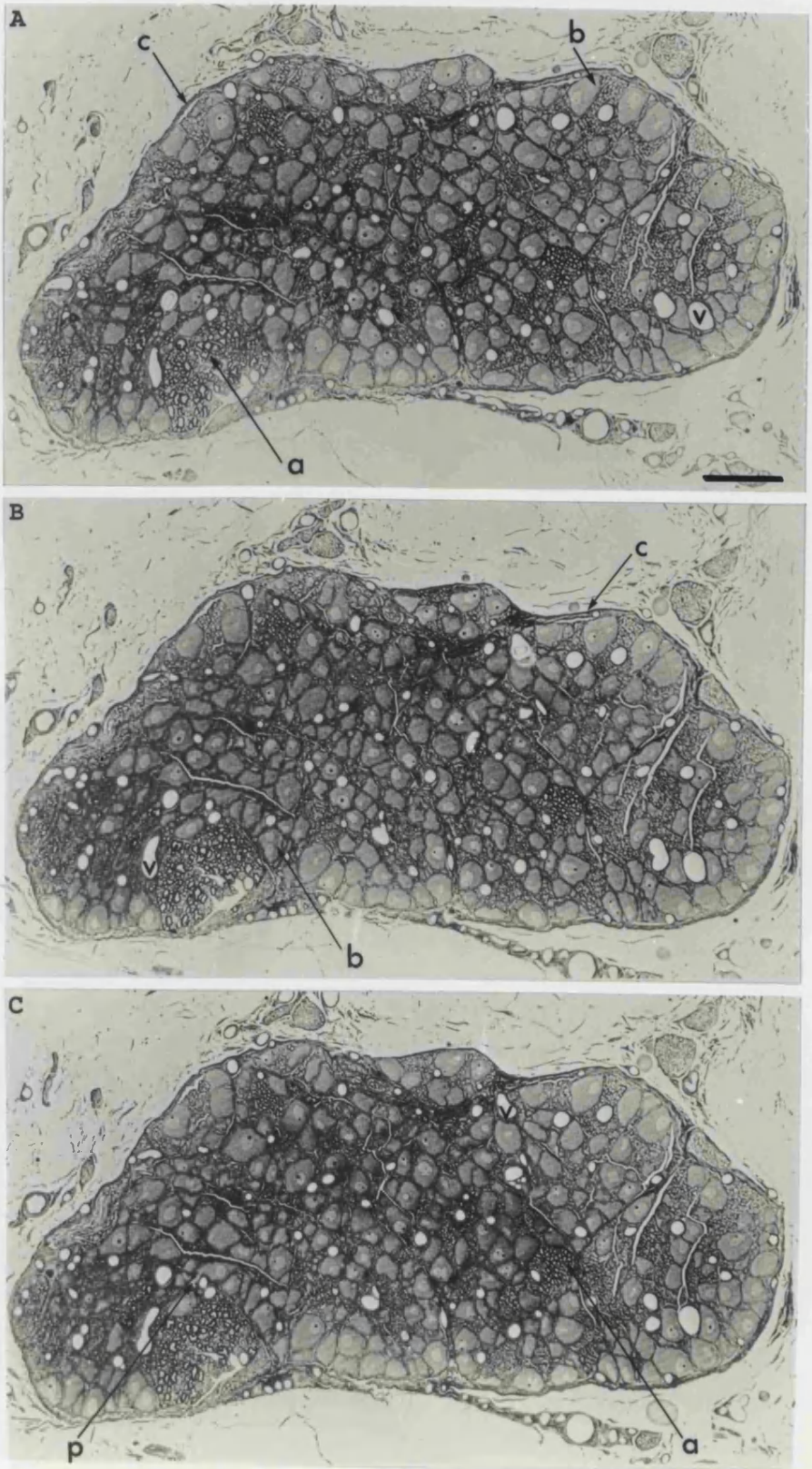
A
c
b
v
a
B
c
v
b
C
v
p
a

Figure 9

Light micrographs of major pelvic ganglia from adult rats. Artefactual cracking (produced possibly during tissue dehydration) is observed at points throughout both ganglia.

A) Male. The various cell types in the ganglion: **f**, fibroblast; **g**, nucleus of satellite glial cell; **n**, ganglion neurons many of which display pale nuclear profiles; **p**, pericyte. Blood vessels (**bv**) in cross section are apparent, as are septa (arrowhead) that divide groups of ganglion neurons.

B) Female. The various cell types in the ganglion: **e**, endothelial cell **f**, fibroblast; **g**, nucleus of satellite glial cell; **n**, ganglion neurons many of which display pale nuclear profiles; **p**, pericyte; **s**, nucleus of small intensely fluorescent (SIF) cells. Blood vessels (**bv**) and myelinated fibres (**m**) in cross section are apparent. The outer capsule (two small arrowheads) is observed to continue into septa (arrowhead) that divide the ganglion neurons.

(Scale Bar = 20μm applies to both).

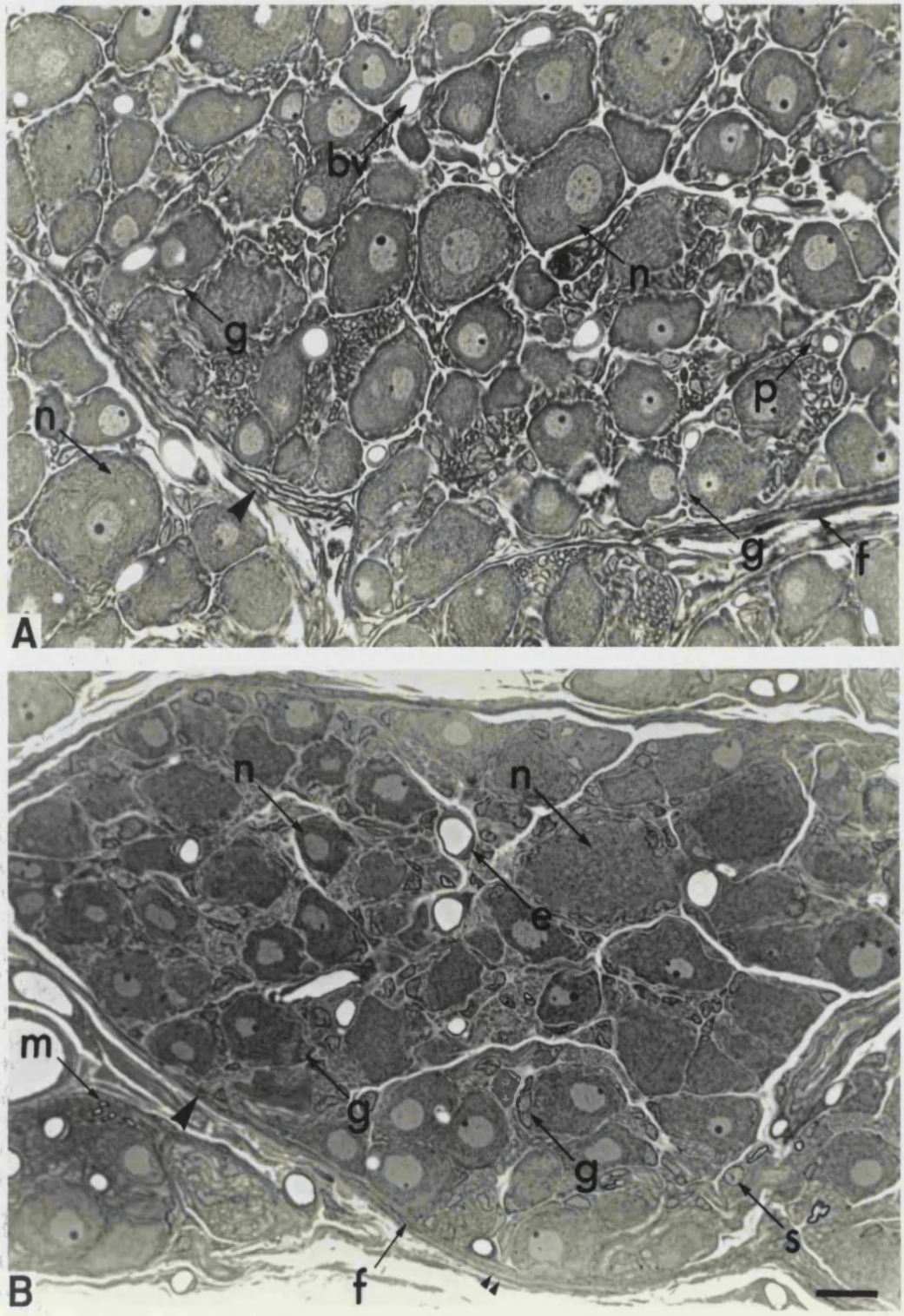
bv
n
g
n
p
g
f
A
n
n
e
m
g
g
s
f
B

Figure 10

Light micrographs of sections of the pelvic nerve from an adult male rat.

A) Portion Distal to Pelvic Ganglion. Five fascicles are observed packed full of nerves fibres mainly in cross section. Large myelinated fibres can be seen (arrow). A thick epineurium (arrowhead) completely surrounds the separate fascicles and blood vessels; some larger blood vessels (asterisk) continue in the core of the fascicles.

B) Portion Proximal to Pelvic Ganglion. Five fascicles (observed in **A**) packed full of nerves fibres mainly in cross section; large myelinated fibres can be seen (arrow). Close to the ganglion the fascicles are less closely associated to one another. A thick epineurium (arrowhead) completely surrounds the separate fascicles and a perineurium surrounds individual fascicles, some of which contain large blood vessels (asterisk, as in **A**). (Scale Bar = 12.5μm applies to both).

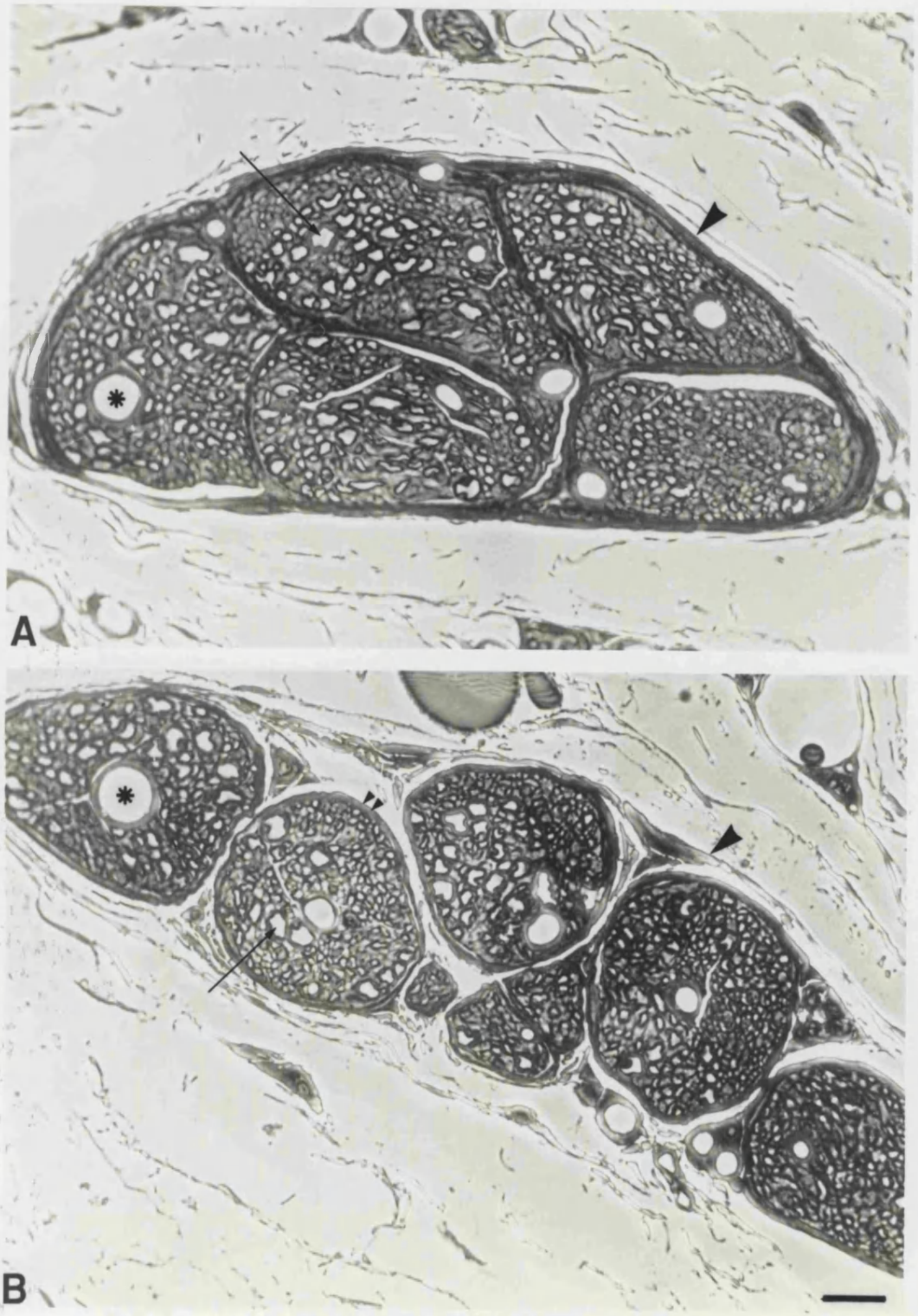
A
B

Figure 11

A series of 12 light micrographs showing a binucleate vacuolated neuron . The sections are 1μm thick and 8μm apart. Profiles of one of the nuclei appear in micrographs **D** and **E** while profiles of the second nucleus appear in micrographs **H** and **I**. The nucleus of an ensheathing satellite cell is visible in micrograph **I**. Granular bodies are seen in some of the vacuoles (**b**) of micrograph **B**.

(Scale Bar in **L** = 20μm and applies to all)

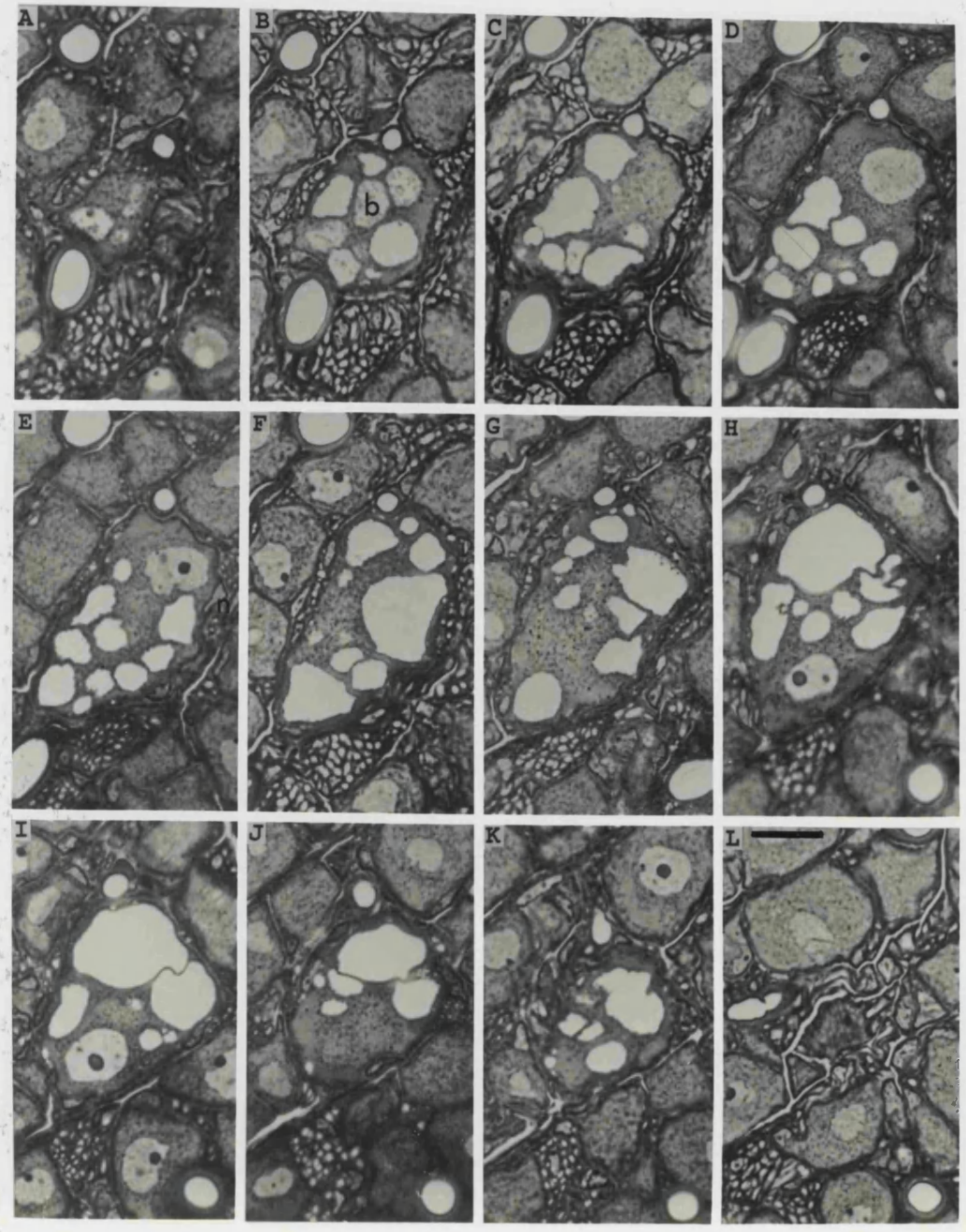
A
B
b
C
D
E
n
F
G
H
I
J
K
L

Figure 12

Light micrographs of an area of two serial sections of a pelvic ganglion from an adult female rat. The sections are separated by 6μm and represent a disector pair.

A) 'Reference' Section. Neuronal profiles observed in **A** that are not observed in **B** are disector 'tops' (asterisks); 5 such profiles are evident. Neuronal profiles (arrowheads) are not 'tops' as profiles are still evident in **B**.

B) 'Look-Up' Section. Neuronal profiles marked with asterisks in **A** are not visible in this section. Neuronal profiles (arrowed) are profiles of the same neurons marked with arrowheads in **A**.
(Scale Bar = 20μm applies to both).

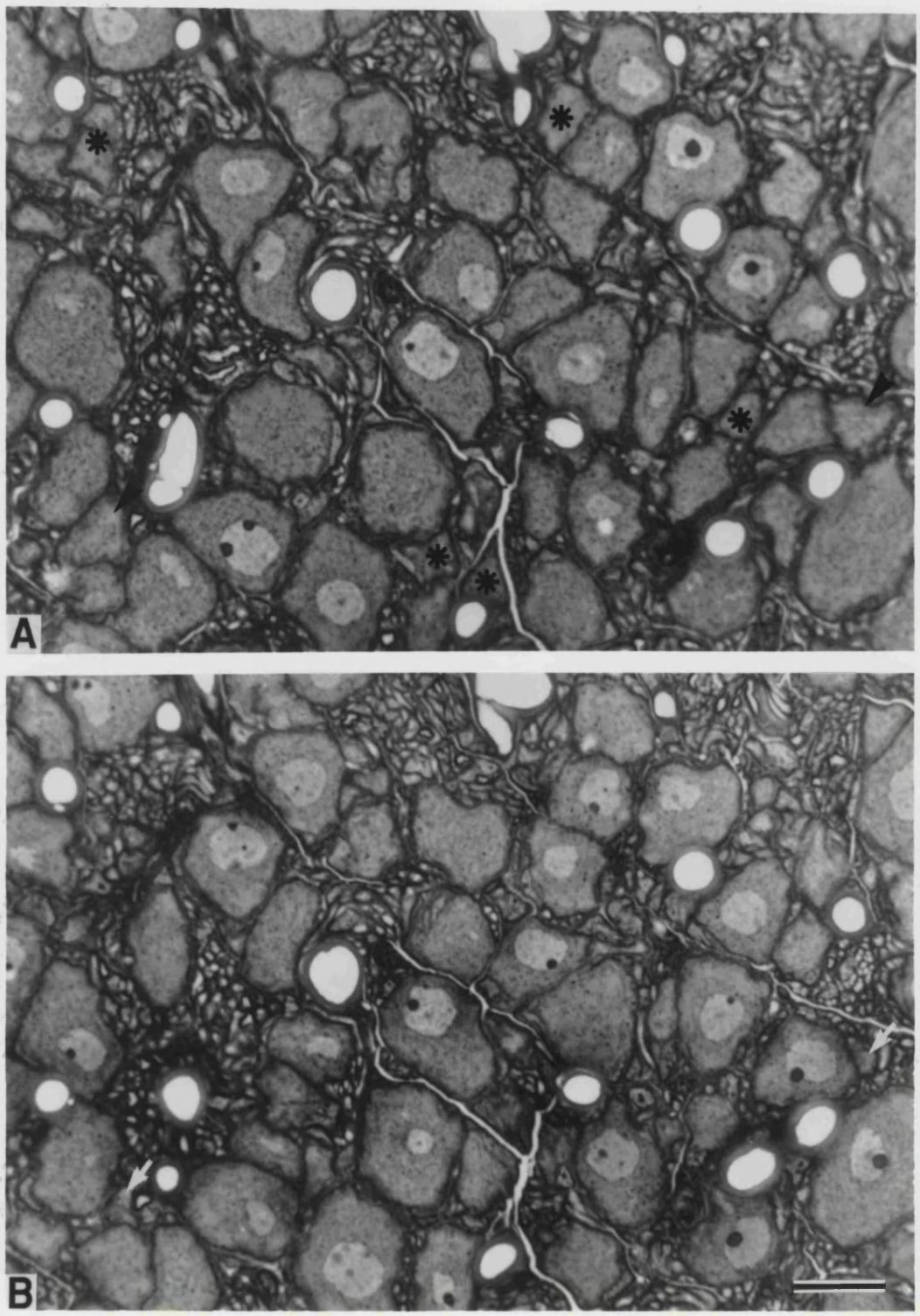
A
B

Figure 13

Scanning electron micrograph of pelvic ganglion from an adult female rat.

A) Note the layered appearance of a portion capsule (**C**), remaining despite enzymatic digestion. Neurons (**n**) are present, although, more precisely, the surface being viewed is more likely to be the cell membrane of the encapsulating glial cells.
(Scale Bar = 10μm).

B) The inside of pelvic ganglion exposed by enzymatic digestion. Note the prominent neuron/glial units (three of which are labelled with **n**) which show clear separation from one another. From the uppermost labelled neuron emerges what appears to be a neuronal process (white arrow), possibly an axon. Between the neurons, and spread across their surfaces is an abundance of collagen fibres (black arrows).
(Scale Bar = 10μm).

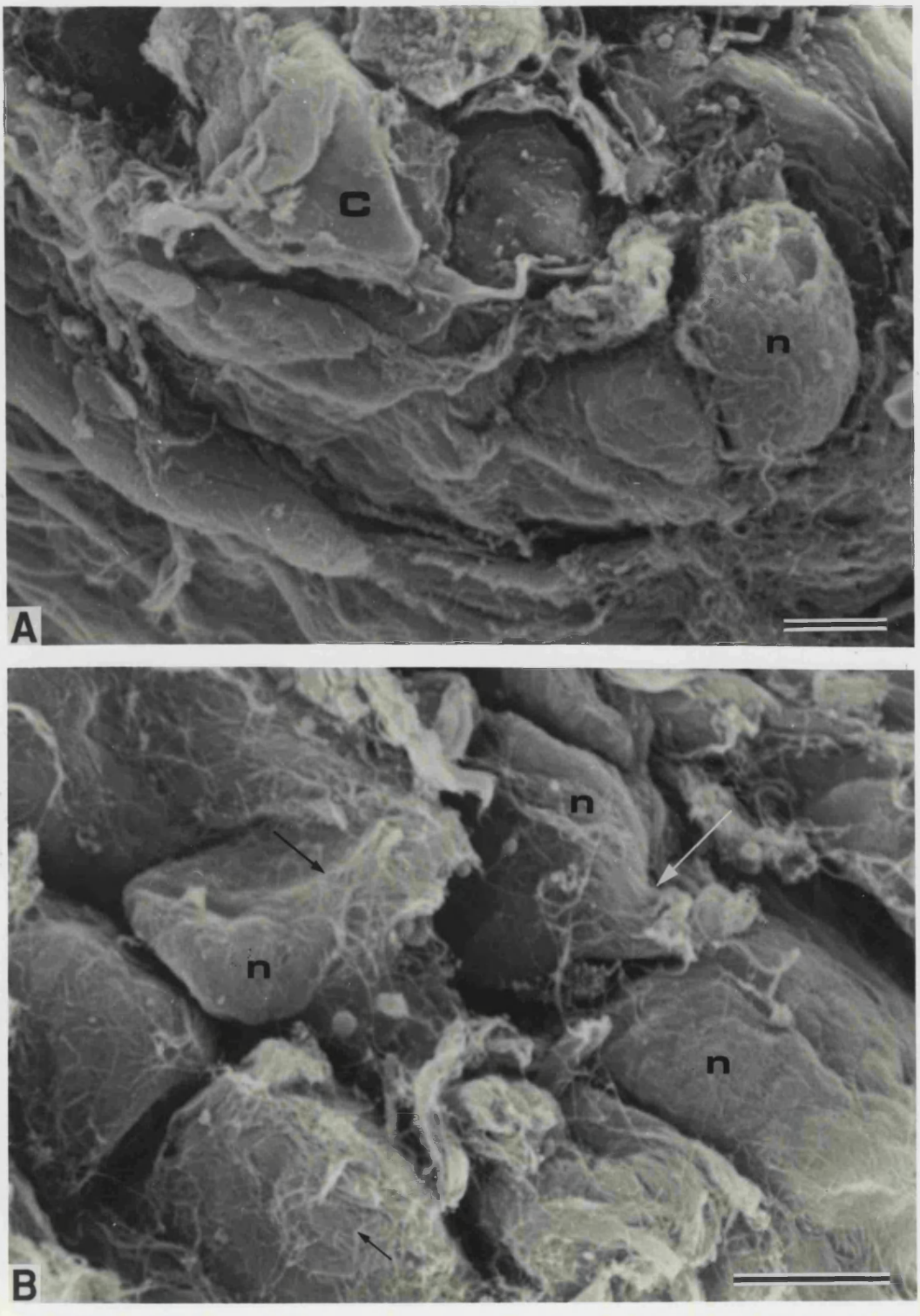
C
n
A
n
n
n
B

Figure 14

Scanning electron micrograph of pelvic ganglion from an adult female rat.

A) A portion of the ganglion with partially removed capsule (**C**); the capsule appears to be removed to differing degrees, demonstrating a composition of several layers. To the right of the micrograph a sizeable post-ganglionic (white arrow) nerve emerges from the ganglion and is accompanied by a smaller nerve (arrowhead); the perineurium (**p**), formed from a continuation of the ganglion's capsule, covers the two nerves. The area boxed is shown in **B** below.
(Scale Bar = 50μm).

B) The area boxed in A (above) exposed by enzymatic digestion. Three neurons (**n**) are present; the actual surface viewed is the surface of the encapsulating glial cells, of which the borders of the overlapping processes are apparent (small white arrow).
(Scale Bar = 5μm).

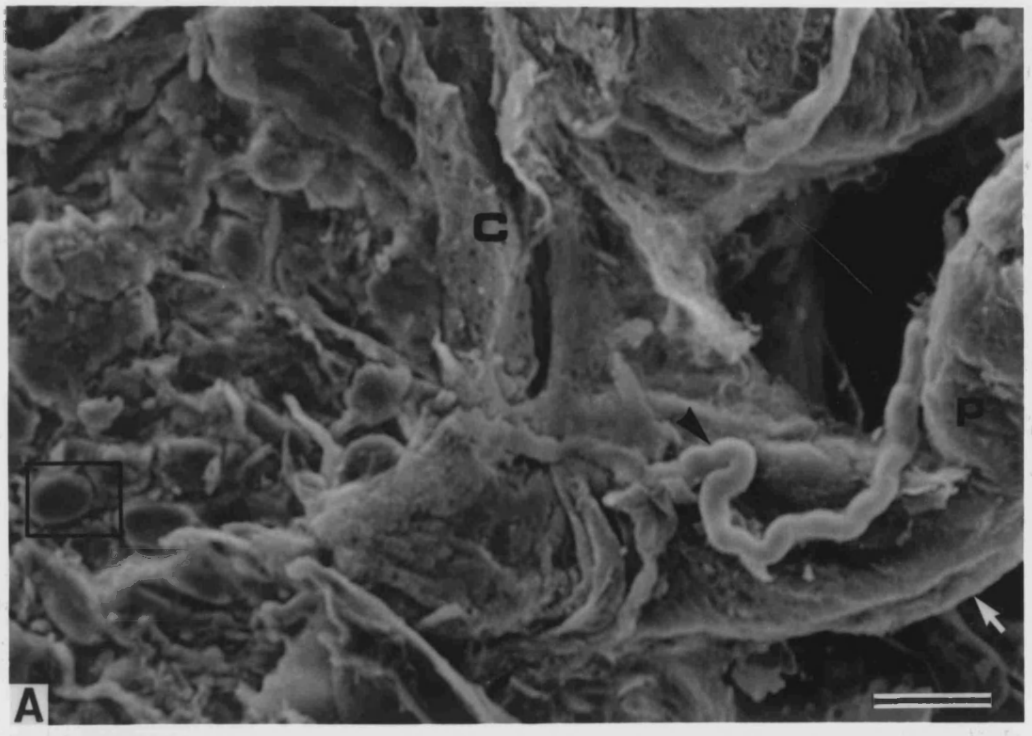
C
P
A

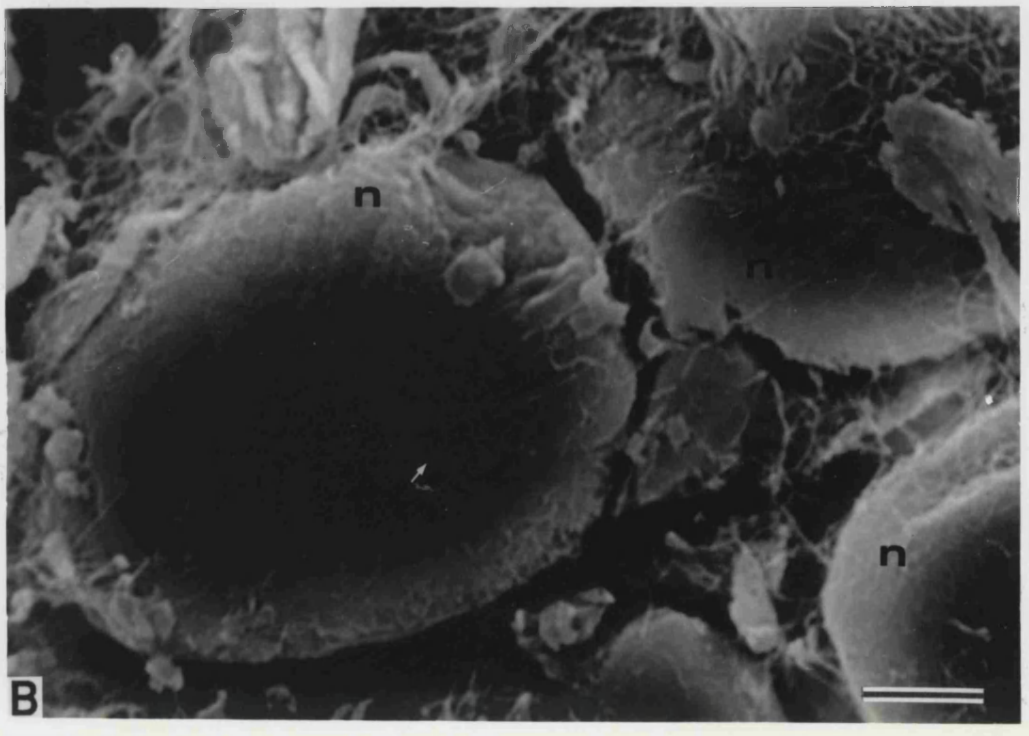
n
n
n
B

Figure 15

Electron micrograph from the pelvic ganglion of an adult female rat showing a neuron and associated satellite glial cell. The neuron shows a prominent pale nucleus (**n**). The neuronal perikaryon (**p**) is surrounded by many layers (arrowed) of glial cell processes, some of which presumably extend from the associated glial cell that exhibits a dense nucleus (**gn**). Midway up the left-hand edge of the micrograph is a part of a blood vessel (**v**) and bundles of collagen fibrils (**c**), mainly in transverse section are evident throughout the neuropil and between the glial laminar processes.
(Scale Bar = 2μm).

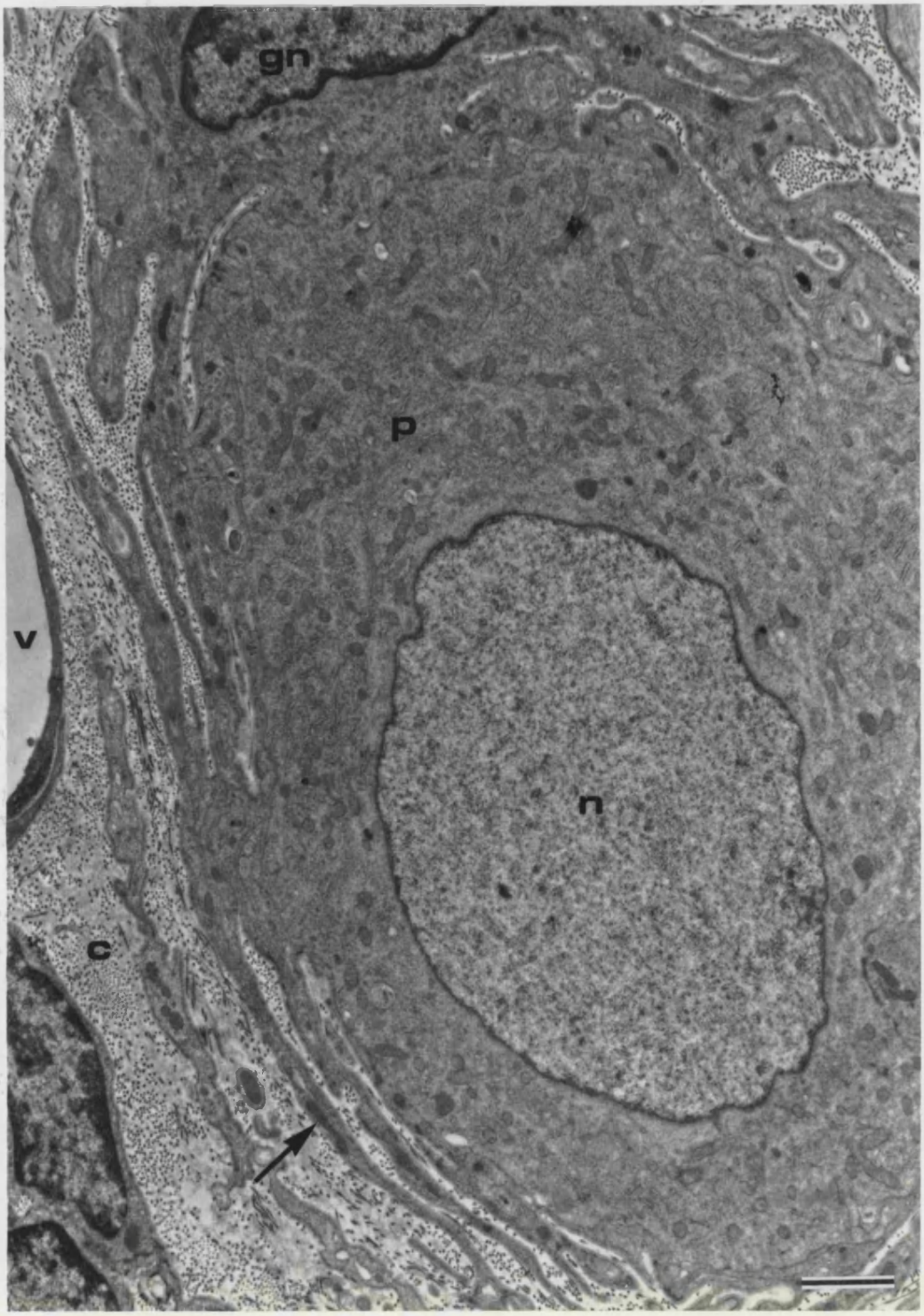
gn
p
v
n
c

Figure 16

Electron micrograph from the pelvic ganglion of an adult male rat showing a neuron and associated satellite glial cell. The neuron shows a prominent pale nucleus (**n**) and a dark nucleolus (white arrowhead). Particularly abundant in the neuronal perikaryon are mitochondria (white arrow). Closely apposed to the neuron is a satellite cell that demonstrates a dense nucleus (**gn**) and the beginning of a thin, encapsulating process (black arrow).
(Scale Bar = 1μm).

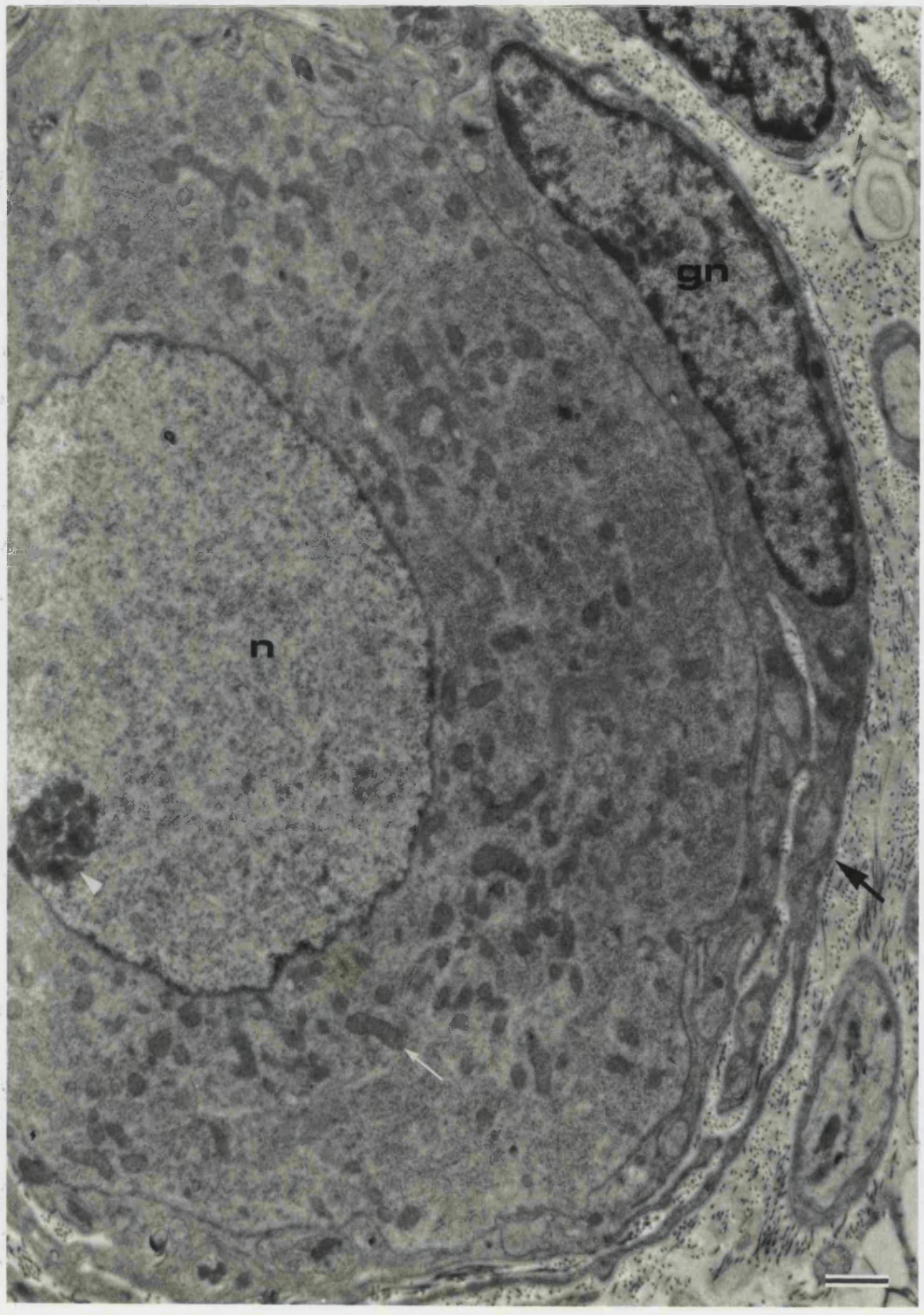
gn
n

Figure 17

A) Electron micrograph a portion of the outer capsule of a pelvic ganglion from an adult male rat. The capsule is comprised of long thin fibroblast processes (arrowed) with intervening collagen fibrils (**c**) (seen here cut in both transverse and longitudinal planes). A fibroblast perikaryon, elongated in shape and exhibiting a dense nucleus (**fn**) is also present. To the left of the micrograph is an area of neuronal perikaryon (**p**) and its thin glial wrapping. (Scale Bar = 1μm).

B) Electron micrograph of a pelvic ganglion of an adult male rat. A portion of a neuronal perikaryon (**p**) is visible and contains many mitochondria (white arrow). The perikaryon shows a intracapsular dendrite (**d**), which is in synaptic contact (black arrow) with a varicose pre-ganglionic fibre. Note that the varicosity is packed with electron lucent synaptic vesicles (arrowhead).
(Scale Bar = 1μm).

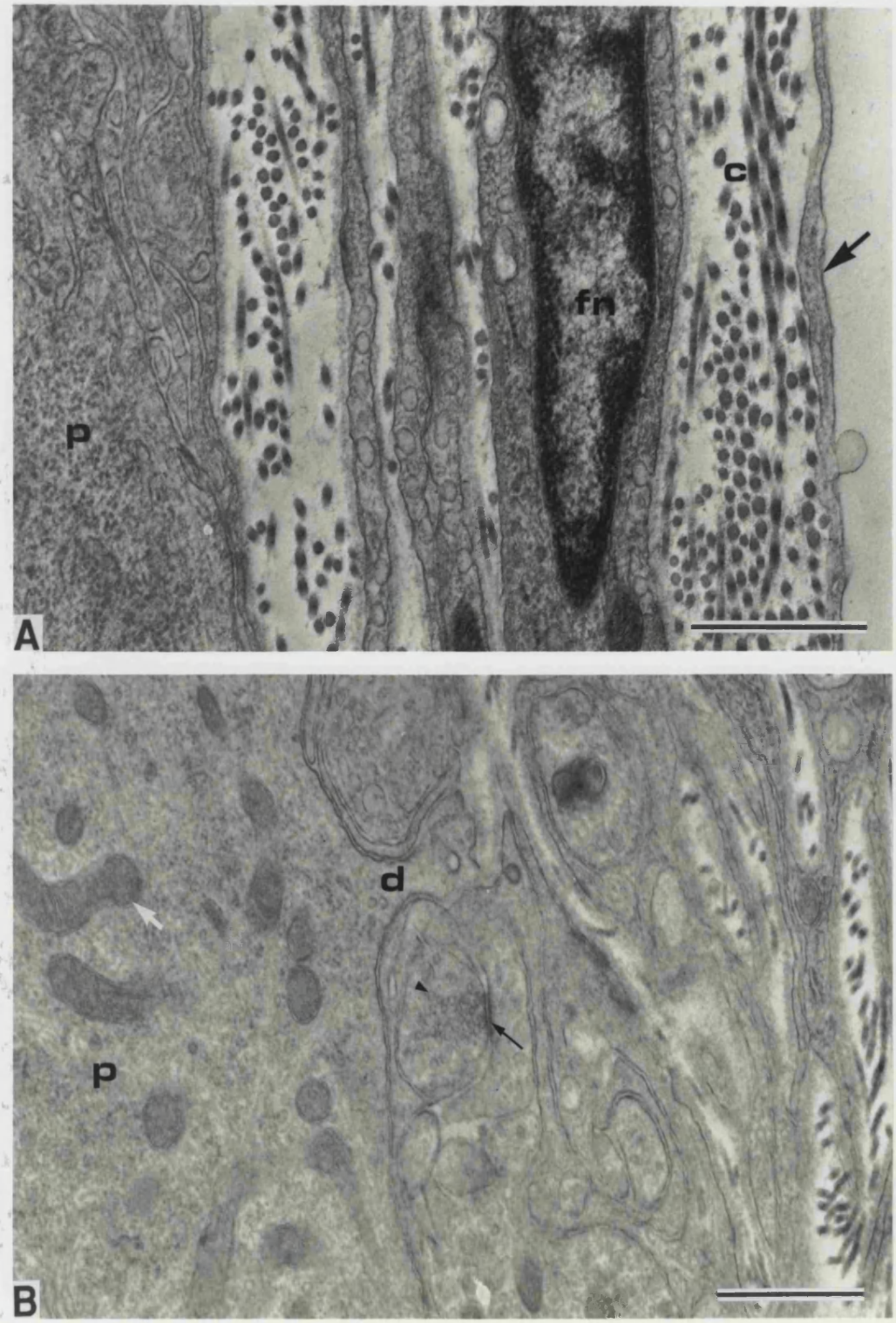
c
fn
p
A
d
p
B

Figure 18

A) Electron micrograph of a pelvic ganglion from an adult female rat. To the bottom right of the figure is a neuronal perikaryon (**p**) amongst the organelles of which can be seen Golgi apparatus (arrowhead). Emanating from this neuronal somata is a process (**pr**), possibly a rare dendrite, that contains many of the same cytoplasmic structures.
(Scale Bar = 1μm).

B) Electron micrograph of a blood vessel (**bv**) in transverse section present in the pelvic ganglion of an adult female rat. An endothelial cell (arrowed) that forms the blood vessel is observed, dominated by its dense nucleus (arrowhead).
(Scale Bar = 1μm).

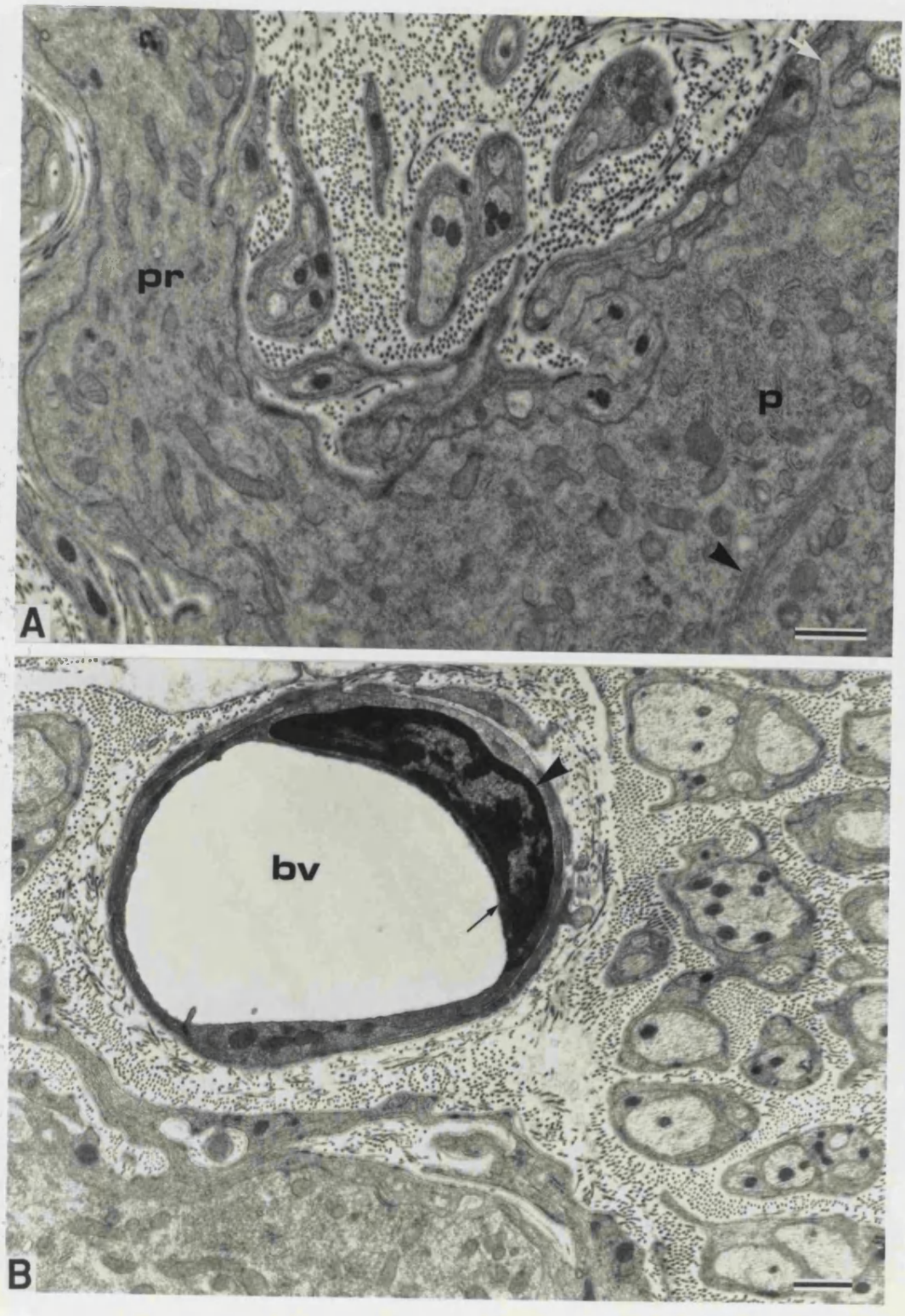
pr
p
A
bv
B

Figure 19

Electron micrograph from the pelvic ganglion of an adult female rat. Shown is region composed mainly of fibres (**a**) (presumably axons) in transverse section. The fibres are unmyelinated and some are surrounded by processes from a Schwann cell which displays a dense nucleus (**sn**). The group of fibres are enclosed by thin septum of connective tissue that is an extension of the outer ganglionic capsule. The fibres are separated by extensive bundles of collagen fibrils (**c**) in transverse section.
(Scale Bar = 1μm).

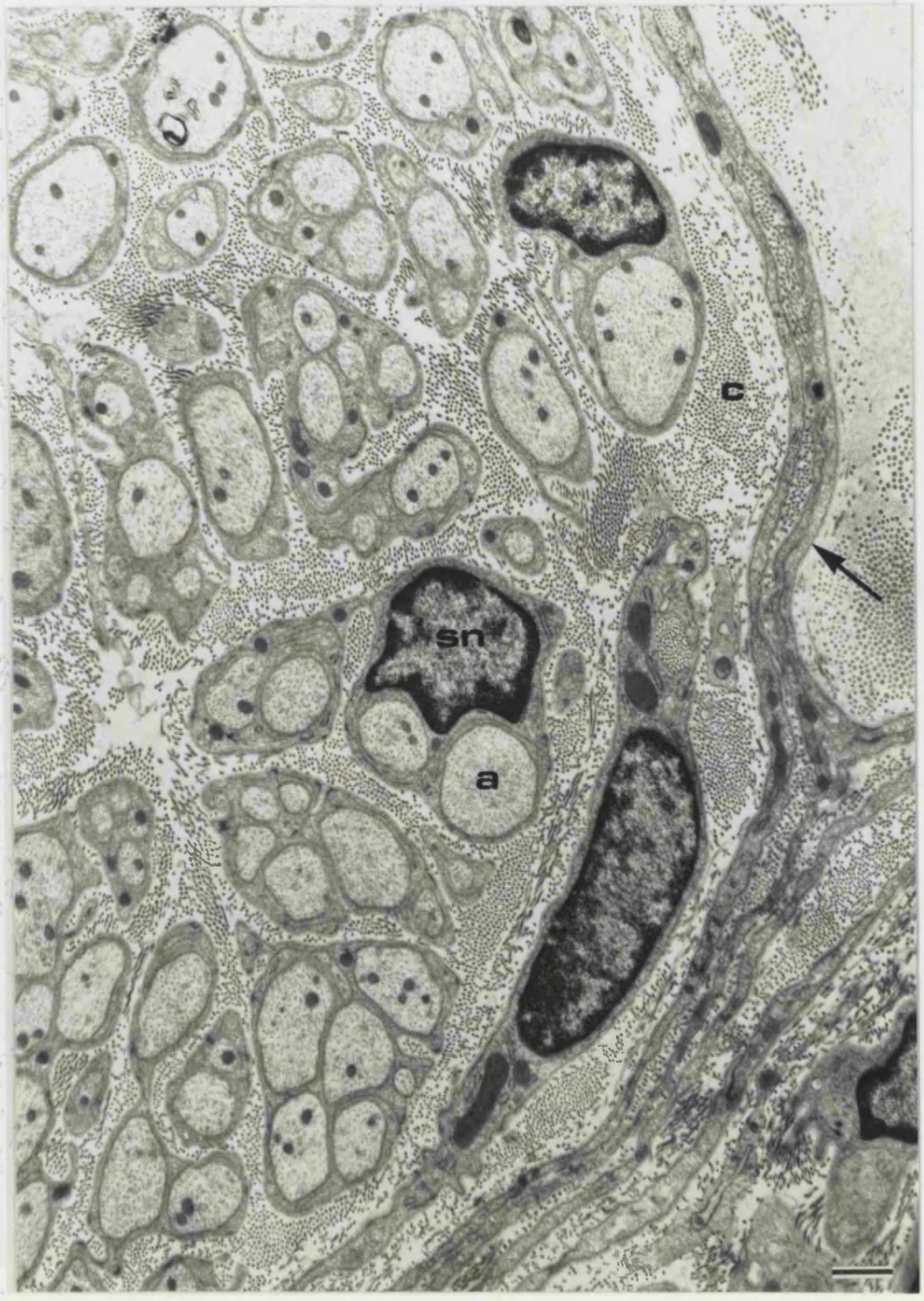
c
sn
a

Figure 20

A) Electron micrograph of a pelvic ganglion from an adult female rat showing S.I.F. cells. A large nucleus (**sn**) is observed in one of the cells (left). Both cells exhibit numerous large (many approximately 300nm in diameter) dense-cored vesicles (white arrow) that contain eccentrically positioned osmophilic material and are distributed throughout the cytoplasm. (Scale Bar = 1μm).

B) Electron micrograph of a mast cell present in the pelvic ganglion of an adult male rat. The large secretory vesicles are clearly evident in the perikaryon surrounding a dense nucleus (**mn**). The mast cell is surrounded by bundles of collagen fibrils (arrowhead) mainly appearing in transverse section.
(Scale Bar = 1μm).

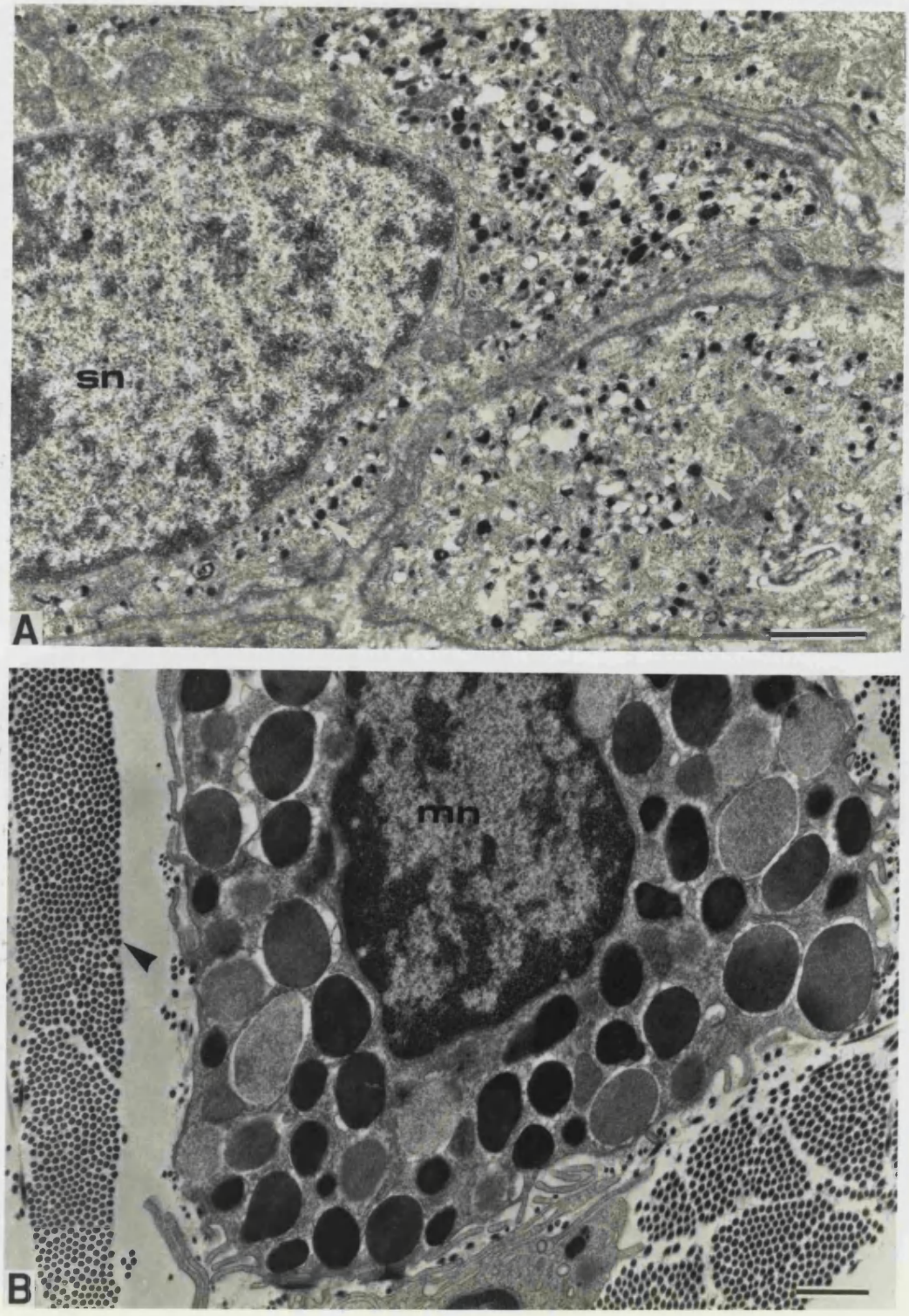
sn
A
mn
B

Figure 21

A) Cryostat section of control adult male rat histochemically stained for NADPH-diaphorase. Strongly and weakly positive neurons can be seen, as well as a positive neuronal process. (Scale Bar = 12.5μm also applies to **B**)
B) Example of NADPH-diaphorase staining showing smaller, positive neurons and a larger negative neuron.

C) Cryostat section of control adult male rat histochemically stained for NADPH-diaphorase displaying a range of staining intensities.
(Scale Bar = 20μm also applies to **C, D, E** and **F**).
D) Adjacent section to that in **C** immunohistochemically stained for nitric oxide synthase (NOS). Note that all neuronal perikarya immunoreactive to NOS are also histochemically positive to NADPH-diaphorase in **C**.

E) Cryostat section of a pelvic ganglion from a pre-pubertally castrated, adult male rat histochemically stained for NADPH-diaphorase. Neuronal perikarya display a range of staining intensities.
F) Same section as that in **E**, immunohistochemically stained for nitric oxide synthase. Note that all neuronal perikarya positive to NOS are also positive to NADPH-diaphorase in **E**.

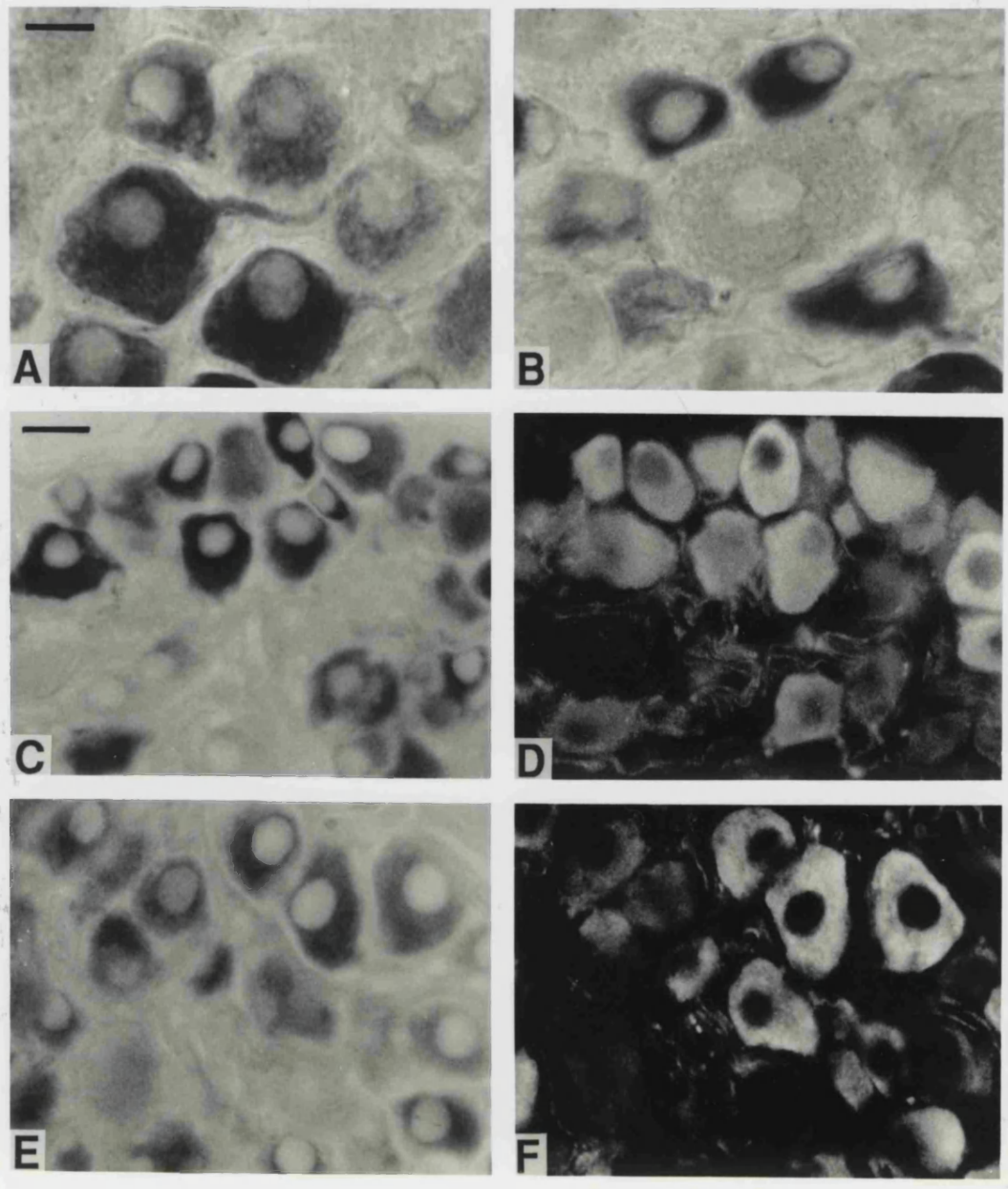
A
B
C
D
E
F

Figure 22

Co-localisation of NADPH-diaphorase and nitric oxide synthase immunoreactivity in a pelvic ganglion from an adult male rat.

A) Cryostat section histochemically stained for NADPH-diaphorase. (Scale Bar = 100μm also applies to **B**).

B) Fluorescent micrograph displaying the same area of cryostat section as above, immunohistochemically stained for nitric oxide synthase. Note that all neuronal perikarya displaying immunoreactivity to nitric oxide synthase also NADPH-diaphorase positive in **A**.

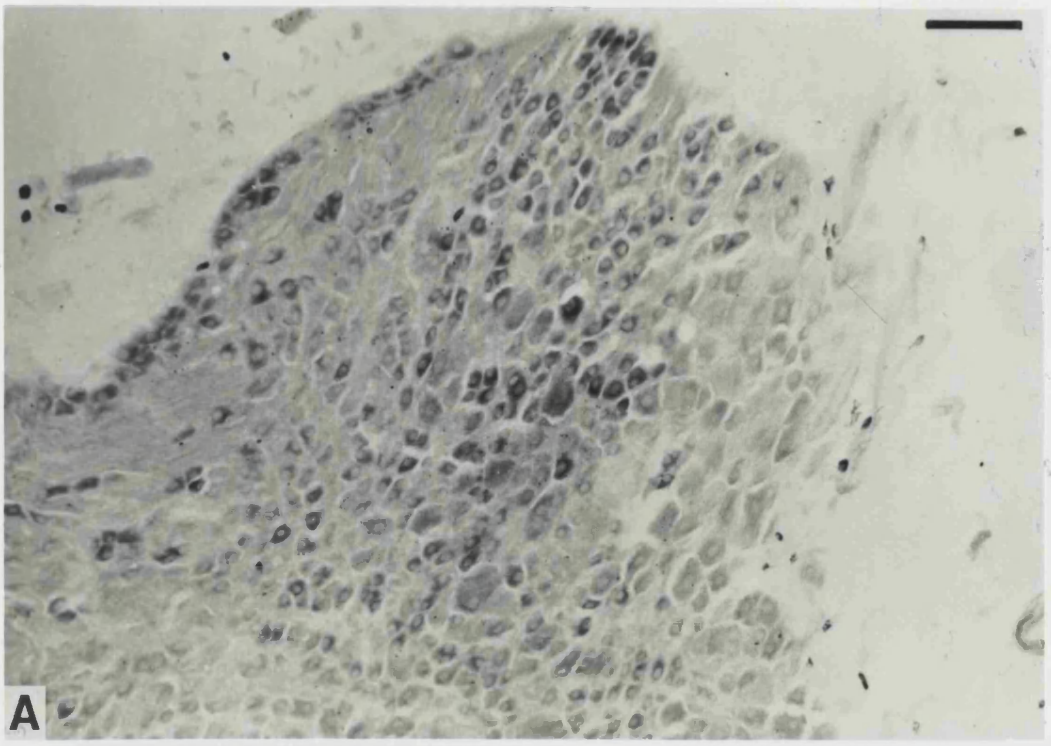
A


B

Figure 23

Longitudinally cryosectioned (10μm thick) pelvic ganglion from an adult male rat histochemically stained for NADPH-diaphorase.

A) A proximal portion of the genital nerve displaying neuronal perikarya positively stained for NADPH-diaphorase.
(Scale Bar = 12.5μm).

B) Longitudinal section of pelvic ganglion displaying topographical distribution of NADPH-diaphorase positive neurons near the emergence of the genital nerve (GN).

GN	Genital Nerve
PN	Pelvic Nerve

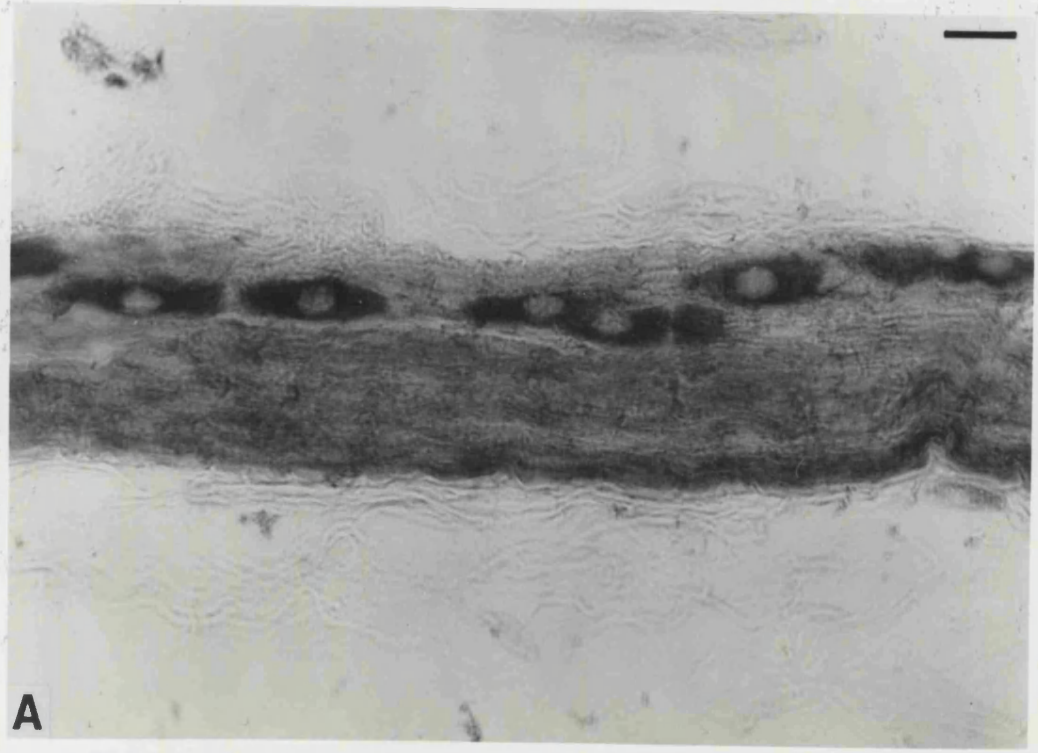
A

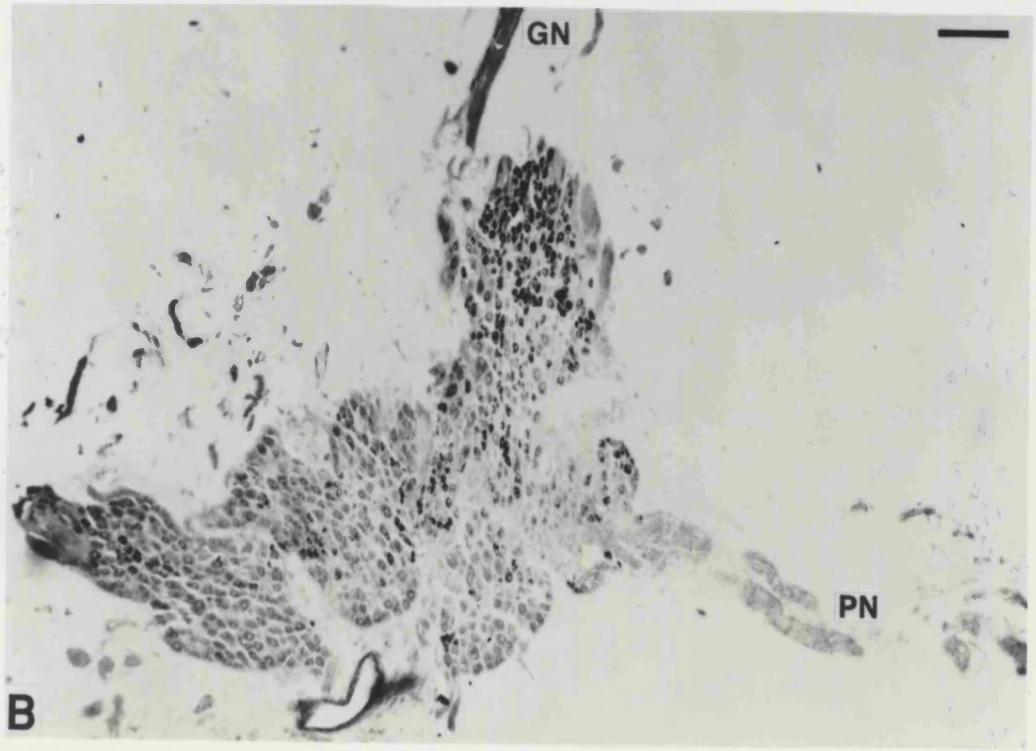
GN
PN
B

Figure 24

Tracings from a longitudinally cryosectioned (10μm thick) pelvic ganglion from male rats indicating the positions (marked with black dots) of neuronal perikarya histochemically stained for NADPH-diaphorase.

A) Adult Male

GN	Genital Nerve
PN	Pelvic Nerve

(Scale Bar = 160μm applies to both).

B) Pre-pubertal Male.

GN	Genital Nerve
PN	Pelvic Nerve

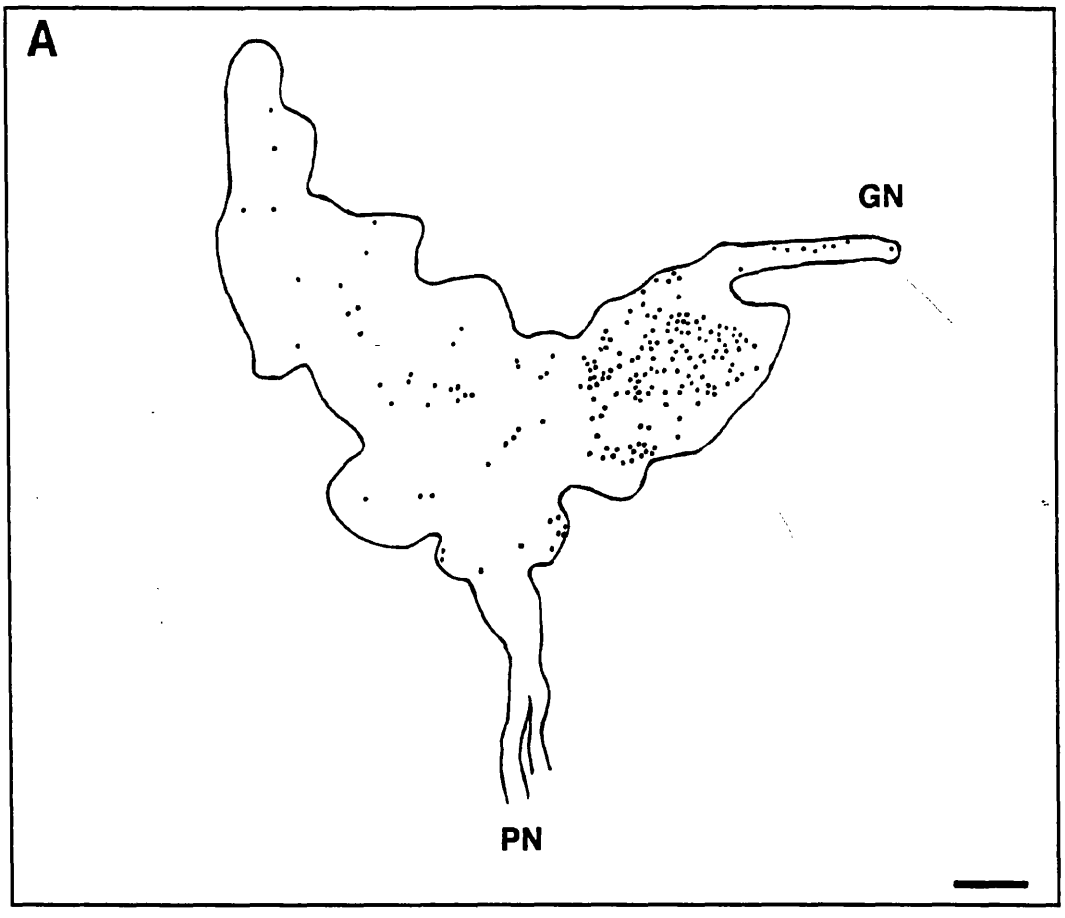
A
GN
PN

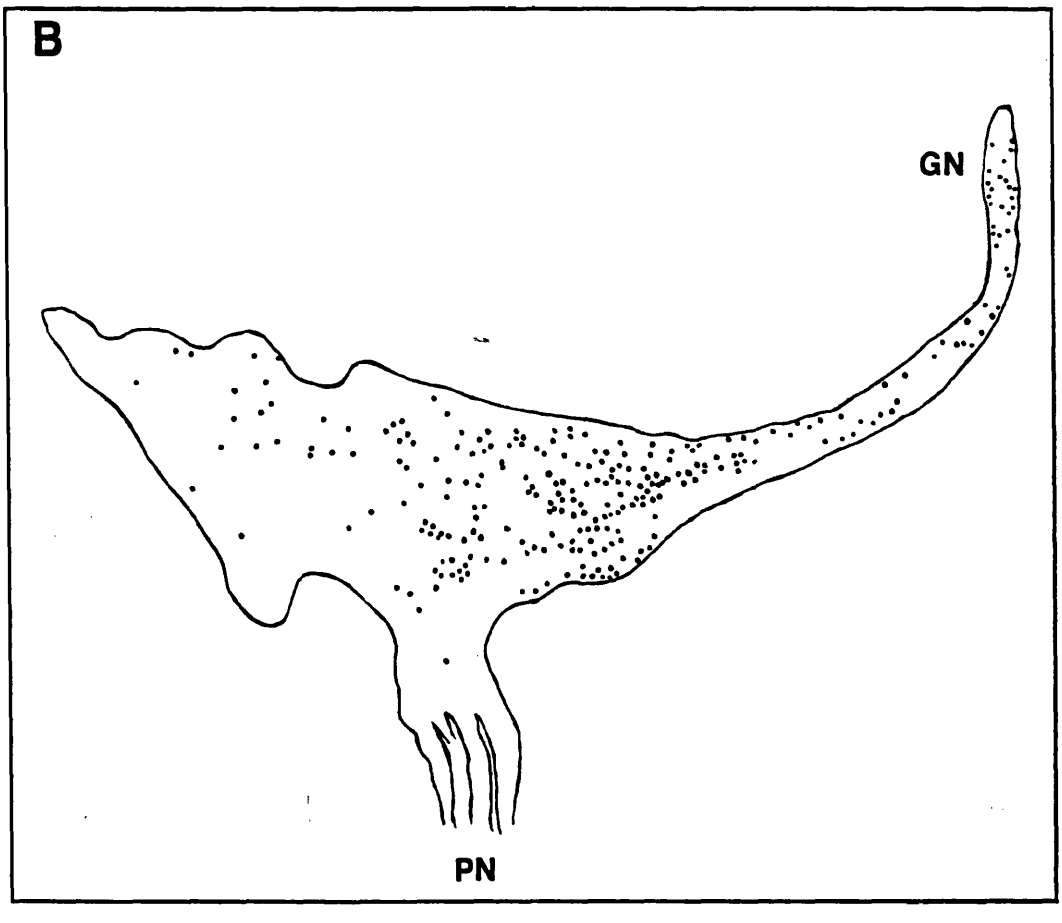
B
GN
PN

Figure 25

Cryostat sections of the major pelvic ganglion from control adult male rats. (Scale Bar = 20μm applies to all).

A) Section histochemically stained for NADPH-diaphorase displaying one strongly positive neuron and five weakly positive neurons.

B) The same section from **A** immunohistochemically stained for Neuropeptide Y. Immunoreactivity is present in the perikarya of five neurons, but not in the neuron that is strongly positive to NADPH-diaphorase in **A**.

C) Frozen section histochemically stained for NADPH-diaphorase displaying weakly and strongly positive neurons.

D) The same cryostat section from **C** immunohistochemically stained for vasoactive intestinal polypeptide. Immunoreactivity is present in the perikarya of both weakly and strongly positive neurons. VIP immunoreactivity is also seen in the nerve process that travels diagonally, from the strongly fluorescent neuron in the bottom right corner of the micrograph towards the top left corner.

E) Immunohistochemical staining for substance P. Immunoreactivity is not present in neuronal perikarya, but is seen in fibres that surround the ganglion cells where they form characteristic 'baskets'.

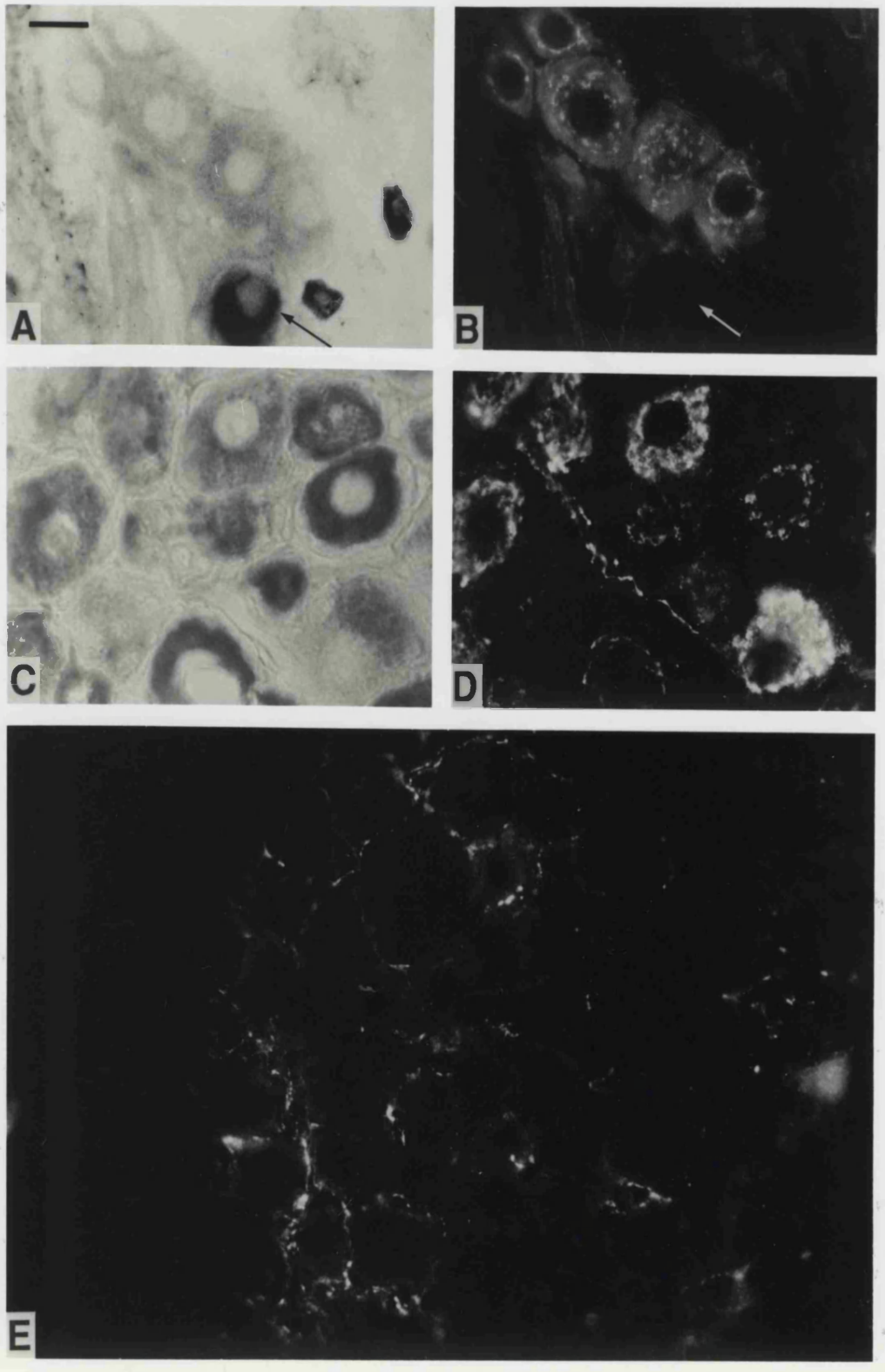
A
B
C
D
E

Figure 26

A) Light micrograph displaying an area of pelvic ganglion (frozen section) from a control male rat, histochemically stained for NADPH-diaphorase. Unstained neurons (e.g. neuron marked with *) are positively stained in micrograph **B**.

B) Fluorescent micrograph displaying the same area of pelvic ganglion frozen section as above, immunohistochemically stained for tyrosine hydroxylase. Note that the strongest immunoreactive signal (arrowed) is contained just below the neuronal cell membrane. Immunoreactivity is also present in nerve fibres.
(Scale Bar = 20μm - applies to both.)

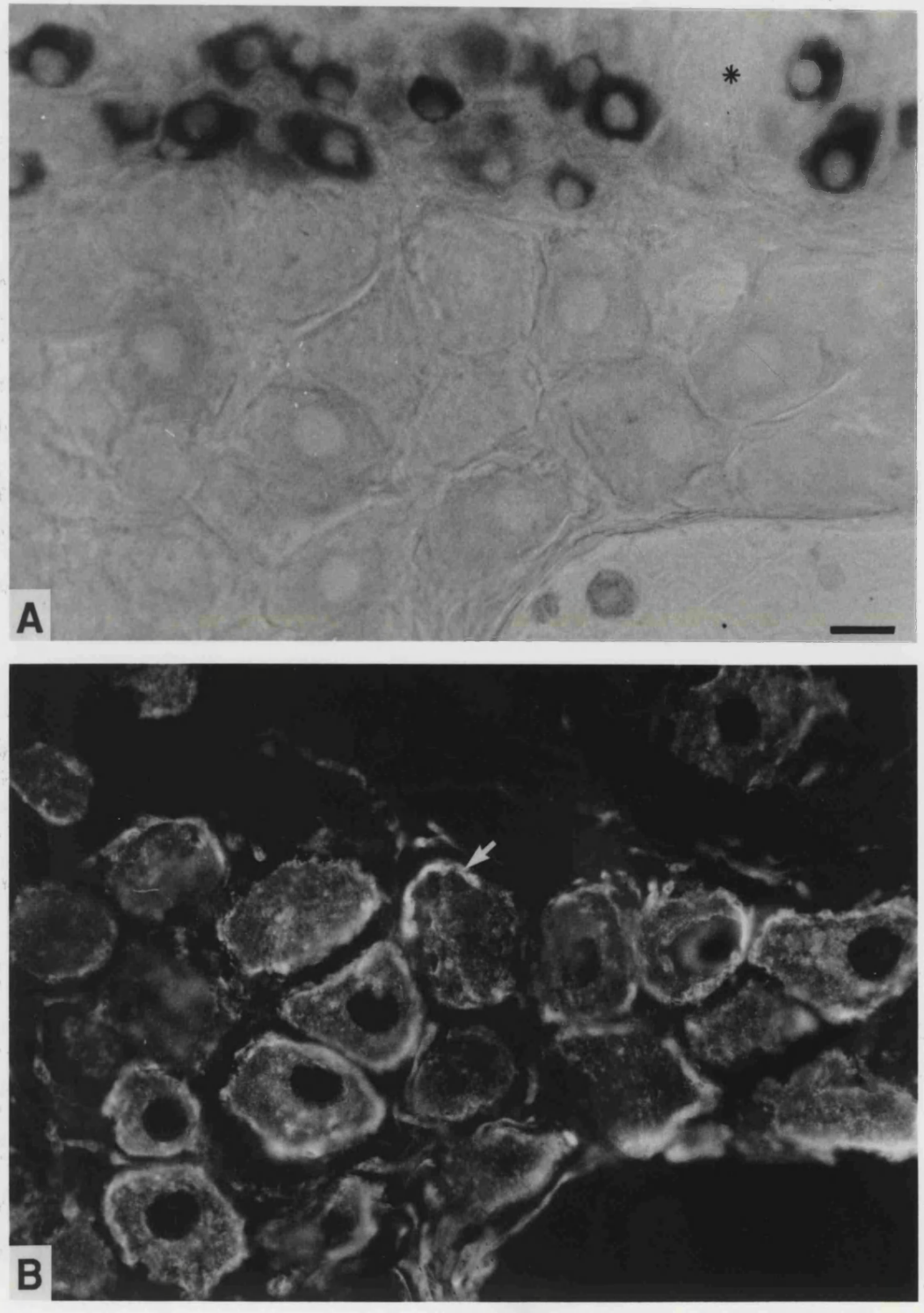
A
B

CHAPTER 4

RESULTS II: PRE-PUBERTAL RATS

4.1 Anatomy of Pelvic Ganglion

To study the pelvic plexus in pre-pubertal rats, fresh dissections were viewed through a dissecting microscope. Generic acetylcholinesterase neuronal staining aided viewing of the components of the plexus, and this was generally more complete and extensive than in adult rats, due to smaller amounts of adipose tissue. In the pre-pubertal animals of both sexes the anatomical structures of the pelvic plexus observed in adult animals were already present at this stage of development. The main connections with the bladder, genital organs and gut were as observed in more mature individuals.

In the female rat the main component of the plexus was the major pelvic ganglion (Fig. 28) which was located on the lateral aspect of the vaginal wall, in its cranial most portion near the uterine cervix. The ganglion was embedded in parametrial tissue, and attached to the vaginal muscle coat making dissection of the structure difficult. Viewed from the side, the ganglion measured approximately 1.5 x 3mm and was roughly triangular in shape, the ventral edge of the ganglion being the base edge of an inverted isosceles triangle. Further dissection (Fig. 29B) and removal of the structure along with the computer assisted reconstruction (Fig. 33A) revealed that the female ganglion was flat. The pre-ganglionic pelvic nerve entered at the dorsal pole of the ganglion and was comprised of several fascicles (Fig. 27 & 29B). The long, slender pre-ganglionic hypogastric nerve arrived at the cranial border (Fig. 30A); often a little distance cranial from the major pelvic ganglion was the hypogastric ganglion swelling (Fig. 29B & 32F). Numerous fine nerves left the pelvic

ganglion from the ventral border and travelled towards the pelvic organs; in many of these fibres clusters of neuronal perikarya were present (Fig. 30B). A group of between 3 and 4 accessory ganglia (Fig. 27 & 32D) that varied in size, shape and position were found ventral and cranial to the major ganglion, in proximity of the distal part of the ureter.

Running from the caudal pole of the ganglion to the pudendum was the prominent genital nerve, which also gave small branches to the rectum from its proximal portion (Fig. 32E). The rectum also received small nerves from the dorsal edge of the ganglion (Fig. 30A). The vagina received numerous nerves of various sizes from the ventromedial aspect of ganglion. From the ventral edge of the ganglion ran nerves to the surface of the bladder; these numbered about eight and ran in front and behind the ureter, branches of which reached the urethra and cranial portion of the vagina. The accessory ganglia received nerves running from the ventrocranial edge. Arriving at the lateral and dorsal surface of the bladder were nerves from the most caudal accessory ganglia while nerves from the more cranial accessory ganglia reaching the ureter and uterus. Occasionally the hypogastric nerve branched before it reached the pelvic ganglion, this accessory hypogastric nerve travelling to the accessory ganglia; when no hypogastric nerve branching was observed, a nerve often ran directly from the pelvic ganglion to accessory ganglia from a point close to the site of entry of the hypogastric nerve.

The major pelvic ganglion was the central element of the pelvic plexus in the male rat (Fig. 27). It was situated in the investing fascia of the posterior lobe of the prostate gland; the ganglion could partially be viewed without reflection of the seminal vesicle as this structure was much reduced in the pre-pubertal animals as compared to the adult. The ganglion was crescent shaped and measured approximately 1.5 x 2.5mm. It was apparent with further dissection (Fig. 29A) and with the computer assisted reconstruction (Fig. 33B) that the ganglion was larger and more rounded than its female counterpart. The pelvic nerve was multi-trunked and entered the ganglion at the dorsal edge of the ganglion while midway along the cranial border entered the long thin hypogastric nerve. Many nerves left the ganglion from its ventral border and reached the pelvic organs; small clusters of neuronal perikarya were often present within these visceral nerves. Between 2 and 4 accessory ganglia of varying size and shape, just visible through the dissecting microscope,

accompanied the main ganglion and were positioned close to the ureter and vas deferens (Fig. 28 & 29A).

The prominent genital nerve (Fig. 28 & 32A) exited from the caudal pole of the pelvic ganglion and terminated in the penis. The proximal portion the genital nerve gave branches that travelled to the rectum, which also received small nerves from the dorsal edge of the pelvic ganglion. The concave ventromedial edge of the ganglion produced numerous nerves of various sizes that ran to the prostate gland (Fig. 31B). The most ventral edge issued nerves, numbering about eight, that coursed to the ventral portion of the bladder and these travelled both behind and in front of the ureter with branches that reached the urethra. The accessory ganglia were connected by nerves running from the craniolateral edge of the ganglion (Fig. 31A). The lateral and dorsal bladder surfaces received nerves running from caudal accessory ganglia while nerves from more cranial accessory ganglia terminated at the ureter and in the seminal vesicles or entered a plexus found along the vas deferens. The hypogastric nerve passed dorsal to the ureter and then separated, before it reached the pelvic ganglion, into two branches, the main and accessory hypogastric nerves; this accessory hypogastric nerve reached the accessory ganglia near the ureters. Occasionally a small ganglion was observed caudal to the junction of the main and accessory hypogastric nerve, and running from this a nerve that entered the ganglion ventral to main hypogastric nerve (Fig. 32B).

Many of the several thousand post-ganglionic neurons that are the main component of the pelvic ganglion were observed in the acetyl cholinesterase whole mount preparations (Fig. 31A). In addition to the larger accessory ganglia that appear to contain about a hundred neurons there were irregular small aggregations ranging from 2-10 neurons situated outside the main ganglion (Fig. 31B).

4.2 Histology of Pelvic Ganglion

4.2.1 General Histology

The pelvic ganglia from pre-pubertal animals were composed of neurons, connective tissue, small blood vessels and a large amount of neuropil and differed little from those of adult animals (Fig. 34 & 36). Nerve fibres mainly in cross section were observed and were

predominantly unmyelinated with some myelinated. Different areas of the ganglion exhibited considerable variation in the proportion of neuropil. There appeared to be no sex related difference with regard to these features.

4.2.1.1 Capsule

The immature ganglia from rats of both sexes demonstrated a thin capsule of connective tissue that sheathed the entire ganglion and continued over the emerging nerves. This capsule was also seen to send septa that partially separated different groups of neurons in a similar fashion to that in the mature animal, although this separation was less extensive than in the older animals (Fig. 35).

4.2.1.2 Neurons

The neurons of the pre-pubertal specimens were ovoid and smooth surfaced, although less regular in shape than those in adult animals of both sexes. The occasional emerging axon the only process observed; as in the adult specimens no dendrites were in evidence. Neurons in both sexes were entirely encapsulated in glial cells, the nuclei of which were visible in the light microscope (Fig. 35). No vacuolated neurons were seen in the pre-pubertal animals of either sex.

4.2.1.3 Packing

Neurons of pre-pubertal animals of both sexes showed clear separation and were completely surrounded by neuropil; they generally appeared to lay closer to one another than neurons in the adult with less neuropil in evidence overall (Fig. 35 & 36); it also seemed as if fewer neurons existed in solitude as opposed to being in a larger group. Throughout the ganglia of both sexes all neurons, whether grouped together or singularly, were clearly individual and encapsulated by glial cells. Clusters of neurons were never contained in the same sheath.

4.2.1.4 Blood Vessels

The vascular tree permeated throughout the entire ganglion with no stark variations in supply density (Fig. 35). Arterioles and venules were differentiated according to the thickness of the vessel wall. Most vessel profiles were circular or ovoid suggesting that the predominant direction of travel was perpendicular to the sectioning plane i.e. dorsoventral.

Different shaped profiles were observed which probably arise due to vascular branching and looping.

4.2.1.5 SIF Cells and Other Cell Types

Clusters and lone SIF cells were present throughout the ganglia from rats of both sexes. No firm counts were undertaken; SIF cells appeared neither more or less abundant than in ganglia from mature rats nor was there any sex related difference observed in pre-pubertal animals. Other non-neuronal cells present in both male and female ganglia were mast cells, fibroblasts, Schwann cells and endothelial cells (Fig. 35).

4.2.2 Ganglion Volume

The ganglion volume, estimated morphometrically, in 3 male pre-pubertal rats ranged between 226.4 $x10^6\mu m^3$ - 272.1 $x10^6\mu m^3$ with an average of 251 ± 23 $x10^6\mu m^3$ (251 million cubic microns or approximately $0.25mm^3$). In 3 female, pre-pubertal rats ganglion volume ranged between 116.7 $x10^6\mu m^3$- 148.4 $x10^6\mu m^3$ with an average value of 129 ± 17 $x10^6\mu m^3$ (129 million cubic microns or approximately $0.13mm^3$); values for the male and female animals show a statistically significant difference ($P < 0.01$ with application of t-test, see Appendix 5).

4.2.3 Nerve Cell Size

Neuron size (the area of the largest profile of a neuron identified from serial sections at $2\mu m$ intervals) was measured in the ganglia from 3 pre-pubertal male and 3 pre-pubertal female rats; approximately one hundred neurons were measured in each animal. The largest sectional profile of a neuron almost invariably displayed the nucleus. In all ganglia, whether from male or female rats, the range of nerve cell sizes was wide, continuous and gave no indication of sub-classes (Graph. 3 & 4). In male rats the neurons ranged in size from $101\mu m^2$ - $819\mu m^2$ and mean neuronal cell sizes from 3 animals ranged from $262\mu m^2$ -$395\mu m^2$ and the average of the means was $338\mu m^2 \pm 68$. In female rats neurons ranged in size from $63\mu m^2$ -$671\mu m^2$ and the mean neuronal cell size ranged between $198\mu m^2$ -$257\mu m^2$; the average of the means was $237\mu m^2 \pm 34$. The data reveal little variability between neuron size ranges and means neuron sizes in ganglia of animals of the same age and sex. Generally smaller neurons predominated in both sexes and there was a wider range

of neuronal sizes in ganglia of male rats (where the histogram is observed to be skewed to the right). Despite neurons of the male having a broader range and a larger average size, overall the average of the mean cross sectional area values for male and female animals showed no statistically significant difference ($P>0.1$ with application of t-test, see Appendix 5).

4.2.4 Neuron Number

Disector-estimated neuronal numbers in 3 pre-pubertal male rats ranged between 12,003 - 14,951 with a group average of 13,605 ± 1,490. The neuronal numbers in 3 pre-pubertal female rats ranged from 5,792 - 7,121 with an average value of 6,563 ± 689; there was a statistically significant difference between estimated neuronal populations in male and female animals ($P < 0.001$ with application of t-test, see Appendix 5).

4.3 Cytology of Pelvic Ganglion

4.3.1 Transmission Electron Microscopy

The ultrastructural features of ganglia from pre-pubertal animals of both sexes, observed through the electron microscope, were generally very similar to those in the adult animals.

4.3.1.1 Neurons

Pre-pubertal principal neurons were as easy to identify as mature neurons, primarily due to their large size, and characteristic nucleus and cytoplasm. The dominating feature of these cells was the large, electron lucent nucleus (Fig. 38B). As in the adult neurons, the pre-pubertal neuronal nuclei often contained several nucleoli (between one and four) and other less electron dense clumps situated close to the nuclear membrane; in contrast to the mature counterparts, apart from the distinct nucleoli, pre-pubertal nuclei were more electron dense and granular throughout. The shape of the neuronal nuclei was generally more invaginated and indented than those of adult neurons.

Rough endoplasmic reticulum was abundant throughout the perikaryon, the paired cisternae of which demonstrated a parallel configuration (Fig. 40B). Golgi apparatus was regularly present, usually positioned fairly close to the nucleus. One of the most conspicuous perikaryal organelles were mitochondria which were numerous, displayed

internal cristae and were distributed in all cytoplasmic regions (Fig. 40B). Most mitochondria were small (even when in longitudinal section and not displaying cristae) while others were substantially larger and of a magnitude not observed in mitochondria of mature neurons. Polysomes and free ribosomes were widely present while lysosomes were less numerous. Multivesicular bodies were occasionally evident and these contained a mixture of electron dense and electron lucent vesicles of variable size (although the dense cored vesicles were generally the larger of the two types). Neurons displayed areas rich in neurofilaments (Fig. 40B), and microtubules were also common.

Dendritic processes were extremely rare, whereas short intracapsular dendritic spines were a consistent feature (Fig. 37). Nerve fibres, presumably pre-ganglionic fibres were usually present close by, and these formed synapses with both the spines (Fig. 37), and with the perikaryon itself; larger undulations of the perikaryon were also a common characteristic of pre-pubertal ganglion cells, which is in contrast to the smoother profiles of more mature neurons.

4.3.1.3 Satellite Cells

All neurons were completely wrapped by satellite glial cells which formed a continuous sheath that enclosed the entire perikaryon (Fig. 37). The dominating feature of these cells was a large, electron dense nucleus the presence of which corresponded to the widest part of the cell (Fig. 38A), despite there being only a meagre surrounding cytoplasm. Processes extended from this glial perikaryon that gradually narrowed with distance from the cell body ultimately reaching a minimum width of roughly 1μm. These glial processes were closely associated with the neurolemma and followed intricately the contours of the neuronal perikaryon (Fig. 38A & 40B). Sometimes a couple of concentric glial processes were present, interleaved with collagen fibrils, but the wider, multiple layered configuration regularly observed surrounding mature pelvic ganglion cells was rare.

4.3.1.4 Nerve Fibres in Transit

Large regions of the ganglion consisted almost entirely of nerve fibres in transit (Fig. 37), with only occasional neuronal perikarya present. Most of these fibre profiles were in transverse section due to the plane of section, although some were obliquely cut. These nerve fibres, presumably axonal profiles, were of myelinated and unmyelinated type (with

the latter predominant) and contained mitochondria, neurofilaments and microtubules (Fig. 39B). Fibres of both types were contained within Schwann cell processes; sometimes between 6-8 unmyelinated axons were associated with a single glial cell, while myelinated axons were associated with just one (Fig. 39B). Myelin was electron-dense and consisted of regular, thin concentric, lamellae. Schwann cells had large, electron dense nuclei surrounded by a cytoplasm containing many organelles (rough endoplasmic reticulum, Golgi apparatus and mitochondria), although these were much reduced in density in the fibre-surrounding cell processes.

4.3.1.5 Connective Tissue Elements

All neuronal perikarya (neuron/satellite glia associations) and nerve fibres (fibre/Schwann cell associations) of the ganglia from rats of both sexes were surrounded by numerous collagen fibrils (Fig. 39B & 40A). Collagen fibrils were usually seen in transverse section and were uniformly distributed throughout the ganglion, rather than forming discrete bundles and fibres. Where fibrils were caught in longitudinal section they appeared as thin, tortuous structures of alternating light and dark striation.

At the border of the ganglion was the capsule that sheathed the entire ganglion and occasionally extended septa to the interior of the ganglion that partially separated different groups of neurons. The capsule was constructed from between 2-6 concentric layers of elongated cells identified as fibroblasts, interleaved with collagen fibrils (Fig. 40A). The widest point of these cells was the cell body that surrounded a large, elongated, electron dense nucleus. The fibroblasts were rich in rough endoplasmic reticulum and mitochondria with occasional Golgi structures, all indicators of metabolically active cells. The cell bodies extended into numerous, thin processes, that mainly travelled circumferentially in relation to the interior of the ganglion, although extensions in other directions were also present. The features of the pre-pubertal capsule showed little difference between the sexes, or with those from adult age-groups.

Large cells that contained dense nuclei and numerous large dense cored vesicles were regularly observed and identified as mast cells. Other cells that were less common were identified as leukocytes.

4.3.1.6 Blood Vessels

Capillary profiles were present at many different points throughout the ganglia from animals of both sexes (Fig. 39A). Curved flattened endothelial cells gave thin extensions from their cell body that continued to form close association with neighbouring endothelial cells, in so doing enclosing the vessel's lumen. Endothelial cells had dense nuclei (Fig. 39A) which were surrounded by cytoplasm that contained some rough endoplasmic reticulum and very few mitochondria. The capillaries were continuous and the lumenal endothelial surface occasionally formed pinocytotic blebs that protruded away from the vessel wall. Endothelial cells had a pronounced basal lamina that abutted the outer surface. Certain vessel profiles, in addition to the comprising endothelial cells, also were partially ensheathed by cells that were identified as pericytes.

4.3.1.7 S.I.F. Cells

Many small cells that contained numerous electron dense vesicles were present in ganglia from both male and female rats and were identified as S.I.F. cells (Fig. 38B). The populations seemed similar between the sexes, but in general they appeared more numerous in the pre-pubertal ganglia than in ganglia from adult animals. The dense core vesicles were distributed throughout the cytoplasm and were variable in size (Fig. 38B); whereas in adult animals it was possible to differentiate between classes of S.I.F. cell according to the size and distribution these vesicles, this was not possible in pre-pubertal specimens where both large and small vesicles were present both close to the cell surface and nearer to the nucleus. The large nuclei dominated the S.I.F. cells and were composed of electron dense clumps close to the nuclear membrane interspersed by regions of higher electron lucency. Some S.I.F. cells were in synaptic contact with pre-synaptic fibres that were densely packed with small clear vesicles at these sites (Fig. 38B); while most of these S.I.F. cells formed synapses with one or two pre-synaptic swellings, some cells were in contact with a greater number and in such regions exhibited a folds and grooves in the perikaryal membrane.

4.4 Cytochemistry

4.4.1 NADPH-diaphorase/ NOS

The intense blue-purple NADPH-diaphorase reaction product was produced in many neurons in pre-pubertal animals of both sexes (Fig. 41A, C). NADPH-diaphorase staining varied in intensity, was present throughout the cytoplasm but not in the nucleus. The formazan reaction product was also present in occasional neuronal processes (presumably axons).

Immunocytochemical staining for NOS produced neuronal perikarya with a bright fluorescence. Where NOS immunostaining was carried out on sections previously incubated with NADPH-diaphorase there was extensive co-localisation (Fig. 41B, D) of the two signals. There was a near total coincidence NOS immunofluorescence in neurons that were intensely stained for NADPH-diaphorase, as were most of the moderately NADPH-diaphorase stained neurons (Fig. 41). It is therefore assumed that a strongly positive NADPH-d reaction product demonstrates a neuron that also contains NOS and is thus able to synthesise nitric oxide.

4.4.1.1 NADPH-diaphorase Neurons Per Unit Area

The average number of NADPH-diaphorase positive neurons per unit area (each approximately 12,000μm^2, randomly selected from every 4th serial, 10μm cryosection) in 3 pre-pubertal male animals ranged between 27±15 - 38±14 with a group average of 33±6. Average numbers per unit area for NADPH-diaphorase positive neurons in the 3 female animals ranged between 14±5 - 23±7 with a group average of 18±5. These figures represent a sex related statistically significant difference ($P<0.05$ with application of t-test, see Appendix 5).

4.4.1.2 Distribution of NADPH-diaphorase

In the pre-pubertal male pelvic ganglion the majority of the NADPH-diaphorase-stained neurons were located in the dorsal region and close to the exit of the penile nerve, with many actually within this nerve (Fig. 24B & 41E). A smaller proportion of the population were observed evenly spread throughout the rest of the ganglion with some positive neurons in the adjacent accessory ganglia.

A contrasting situation occurred in the pre-pubertal female pelvic ganglion where neuronal somata that stained positive for NADPH-diaphorase were sparsely and more uniformly spread throughout the ganglion (Fig. 41F). As observed in the adult female animal there was no grouping at the exit of the genital or any other nerve and in general no particular grouping pattern was noticeable.

GRAPH 3

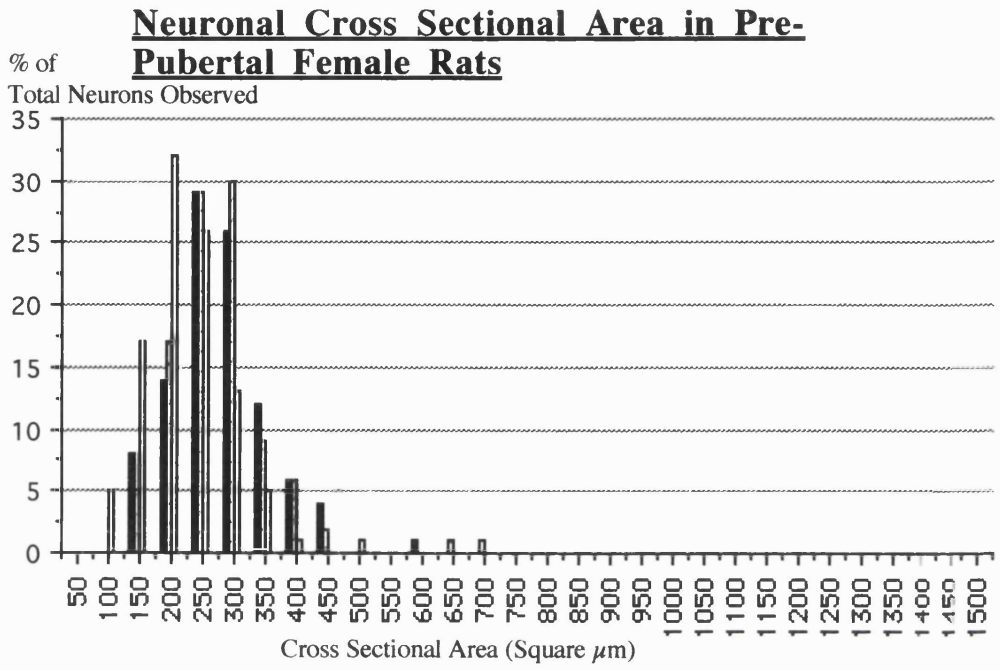

GRAPH 4

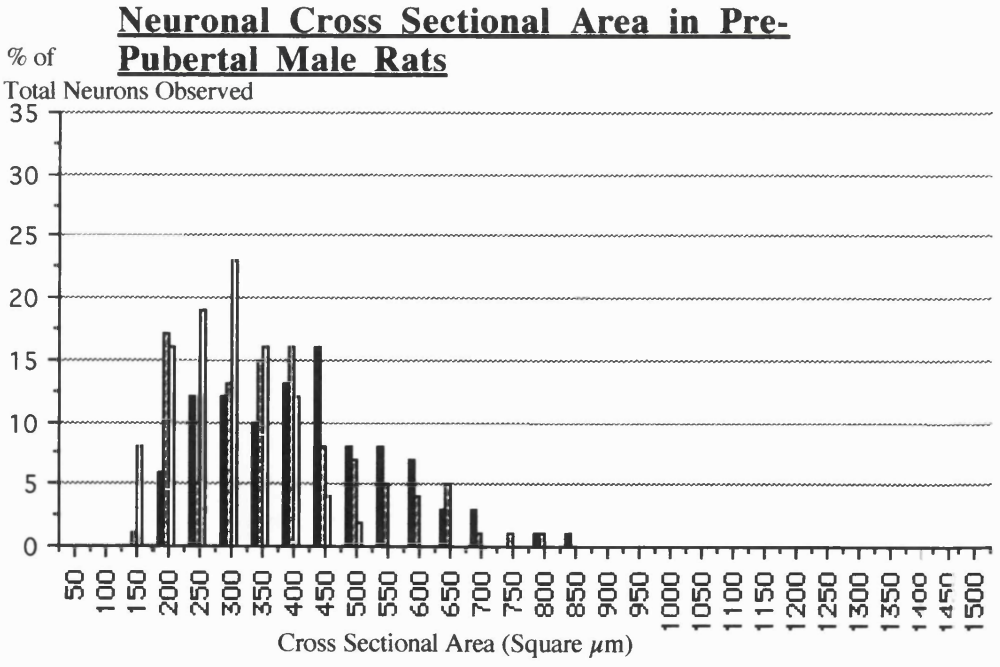

Figure 27

Side view of an acetyl cholinesterase stained preparation (Top) and diagrammatic representation (Bottom) of the right pelvic viscera and pelvic plexus of a **pre-pubertal male** rat. In the diagram neural structures have been represented by filled black artwork. For clarity only two small portions of the enteric plexus have been shown and only one accessory ganglion labelled (which is practically unstained in the actual acetyl cholinesterase preparation).

(Scale Bar = 2.5mm)

AG	Accessory Ganglion
BL	Bladder
ET	Enteric Plexus
GN	Genital Nerve
HN	Hypogastric Nerve
MPG	Major pelvic Ganglion
PN	Pelvic Nerve
PR	Prostate Gland
RT	Rectum
SV	Seminal Vesicle
UT	Ureter
VD	Vas Deferens

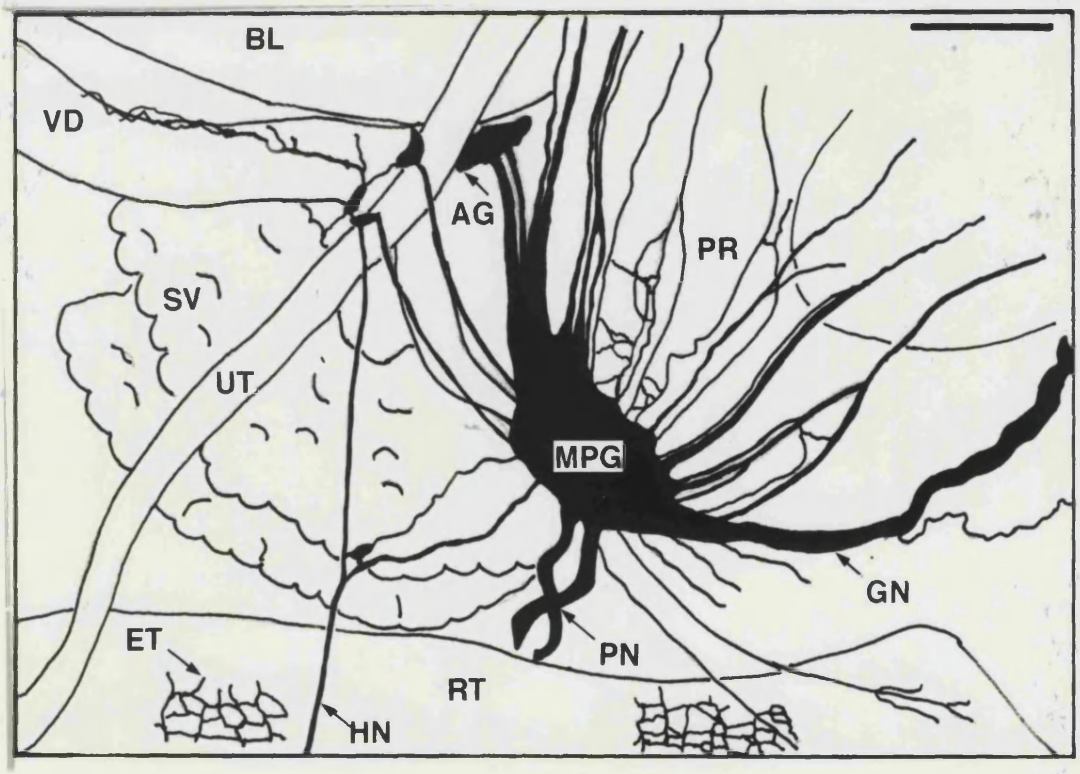
BL
VD
AG
PR
SV
UT
MPG
GN
ET
PN
RT
HN

Figure 28

Side view of an acetyl cholinesterase stained preparation (Top) and diagrammatic representation (Bottom) of the left pelvic viscera and pelvic plexus of a **pre-pubertal female** rat. In the diagram neural structures have been represented by filled black artwork. For clarity only two small portions of the enteric plexus have been shown and only one accessory ganglion labelled.

(Scale Bar = 1.25mm)

AG	Accessory Ganglion
ET	Enteric Plexus
GN	Genital Nerve
HG	Hypogastric Ganglion
HN	Hypogastric Nerve
MPG	Major Pelvic Ganglion
PN	Pelvic Nerve
RT	Rectum
UR	Ureter
UT	Uterus
VA	Vagina

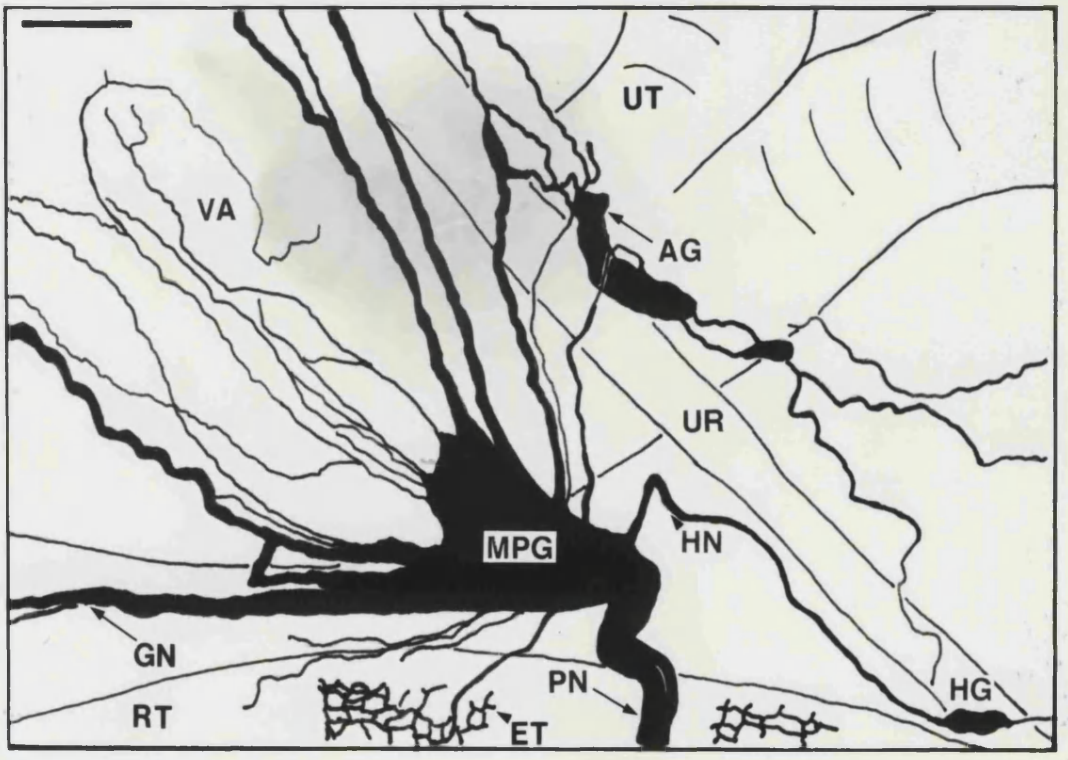
UT
VA
AG
UR
MPG
HN
GN
PN
HG
RT
ET

Figure 29

A) Acetyl cholinesterase stained pelvic ganglion and associated nerves dissected from a **pre-pubertal male** rat.
(Scale Bar = 1.25mm applies to both).

B) Acetyl cholinesterase stained pelvic ganglion and associated nerves dissected from a **pre-pubertal female** rat.

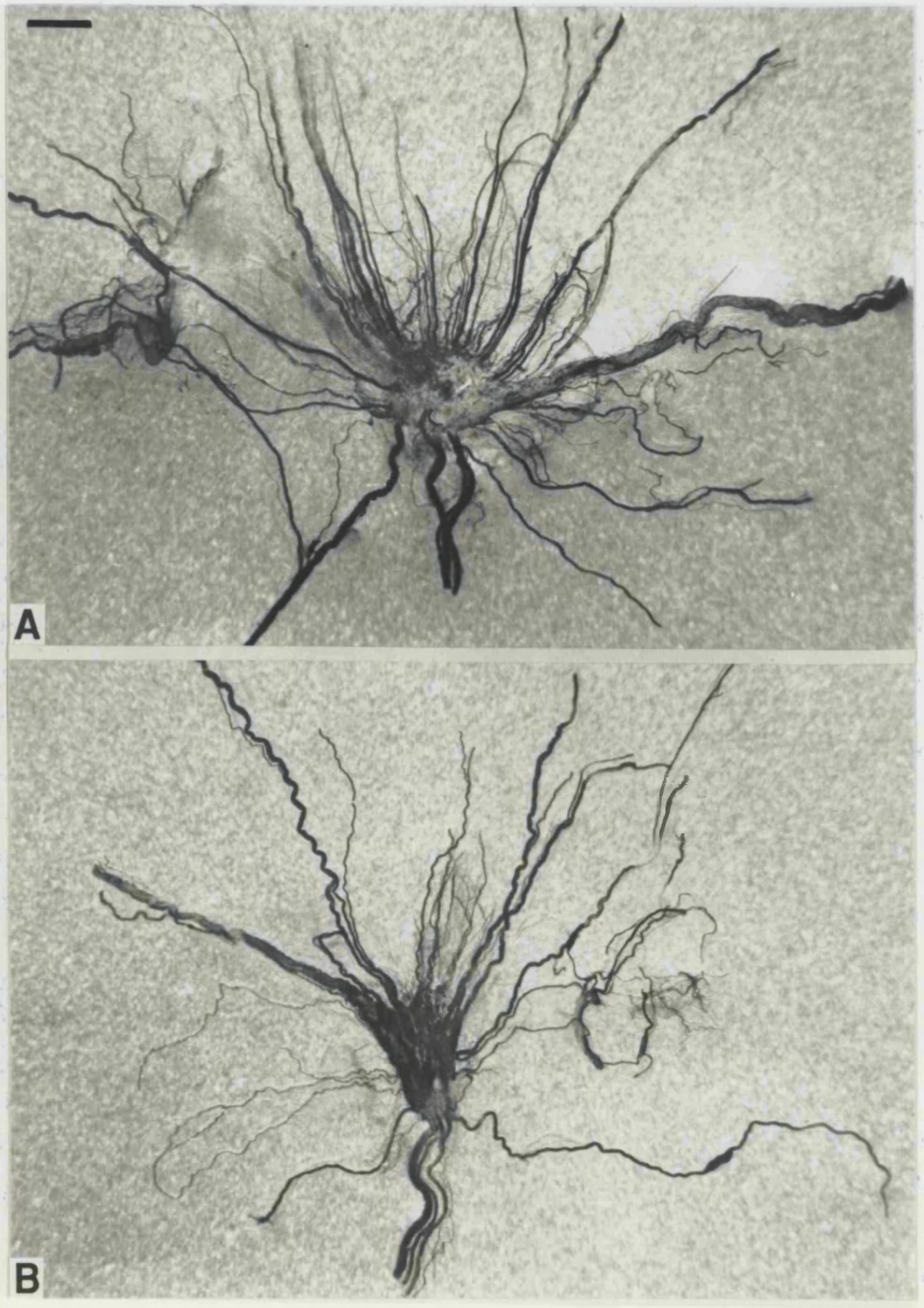
A
B

Figure 30

Anatomical details of a pelvic ganglion from a **pre-pubertal female** rat stained using acetyl cholinesterase.

A) The edge of the ganglion is in evidence with stained ganglion cells. The pre-ganglionic hypogastric nerve can be seen entering the ganglion, and three post-ganglionic nerves that travel to the enteric plexus of the rectum.

B) The post-ganglionic genital nerve with stained neuronal cells contained within. Stained neurons are also in evidence in the post- ganglionic nerves to the bladder.

(Scale bar-50μm applies to both).

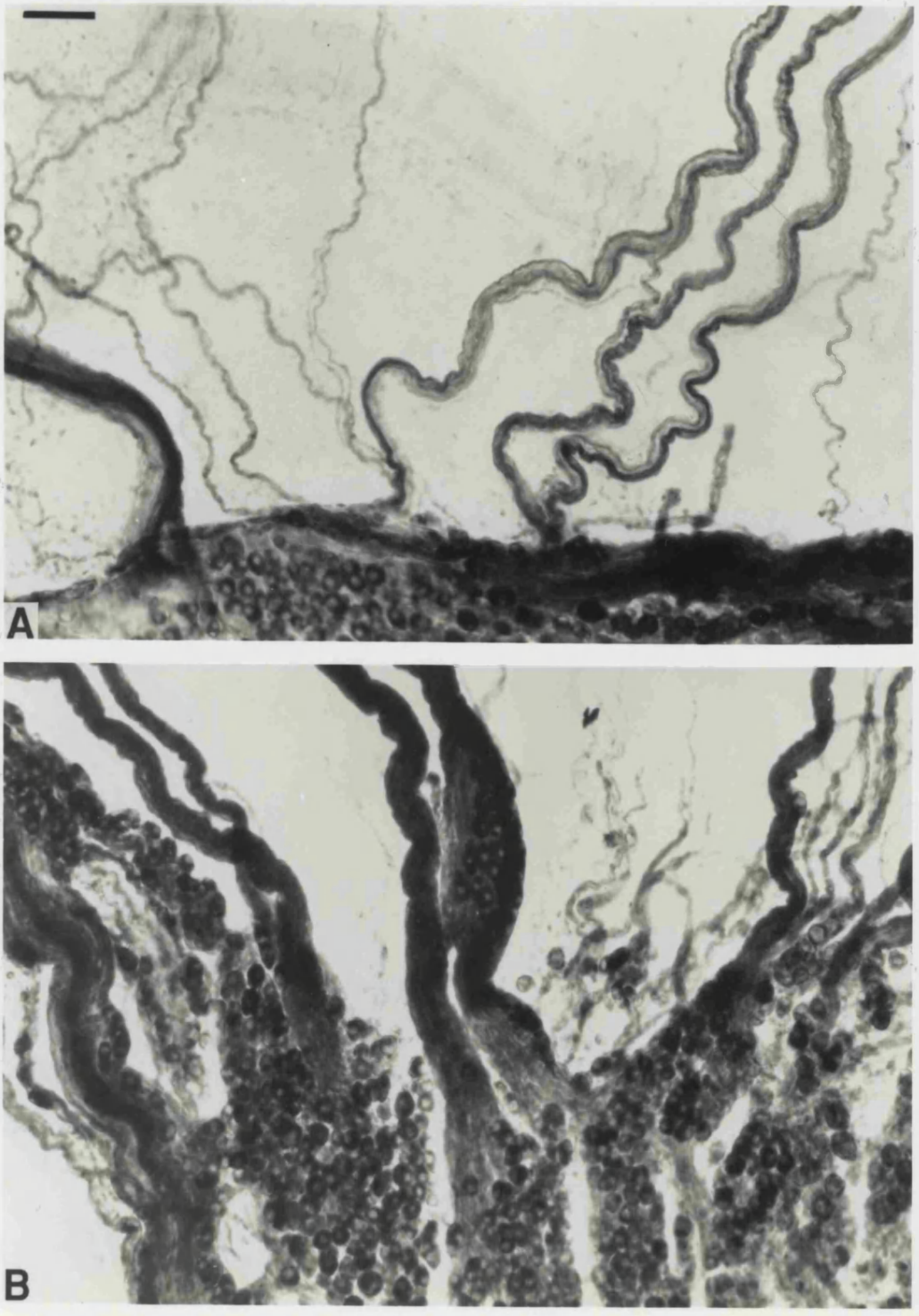
A
B

Figure 31

Anatomical details of a pelvic ganglion from a **pre-pubertal male** rat stained using acetyl cholinesterase.

A) The edge of the ganglion is in evidence showing stained ganglion cells. Post-ganglionic nerves that travel to the accessory ganglia can be seen. Also visible is an incoming pre-ganglionic nerve along which a mini-accessory ganglion is present.

B) The post-ganglionic nerves travelling to the bladder. The intricate plexus is observed and contains numerous aggregations of neurons of variable size. (Scale bar-50μm applies to both.)

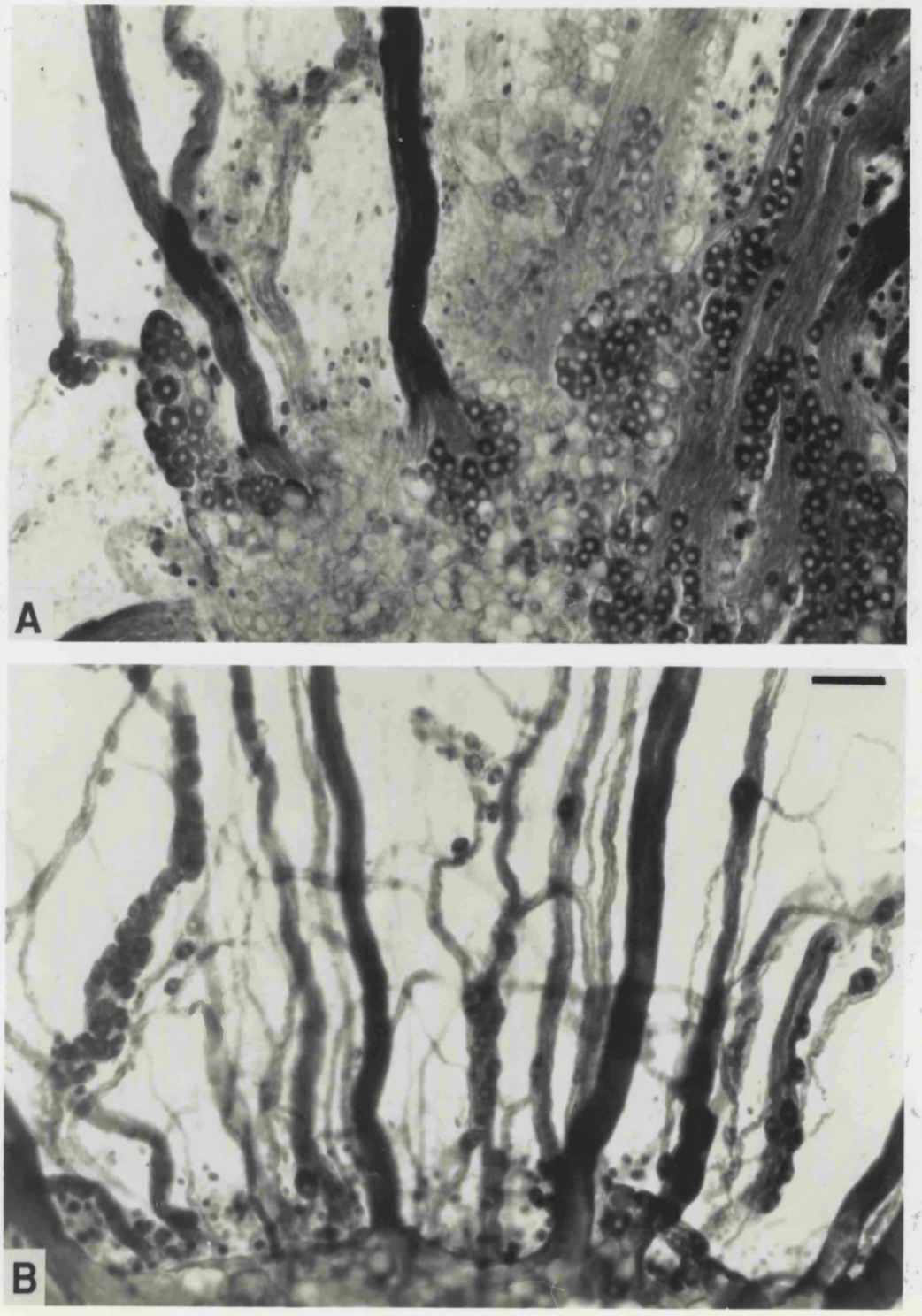
A
B

Figure 32

Anatomical details of a pelvic ganglion from an **pre-pubertal male** (**A** and **B**) and **female** (**C, D, E** and **F**) rat stained using acetyl cholinesterase.

A) The emergence of the genital nerve displaying a speckled appearance due to the acetyl cholinesterase staining of the neuronal perikarya within. Branches from the main trunk can be observed; these terminate in the rectum.

B) Small aggregations of ganglion neurons forming a mini-accessory ganglion at the branch of the main and accessory hypogastric nerves. The ganglionic aggregation issues a postganglionic trunk that travels to the major pelvic ganglion.

C) The genital nerve some distance from its origin demonstrating a branch that travels to the rectum.

D) A group of accessory ganglia.

E) A post-ganglionic nerve joining a separate post ganglionic nerve.

F) Swelling situated on the hypogastric nerve termed in this thesis the hypogastric ganglion.

(Scale Bar = 200μm - applies to all.)

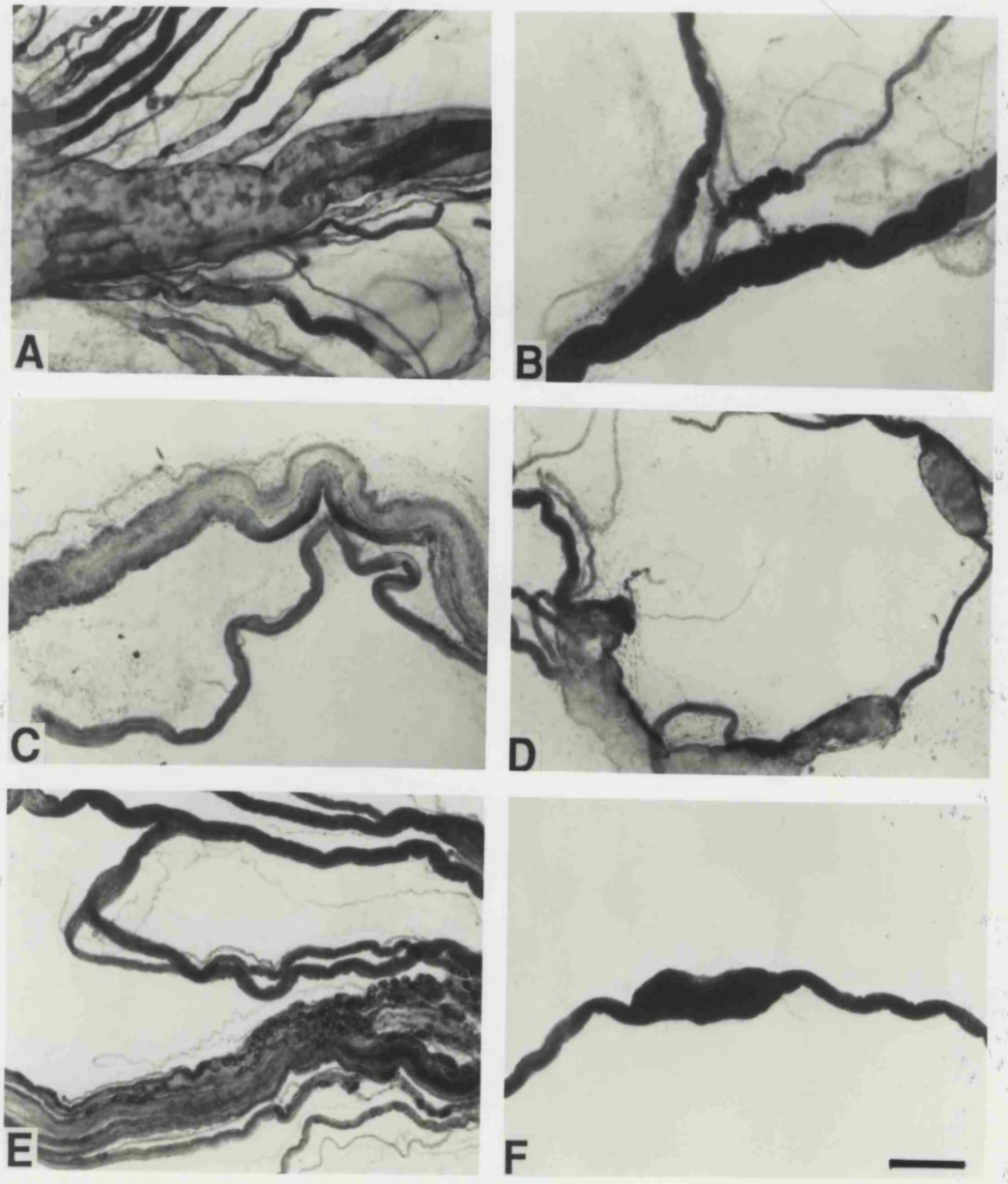
A
B
C
D
E
F

Figure 33

Line drawings representing the three dimensional outline of sections, 100μm apart, from pelvic ganglia of **pre-pubertal** rats.

A) Female

Note the flat shape of the ganglion demonstrating very little medial depth.

B) Male

Note the rounded shape and marked medial depth. Elongations from the dorsocranial edge represent the entrance of the pre-ganglionic hypogastric nerve.

(Axis bars: **V**, ventral; **M**, medial; **Cr**, cranial; **D**, dorsal; **L**, lateral; **Ca**, caudal).

(Scale Bar = 500μm applies to both)

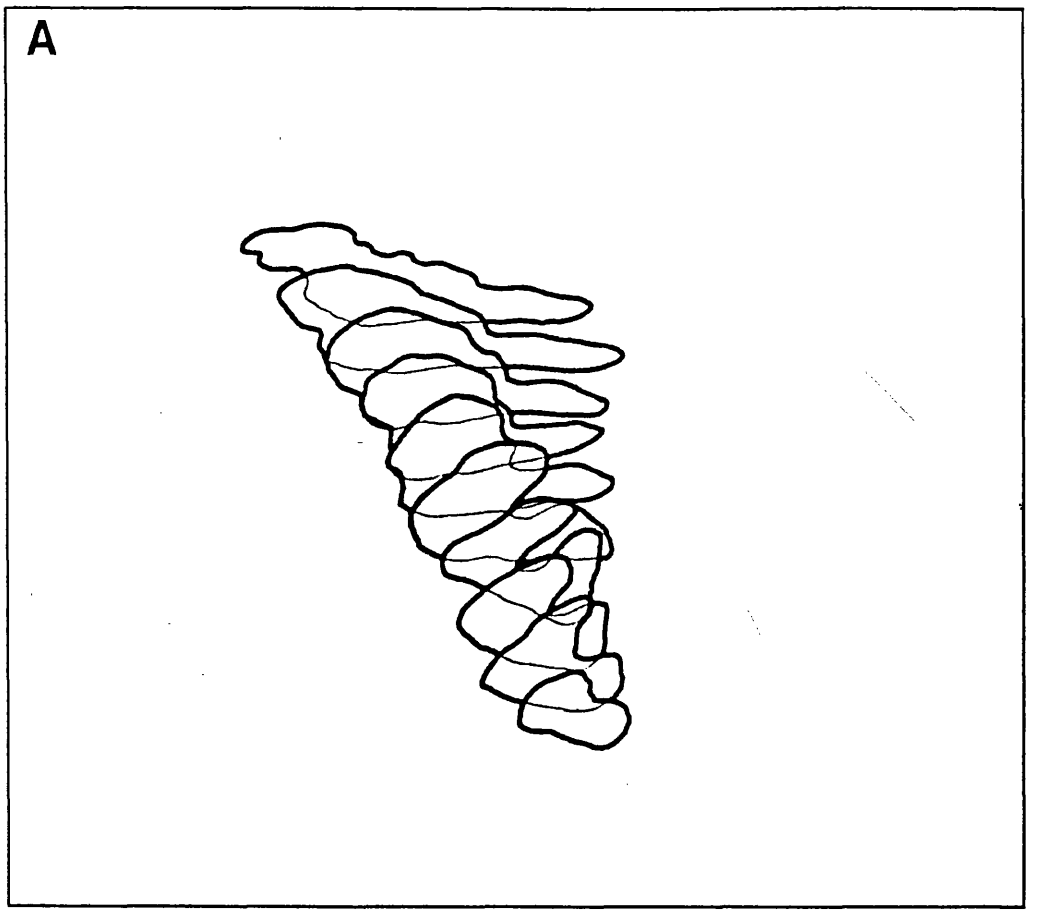
A

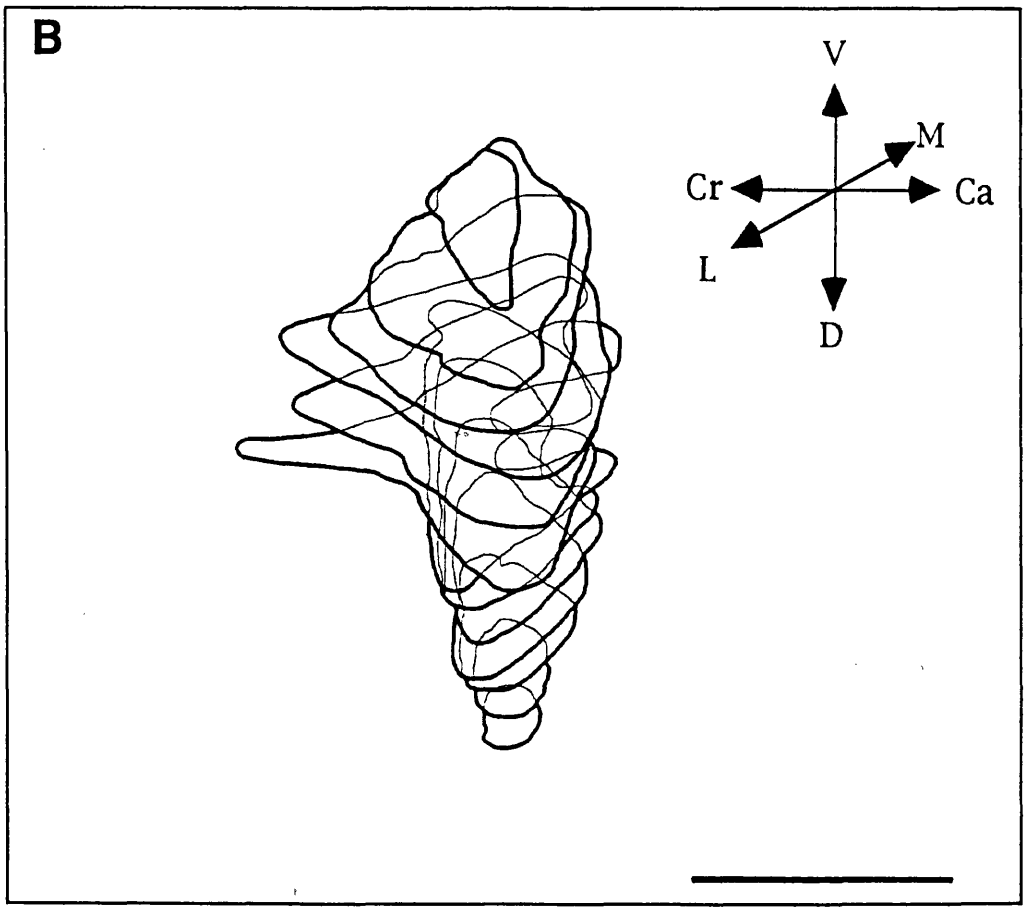
B
V
M
Cr
Ca
L
D

Figure 34

Light micrographs of major pelvic ganglia from pre-pubertal rats.

A) Male. The ganglion is completely covered by an outer capsule (arrowhead) within the boundaries of which the many neurons are observed.

B) Female. The ganglion is completely contained within an outer capsule (arrowhead) and is accompanied by large blood vessels (asterisk). The numerous neurons can be seen within the ganglion.
(Scale Bar = 100μm applies to both).

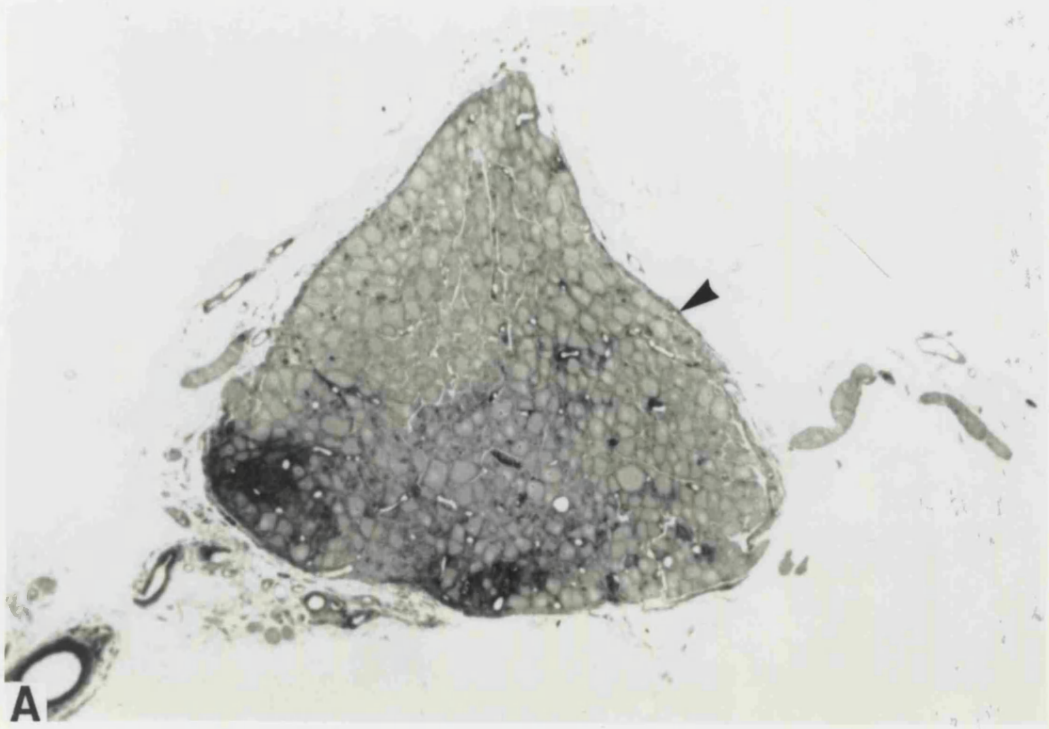
A

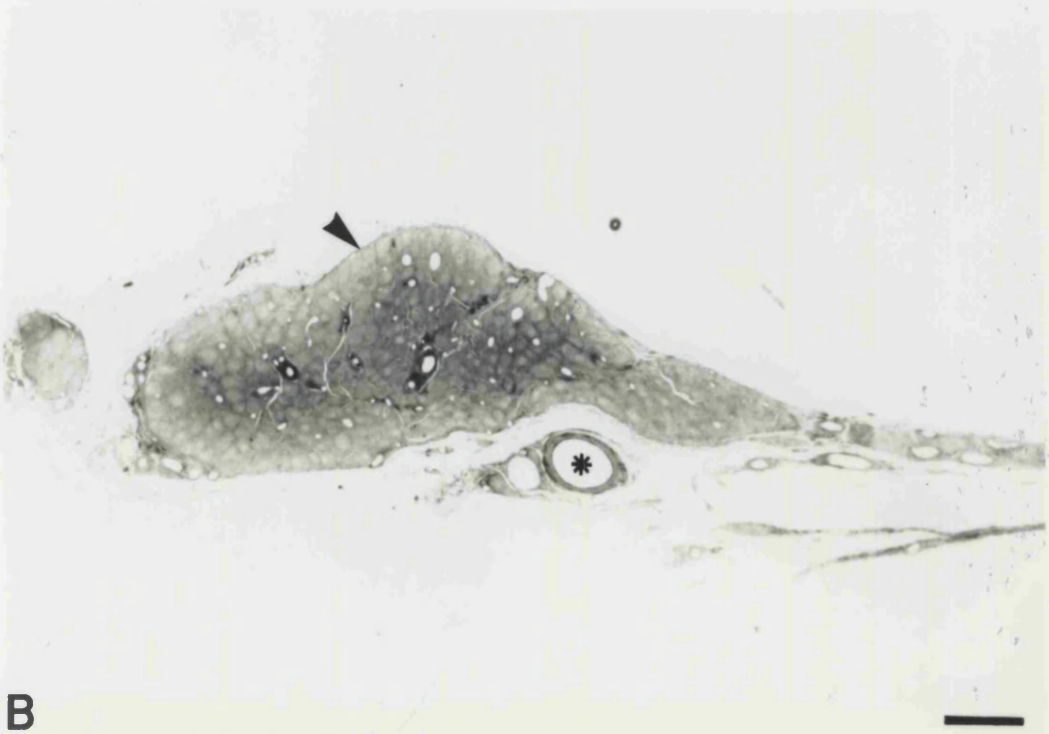
B

Figure 35

Light micrographs of major pelvic ganglia from pre-pubertal rats. Artefactual cracking (produced possibly during tissue dehydration) is observed at points throughout the ganglion.

A) Male. Major cell types of the ganglion: **g**, nucleus of satellite glial cell; **n**, ganglion neurons many of which display pale nuclear profiles; a process (**p**) emanating from a neuron is present. Blood vessels (**bv**) in cross section are observed.

B) Female. Some of the various cell types in the ganglion: **g**, nucleus of satellite glial cell; **n**, ganglion neurons many of which display pale nuclear profiles; **p**, pericyte; **s**, nucleus of small intensely fluorescent (SIF) cells. Blood vessels (**bv**) and myelinated fibres (arrowhead) in cross section are apparent. The outer capsule (two small arrowheads) is observed.
(Scale Bar = 20μm applies to both).

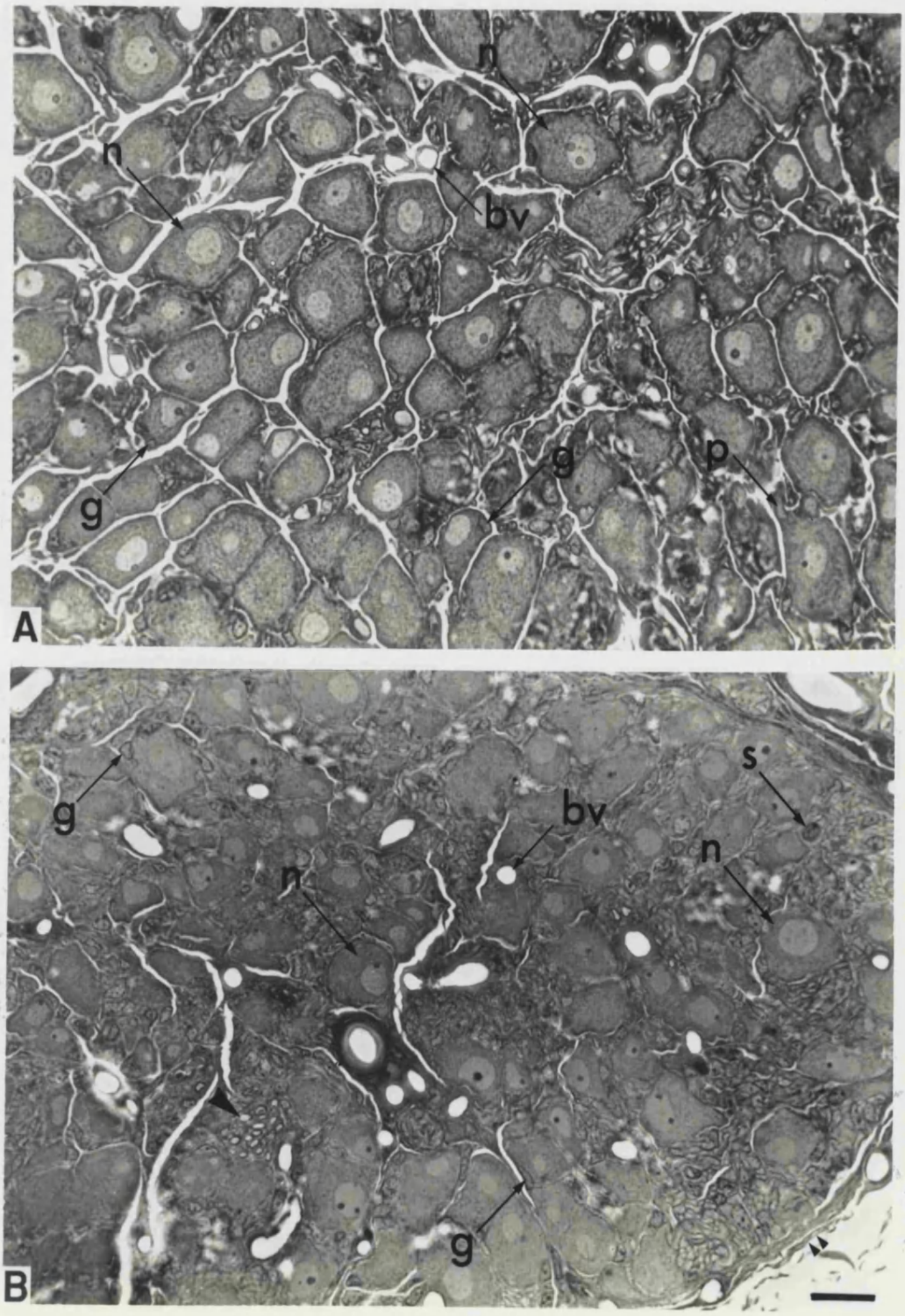
n
n
bv
g
g
p
A
g
bv
s
n
n
g
B

Figure 36

Light micrograph montage of a pelvic ganglion from a pre-pubertal male rat, stained with toluidine blue.

(Scale Bar = 100μm)

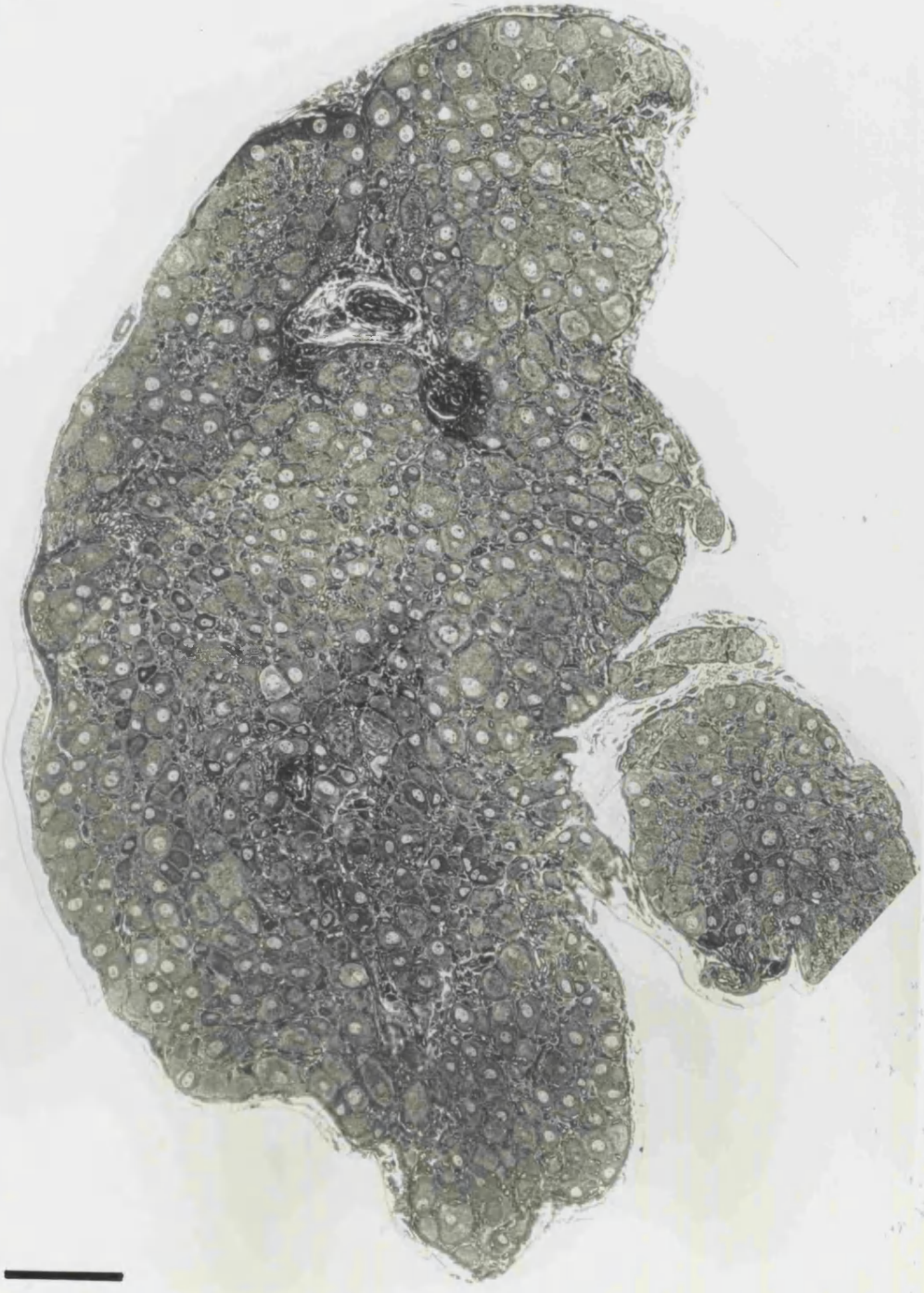

Figure 37

Electron micrograph from the pelvic ganglion of a pre-pubertal female rat. Shown is large region of a neuronal perikaryon (**p**) that is surrounded by neuropil. The perikaryon is entirely encapsulated by satellite cell processes (black arrowhead) and a basal lamina. Most parts of the perikaryal surface are smooth, although at one point a small intracapsular dendrite is observed (**d**). The dendrite shows dense, synaptic regions (white arrow) and is in synaptic contact with an axon. The latter is presumably a pre-ganglionic fibre, which is full of clear synaptic vesicles (white arrowhead), and also shows a mitochondrion and pre-synaptic densities.

The surrounding neuropil is composed of unmyelinated nerve processes and a supporting Schwann cell, with intervening collagen fibrils; in a nerve fibre (toward the bottom right-hand corner of the micrograph) is a multi-vesicular body (black arrow).

(Scale Bar = 0.5μm).

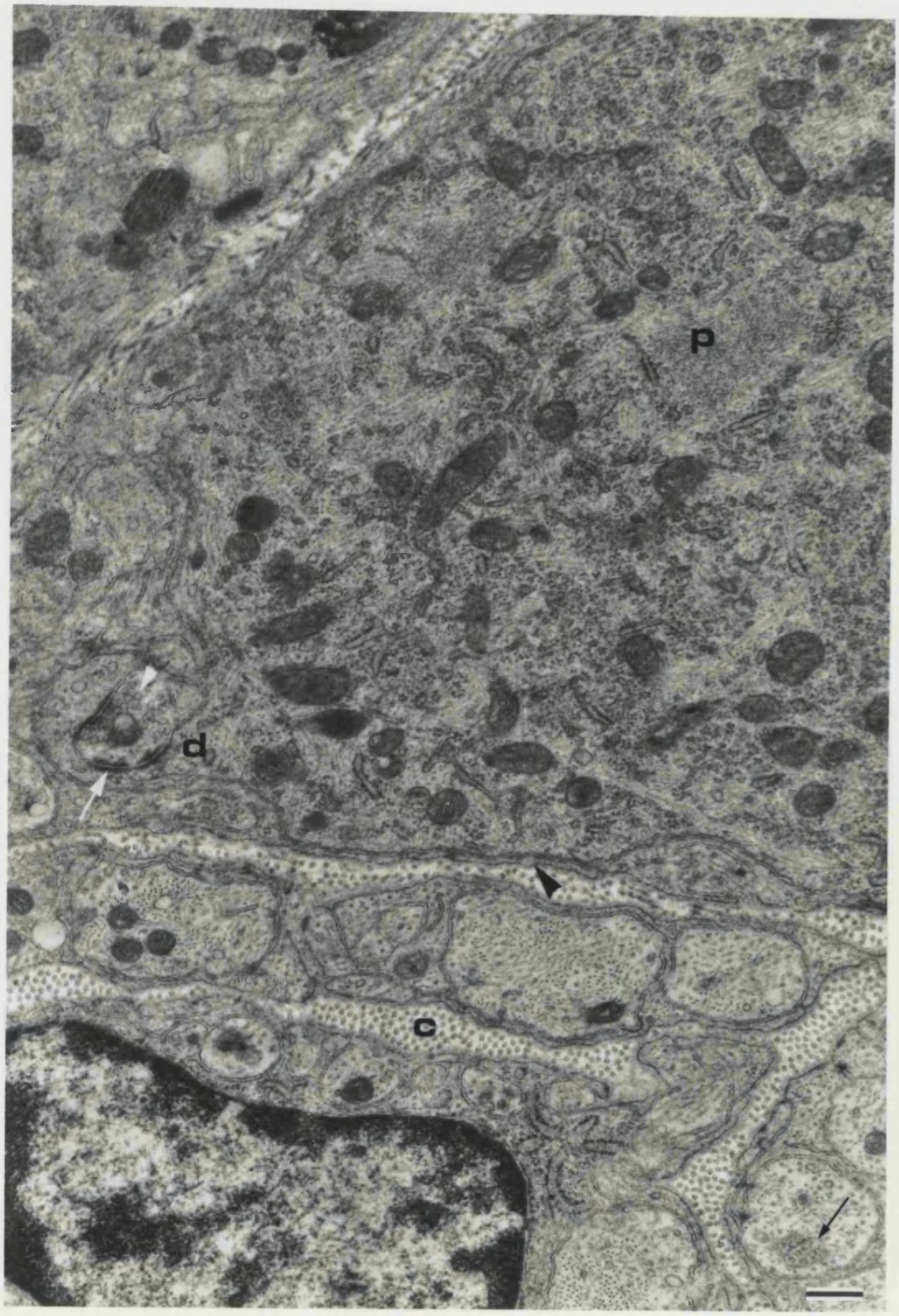
p
d
c

Figure 38

A) Electron micrograph from a pelvic ganglion of a pre-pubertal male rat showing a neuron and an associated satellite glial cell. The neuronal perikaryon surrounds the pale neuronal nucleus (**n**) and contains many organelles while the satellite cell body contains a large dense nucleus (**gn**). The boundary between the two cells is a direct apposition of the cell membranes (two black arrows).

B) Electron micrograph of a portion of a S.I.F. cell present from the pelvic ganglion of a pre-pubertal female rat. To the right is the large nucleus (**sn**) of the cell. The cytoplasm, as well as containing numerous prominent mitochondria and Golgi apparatus, also contains many characteristic dense-cored vesicles (two marked with white arrows). The cell surface is indented and in such regions is in close association with several neuronal processes in transit. One such process is packed with small clear vesicles as well as larger dense cored vesicles, although no membrane synaptic specialisation is observed.

(Scale Bar = 0.5μm applies to both **A** and **B**).

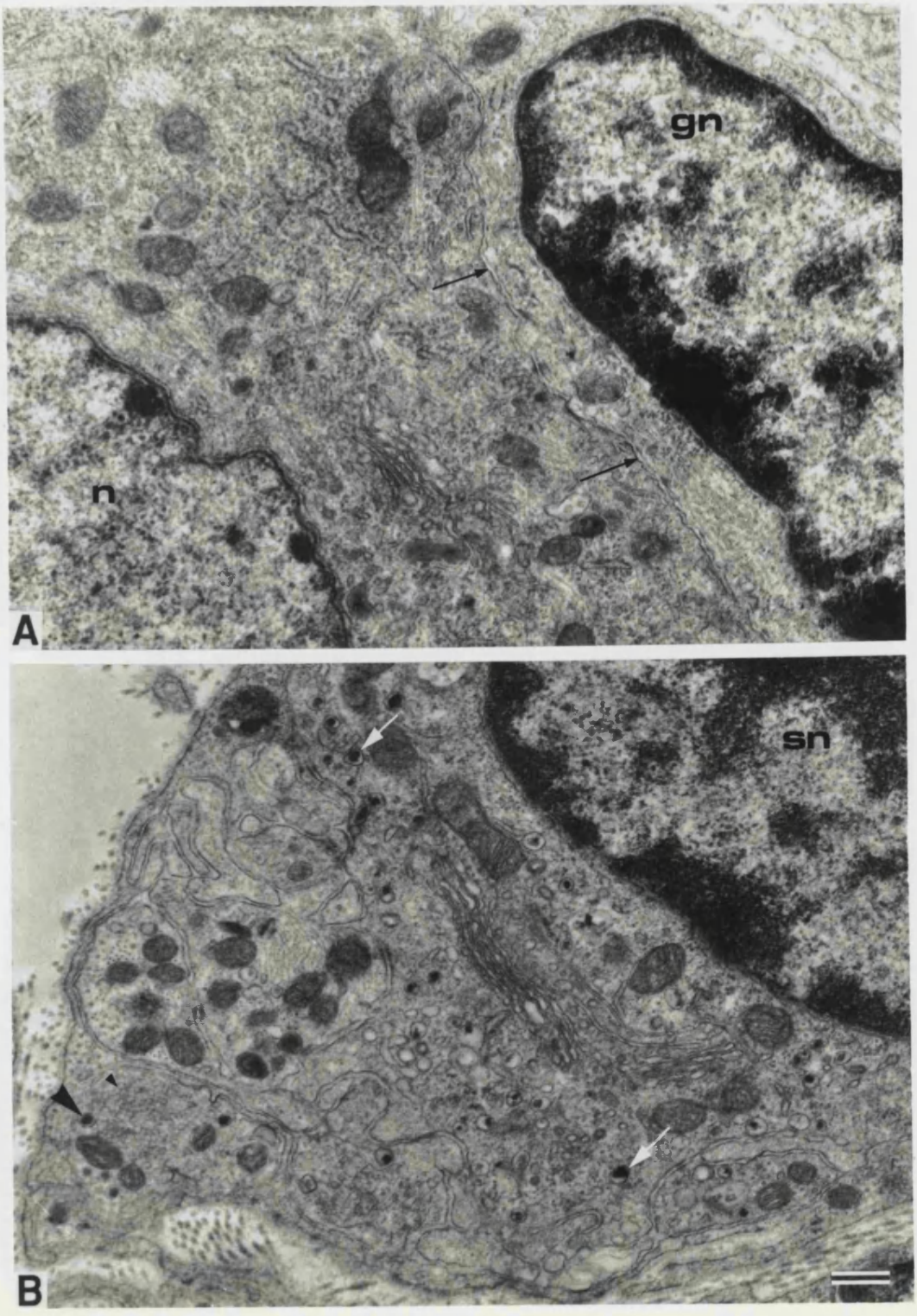
gn
n
A
sn
B

Figure 39

A) Electron micrograph of a pelvic ganglion from a pre-pubertal female rat. To the right of the micrograph is a profile of a blood vessel (lumen marked **v**). Endothelial processes (black arrowhead) extend from the cell body (where a portion of the nucleus is present [white arrow]). The neuron (left) shows a pale neuronal nucleus (**n**) that is surrounded by a characteristic perikaryon (**p**) which is rich in cell organelles.
(Scale Bar = 1μm).

B) Electron micrograph of two Schwann cells from the pelvic ganglion of a pre-pubertal male rat. Both cells possess large, dense nuclei (**sn**), and both cells extend processes that encapsulate nerve fibres. The Schwann cell towards the top of the micrograph encapsulates at least six axons (one of which is marked **a**), all of which are unmyelinated. The Schwann cell towards the bottom of the micrograph encloses only one axon (**ma**) which is myelinated. The Schwann cells and nerve processes in transit are surrounded by numerous collagen fibrils (**c**) and fibroblast processes (black arrow).
(Scale Bar = 1μm).

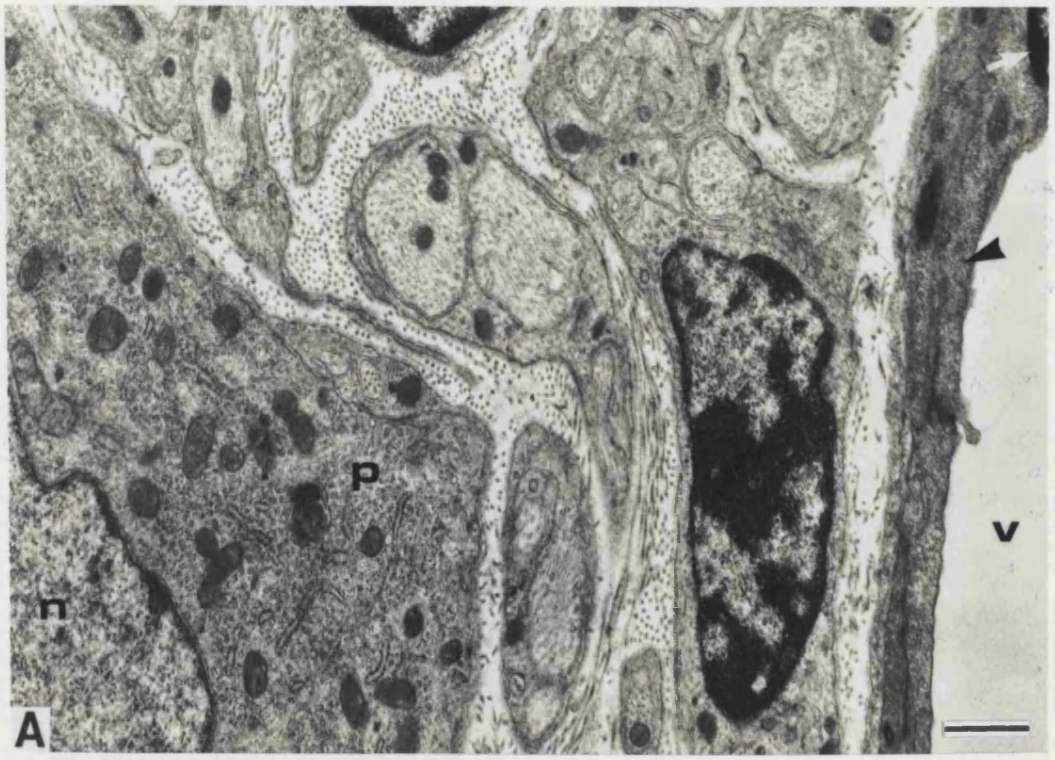
p
n
v
A

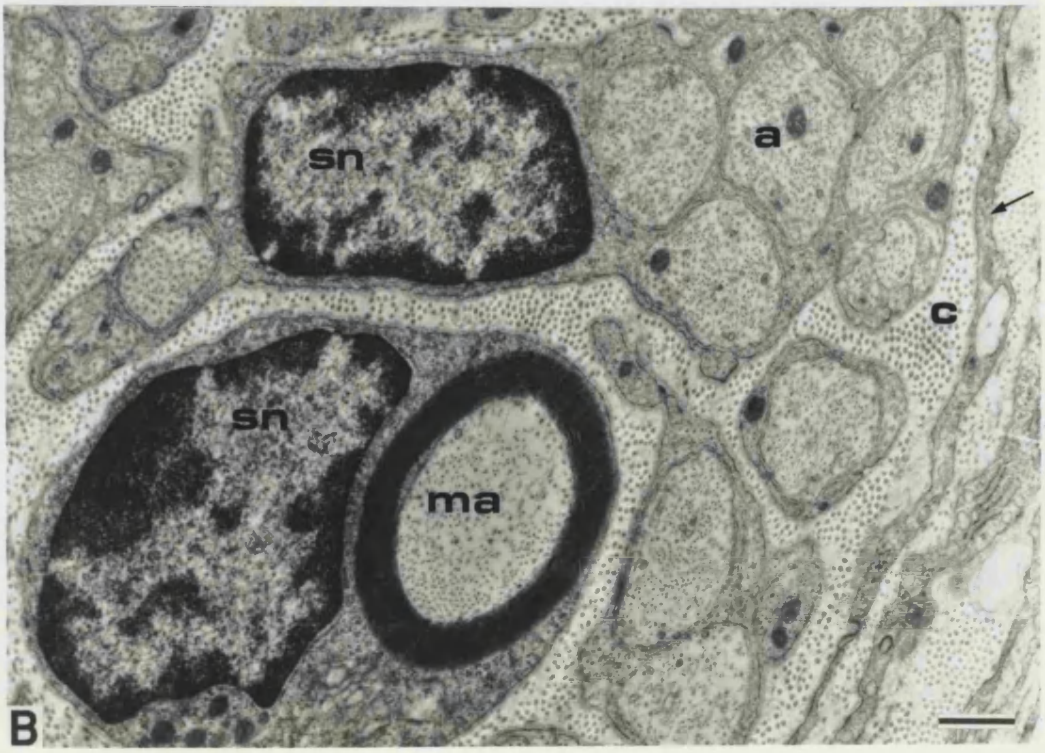
sn
a
c
sn
ma
B

Figure 40

A) Electron micrograph of the capsule of the pelvic ganglion from a pre-pubertal female rat. Five fibroblast profiles are observed, one of which contains a large, dense nucleus (black arrow). The processes form concentric lamellae arranged circumferentially to the interior of the ganglion (lower left-hand corner of the micrograph) and are interspersed with numerous collagen fibrils (**c**).
(Scale Bar = 0.5μm).

B) A high magnification electron micrograph demonstrating cytological detail of two neurons from the pelvic ganglion of a pre-pubertal female rat. One neuronal perikaryon (left) shows part of its nucleus (**n**) and is lined by a satellite cell (large black arrowhead). Amongst the organelles in evidence are two elements of Golgi apparatus (both marked with a white arrow), many mitochondria (the largest profile of which is marked with a large black arrow) and rough endoplasmic reticulum (twin black arrowheads). The other neuron (right) is also lined by a satellite cell and exhibits extensive bundles of neurofilaments, one in longitudinal section (small black arrow) and another in transverse section (small white arrow).
(Scale Bar = 0.5μm).

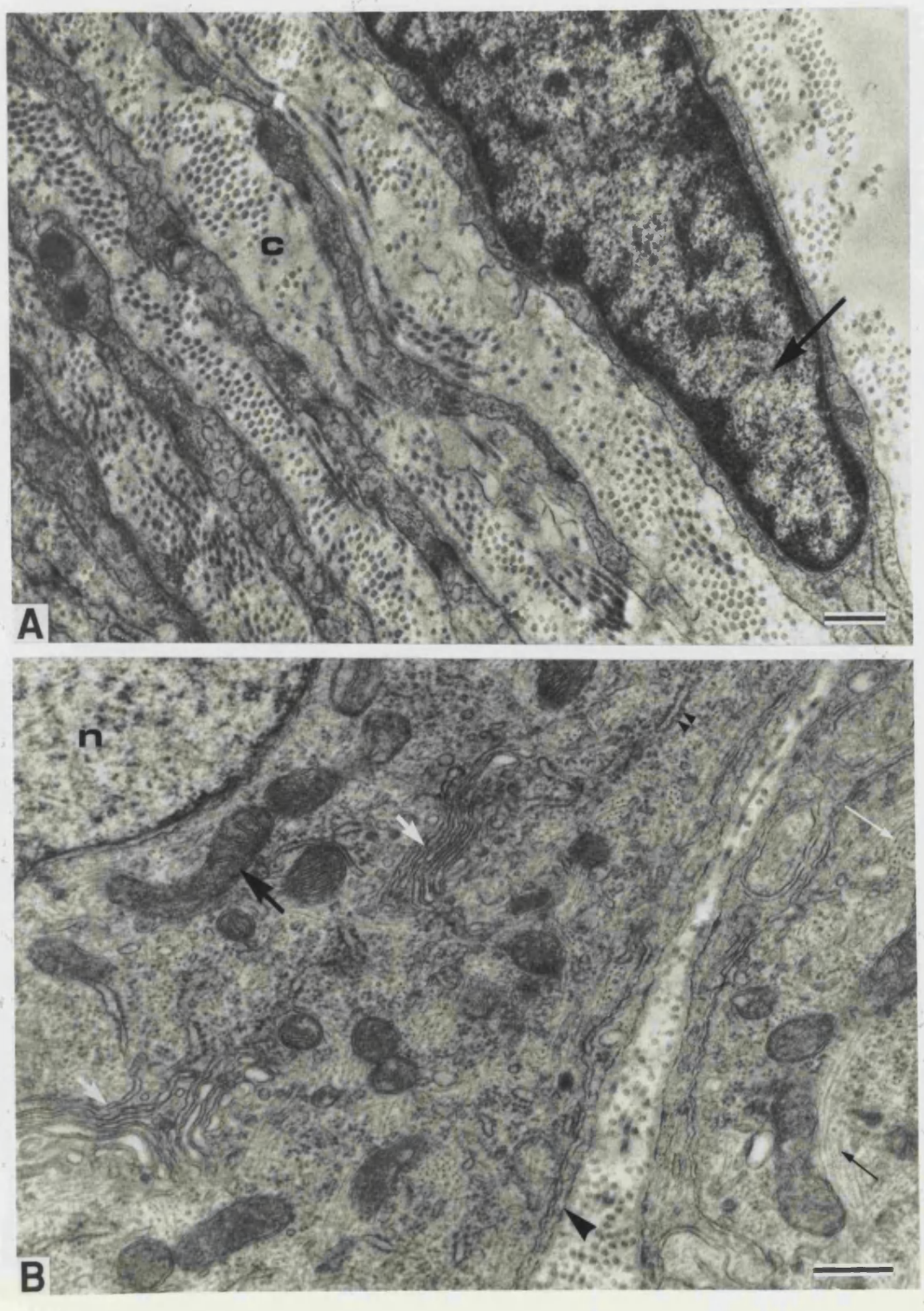
c
A
n
B

Figure 41

Cryostat sections stained for NADPH-diaphorase in **A**, **C**, **E** and **F**.

A) Pre-pubertal male rat. Neuronal perikarya display a range of staining intensities.

B) Same section as that in **A**, immunohistochemically stained for nitric oxide synthase (NOS). Note that all neuronal perikarya positive to NOS are also positive to NADPH-diaphorase in **A**.

C) Pre-pubertal female rat.

(Scale Bar = 15μm also applies to **A**, **B** and **D**).

D) Same section as that in **C**, immunohistochemically stained for nitric oxide synthase (NOS). Note that all neuronal perikarya positive to NOS are also positive to NADPH-diaphorase in **C**.

E) Longitudinal section of a pelvic ganglion from a pre-pubertal male rat. The post ganglionic nerve marked with an asterisk is the genital nerve and contains many neuronal perikarya that are positively stained for NADPH-diaphorase; the region of the ganglion closest to the emergence of the genital nerve is densely populated with NADPH-diaphorase positive perikarya.

(Scale Bar = 150μm).

F) Longitudinal cryostat section of a pelvic ganglion from a pre-pubertal female rat. The post ganglionic nerve marked with an asterisk is the genital nerve and contains very few neuronal perikarya that are positively stained for NADPH-diaphorase; NADPH-diaphorase positive perikarya are distributed throughout the body of the ganglion.

(Scale Bar = 175μm).

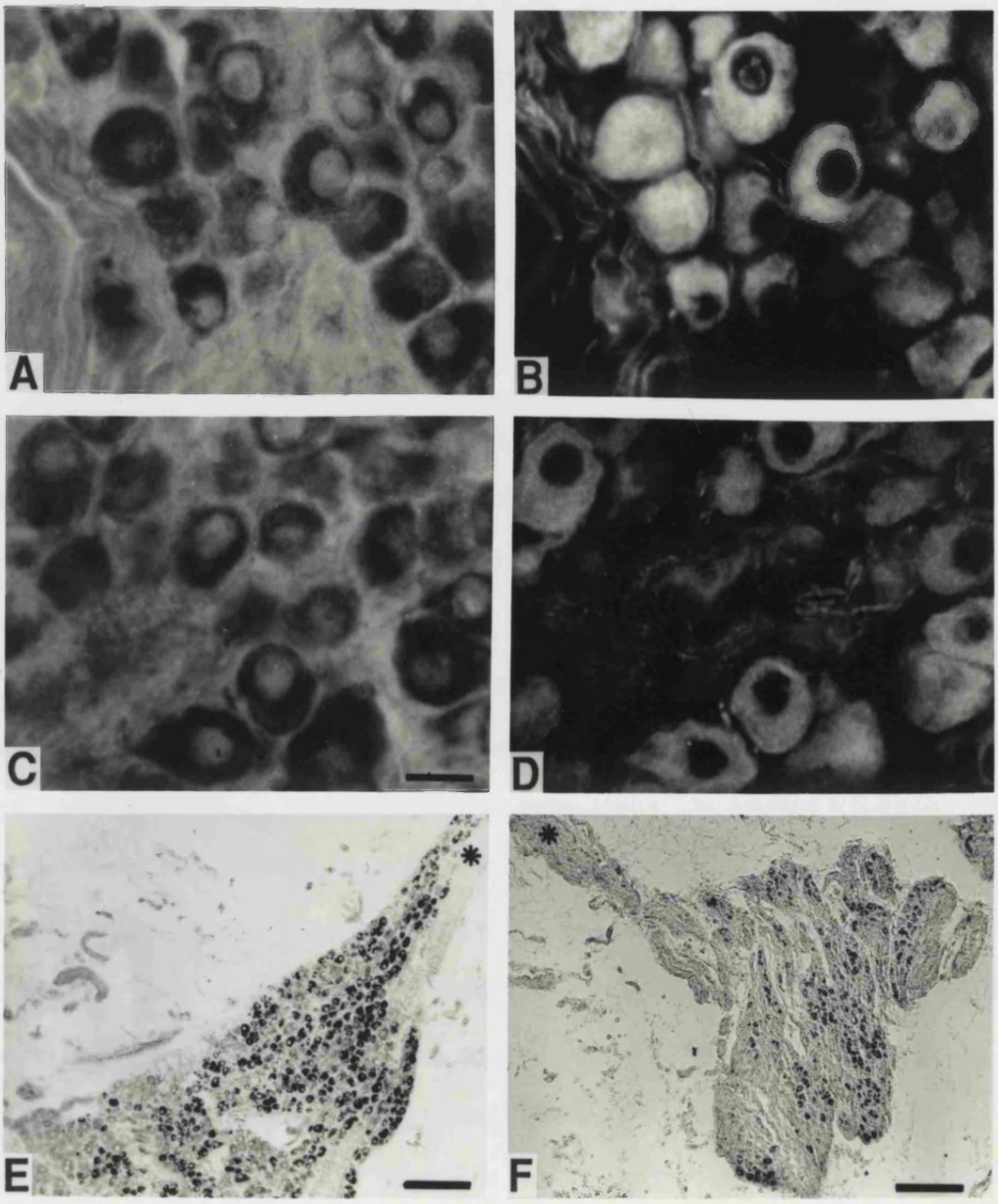
A
B
C
D
E
F

CHAPTER 5

RESULTS III: NEWBORN RATS

5.1 Anatomy of Pelvic Ganglion

Fresh dissections viewed through a dissecting microscope were used to study the pelvic plexus. Generic neuronal staining (acetylcholinesterase) helped in the identification of the comprising structures. In general the appearance of the pelvic ganglion in newborn animals of both sexes was very similar.

The major pelvic ganglion was the central element of the plexus in the female rat (Fig. 42). The ganglion was large and dominating, and was located on the lateral aspect of the vaginal wall, in its cranial most portion near the uterine cervix. The ganglion was loosely contained in parametrial tissue lying in fascia of the vaginal muscle coat; this loose attachment made dissection less difficult than in more mature animals. The ganglion measured approximately 1.5 x 2mm and, viewed from the side, was a pronounced triangular shape in stretched preparations, the ventral, dorsolateral and cranial edges all be roughly of equivalent length. On removal it became apparent that the newborn female ganglion had significant depth with extending medial volume, this also being in evidence in the computer assisted reconstructions (Fig. 44A). At the dorsal triangular point of the ganglion the multi-trunked pelvic nerve entered while the slender hypogastric nerve reached the dorsal portion of the cranial border; in some preparations a slight swelling (the hypogastric ganglion) was present at a small distance cranial from the major pelvic ganglion, some distance from the issue of the nerve from the inferior mesenteric ganglion. Numerous nerves, many containing neuronal perikarya, left the pelvic ganglion from the ventral border and travelled towards the

pelvic organs. Accessory ganglia numbering between 3 and 4, of variably size and shape, and often amalgamated into a larger mass, were found ventral and cranial to the major ganglion.

The prominent genital nerve emanated from the caudal pole of the ganglion (Fig. 42) and was observed to run to the pudendum; it appeared proportionally bigger in the newborn than in more developed female rats. The genital nerve issued small branches at intervals along its length that travelled to rectum, which also received small nerves direct from the dorsal edge of the ganglion. Situated ventral and medial from the genital nerve were numerous nerves of various sizes that ran to the vagina some of which formed plexi in the adventitia. The most ventral edge of the ganglion issued nerves that ran to the ventral surface of the bladder; these varied in thickness and numbered about eight, running both in front and behind the ureter; some also formed anastomoses with contralateral post-ganglionic nerves. Branches from these bladder nerves also ran to the cranial portion of the vagina and urethra. Nerves from the craniolateral edge of the ganglion ran to the accessory ganglia; nerves running from caudal accessory ganglia arrived at the lateral and dorsal surface of the bladder, while those issued from more cranial accessory ganglia terminated at the ureter and uterus. Branching before it reaches the pelvic ganglion, the hypogastric nerve issued the accessory hypogastric nerve which ran to the accessory ganglia near the ureter.

In the male, similarly the main aspect of the pelvic plexus was the major pelvic ganglion (Fig. 43). This was positioned in the investing fascia of the developing prostate gland; in contrast to the adult, exposure of the ganglion was simple, requiring no reflection of the vas deferens due to the presence of the testis. When viewed from the side, the ganglion was triangular in shape and measured approximately 1.5 x 2mm. It was clear with subsequent removal, and with the computer assisted reconstruction (Fig. 44B) that the ganglion extended medially and was extensively thicker than it first appeared when only viewed from the side. The multi-fascicled pelvic nerve entered the ganglion at the dorsal pole, and the slender hypogastric nerve entered the ganglion midway along its cranial border. Many nerves left the pelvic ganglion from the ventral border and travelled towards the pelvic organs; neuronal perikarya were often present within these nerves (undocumented

observations). Lying close to the ureter and vas deferens were between 2 and 4 accessory ganglia which again were sometimes amalgamated into a larger continuous structure.

Running from the caudal pole of the ganglion was the genital nerve; this was the most prominent postganglionic nerve and reached the corpus cavernosum. The rectum received branches that ran at intervals from the proximal portion of the genital nerve, and other small nerves directly from the dorsal edge of the ganglion. The prostate gland was supplied by numerous small nerves that ran from the ventral border of ganglion. From the most ventral edge and pole of the ganglion emanated nerves that ran to the ventral portion of the bladder; these numbered about eight, were of various sizes and ran in front and behind the ureter with branches that reached the urethra; some also formed contralateral anastomoses. The accessory ganglia were connected by nerves running from the craniolateral edge of the ganglion. Running from the most caudal accessory ganglia emerged nerves that supplied the lateral and dorsal surface of the bladder, while more cranial accessory ganglia terminated at the ureter and the vas deferens. The hypogastric nerve separated, before it reached the pelvic ganglion, into two branches, the main and accessory hypogastric nerves; this accessory hypogastric nerve reached the accessory ganglia near the ureters.

Ganglia in both sexes appeared more prominent in their respective topographical positions than in the more mature animals due their increased relative size (compared to the adjacent immature pelvic viscera) and total absence of peritoneal adipose tissue. Overall the gross morphology of the main body of the ganglia in both sexes was very similar, neither one or other sex demonstrating a noticeable difference in size. The newborn ganglia in both sexes had less lobed portions proximal to post-ganglionic nerves and the marked protrusions in the ganglion body of adult animals were absent.

5.2 Histology of Pelvic Ganglion

5.2.1 General Histology

There was a marked comparability in the histology of ganglia from rats of both sexes.

5.2.1.1 Capsule

Although having a clear boundary demarcation, the ganglia in both sexes had a much reduced, and in some areas almost absent capsule (Fig. 45 & 46). Where encapsulating

structures were visible they appeared fine and delicate. The septa observed dividing the ganglia in more mature animals were absent, although a limited separation was visible in regions near the exit of post ganglionic nerves.

5.2.1.2 Neurons

There was a great uniformity in the appearance of neurons in the ganglia from both sexes (Fig. 46). The neurons were more circular than those seen in older animals. Each displayed a prominent nucleus that seemed to inhabit proportionally more of the cytoplasm than was the case in mature counterparts. Numerous nucleoli (1-4) were also clearly visible and these structures were more conspicuous than was the case in adult animals. Glial cell nuclei were visible loosely associated with the neuronal cell bodies; no clear glial cell encapsulation was observed at the light microscopic level (Fig. 46).

5.2.1.3 Cell Packing

The newborn ganglion neurons were packed densely within the ganglion; many neurons lay close to one another with little or no intervening neuropil (Fig. 46). Overall the quantity of neuropil appeared far less than that in the more mature animals, and areas primarily composed of nerve fibres were also less obvious than in histological section from older rats.

5.2.1.4 Blood Vessels

Profiles of blood vessels, often still containing erythrocytes due to incomplete perfusion, were visible throughout the ganglion and were usually in transverse section. Some vessels, presumably arterioles, displayed thicker walls; endothelial cells bodies could often be distinguished in the walls of some blood vessels (Fig. 46).

5.2.1.5 Other Cell Types

Clusters of smaller cells were observed in ganglia of both sexes. These had nuclei that were proportionally larger relative to cell size as compared to those of principle neurons, and these were identified as developing S.I.F. cells (Fig. 46).

5.2.2 Ganglion Volume

The average ganglion volume estimated by the Cavalieri method (example of sections in Fig. 47) was very similar in newborn male and female rats. In 3 newborn male rats ganglion volume ranged from 48 $x10^6\mu m^3$ to 77 $x10^6\mu m^3$ with an average value of was 66 $x10^6\mu m^3$

± 16 (66 million cubic microns or approximately 0.06mm^3). In the female animals ganglion volumes ranged between 49 x10$^6\mu$m^3 and 66 x10$^6\mu$m^3 with an average value of 59 x10$^6\mu$m^3 ±9 (59 million cubic microns or approximately 0.06mm^3) (P>0.10 with application of t-test, see Appendix 5).

5.2.3 Nerve Cell Size

Neuron size (the area of the largest profile of a neuron identified from serial sections at 2μm intervals) was measured in the ganglia from 3 adult male and 3 adult female rats; roughly one hundred neurons were measured in each animal. The largest sectional profile of a neuron always displayed the nucleus. In both male or female rats, there was a small, continuous range of nerve cell sizes, and gave no indication of sub-classes (Graph 6 & 7). In male rats the neurons ranged in size from 33μm^2 to 179μm^2 and mean neuronal cell sizes from 3 animals ranged from 80μm^2 to 83μm^2 and the average of the means was 81μm^2 ± 2. In female rats neurons ranged in size from 32μm^2 to 177μm^2 and mean neuronal cell size from 3 animals ranged between 77μm^2 to 82μm^2 and the average of the means was 80μm^2 ± 3. The data reveals little variability in neuron size ranges and means neuron sizes between ganglia of animals of the same age and sex. There was no significant difference between the average neuronal sizes in pelvic ganglia of newborn male animals compared to those in the female.

5.2.4 Neuron Number

Ganglia from newborn male rats exhibited estimated neuronal cell numbers ranging from 10,989 to 13,531 with an average of 12,604 ± 1403. In the female neonates this estimated populations ranged from 10,652 to 12,384 with an average of 11,640 ± 892. Neuronal populations of pelvic ganglia from newborn animals therefore displayed no statistically significant gender difference.

5.3 Cytology of Pelvic Ganglion

5.3.1 Transmission Electron Microscopy

5.3.1.1 Neurons

The dominant feature of the neuronal cell bodies was a large nucleus (Fig. 48 & 49). Electron dense material (presumably chromatin) appeared to be less uniformly spread throughout the nucleus than in more mature animals and was generally more clumped, especially close to the nucleolemma (Fig. 48). Multiple nucleoli were present in many nuclei (Fig. 50A). Bi-nucleate neurons were not observed in animals of either sex.

Rough endoplasmic reticulum and polysomes were plentiful throughout the perikaryon (Fig. 50B) as were small mitochondria that generally exhibited cisternae in transverse section (Fig. 50A). Golgi apparatus was also common usually positioned close to the nucleus and multivesicular bodies were (often containing electron dense material) of various shapes and sizes were distributed throughout the cytoplasm. Structures identified as neurofilaments and microtubules were observed.

Vacuolated neurons were not observed, although in some perikarya sizeable vacuoles were seen but not to the extent at which the cell would fit the characteristics of a large vacuolated neuron.

5.3.1.2 Synapses

Many large fibres, presumably varicosities in cross section, were observed abutting the somatic membranes of many ganglion cells but synapses were not observed. The neuronal cell body membrane also appeared less complicated in structure than that of adult animals in that, rather than intricate intracapsular dendritic mounds, the somal surface was not highly cavernous (Fig. 50B).

5.3.1.3 Glia

Glial cells displaying their nuclei and a limited amount of cytosol were common, but in contrast to adult animals complete encapsulation of neurons was not observed (Fig. 48, 49 & 50A). Some glial cells were clearly associated with a particular neuron which was partially in contact with the glial cell processes (Fig. 50A). Other neurons had no associated glial cells, while another group of neurons exhibited a situation between these two extremes,

where although there was no close glial contact, satellite cells were present close by the neuronal soma Fig. 48). Many neurons were extremely close to one another and cells that had no glial association demonstrated extensive membrane/membrane contact with neighbouring neurons (Fig. 48 & 49).

5.3.1.4 Fibres in Transit

Usually toward the periphery of the ganglia were sizeable groups of fibres in cross section. All these fibres appeared to be unmyelinated although many at a time were in close association with a cells with a large dense nucleus identified as a Schwann cell. Mitochondria were often present within the fibres and as well as neurofilaments and microtubules (Fig. 50B).

5.3.1.5 Connective Tissue

Generally the components of the ganglia were densely packed and there was very little extracellular space. The neuron to neuropil ratio was high and while collagen fibres was observed throughout ganglia overall connective tissue was small (Fig. 48 & 49).

5.3.1.6 Blood Vessels

Endothelial cells forming blood vessels were seen throughout the ganglia. These cells were convoluted in appearance giving the vessel lumen a less smooth surface than that in more mature ganglia.

5.3.1.7 Other Cell Types

Clusters of cells with dense core vesicles (Fig. 52) distributed uniformly in the cytosol were present throughout the ganglia, and especially close to blood vessels (Fig. 51). These cells were identified as S.I.F. cells and were often in direct soma-soma contact with neighbouring S.I.F. cells (Fig. 51). Identification of these cells was not always strait forward as some cells demonstrated a lower concentration of dense core vesicles present only at the cell membrane and also a less electron dense nucleus reminiscent of that of a principal neuron.

Other blood borne cells were observed including mast cells with their characteristic secretory vesicles, eosinophils and neutrophils with characteristic lobulated nuclei.

5.4 Developmental Cell Death

5.4.1 Newborn

Peroxidase visualised TUNEL staining was observed in neuronal cells of ganglia from both male and female animals. Staining was very sparse; although quantitation was not undertaken, it appeared that no more than between 4-6 stained cells were observed in an entire ganglion section. The dark peroxidase stain was restricted to the nucleus of positively stained cells, indicating the specific site of action of this method.

5.4.2 Week Old

Nuclear TUNEL staining was observed in neurons in ganglion sections from 7 day old animals of both sexes (Fig. 53). In contrast to the neonates, a gender difference was apparent in this age group, where, although absolute quantitation was not performed, positive TUNEL staining seemed more abundant in the neurons of ganglia from female rats. Whereas in the male, the largest section from a serially cryosectioned ganglion yielded few positive cells (1-2), such a maximal section of a ganglion from a female rat sometimes revealed as many as 8 positively stained neurons.

GRAPH 5

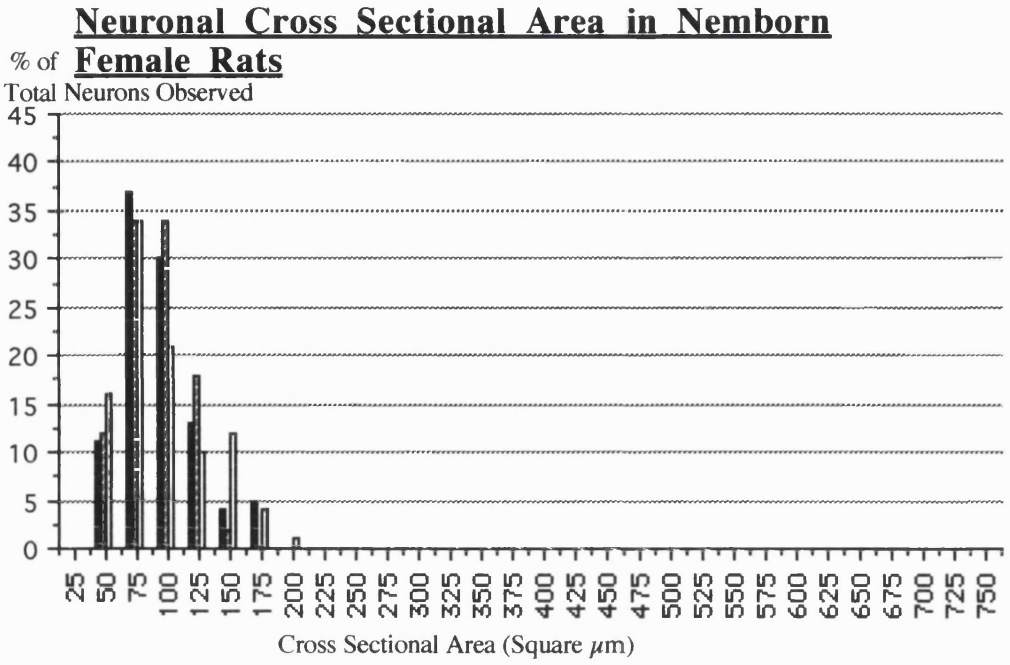

GRAPH 6

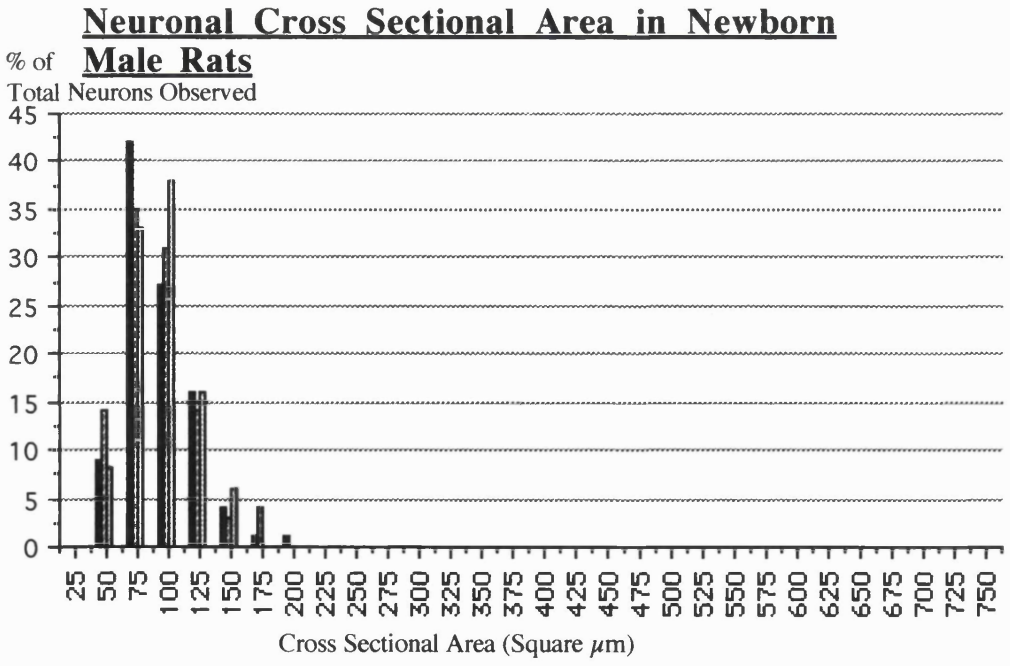

Figure 42

Side view of an acetyl cholinesterase stained preparation (Top) and diagrammatic representation (Bottom) of the left pelvic viscera and pelvic plexus of a **newborn female** rat. In the diagram neural structures have been represented by filled black artwork. For clarity only two small portions of the enteric plexus have been shown and only one accessory ganglion labelled.

(Scale Bar = 1.25mm)

AG	Accessory Ganglion
BL	Bladder
ET	Enteric Plexus
GN	Genital Nerve
HN	Hypogastric Nerve
MPG	Major pelvic Ganglion
PN	Pelvic Nerve
RT	Rectum
UA	Urethra
UR	Ureter
UT	Uterus
VA	Vagina

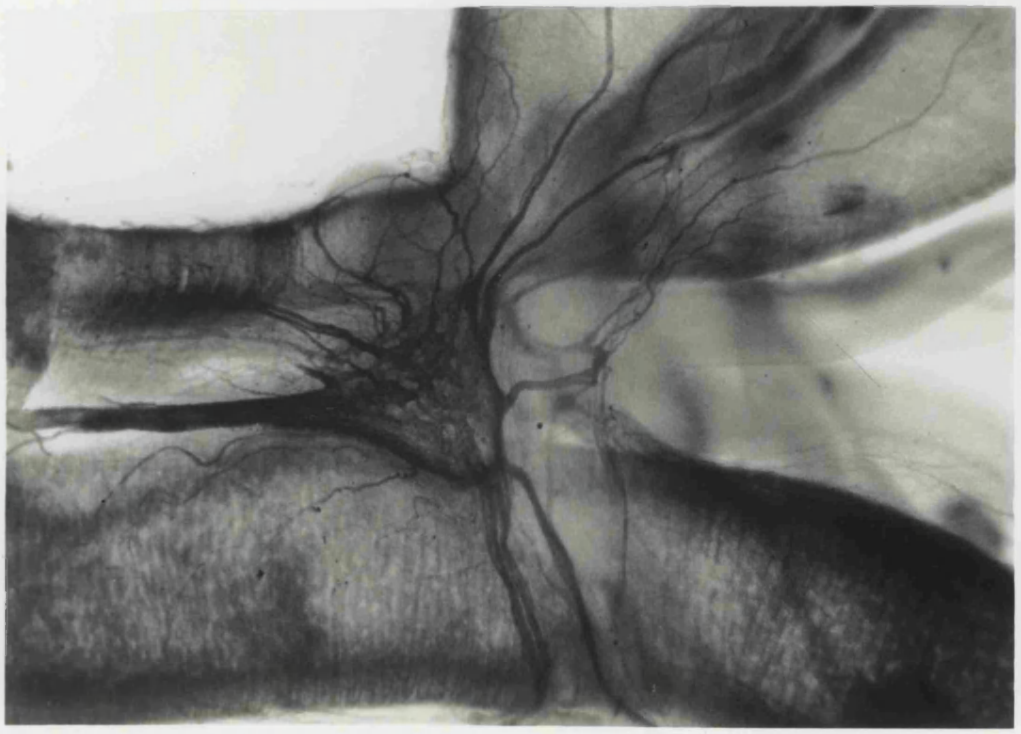

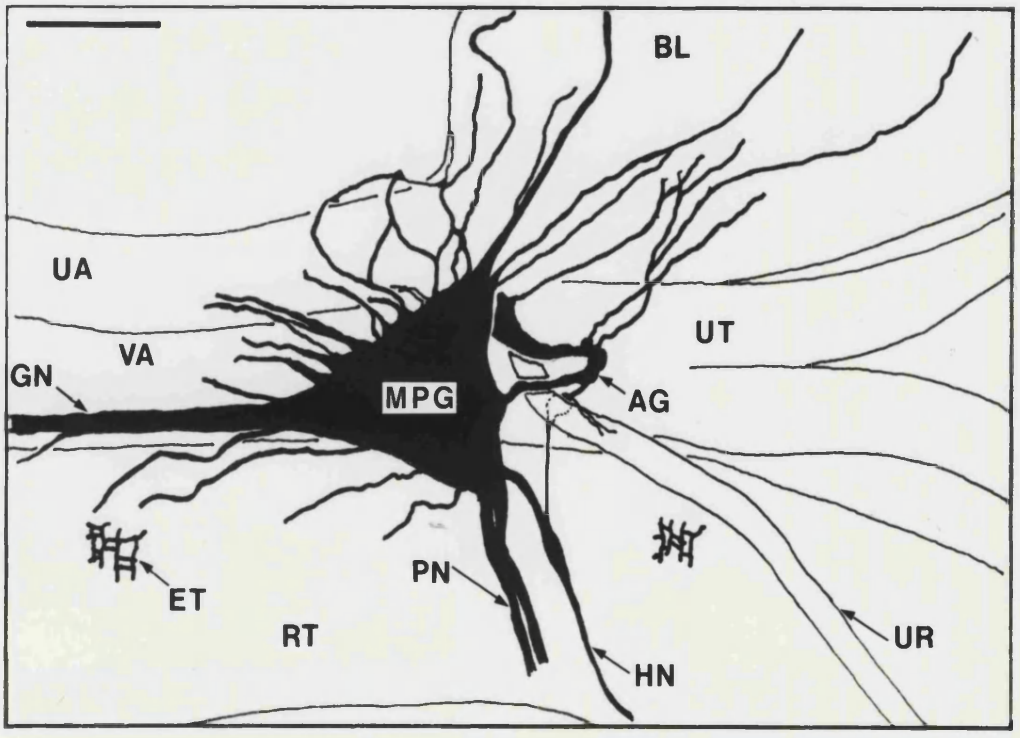
BL
UA
VA
UT
GN
MPG
AG
ET
PN
RT
UR
HN

Figure 43

Side view of an acetyl cholinesterase stained preparation (Top) and diagrammatic representation (Bottom) of the left pelvic viscera and pelvic plexus of a newborn male rat. In the diagram neural structures have been represented by filled black artwork. For clarity only two small portions of the enteric plexus have been shown.
(Scale Bar = 1.25mm)

AG	Accessory Ganglion
BL	Bladder
ET	Enteric Plexus
GN	Genital Nerve
HG	Hypogastric Ganglion
HN	Hypogastric Nerve
IMG	Inferior Mesenteric Ganglion
MPG	Major pelvic Ganglion
PN	Pelvic Nerve
RT	Rectum
TE	Testis
UA	Urethra
UR	Ureter
VD	Vas Deferens

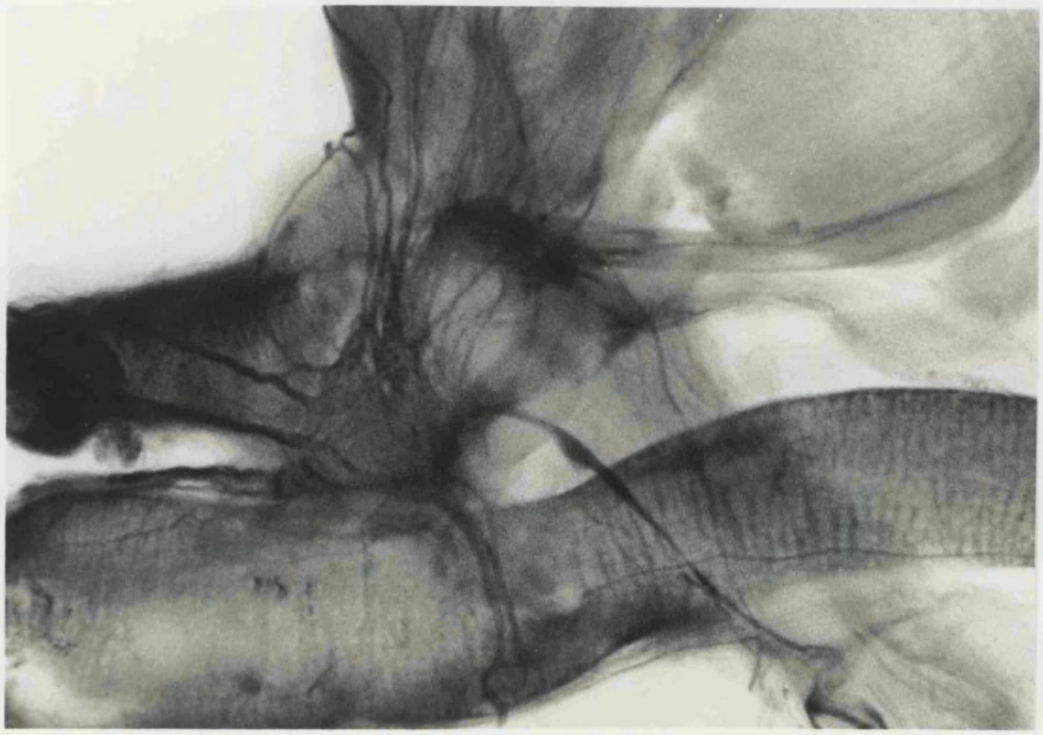

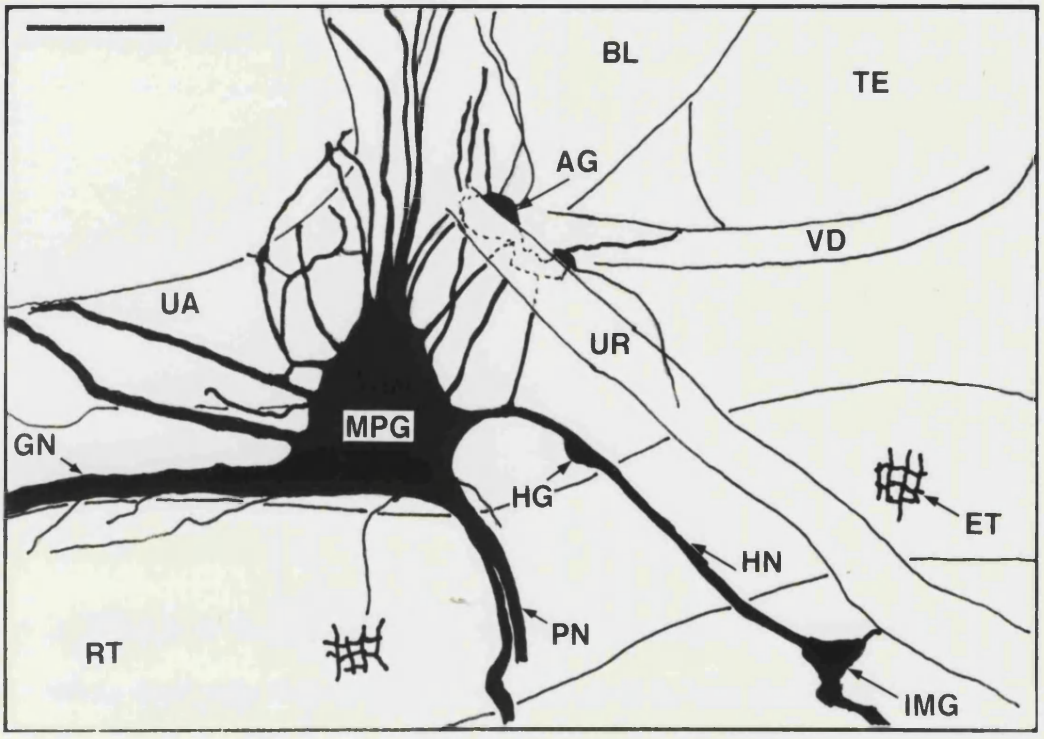
BL
TE
AG
VD
UA
UR
MPG
GN
HG
ET
HN
PN
RT
IMG

Figure 44

Line drawings representing the three dimensional outline of sections, 50μm apart, from pelvic ganglia of newborn rats.

A) Female

Note the barrel shape of the ganglion demonstrating extensive medial depth. (Axis bars applies to both: **V**, ventral; **M**, medial; **Cr**, cranial; **D**, dorsal; **L**, lateral; **Ca**, caudal).

B) Male

Note the shape shows marked medial depth. The elongation from the ventrocaudal edge represents the emergence of the post-ganglionic genital nerve.

(Scale Bar = 500μm applies to both)

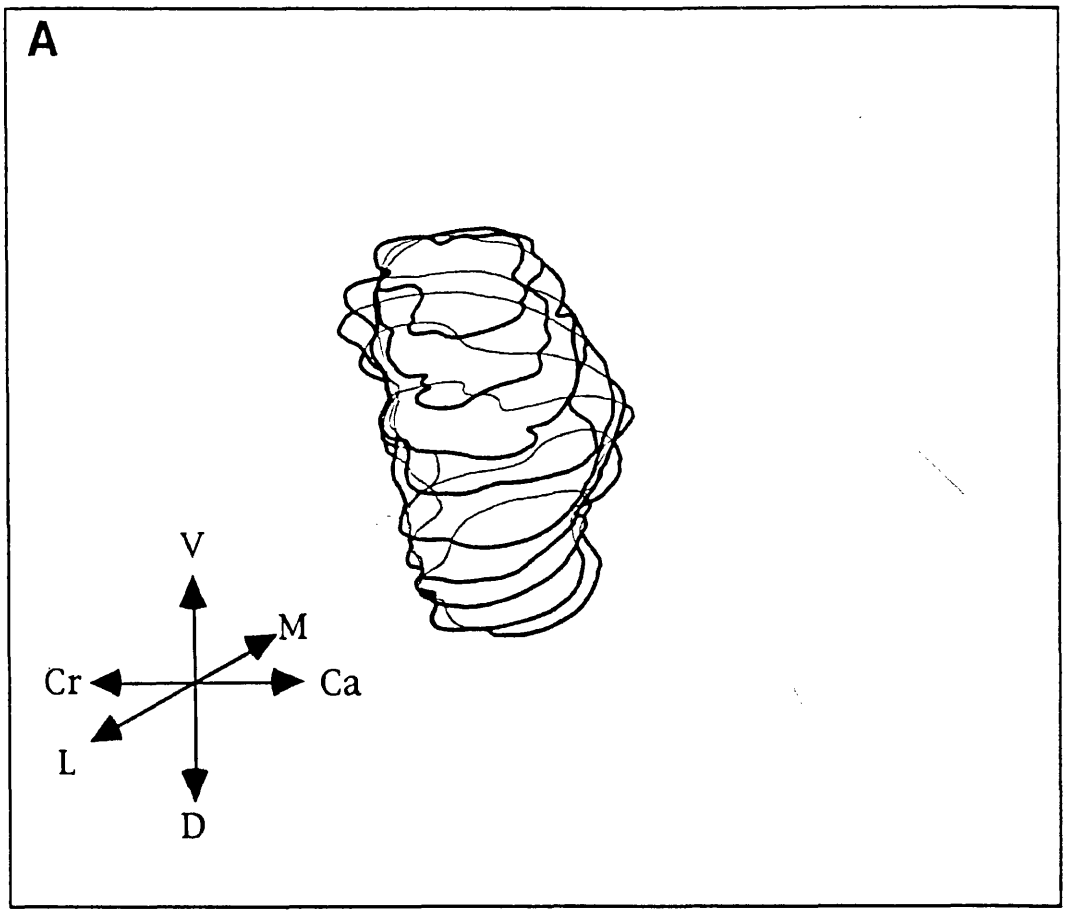
A
V
M
Cr
Ca
L
D

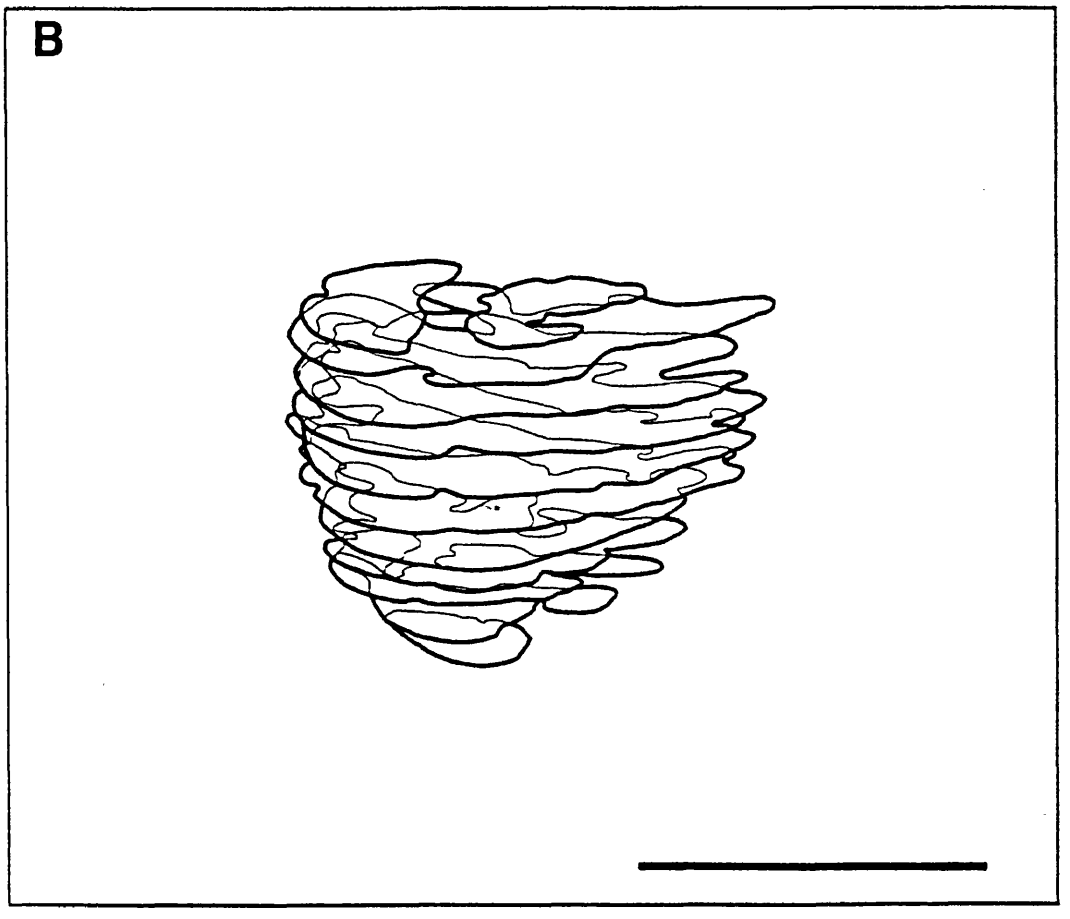
B

Figure 45

Light micrographs of major pelvic ganglia from new-born rats.

A) Male. The ganglion is covered by a diffuse outer capsule (arrowhead). The numerous neurons within the ganglion are observed partially separated by spaces surrounding developing blood vessels (arrow).

B) Female. The ganglion is covered by a diffuse outer capsule (arrowhead) and has a large developing blood vessel (possibly an arteriole) (arrow) passing through it. The numerous neurons can be seen within the ganglion. (Scale Bar = 50μm applies to both).

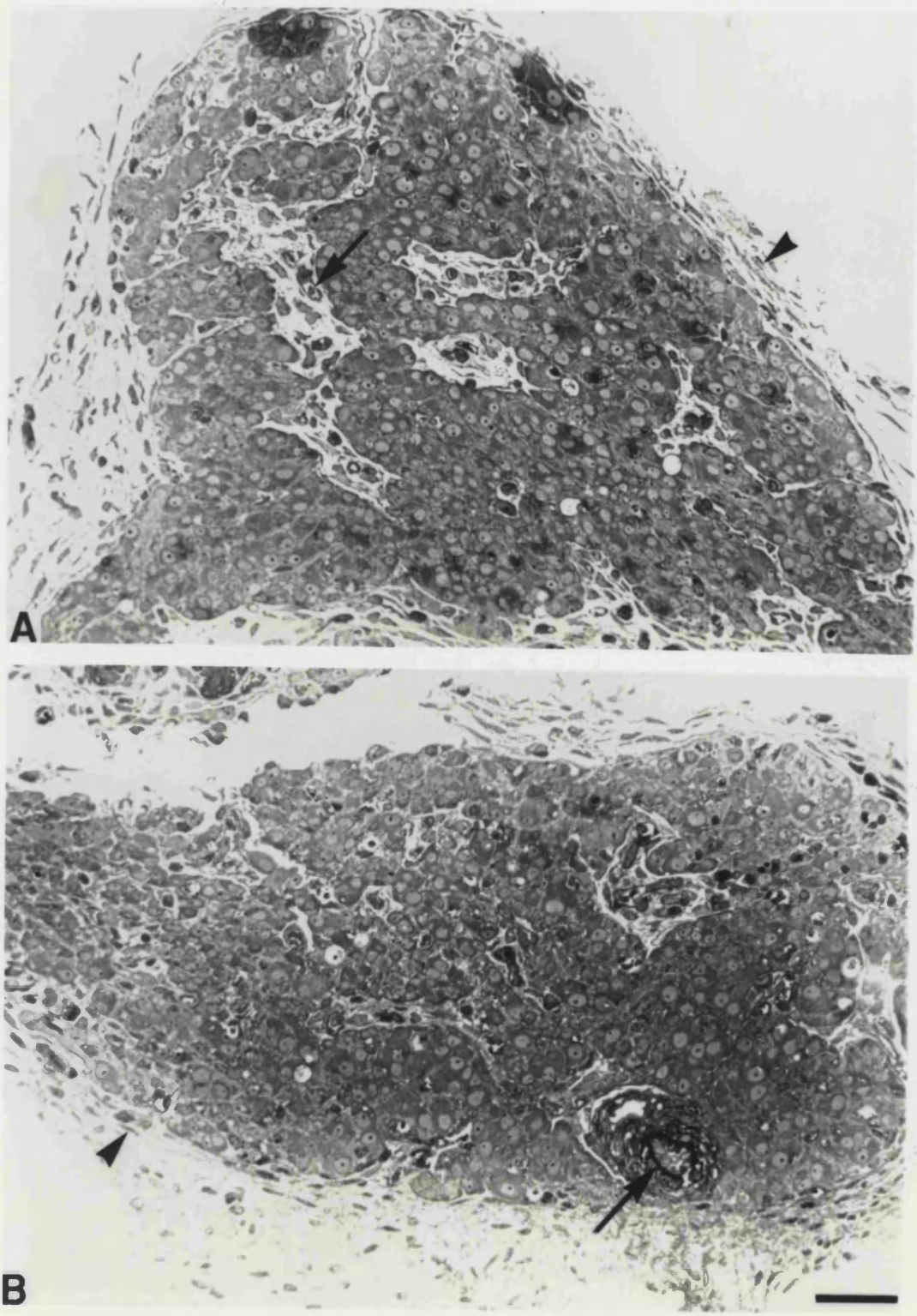
A
B

Figure 46

Light micrographs of major pelvic ganglia from new-born rats.

A) Male. Major cell types of the developing ganglion: **e**, endothelial cell; **f**, nucleus of fibroblast; **g**, nucleus of satellite glial cell; **n**, ganglion neurons dominated in appearance by their pale nuclear profiles; **s**, nucleus of a small intensely fluorescent (SIF) cells. Fibroblastic processes form the immature outer capsule (twin arrowheads) and beginnings of septa (arrowhead).

B) Female. Major cell types in the developing ganglion: **e**, endothelial cell; **f**, nucleus of fibroblast; **g**, nucleus of satellite glial cell; **n**, ganglion neurons many of which display pale nuclear profiles. Fibroblastic processes form the immature outer capsule (twin arrowheads) and segregating septa (arrowhead).

(Scale Bar = 20μm applies to both).

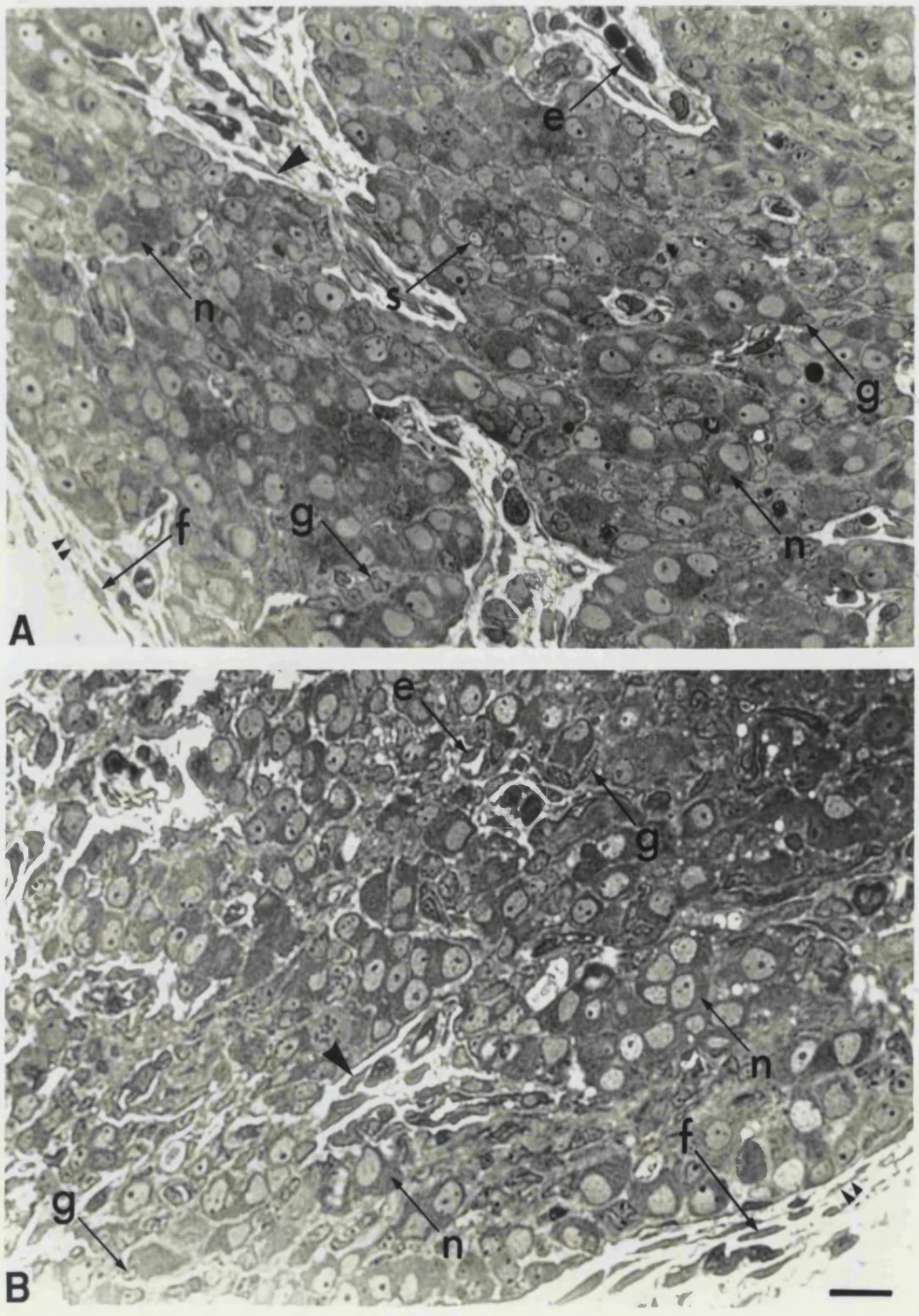
e
n
s
g
f
g
n
A
e
g
n
f
g
n
B

Figure 47

Five (numbered 1-5) serial resin sections (2μm thick) of a pelvic ganglion from a newborn male rat. The sections are stained with toluidine blue and each is separated from the next by 100μm. (Scale Bar = 250μm).

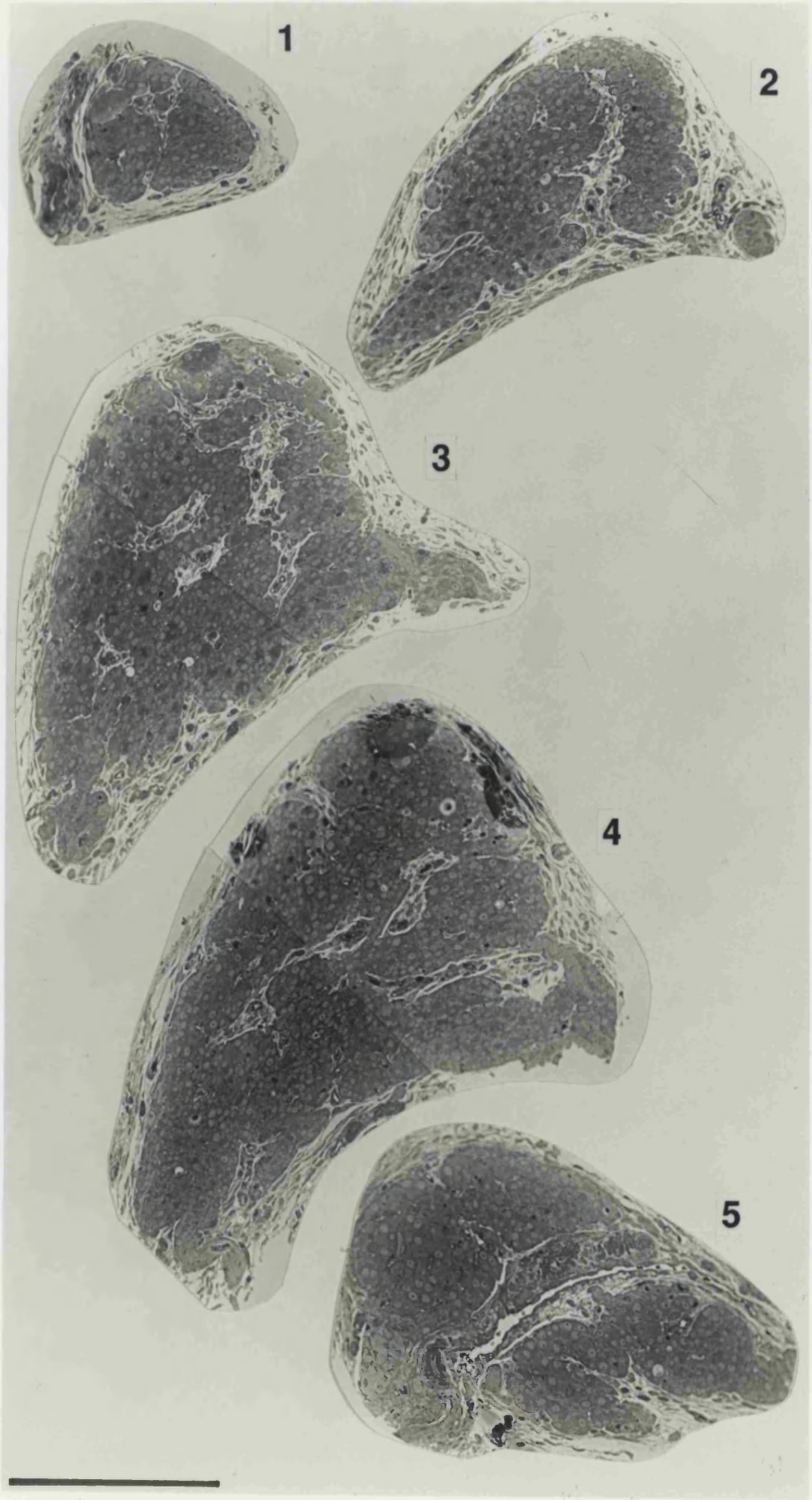
1
2
3
4
5

Figure 48

Electron micrograph from the pelvic ganglion of newborn female rat showing two developing neurons. The neurons exhibit prominent neuronal nuclei (**n**). Loosely associated to one neuron is a developing glial cell with has a dense nucleus (white arrow) but does not demonstrate encapsulation of the neuron. An area of neuronal soma-soma contact (arrowhead) is present in the lower neuron. Practically no extracellular space is evident and generally the tissue is densely packed. The area boxed is shown at higher magnification in Fig. 50B.

(Scale Bar = 1.2μm).

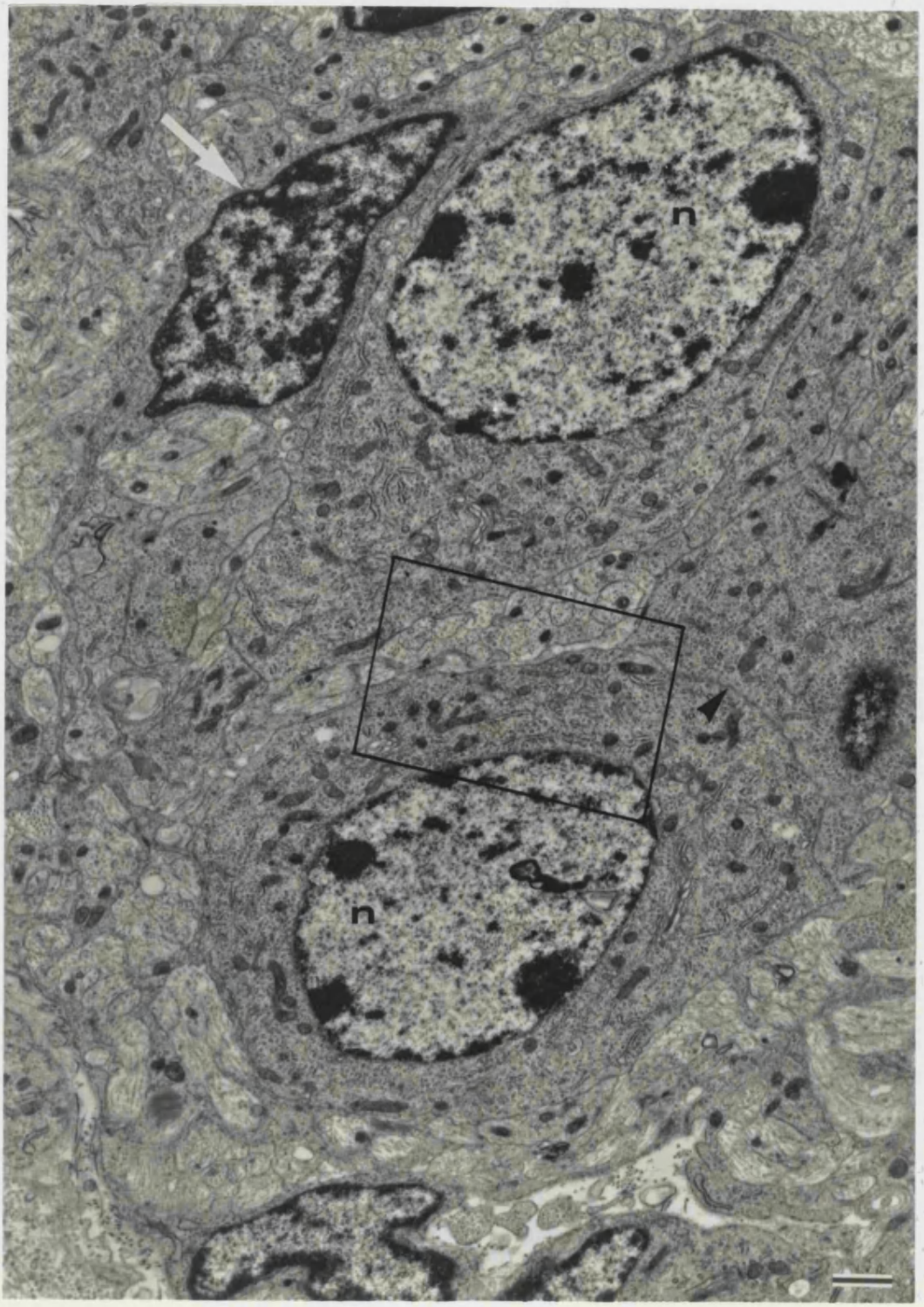
n
n

Figure 49

Electron micrograph from the pelvic ganglion of newborn male rat showing three developing neurons. The neurons exhibit prominent neuronal nuclei (**n**), and are packed closely together with no glial cell encapsulation present. Extensive areas of neuronal soma-soma contact (white arrows) are evident. (Scale Bar = 1.2μm).

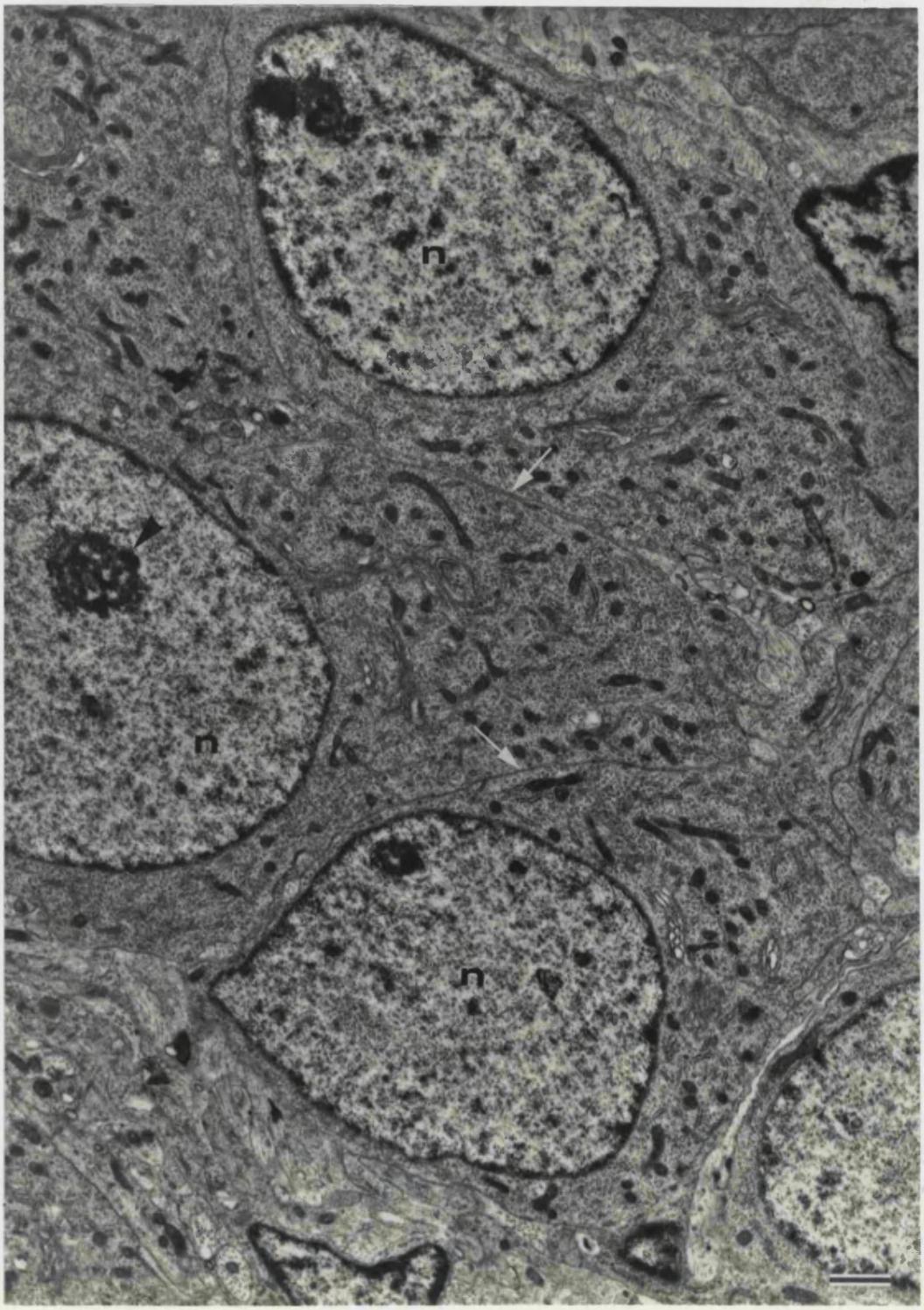
n
n
n

Figure 50

A) Electron micrograph showing a neuron and associated glial satellite cell from a pelvic ganglion of a newborn female rat. The prominent neuronal nucleus (**n**) exhibits two nucleoli (one arrowed [black]). The neuronal perikaryon contains many mitochondria (black arrowhead). The more dense satellite cell nucleus (white arrow) is surrounded by a limited cytoplasm but does not seem to form a full sheath around the neuron. The neuron is present in a less densely packed area of the ganglion with a greater extracellular space; collagen fibrils (**c**) are widely distributed in this space.
(Scale Bar = 1.2μm).

B) Higher magnification electron micrograph of the area boxed in Fig. 48. A portion of a developing neuron from a pelvic ganglion of a newborn male rat is shown and demonstrates a pale granular nucleus (**n**) and a perikaryon packed with rough endoplasmic reticulum (arrowhead). Close by to the neuron is a group of unmyelinated fibres in transit (**a**) (presumably axons) which contain mitochondria (large black arrow) and neurofilaments (small black arrow). Again, there is no glia between the neuronal perikaryon and the bundle of nerve processes. (Scale Bar = 1μm).

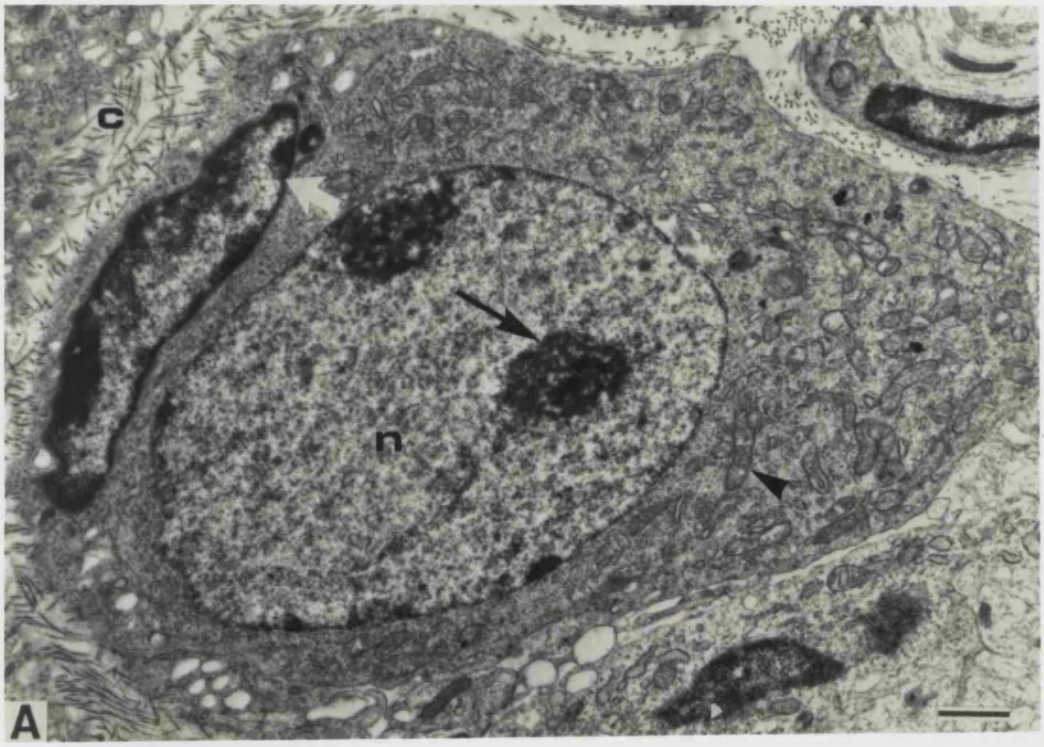
c
n
A

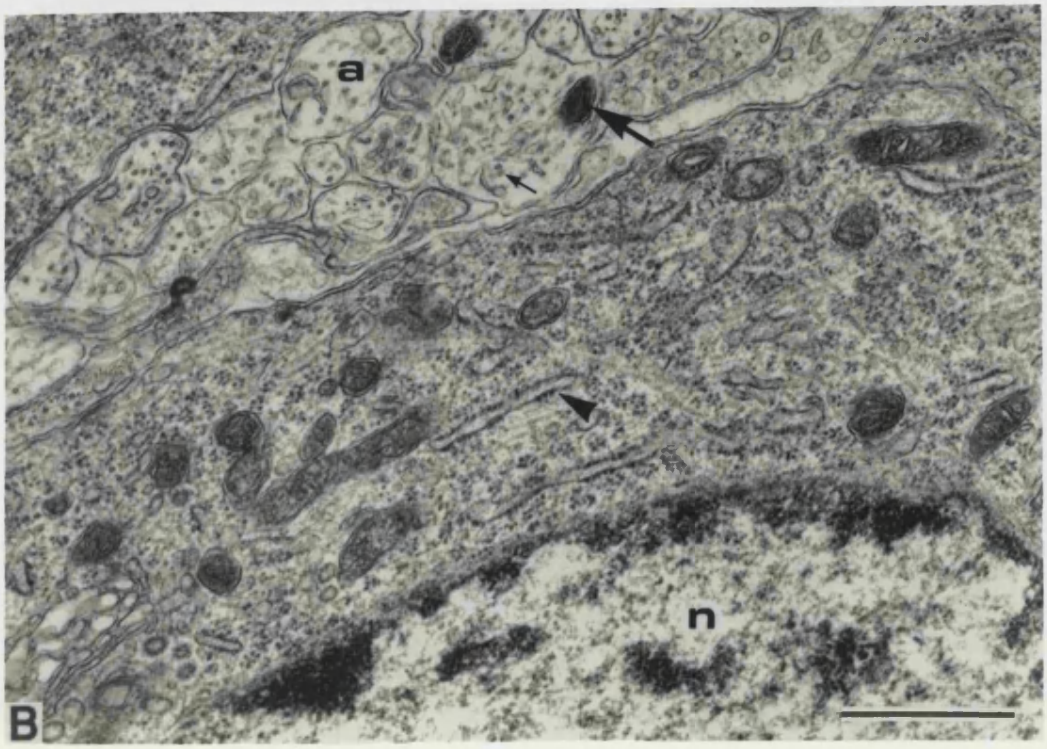
a
n
B

Figure 51

Electron micrograph from the pelvic ganglion of newborn female rat showing a developing S.I.F. cell. A large nucleus (sn) dominates the cell, which is positioned close to another S.I.F. cell; an area of soma-soma contact exists between the two cells, along which a desmosome (small white arrow) is observed. The S.I.F. cell is close by to a blood vessel (lumenal surface - large white arrow) which still contains erythrocytes.
(Scale Bar = 1μm).

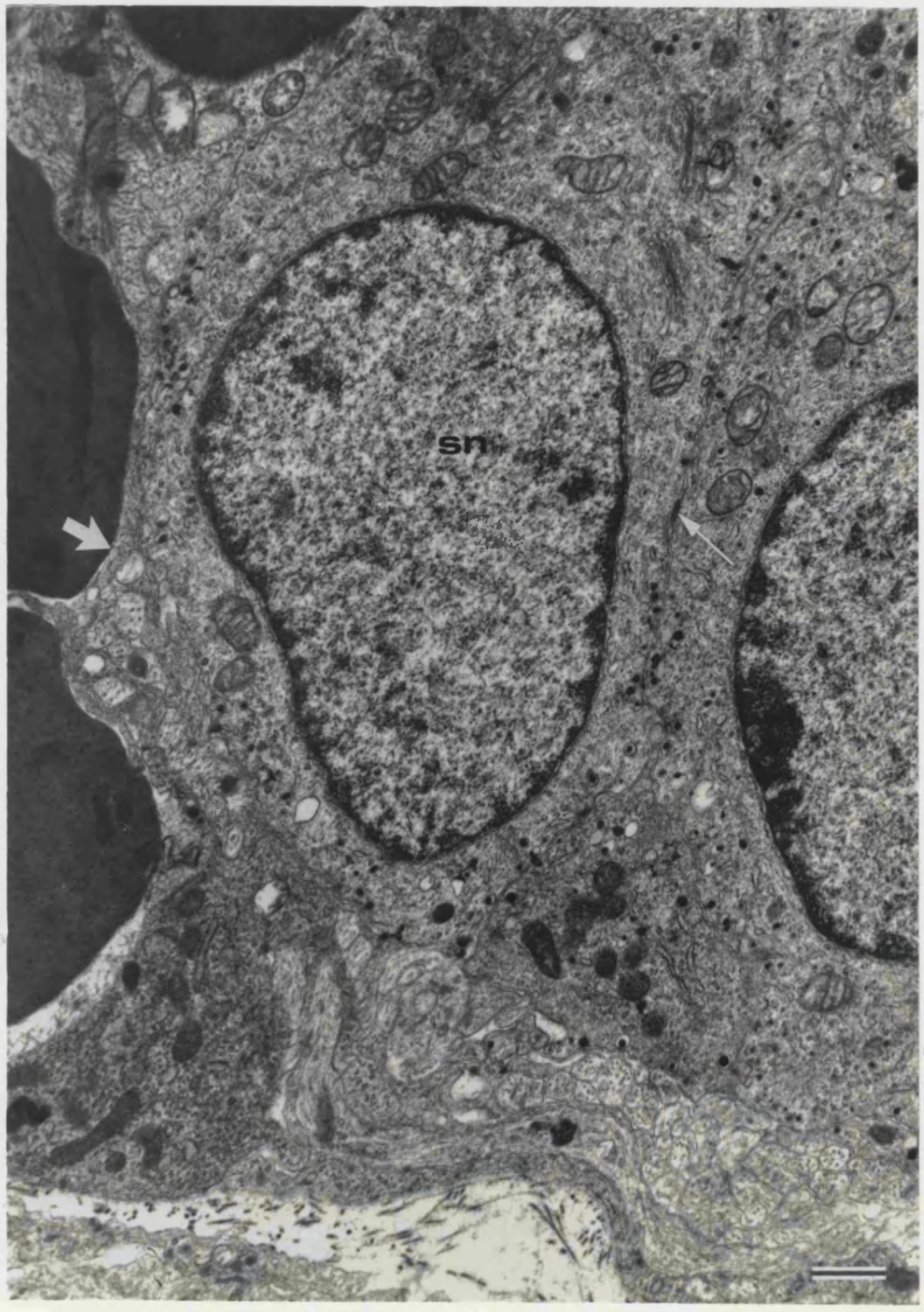
sn

Figure 52

Electron micrograph from the pelvic ganglion of newborn female rat showing a developing S.I.F. cell. The large nucleus (**sn**) dominates the cell. Dense core vesicles (arrowed) are distributed throughout the cell, although appear to more concentrated beneath the cell membrane. A developing glial cell (white arrow) is close by and is probably a developing Schwann cell as it is closely associated with many fibres.

(Scale Bar = 1μm).

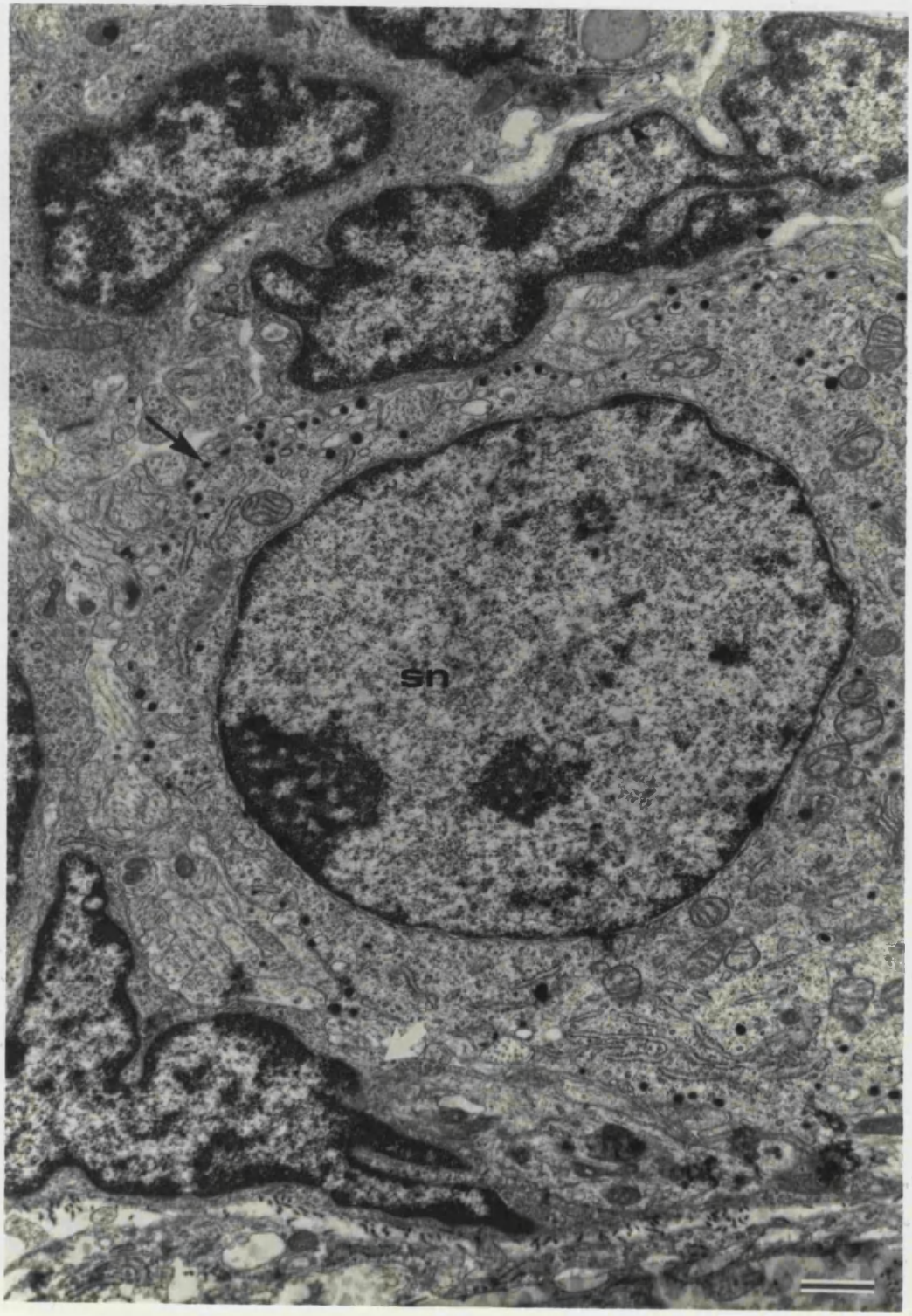
sn

Figure 53

Light micrographs of cryosectioned ganglia from week old rats stained using the TUNEL method.

A) Pelvic ganglion from a female rat.

(Scale Bar = 100μm, also applies to B).

B) Pelvic ganglion from a male rat.

C) Higher magnification light micrograph of a developing neuron positively stained by the TUNEL method. Note how the peroxidase stain is restricted to the cell nucleus. (Scale Bar = 50μm).

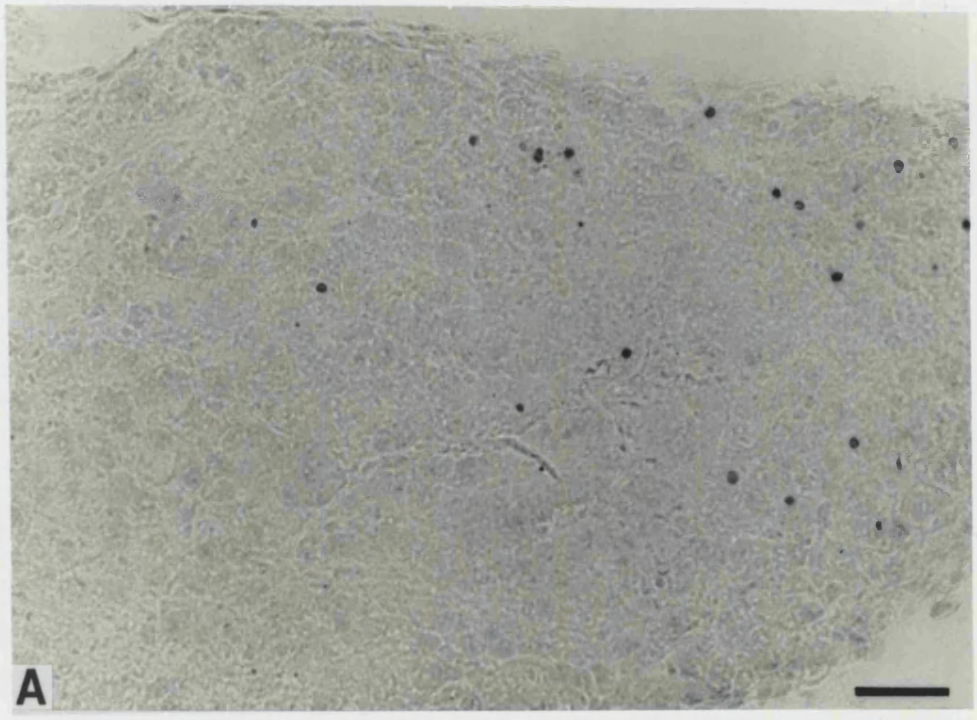
A

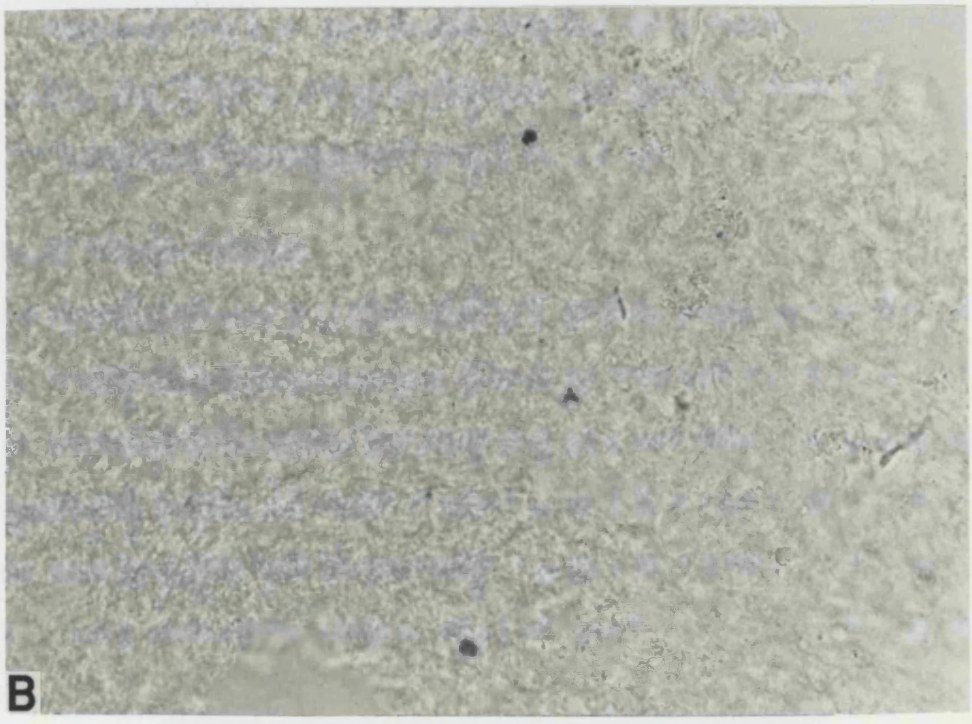
B

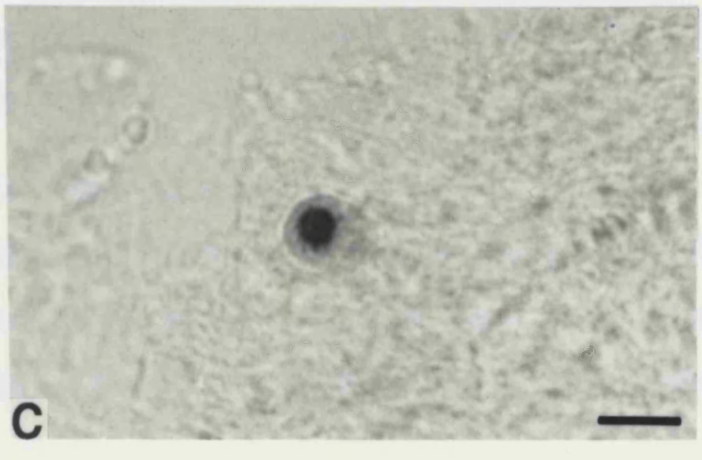
C

CHAPTER 6

RESULTS IV: CASTRATED MALE RATS

6.1 Body Weight

The average body weight of 3 pre-pubertally, surgically castrated male rats, three weeks post-operative was 174g ±5.2. In 3 control littermates this figure was 188.5g ±3.5 ($P<0.05$). The weight of testes in control animals was 2.4 g ±2.

6.2 Pelvic Viscera Weight

On opening the pelvic cavity extensive atrophy of the pelvic viscera was immediately in evidence in comparison to the pelvic organs of the control littermates (Graph 7). The recorded wet weights of the seminal vesicles, prostate gland and penis in the castrated rats were significantly less than the weights recorded in control littermates ($P<0.001$); these findings are in accordance with data recorded by Wakade and co-workers (1975). The seminal vesicles underwent on average a 77% weight reduction, the prostate gland an 80% reduction and the penis a reduction of 60%. The bladder showed a 36% reduction in average weight. The appearance of the penis, seminal vesicles prostate gland and bladder was unchanged in control rats.

6.3 Anatomy of Pelvic Ganglion

The main component of the pelvic plexus was the pelvic ganglion that was positioned in the investing fascia of the posterior prostate lobe of the gland. The general appearance of the ganglion was similar to that in the control animals although it appeared more conspicuous

due to the atrophy of the prostate gland. The pelvic nerves and hypogastric nerves, the main pre-ganglionic trunks entered the ganglion at the dorsal pole and cranial edge respectively. From the ventral border postganglionic nerves ran to the pelvic organs which appeared to be of the same extent as in control animals despite travelling to atrophied tissues. A cluster of between two and four accessory ganglia were present close to the ureter and vas deferens, and as with the main ganglion, these structures were more conspicuous than those in control animals due the reduction in size of the vas deferens.

6.4 Histology of Pelvic Ganglion

6.4.1 General Histology

The overall appearance of the ganglion from the castrated animals was similar to that in the control animals (Fig. 54). The ganglion was entirely contained within a membranous capsule which continued over the nerves. The main components were principal neurons that rarely displayed dendrites. Each neuron was entirely wrapped in glial cells. Clusters of SIF cells were in evidence although vacuolated neurons were absent. The neuronal packing density appeared similar to that of control, as did the areas of neuropil and nerve fibres. Blood vessels in cross section were observed with apparently uniform distribution throughout the ganglion, and the ganglion received vascularisation from a branch of the obturator artery as recorded in the control male rat (Fig. 54).

6.4.2 Ganglion Volume

The ganglion volume estimated morphometrically by the Cavalieri method ranged between 191 - 251 $x10^6 \mu m^3$ in 3 operated rats with an average of 249 $x10^6 \mu m^3$ ±34 (249 million cubic microns or approximately $0.25mm^3$). In 3 unoperated male rats of the same age from the same colony (animals used elsewhere in other experiments, see section 3) the ganglion volume ranged between 278.6 - 307.4 $x10^6 \mu m^3$ with a group average of 296 ± 15 $x10^6 \mu m^3$ (296 million cubic microns or approximately $0.3mm^3$). A reduction in the average ganglion volume of 16% was observed in castrated animals as compared unoperated equivalents ($P<0.10$ with application of t-test, see Appendix 5).

6.4.3 Neuron Cell Size

Neuron size (the area of the largest profile of a neuron identified from serial sections at 2μm intervals) was measured in the ganglia from 3 operated rats; roughly one hundred neurons were measured in each animal. The largest sectional profile of a neuron almost invariably displayed the nucleus. In all ganglia the range of nerve cell sizes was wide (Graph 8), continuous and gave no indication of sub-classes. Neurons ranged in size from 68 - 619μm^2 and mean neuronal cell sizes from 3 animals ranged from 224 - 293μm^2 and the average of the means was 252μm^2 ± 37. The data reveals some variability between neuron size ranges but little between means neuronal sizes. In three control adult male rats (section 3.0) the neuron ranged in size from 121 - 1155μm^2 and mean neuronal cell size ranged between 489 - 513μm^2; the average of the means was 501μm^2 ± 13. The reduction in the average neuronal cross sectional area in castrated animals compared to unoperated animals of the same age was 50% ($P<0.001$ with application of t-test, see Appendix 5) and was accompanied with a marked reduction in the range of neuronal sizes (the curve is shifted to the left).

6.4.4 Neuron Number

Disector estimated neuronal populations in ganglia from 3 castrated rats ranged between 12,873 - 14,386 with an average value of 13,619 ±616. In unoperated adult male rats the neuronal population ranged between 11,951 - 13,247 with an average of 12,506 ± 668 and there was no statistical difference between the two groups.

6.5 Cytochemistry

6.5.1 NADPH-diaphorase/NOS

Many neurons in the ganglia of adult, pre-pubertally castrated rats exhibited intense blue-purple NADPH-diaphorase staining (Fig. 55A & C). A range of NADPH-diaphorase staining intensities was observed, ranging from weakly positive to intensely positive. The formazan reaction product was limited to the perikaryon leaving the nucleus unstained at the centre of each positive profile; sometimes stained processes, interpreted as axons, extended from the NADPH-diaphorase positive perikarya. Neurons stained for NADPH-diaphorase

were distributed throughout the ganglia, but topographical distribution was not studied due to the lack of known orientation in ganglion sectioning.

There was an almost total coincidence of intense NADPH-diaphorase staining and fluorescence with subsequent immunohistochemical staining for nitric oxide synthase. There was also extensive, but not complete, co-localisation of moderate NADPH-diaphorase staining and NOS immunofluorescence.

The distribution and extent of co-localisation of the NADPH-diaphorase formazan reaction product and immunofluorescence to NOS was similar to that observed in unoperated rats and again demonstrates that these neurons are able to synthesise the putative neurotransmitter nitric oxide.

6.5.2 Co-localisation of NADPH-diaphorase

6.5.2.1 Vasoactive Intestinal Polypeptide

In the castrated male pelvic ganglion many principal neurons contained immunoreactivity for vasoactive intestinal polypeptide (VIP) (Fig. 55D). The perikaryal fluorescence had a speckled appearance and was absent within cell nuclei. The immunosignal was also present in neuronal processes, and in nerve fibres that coursed through the ganglion.

Many neurons previously histochemically stained for NADPH-diaphorase showed immunofluorescence to VIP (Fig. 55C & D); nearly all neurons intensely positive for NADPH-diaphorase were VIP-immunoreactive, as were many that displayed a moderate NADPH-diaphorase stain. Due to the near total coincidence of NOS-immunoreactivity and NADPH-diaphorase staining this indicates co-localisation of VIP and NOS.

6.5.2.2 Tyrosine Hydroxylase

Many neuronal perikarya were positive to immunocytochemical staining for tyrosine hydroxylase (TH) (Fig. 56B). This stain was present throughout the perikaryon and was generally more intense close to the cell membrane. Fluorescent neuronal cell profiles were present throughout the ganglion sections although certain regions were more abundant that others, and in such regions very few unstained profiles were present. In sections previously stained for NADPH-diaphorase, no neuronal perikarya that demonstrated an intense or moderate formazan reaction product were also immunofluorescent for TH, although

NADPH-diaphorase-negative neurons did exhibit TH-immunofluorescence (Fig. 56A & B). It appeared that TH-positive neuronal perikarya were larger than adjacent NADPH-diaphorase positive perikarya although no actual measurements were undertaken.

6.5.2.3 Neuropeptide Y

A positive immunocytochemical reaction to neuropeptide Y was obtained in many neurons (Fig. 55B) that were distributed throughout ganglion sections. The stain appeared as small clumps of fluorescence and was present throughout the perikarya although was more intense close to the nucleus.

When NPY antibody incubation was subsequently carried out on NADPH-diaphorase stained sections, there were no moderate or intense NADPH-diaphorase positive neurons that also demonstrated immunoreactivity to NPY. Occasionally neurons weakly stained for NADPH-diaphorase were also positive to NPY (Fig. 55A & B). NADPH-diaphorase positive neurons were more numerous throughout the ganglia than those immunoreactive for NPY.

6.5.2.4 Substance P

Immunofluorescence from antibodies raised against substance P was observed in many fibres, but not in neuronal perikarya, throughout the ganglion. The immunopositive fibres were mainly in cross section, although occasional fibres in oblique section were also present. Many positive fibres travelled close to, and surrounded neuronal perikarya (Fig. 55E). Many of these abutting fibres were varicosed, while others showed less swellings but intricate interconnections that formed plexi.

GRAPH 7

Atrophy In Pelvic Organs of Castrated Male Rats

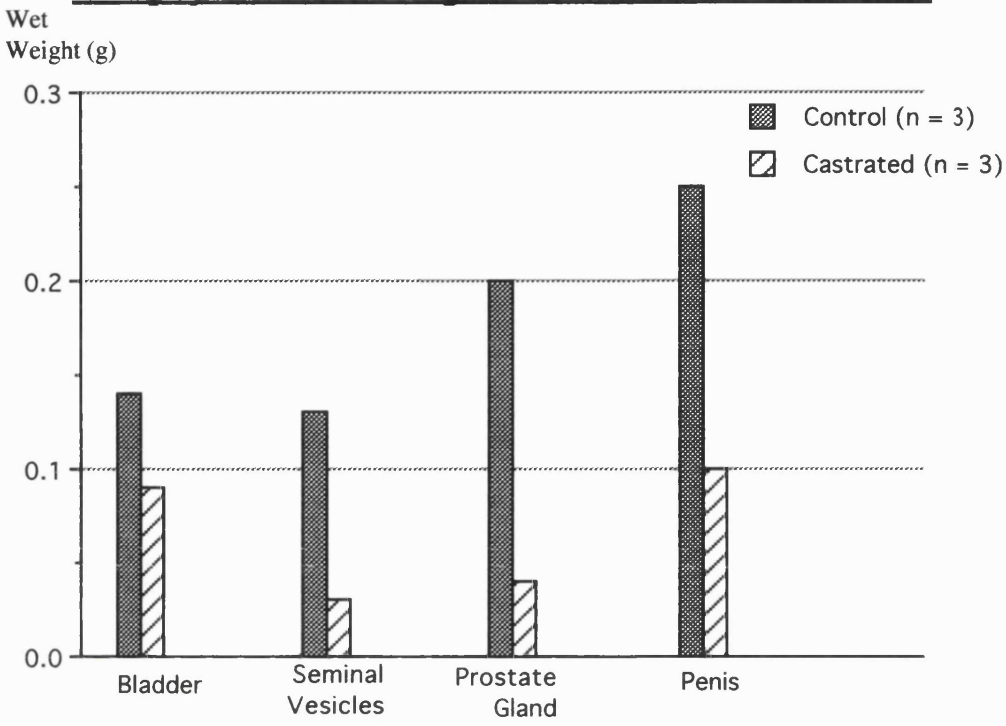

GRAPH 8

Neuronal Cross Sectional Area in Castrated Male Rats

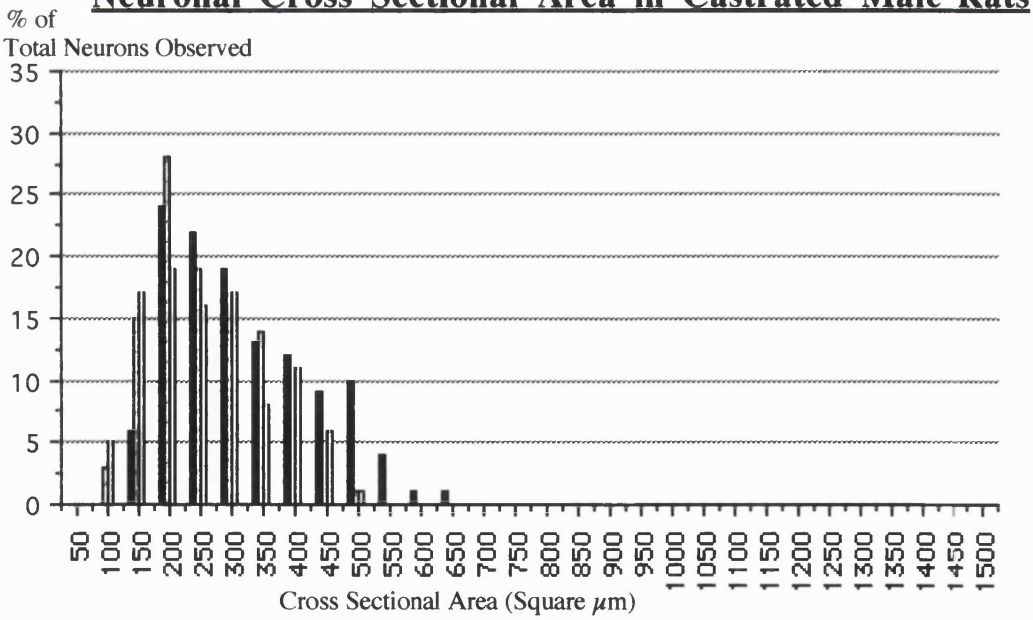

Figure 54

A light micrograph montage of a resin section (stained with toluidine blue) of a pelvic ganglion from a pre-pubertally castrated, adult rat. To the left are the large blood vessels that travel along the ganglion; the vessel marked **a** is the arterial branch of the obturator, while the vessel marked **v** is the accompanying vein. Passing through the interior of the ganglion is an arteriole (filled star) and a venule (unfilled star) paired together.

The ganglion profile is entirely contained within a connective tissue capsule (arrowheads) and contains many of neuronal profiles; an area predominantly composed of myelinated nerve fibres in transverse section (arrow) is seen to the top right of the ganglion.

(Scale Bar = 50μm)

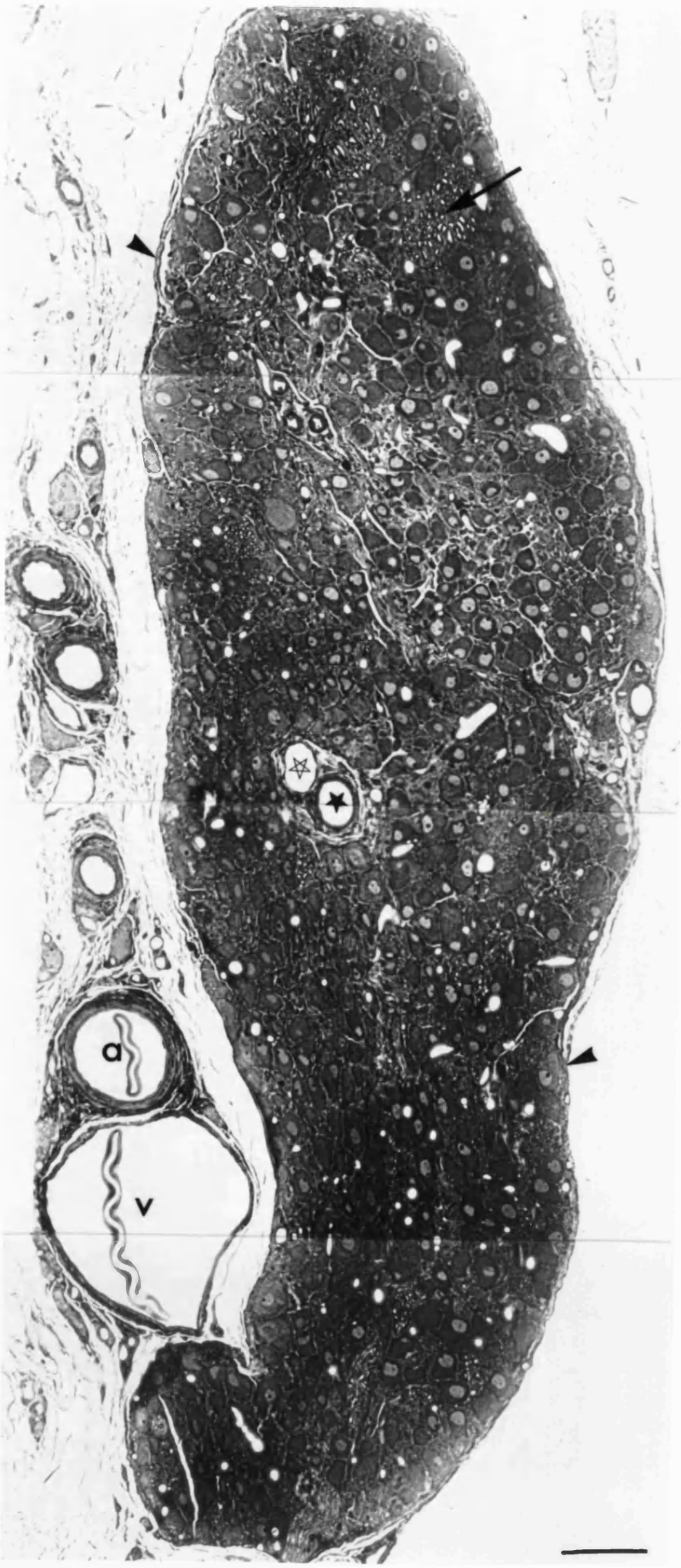
a
v

Figure 55

Cryostat sections of the major pelvic ganglion from pre-pubertally castrated adult male rats.

A) Frozen section histochemically stained for NADPH-diaphorase displaying both strongly and weakly positive neurons.
(Scale Bar = 20μm applies to **A**, **B** and **E**)
B) The same cryostat section from **A** immunohistochemically stained for Neuropeptide Y. Immunoreactivity is present in the perikarya of neurons that are weakly positive to NADPH-diaphorase in **A**, but not in those that are strongly positive.

C) Frozen section histochemically stained for NADPH-diaphorase displaying weakly and strongly positive neurons. (Scale Bar = 40μm applies to **D**).
D) The same cryostat section from **C** immunohistochemically stained for vasoactive intestinal polypeptide. Immunoreactivity is present in the perikarya of both weakly and strongly positive neurons.

E) Immunohistochemical staining for substance P. Immunoreactivity is not present in neuronal perikarya but is seen in fibres surrounding the ganglion cells, forming the characteristic 'baskets'.

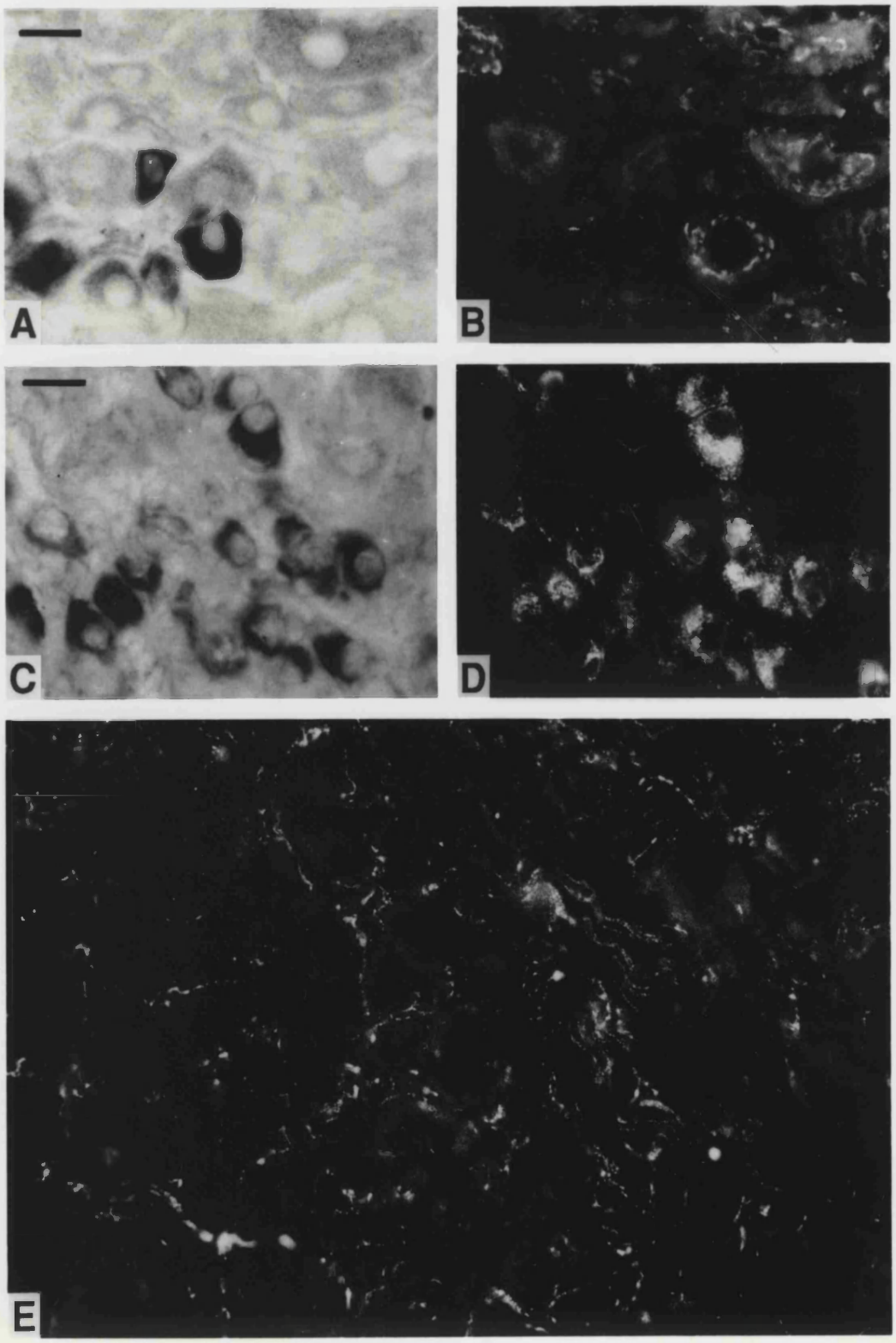
A
B
C
D
E

Figure 56

Cryosections of a pelvic ganglion from a pre-pubertally castrated adult male rat double-stained for NADPH-diaphorase and tyrosine hydroxylase.

A) Light micrograph displaying NADPH-diaphorase histochemistry. Neuronal perikarya stained with the dense formazan reaction product show no immunofluorescence in micrograph **B**.

(Scale Bar = 20μm - applies both.)

B) Fluorescent micrograph displaying the same area of cryosection as **A**, immunohistochemically stained for tyrosine hydroxylase. Immunoreactivity is also present in nerve fibres. Perikarya exhibiting immunoreactivity to tyrosine hydroxylase do not show staining for NADPH-diaphorase in **A**.

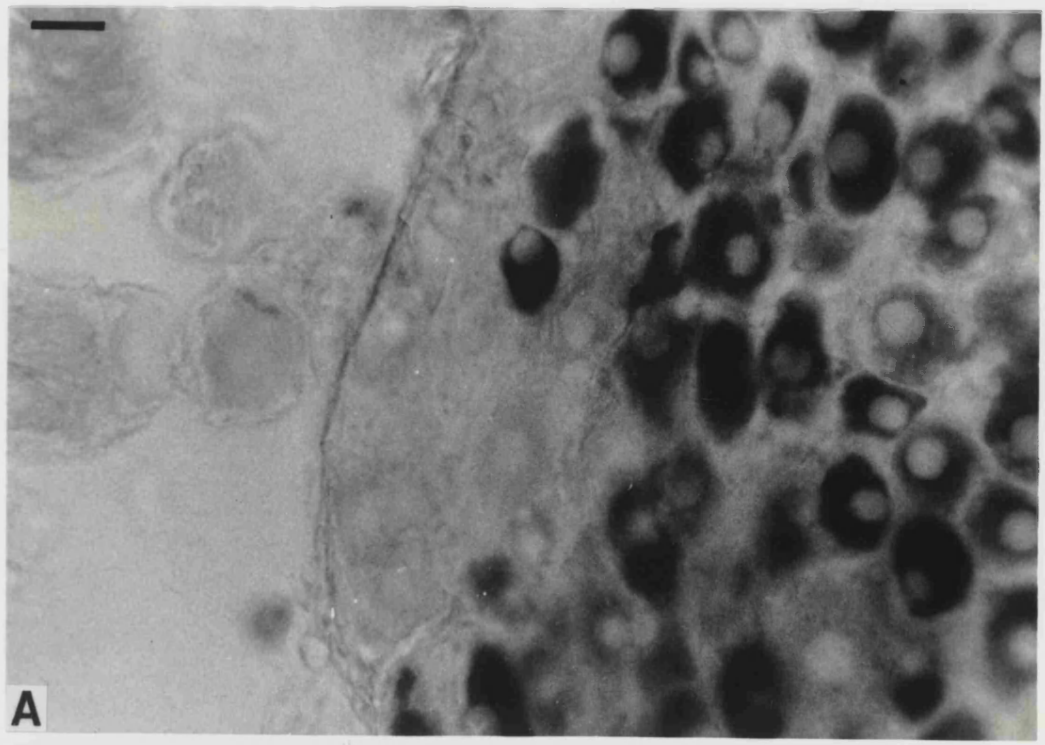
A

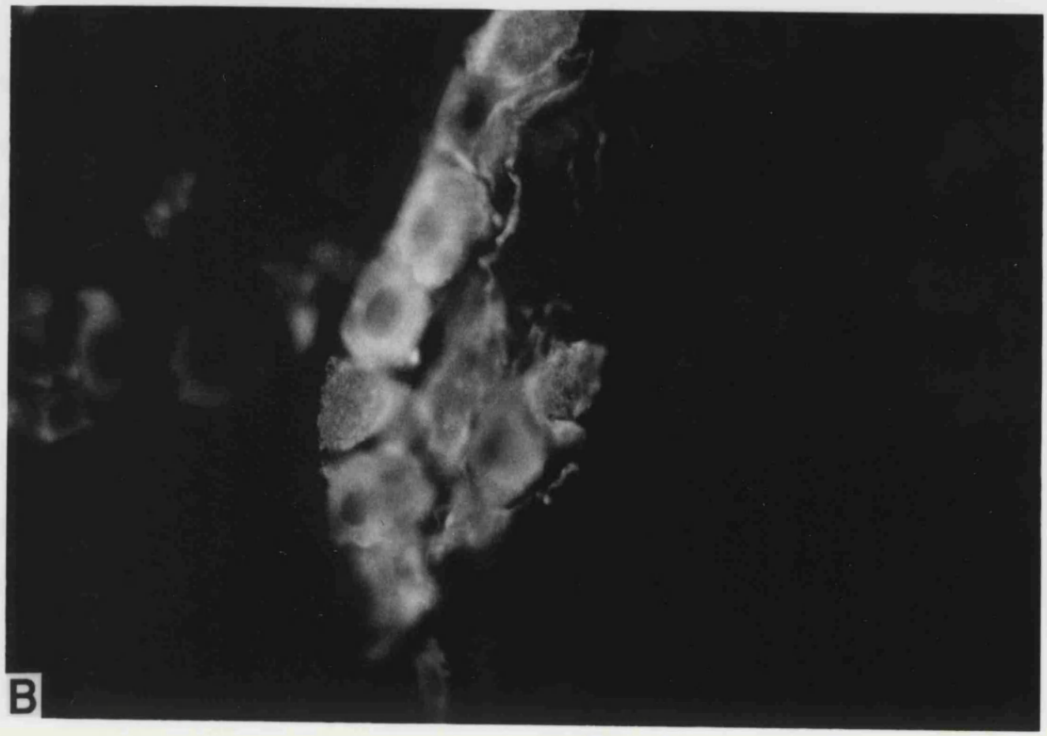
B

CHAPTER 7

DISCUSSION

7.1 Methodology

7.1.1 Neuronal Quantitation

Neuronal counting is an important investigative probe in neurobiology. The microscopic size of neurons requires that counting is undertaken in histological sections. Basically, four methods are available to histologists: serial section reconstruction, stereological methods, profile counts, and methods based on conversion criteria (for reviews see Gundersen et al., 1988a and 1988b; Coggeshall, 1992; Mayhew, 1992; and Coggeshall and Lekan, 1996).

7.1.1.1 Serial Section Reconstruction

Complete serial section reconstruction produces neuron number counts of the highest accuracy because it involves virtually no assumptions (sampling or estimating), but a simple reconstruction of all the neurons in the series of histological sections in which they appear. Despite its accuracy this method is used very rarely (Coggeshall and Lekan, 1996 state its use in only 11% of original articles that involve neuron counts, published in four major journals in the whole of 1994) presumably due to the extensive labour required. Nevertheless, the advantages of complete serial reconstruction are such that it was employed in this thesis, as it was thought important to have some data that was relatively free of bias and therefore of minimal doubt, and as it also provided a reference with which to compare the data produced by the stereological methods (also used in the thesis). In addition, the full reconstructions provided vast quantities of material which allow further

investigation into the pelvic ganglion; where the results in this thesis only describe the total number of neurons in each of the ganglia, many other aspects can still be described (e.g. the extent of the vascular tree within the ganglia, positional relationships of nerve fibres passing through each ganglion and S.I.F. cell counts to name just three).

7.1.1.2 Disector Analysis

In order to compare neuron counts from many different animal groups a less labour intensive method was required. The disector method was chosen, as this stereological technique is reported to be accurate (unbiased), as it is based on serial section analysis, and also relatively efficient (see reviews outlined above) due to its suitability to sampling. There are two types of disector techniques, the physical disector and the optical disector. Briefly, the basis of the former method (as described in section 2) is to locate neuronal profiles in one section (the reference section) but count only those that are not found in a serial section (the look-up section). A complete physical disector reconstruction, where all sections are examined as parts of disector pairs, would obviously be no more efficient than a serial reconstruction. However, physical disectors are suited to sampling (Gundersen et al, 1988a, b) and only necessitate the examination of widely spaced sections pairs to produce an unbiased, efficient estimate (Pakkenberg and Gundersen, 1989; Pover and Coggeshall, 1991; Coggeshall, 1992). The optical disector is similar to the physical disector except that two optical planes are used in one thick section, as opposed to two (physical) sections; instead of counting profiles in one section not found in the another, cells are counted as they come into focus in passing from one optical plane to another. Similarly, if optical disectors are taken throughout an entire series of thick sections then the method would be little more efficient than a serial reconstruction or physical disector (West, 1993). However, as it is suitable for sampling, widely spaced thick sections can be selected, and this produces a method that is more efficient than both the physical disector that selects section pairs, and full serial reconstruction that selects every section (West at al, 1991).

An advantage of the physical disector is that histological detail is preserved and, as this was required for the concomitant qualitative studies, this method was chosen in this thesis. Even though the optical method is more efficient, the staining and observation of

structures deep within the section is difficult, and it cannot match the good histology that results from thin sectioning and resin embedding.

However the physical disector does have certain problems. One such problem is termed 'matching' and arises whenever numerous profiles are present, when it becomes difficult to match up two profiles that come from the same object as opposed to those that come from different objects. However the problems of matching are reduced by reduction of section thickness and/or the disector pair separation; the section thickness in this thesis of only 2μm and the disector height of 6μm minimised errors from this source.

Pover and Coggeshall (1991) investigated the effect of disector height on the accuracy of disector neuronal estimates. They sectioned, at a thickness of 6μm, wax embedded dorsal root ganglia, and calibrated a range of disector sizes against a full serial reconstruction. Their conclusions were that disectors produced from adjacent sections (a 12μm disector) resulted in a consistent underestimation (bias) but that disectors with at least one intervening section (e.g. 18, 24, 30μm) provide accurate estimates. They attributed the inaccuracy in the adjacent section disector to result from 'invisible fragments'. An invisible fragment occurs when a structure is cut by the microtome knife and one of the resulting fragments is too thin to be distinguished from background (Floderus, 1944; Konigsmark, 1970). This problem is usually eliminated by the selection of a disector height that is less than the height that results from combined heights of the lost fragments subtracted from the minimum particle diameter (Sterio, 1984); the thick wax sections employed by Pover and Coggeshall (1991) exacerbated errors of this type.

The disector height of 6μm (one intervening section) selected in this thesis was the smallest size possible without using adjacent sections. It follows that the problem of matching was therefore reduced to a minimum by such a small disector (also helped by the re-evaluation that the physical micrographs allowed, as compared to an optical disector), as was the problem of 'lost' cells which can result when the difference between the reference and the look-up is greater than the diameter of the smallest neurons (Sterio, 1984).

7.1.1.3 Profile Counts

Profile counting is very common in the literature (Coggeshall and Lekan (1996) show that it is used in 76% of original articles containing particle counting, published in four major journals in 1994) and is used primarily because of its efficiency in comparison to serial section methods; it was partly for this reason that some profile counting was also adopted in this thesis. When counts are performed on a single histological plane it is the number of neuronal profiles that are counted rather than the number of neurons themselves and as such is an extreme case of sampling. The main reason for the use of profile counting in this work was to count neurons that were positively stained for NADPH-diaphorase, and to perform histochemistry on approximately 200 serial cryostat sections in a reconstruction would be an unrealistic undertaking, not to mention the excessive requirement of chemical reagents.

Profile counts are hardly suitable to estimate total neuron numbers and consequently it is more common to determine the spatial density of cells in a given space or ratios of such figures. The commonest method in the literature (93 out of 112 studies published in four major journals that used profile counts in 1994;Coggeshall and Lekan, 1996) is to count profiles per unit area. Usually the number of profiles in an area is determined in the control and experimental situation, and the ratio between the two values is calculated; this essentially was the method employed in the analysis of the NADPH-diaphorase positive neurons in this thesis but comparisons were drawn between ganglia from male and female animals. However there are some reservations relating to the value of such comparisons. The first is in the assumption that there is a proportional relationship between profile counts and actual neuronal numbers, although even in the absence of one, the data may be used to simply analyse the ratios rather than absolute profile numbers. A further problem is that changes in cell size and shape result in altered profile densities which have no relation to changes in cell number. Neurons in the pelvic ganglion range in size, and there are differences in cell size between male and female animals, observations which may reduce the value of the profile counts obtained for the NADPH-diaphorase positive neurons. However, it is widely reported that the diaphorase reaction is limited to population of small neurons (Papka et al., 1995; Schirar et al., 1994) in rats of both sexes

and this may therefore reduce errors that would arise if the entire neuronal size range was incorporated. Furthermore, it may be more appropriate only to make comparisons between profile densities from animals of the same age group rather than between different age groups, as there is a marked increase in cell size in development and this may effect NADPH-diaphorase positive neuron density ratios.

7.1.1.4 Methods Based on Conversion Criteria

All methods of this type determine profile numbers which are then converted to cell numbers by combination with certain geometrical criteria. Developed to alleviate difficulties with profile counts, Abercrombie (1946) proposed a method that produces cell counts by multiplying nuclear profile counts by mean nuclear diameter, and then dividing this figure by the mean nuclear diameter plus section thickness. The reasoning behind this method is sound as long as the assumptions made, that nuclei are spherical and that all nuclear fragments are identified, are true. Coggeshall and co-workers (1990) suggested that this was often not the case, as they found that Abercrombie estimates were inaccurate as compared to neuronal numbers determined by serial reconstruction of adult rat dorsal root ganglia.

Further methods were developed by Floderus (1944), Konigsmark (1970) and Hendry (1976) which introduced adjustments to the Abercrombie method regarding the assumptions made. However, unless calibration against serial reconstruction is performed, it is not possible to tell whether the criteria have been met, and therefore to what extent bias has been introduced. The extent of this problem is illustrated by Smolen and co-workers (1983) who show that in 10 studies between 1960 and 1981 that used a range of different methods, the number of neurons reported in the SCG of the rat ranged between 13,000 (Hendry and Campbell, 1976) and 45,000 (Davies, 1978); the Smolen group then went on to propose modifications of their own.

7.2 Nomenclature

Few studies in the field of pelvic autonomic innervation directly compare the nature of this nervous control between male and female animals. Consequently in the literature the anatomical structures studied in each sex have been awarded terminology that is generally

gender specific and thus inappropriate for use in both sexes (e.g. Paracervical ganglion), or at least terminology that is applied in a largely inconsistent manner by authors studying one or other sex. An effort was therefore made to use consistently a nomenclature which could be applied to both sexes.

The main aggregation of ganglion cells in the pelvic plexus was called the major pelvic ganglion (also adopted in amongst others in the works of Purinton et al 1973; Dail et al., 1975); this structure, although variable in size and shape, was present in rats of both sexes and all age groups studied (sometimes when the major pelvic ganglion was the only structure being discussed the term 'pelvic ganglion' was used). The smaller ganglia positioned ventrocranially to the major pelvic ganglion were termed accessory ganglia in this thesis, again a term that is applicable to both sexes and allows no confusion between other related structures. The selection of these two terms also removes the inconsistencies present in the literature where the term hypogastric has been used in some instances to describe the major pelvic ganglion (Wang et al., 1990; Warburton and Santer, 1993) and in others to describe the accessory ganglia (Melvin and Hamill, 1986; Hamill and Schroeder, 1990). Due to its anatomical position and origin, the sympathetic pre-ganglionic input was termed the hypogastric nerve and correspondingly the small ganglion often observed along this nerve was called the hypogastric ganglion. Conflicting terminology in the literature is not present regarding the parasympathetic pre-ganglionic supply to the pelvic ganglion, and this nerve was thus termed the pelvic nerve.

7.3 Sexual Dimorphism of Pelvic Ganglion in Adult Rats

Structural differences in the CNS between males and females include the frog (Kelley and Dennison, 1990) and songbird (Nottebohm and Arnold, 1976) vocal control regions, the innervation (spinal nucleus of the bulbocavernosus) of the rat perineal muscles (Sengelaub and Arnold, 1986) and the preoptic area of the rat brain (Gorski et al, 1978).

This topic has not been extensively studied in the autonomic nervous system and few studies have directly compared structures in males and females. Sexually dimorphism is described in the rat superior cervical ganglion (Wright and Smolen, 1983), the mouse hypogastric ganglion (equivalent of the pelvic ganglion in this species) (Suzuki et al,

1983) and the major pelvic ganglion of the rat (Greenwood et al, 1985). The only study showing sexually dimorphism in the SCG was carried out before the introduction of modern stereometric methods and described neuron numbers which are approximately 50% greater in male animals as compared to females.

7.3.1 Pelvic Ganglion

Surprisingly, only Purinton et al. (1973) and Greenwood et al. (1985) have performed comparative studies on male and female rats. The former study was a purely qualitative evaluation, while even the latter that performed quantitation of neuronal numbers did not undertake basic morphometric analysis (e.g. volume calculations). The data in this thesis reinforce and expand on the meagre data available, and documents the development of the sexual dimorphism observed in the adult.

7.3.1.1 Common Structural Plan

Pelvic ganglia of both sexes are similar in that they are both bilaterally symmetrical, close to the midline and are at the centre of radially emerging nerves. Ganglia from rats of both genders are supplied by the pelvic and hypogastric nerves (Langworthy, 1965; Purinton et al., 1973), and both are mixed ganglia i.e. they contain neurons in contact with sympathetic and parasympathetic pre-ganglionic axons. The principal neurons issue axons that leave the ganglion in nerves that travel to the pelvic organs. The ganglion body becomes elongated at the position of these emerging nerves, and further narrowing culminates in the post-ganglionic nerve itself.

There are anatomical differences related to topography and target-projection. The arrangement of the nerves to the bladder and the rectum is indistinguishable (Langworthy, 1965; Purinton et al., 1973; Baljet and Drukker, 1980) while, of course, specific features are found in nerves supplying the genital organs.

Principal ganglion neurons have very few processes, are predominantly uninucleate (with a small number of binucleate examples) and are encapsulated by glial cells and a basal lamina (Dail et al., 1975, Kanerva and Hervonen, 1976; Tabatabai et al., 1986). Pelvic ganglia contain small intensely fluorescent (SIF) cells and large vacuolated neurons. Large numbers of both myelinated and unmyelinated axons (some presumably

afferent fibres) pass through the ganglion. The ganglion receives its blood supply from a branch of the obturator artery; this blood vessel provides vascularisation to the ganglion and it passes close to, and often actually through the ganglion itself. All these features are, at least as assessed qualitatively, identical between male and female animals.

7.3.1.2 Gross Anatomy, Position and Volume

Several authors (Langworthy, 1965; Purinton, 1973; Baljet and Drukker, 1980) have described significant anatomical differences between the sexes in adult animals, and their main conclusions have been confirmed in this thesis. Firstly, the ganglion in the male rat is positioned loosely in the investing fascia of the posterior lobe of the prostate gland while that of the female is located at the transition of uterine cervix to vagina and is firmly attached to parametrial tissue. The ganglion of the male rat is globular and bulbous while, in contrast, that of the female rat is much flatter, these differences graphically demonstrated by the computer reconstructions. At this level of investigation it is not possible to conclude whether these anatomical differences result from ganglia of different sizes in either sex, or whether they are simply different shapes that result from the physical impact of the surrounding anatomy e.g. physical pressure on the female ganglion from its closeness to the cervix may contribute to its flattened shape.

The male ganglion is, on average roughly 40% larger in volume (calculated by the Cavalieri method) than its female counterpart (male : female 0.30 : 0.18mm^3); there are no estimates of the ganglion volume in the literature in the rat. Suzuki and Arai (1986) undertook a similar study of the mouse hypogastric ganglion which is also significantly greater in volume in the male than in the female (approximately male : female 0.02 : 0.01mm^3). An objective of this thesis was, therefore, to investigate the basis of this difference in ganglion size i.e. whether it arises from differences in neuron number, in neuronal size, in other ganglion constituents (e.g. fibres in transit, glial cells and blood vessels) or a combination of these factors.

7.3.1.3 Neuron Number

Average estimated neuronal cell populations in the pelvic ganglion of the male rat are approximately double that of the female animal; male estimates in this thesis are 12,506 ± 668 while female estimates are 6,845 ± 717. This result is broadly in agreement with that

of Greenwood and co-workers (1985) who also documented a gender difference in neuron number in the rat pelvic ganglion where male animals had 14,654 ±936 and females 5,892 ±797. Hondeau and co-workers (1995) obtained a similar number (5,069 ± 1,525) in ganglia of female rats, and in addition 414 ±149 neurons in the associated accessory ganglia; accessory ganglia were not studied in this thesis. The superior cervical ganglion, the only other autonomic ganglion where sexual dimorphism is documented, has 38,920 ± 1,160 neurons in the male and 26,580 ± 3,340 in the female (Wright and Smolen, 1983). Presumably the different genital organs innervated by the pelvic ganglion in males and females exert an effect on the neuronal population, and there is evidence that indicates a mechanisms controlled by sex steroid (testosterone being the major candidate) and target-derived trophic factors; as there are no overt differences between males and females in the tissues of the head and neck the gender difference in the SCG is less intuitive, although one possibility is that it may be linked with pheromone production

7.3.1.4 Neuron Size

Pelvic ganglion neurons are heterogeneous in size: the mean diameter ranges between 11μm and 35μm in females and between 12μm and 39μm in males. What is the significance of this heterogeneity? Two factors will be discussed: i) even neurons projecting to a single target display a range of neuronal sizes. ii) populations of neurons of different function display different ranges of cell sizes.

Neuronal 'Size Principle'

In the pelvic ganglion, a degree of topographical specialisation has been noted, with certain areas of the ganglion predominantly innervating a single target organ (Dail et al., 1986; Keast et al., 1989; Keast, 1992; Kepper and Keast, 1995). Even within these target specific, transmitter-specific groups of neurons (identified usually by retrograde dye labelling) large ranges of somal size are observed. This is also the case in sympathetic ganglia of the rat and other mammalian species (Purves, 1975; Bowers and Zigmond, 1979; Gabella et al., 1988) where in areas predominantly supplying a single organ, ranges in neuron size are present. In the pelvic ganglion, large and small neurons are evenly spread throughout the ganglion and no single topographical location predisposed to large or small neurons. This observation, combined with the evidence that in the rabbit SCG,

large neurons have been reported to be as likely to innervate the iris as they are various other glands of the head (Dail and Barton, 1983), leads to the conclusion that neurons of a range of sizes innervate each target organ.

It is not obvious why certain neurons that supply a single target remain small, while others grow to a larger size. There is evidence of a relationship between autonomic innervation and body size; Gabella and Trigg (1984) supplied evidence that enteric neuron size increases between different species of increasing body weight, and Purves and colleagues (1986) show it involves not only variations in neuron size and number, but also in dendritic branching and in divergence and convergence of synaptic inputs.

Study of somatic motoneurons (McPhedran et al., 1964) has shown that large motoneurons have large axonal diameter, and that these neurons innervate more muscle fibres than do smaller neurons that have smaller axonal diameters. It is also known that the larger the axon, the faster the neuronal conduction velocity (Rushton, 1951), and that conduction velocity is faster in larger motoneurons than in smaller ones. The conclusion of these observations is that motoneurons of different size have fundamental functional differences, namely that large neuronal size is accompanied by faster conduction velocity and amounts of activated muscle fibres. There is also variation seen in the reflex excitability in motoneurons where small motor units have lower thresholds of excitation than do larger units (Henneman et al., 1965). Whereas small motor units with low excitation thresholds generate a moderate amount of force in muscle fibres, larger motor units have a higher threshold and thus require a greater stimulus, and result in greater generation of force in the muscle. Physiologically these phenomena enable skeletal muscle contraction of either precision or strength; Henneman and colleagues (1974) described this relationship as the 'size principle' where cell size determines the rank order of recruitment of motoneurons.

How far the recruitment relationships observed in somatic motoneurons apply to the autonomic nervous system is uncertain. While motor neuron axons are heavily myelinated, autonomic post-ganglionic axons are mainly un-myelinated. A limited amount of investigation into conduction velocities in the periphery has been undertaken, where calculations converting un-myelinated axonal diameter into conduction velocities (Cottrell,

1984), and the average conduction velocity in feline post-ganglionic sympathetic axons is $0.59ms^{-1}$ (Jänig, 1988). However, although probably present, there is no direct evidence that shows a relationship between un-myelinated axonal size and somal size. Dahlstrom and Haggendal (1966) showed there to be many thousands of varicosities in terminal neuronal processes, although variation in the diameter of more proximal parts of the axon is unknown.

The large variation in cell sizes in the pelvic ganglion is probably partly accounted for by a range of neuronal sizes within the same autonomic sub-population that innervates the same target. A conceivable hypothesis is that an arrangement of type would provide a control of effector activity, smaller neurons of the pelvic ganglion, with weaker levels of stimulation bringing fine effector control, while more intense stimulations, via more sizeable neurons, providing large and fast increases in the activity of smooth muscle targets. In addition to the 'size principle' there is also much evidence that suggests that the size of the target influences the neuronal morphology (see Section 7.4)

Noradrenergic and Cholinergic Phenotypes

A source of diversity in the pelvic ganglion is that it contains neurons from both the sympathetic and parasympathetic divisions. Broadly speaking, neurons from either division have different size ranges, and this diversity may partly account for the range of neuronal sizes in male and female ganglia. Sympathetic neurons (that express noradrenaline and stain positively for tyrosine hydroxylase) are the largest neurons of the pelvic ganglion and have diameters ranging between 30μm and 40μm (Dail et al., 1975; Papka et al., 1987), while Kanerva and Teräväinen (1972) describe some, possibly vacuolated neurons, as large as 60μm. Parasympathetic neurons are smaller cells and range between 15μm and 25μm in diameter (Dail et al, 1975; Papka et al., 1987; Keast and de Groat, 1989; Keast, 1991). The literature also indicates a difference in the proportions of the two neuronal types in ganglia between the sexes. Approximately 25-35% of neurons in the pelvic ganglion of the male contain noradrenalin (Dail et al., 1975; Keast et al., 1989) and, while early reports also indicated roughly a third of all principal neurons in the female were noradrenergic (Kanerva et al., 1972), subsequent investigation showed these neurons to be much fewer (Papka et al., 1987) and as little as 9%

(Rousseau et al., 1995) in this sex. The gender difference possibly reflects the dense noradrenergic innervation of the male internal reproductive organs, in particular the vas deferens (Sjöstrand, 1965) as compared to the sparse noradrenergic innervation of the female reproductive tract (Papka et al., 1985). The overlap between range in cell size of the two neuronal phenotypes would contribute to the range of neuronal sizes observed in pelvic ganglia of both sexes, and differences between the numbers of each cell phenotype in either sex could result in the gender difference in average and range of neuronal sizes reported in this thesis.

7.3.3.5. Projections and Neuron Type

As well as performing a role in cytotoxic actions of macrophages (Hibbs et al., 1987), much evidence also suggests that nitric oxide (NO) regulates cell-to-cell communication in different organs and cells (for reviews see Moncada et al., 1991; Bredt and Snyder, 1992); Moncada and co-workers (Palmer et al., 1987, 1988) first directly demonstrated that relaxation of vascular smooth muscle was mediated by NO released from the endothelium, these cells having earlier been implicated in this process by indirect evidence produced by Furchgott and Zawadski (1980). Evidence of NO in the brain was first supplied by Garthwaite and collaborators (1988) who noted that dissociated cultures of neonatal cerebellarcells also induced vascular contraction.

Nitric oxide synthase (NOS) is responsible for the calcium/calmodulin-dependent production of NO from arginine (Hope et al., 1991, Vincent and Hope, 1992) and the enzyme differs markedly from that found in macrophages compared to neural and endothelial forms (Bredt et al., 1990). NADPH-diaphorase has been selectively detected since the introduction of tetrazolium salt enzyme histochemistry (Thomas and Pearce, 1964) and was subsequently identified as an electron donor in the synthesis of NO (Förstermann et al., 1991). Much evidence has lead to the acceptance that NADPH-diaphorase is a suitable histochemical marker for neurons containing NOS (and therefore for NO-producing neurons) as both compounds are co-localised (Bredt et al., 1990; Dawson et al., 1991; Hope et al., 1991; Schmidt et al., 1992).

In the peripheral nervous system, NO is thought to act as a non-adrenergic, non-cholinergic (NANC) inhibitory neurotransmitter involved in the regulation of autonomic

functions (see reviews by Sanders and Ward, 1992; Sneddon and Graham, 1992). Immunoreactivity to NOS in this thesis shows overwhelmingly the same distribution as the formazan NADPH-diaphorase stain in pelvic ganglion neurons from adult male and female rats. The coincidence of NADPH-diaphorase reactivity and NOS-immunoreactivity in pelvic ganglion neurons is evidence that these neurons can synthesise NO and may be able to induce relaxation of vascular and non-vascular smooth muscle.

Santer and Symons (1993) observed NADPH-diaphorase positive neurons of varying intensity in paravertebral (superior cervical and stellate ganglia where a light homogenous reaction product was seen), prevertebral (coeliac-superior mesenteric and inferior mesenteric) ganglia and pelvic sympathetic (accessory) ganglia. Intense NADPH-diaphorase staining in certain neurons was demonstrated in the coeliac-superior mesenteric ganglia while in both the inferior mesenteric and pelvic ganglia many very intensely positive NADPH-diaphorase neurons were seen. These strongly positive cells were small in size as compared to the lightly stained neurons, and usually exhibited one (axonal) process. NADPH-diaphorase staining and NOS immunoreactivity has been widely reported in the pelvic ganglia of rats of both sexes (male: Keast, 1992; McNeill et al., 1992a, Santer and Simmons, 1993; Warburton and Santer, 1993, Schirar et al., 1994. female: Papka and McNeill, 1992; Papka et al., 1995). NADPH-diaphorase positive neurons in these reports are also usually small in size; Papka and colleagues (1995) describe the cells in the pelvic ganglion of the adult female rat as oval in shape with an average long axis of about 27μm (and a short axis of 17μm), while Schirar and co-workers (1995) supplied values of 12 to 37μm in diameter in the male rat (the larger cells being less intensely stained), and Vizzard and colleagues (1994) an average of 33μm. Measurements of NADPH-diaphorase stained neurons were not carried out in this thesis, but it was clearly apparent that positive neurons were at the smaller end of the range of neuronal cell sizes in evidence.

The distinct topographical spread of NADPH-d positive neurons in pelvic ganglia from adult male rats (Keast, 1992; Schirar et al., 1994) confirmed in this thesis, occurs as stained neurons densely populated close to the exit of, and within the genital nerve itself. These NOS expressing neurons project to the penis (Ding et al., 1993) where NO is

strongly implicated as transmitter in the control of penile erection (Burnett et al, 1992). Strong functional evidence supports this theory: in vitro studies reveals that NO is released after transmural electrical stimulation, that exogenous NO induces a relaxation similar to that evoked by nerve stimulation and that electrical stimulation is effected by inhibition of NO synthesis (Ignarro et al., 1990; Kim et al., 1991; Bush et al., 1992; Holmquist et al., 1992). Relaxation of cavernous smooth muscle, a process essential for penile erection, has been shown by in vivo studies (in the human and laboratory animals) to be mediated by NO (Holmquist et al., 1991; Burnett et al., 1992).

Investigations reporting the presence of NADPH-diaphorase positive cells in ganglia from adult female rats report no such organ related spread (Papka and McNeill, 1992; Papka et al., 1995) and these agree with the findings in this thesis. A major site of projection of these NADPH-diaphorase positive neurons in female rats is the uterus (Papka and McNeill, 1992) where it is suggested that NO plays a significant role as a transmitter in the control of uterine myometrium and vasculature. NADPH-diaphorase positive neurons have also been reported to project to the urinary bladder (McNeill et al., 1992b; Vizzard et al., 1994) in the male rat but these neurons are few in number and it is not thought that NO acts as a transmitter in this organ; there may be species differences as in the guinea pig most intramural bladder neurons express NO (Saffrey et al., 1994).

Conceptually the sex difference in topographical spread is easily explained where the major innervation of the penis carried in the genital nerve is from a group of neurons close to the site of issue of this nerve. In contrast innervation of the uterus is supplied by several smaller nerves, and the NADPH-diaphorase positive perikarya that issue these projections have a wider distribution throughout the ganglion. However, NADPH-d positive neurons are observed in other areas of the pelvic ganglion (as well as proximal to the genital nerve) and it would seem probable that some of these are the nitrergic neurons that project to bladder; it is also known that neurons that project to the bladder have no particular topographical distribution, but are spread through the entire ganglion (Keast et al, 1989) with a predominance in the ventral half of the ganglion, near the origin to the bladder nerves (Steers et al., 1990).

The sex difference in the number of NADPH-d positive neurons is mainly accounted for by the large number of NO-neurons supplying the penis, as compared to the smaller influence of nitric oxide in the uterus. The data is unable to supply evidence of any differences between the sexes in the numbers of NO neurons that project to specific organs e.g. the bladder and rectum, and to do so retrograde studies need to be performed.

The absence of co-localisation of tyrosine hydroxylase and NADPH-diaphorase staining is evidence that sympathetic, adrenergic neurons do not express NADPH-diaphorase. This observation is endorsed by the literature where it is suggested that NO containing neurons of the pelvic ganglion are confined to the parasympathetic neuron population (Warburton and Santer, 1993 working with male rats and Papka et al, 1995 with female rats) as no co-localisation of tyrosine hydroxylase (TH) or Neuropeptide Y (NPY) with NADPH-diaphorase has been observed. Unequivocal staining of parasympathetic neurons is difficult, but good correlations between staining for acetyl cholinesterase (AChE) and predicted parasympathetic sites (neurons positioned in the pelvic ganglion proximal to the entry of the pelvic nerve) have been described (Dail et al., 1975) and with this method Warburton and Santer (1993) showed extensive co-localisation of NADPH-diaphorase and AChE staining. The weight of evidence therefore points to the fact that NADPH-diaphorase is restricted to parasympathetic neurons, but caution must be exercised if this method is to be used as an absolute parasympathetic cell marker; additional evidence in support of this notion is supplied by Alm and co-workers (1995) who not only corroborate the distribution of NADPH-diaphorase in the pelvic ganglion, but also state its occurrence in other parasympathetic ganglia (sphenopalatine, submandibular, sublingual and otic).

There is evidence that neurons in which VIP-immunoreactivity and NADPH-d staining coexist, of the type outlined in this thesis in the ganglion of the male, project to the penis and rectum (Domoto and Tsumori, 1994). Co-localisation of the polypeptide and neuronal nitric oxide has also been observed in the female where the neurons project to the uterus (Papka et al, 1995). VIP and NO present in parasympathetic neurons, are thought to act concomitantly on the smooth muscle target tissues (corpus cavernosum, myometrium and penile and myometrial blood vessels).

7.4 Autonomic Ganglion Development

7.4.1 Synaptic and Post-Ganglionic Development

The anatomy of pelvic plexus of the new-born rats displays post-ganglionic nerve trunks that travel to the target organs, as well as incoming pre-ganglionic trunks. This arrangement is identical to that of the ganglia from pre-pubertal and adult animals, and indicates that already at this stage of development axons have been issued by the ganglion neurons and that preganglionic axons have reached the ganglion. However, synaptic specialisations were not observed in the pelvic ganglion in this thesis which suggests that at birth there is no functional control of target organs. Unfortunately, due to the dearth of embryonic and neonatal studies of the pelvic plexus, in order to understand its synaptic development one must relate observations made in this structure to those in the rat superior cervical ganglion (the tissue in which most information is available).

The SCG begins to form on embryonic day 12 (E12) with the coalescing of sympathetic precursor cells along the dorsal aorta. The first post-mitotic principal neurons appear at E12 and they continue to be born up to E20 (Hendry, 1977). On E12 some of these differentiated sympathetic neurons have extended post-ganglionic axons which can be followed beyond the developing ganglion into exiting nerve trunks (Rubin, 1985a). The following day (E13) pre-ganglionic axons from the spinal cord first enter the SCG; electrophysiological evidence suggests synaptic formation occurs within hours of axon arrival and the first morphologically distinct synapses are viewed on E14 (Rubin, 1985b). If events in the pelvic ganglion parallel those of the SCG, (which is likely bearing in mind that the pelvic ganglion also contains sympathetic as well as parasympathetic neurons) it seems strange that no synapses are present in this structure in the newborn when at this age specialisations have been present in the SCG for about 7 days.

In contrast to neurons of pelvic ganglia, SCG neurons have many dendritic processes and these begin to form on the fourteenth day of gestation. Retrograde labelling studies by Rubin (1985a) using horseradish peroxidase showed that many short dendrites initially protrude from the cell soma, but that during subsequent days only some continue to extend while others retract; the adult number of dendrites is present at birth although they

are shorter in length at this stage. Synapses present at the end of embryogenesis are made with these dendritic processes (Rubin, 1985b), whereas the first identifiable synapses are axosomatic and formed with the cell soma before the onset of dendritic development (Rubin, 1985b).

Smolen and Raisman (1980) have shown that the number of synapses in the SCG rapidly rises after birth, a 7-8 fold increase in the first 3 post-natal weeks. The rate of increase slows with age when, at between one and three months, there is a 30-40% increase in synapse number (Smolen and Raisman, 1980). The pelvic ganglion also demonstrates numerous synapses in both the three week old animals and adult animals studied in this thesis although quantitation was not undertaken so that it was not possible to highlight any change in the rate of synapse formation.

In sympathetic (Lichtman and Purves, 1980; Snider, 1986) and parasympathetic (Lichtman, 1977) autonomic ganglia (as well as in the central nervous system reviewed by Purves and Lichtman, 1985a) during the early stages of synapse formation there is much rearrangement of these contacts, this process known as 'synaptic elimination'. Whereas initially several different pre-ganglionic axons make synaptic contact with each neuron, shortly after birth (during the first week) some of these axons withdraw their terminals from some cells while increasing their connections with others. The molecular mechanism behind this process is not known but is believed to result from competition among presynaptic axons for some feature of the post-synaptic cell. 'Synaptic elimination' transforms a situation where each axon makes weak contacts on many neurons, to one of stronger contacts on fewer cells. It is possible that initial, weak synapses of this type, although not identified in the neonatal pelvic ganglion are in fact present, and that it is only because they are more mature (and much more numerous) in the pre-pubertal animal that they are only observed by electron microscopy at this later stage.

7.4.2 Neuronal Morphological Development

The neuronal measurements carried out in this thesis suggest that as the whole animal develops, neurons present in the pelvic ganglion also grow. Again most of the work in this area has been carried out on the superior cervical ganglion where dendritic

development is generally the characteristic analysed, although certain studies also investigate somal size. There are two sources described in the literature that are thought to influence this neuronal development: preganglionic innervation and peripheral target size. Each of these influencing factors will now be discussed in turn.

7.4.2.1 Influence of Preganglionic Innervation

Many observations in the central nervous system indicate that pre-ganglionic innervation influences neuronal dendritic development. This notion is supported by normal development studies that show that innervation usually precedes dendrite formation (Berry et al., 1978), and experimental studies that remove presynaptic inputs prevent normal dendritic outgrowth (Levi-Montalcini, 1949; Benes et al., 1977). Smolen and Raisman (1980) describe a relationship in the autonomic nervous system between pre-ganglionic innervation and synapse formation. Their study in the SCG showed that transection of the cervical sympathetic trunk at birth, combined with prevention of re-innervation, eliminates more than 90% of synapses. This procedure is also known to have other developmental effects, both on neuronal ontogeny, where it prevents normal post-natal increases of tyrosine hydroxylase (Smolen et al., 1985) and peripheral target tissue ontogeny (Lawrence et al., 1979). However, dendritic development in the SCG is hardly effected by deafferentation in either adult (McLachlan, 1974) or neonatal rats (Smolen and Beaston-Wimmer, 1986; Voyvodic, 1987). As dendrites continue to grow for up to 6 months after denervation (Voyvodic, 1987) it appears that preganglionic input has little involvement in the control of dendritic maturation. Denervation experiments similar to those described would also be useful in the pelvic ganglion; presumably a relationship similar to that documented by Smolen and Raisman (1980) exists between deafferentation and synapse formation, but whether there would be an effect on postganglionic development is less clear.

7.4.2.2 Influence of Peripheral Target Size

The length and complexity of dendrites in superior cervical neurons increases for as long as the animal, and its comprising neural targets, continue to grow (Rubin, 1985a; Voyvodic, 1987 and 1989a). A similar relationship is also present in phylogeny, where complexity of dendritic and axonal arborisation compensates for the decreases in the ratio

between the number of innervating neurons and overall body weight (target tissue) (Purves and Lichtman, 1985b; Purves et al, 1986; Snider, 1987). This evidence suggests that the increase in size of peripheral target tissues has a regulatory influence on neuronal morphology.

Evidence in this thesis suggests that a similar relationship is present in the pelvic ganglion. Dendritic development aside (it is well established that most mature neurons of the pelvic ganglion have very few dendritic processes: Kanerva and Teräväinen, 1972; Tabatabai et al., 1986), neuronal somal sizes continue to increase in size as the animal develops. Pelvic ganglion neurons from rats of both sexes increase in average size progressively in three developmental stages, the smallest neurons of the adult being roughly twice the volume of those of the pre-pubertal, and 6 times those of neonates. The data also shows that certain populations of neurons undergo a greater increase in size, while others experience less (i.e. there is an increase in the range of neuronal sizes). Overall the data strongly suggests a regulatory influence of the increasing target size (developing pelvic organs) on perikaryal size.

Other indirect evidence to the presence of this relationship in the neurons of the pelvic ganglion is obtained from the reports of neuronal hypertrophy in this structure (Steers et al., 1990; Gabella et al., 1992). Experimental reduction of the lumen of the urethra induces a 6 fold increase in bladder muscle weight after 6 weeks. Retrograde tracing with fluorogold revealed that this muscular hypertrophy is accompanied by a large increase in the size of neurons (neuronal hypertrophy) that project to the bladder (Steers et al., 1990) which is reversed with ligation removal and subsequent reduction in detrusor hypertrophy (Gabella et al., 1992). A regulatory influence of the hypertrophic bladder muscle on the perikaryal size leading to neuronal hypertrophy, was suggested in both of these studies.

Manipulation of Relative Target Size

This relationship has been elegantly investigated in rat SCG neurons that innervate the submandibular salivary gland. Voyvodic (1989a) partially denervated this gland at birth, which resulted in a relative increase in target size, as axotomised neonatal neurons do not survive (Hendry and Campbell, 1976; Wright et al., 1983) and thus the partial denervation produces a normal gland that is supplied by fewer neurons. In the same study Voyvodic

(1989a) carried out salivary duct ligation at four weeks of age. This procedure arrests the growth of the gland (Womble and Roper, 1987) and produces a relative decrease in the target size (i.e. a target significantly smaller than normal is innervated by the same number of neurons). Such manipulations of target size were found to have a profound effect on neuronal morphology, a relative reduction producing projecting neurons of smaller somal size with shorter dendrites, a relative increase producing projecting neurons of increased somal size with more numerous and longer dendrites (Voyvodic, 1989a). Using the same experimental protocol relative increases and decreases in target size have also been shown to induce increases and decreases in the diameter, branching and proportion of myelination of postganglionic axons projecting from sympathetic neurons (Voyvodic, 1989b).

Axotomy

Further evidence of target derived regulatory signals is provided by studies that involve postganglionic axotomy. Studies in which a peripheral nerve is crushed or cut report changes in neuronal perikaryal and dendritic morphology that include chromatolysis (disintegration of Nissl bodies), separation of rough endoplasmic reticulum and nuclear translocation to an eccentric position within the cell body (Lieberman, 1971; Matthews and Raisman, 1972; Matthews, 1973). Additionally, Yawo (1987) documented a reduction in dendritic arborisation in the mouse SCG following axotomy followed by re-expansion if the severed axons are allowed to regenerate; the time-course for this re-expansion is equivalent to that needed for re-innervation of the periphery.

A further feature of motoneuron (Eccles et al., 1958; Mendell et al., 1976; Brenner and Johnson, 1976) and autonomic neuron (Matthews and Nelson, 1975; Purves, 1975) postganglionic severing is a decrease in preganglionic synaptic function. This phenomenon is believed to result from synaptic disconnection (Purves [1975] described a 65-70% reduction in number of synapses on axotomised SCG neurons) and is also induced by interruption (by colchicine) of axonal transport (Pilar and Landmesser, 1972; Purves, 1975).

Experimental evidence from both target size manipulations and axotomy are consistent with the notion that the signal which regulates neuronal morphological development is the

same that is interrupted by axotomy. It therefore seems prudent to suggest that this target regulation occurs in the development of the pelvic ganglion.

7.4.3 Mechanism of Trophic Interaction

In mammalian ontogeny, the final number of nerve cells is generally defined early in development, often in the embryo (Rakic, 1974; Altman and Bayer, 1984). In contrast, overall somatic growth, brought about by the adding of more cells and the enlargement of existing ones, is maintained well into the postnatal period in all mammals. Therefore a body that progressively changes in size and number of constituent cells requires innervation from a relatively fixed number of neurons. In order to ensure efficient neural function during the somatic growth period, the nervous system must also develop in conjunction with the changing targets.

This developmental relationship, powerfully suggested by experiments outlined in the previous section, is widely attributed to trophic interactions (for review see Purves et al, 1988)- 'the long-term interdependent relationship of neurons and the cells they innervate'. These effects take place over days, weeks or even months and are lost when one of the elements in the relationship is removed. The process involves a specific molecular message that passes between the neuron and effector (smooth muscle of the pelvic viscera in this ganglion, although the effector can also be striated muscle fibres or a secretory cells while there is also some evidence that suggests another neuron), in addition to the neurotransmitters released in synaptic transmission. While initially these trophic interactions were put forward as accounting for developmental regulation of neuronal numbers (Hamburger, 1977; Oppenheim, 1981), it is widely suggested that broader based neuronal ontogeny (axonal and dendritic arborisation, somal size and synaptic connections already discussed above) is also subject to this control.

7.4.3.1 Nerve Growth Factor

It is well established that the protein Nerve Growth Factor (NGF) is the target derived substance that controls cell growth and axonal and dendritic development of sympathetic ganglion neurons (Levi-Montalcini and Calissano, 1966; review by Levi-Montalcini,

1987); survival of sympathetic neurons during development is also widely accepted to be dependent on target-derived NGF (see below 7.4.5).

Studies in the superior cervical ganglion support the concept that (at least within this ganglion) throughout life the continuous retrograde transport of NGF produced by the peripheral tissues regulates neuronal morphology. Firstly, NGF is produced by targets innervated by the SCG (e.g. the submandibular gland, Korsching and Thoenen, 1983) and is taken up by sympathetic axon terminals and retrogradely transported to perikarya (Thoenen and Barde, 1980). Secondly, NGF promotes neurite outgrowth *in vitro* (Campenot 1977, 1982a, b), and effects perikaryal size *in vivo* (Hendry and Campbell, 1976; Schafer et al., 1983) and dendritic growth in neonates (Snider, 1988). Thirdly, and most compelling, is evidence supplied by Ruit and colleagues (1990) who exposed adult mice to either prolonged elevated or reduced (by system administration of an NGF antiserum) NGF levels; injection of NGF results in an increase in sympathetic perikaryal size and dendritic length as compared to control animals, while injection of NGF antibodies causes the reverse.

Although most data supporting the notion of NGF developmental control comes from work on sympathetic neurons, Collins and Dawson (1983) supplied evidence of a developmental effect of NGF on the neurite outgrowth from parasympathetic chick ciliary neurons. Furthermore, Steers and colleagues (1989) showed that NGF was present in the bladder detrusor muscle and, combined with the data obtained from urethral obstruction (Steers et al., 1990; Gabella et al., 1992), suggest the possibility of a similar role for NGF in the morphological control of pelvic neuron development.

7.4.4 Control of Neuronal Numbers

The estimated number of neurons in the pelvic ganglion of newborn female rats is 11,640 ± 892 while in pre-pubertal animals of the same sex this figure is 6,563 ± 689, with adults 6,845 ± 717. There is clearly in large reduction in number of neurons during the development of the pelvic ganglion in the female rat; the reduction in neuron number appears to occur during the three weeks of development from the neonate to the pre-pubertal age, as neuron numbers in the pre-pubertal rat are equivalent to those of the adult. The estimated

number of neurons in the pelvic ganglion of newborn male rats is 12,604 ± 1,403 while in pre-pubertal animals this figure is 13,605 ± 1,490. In adult male rats this figure is 12,506 ± 668 which suggests that neuronal populations remain relatively constant in ontogeny of the ganglion of the male rat. However, experimental investigation of cell death using the TUNEL method did provide evidence that some neurons in the pelvic ganglion of the newborn male rat were apoptotic, but presumably the number of cells dying were too few to be highlighted by the stereological estimates made in the three developmental age groups.

7.4.4.1 Neuron Death

Cell death performs an important function in many different areas of vertebrate development (Glücksman, 1951). The phenomenon is divided into three categories (Ernst, 1926): the first (phylogenetic) occurs during disintegration of tissues that develop transiently in the embryo (e.g. the death of neurons in the caudal end of the spinal cord of vertebrate embryos, leaving only glial cells in the filum terminale); the second (morphogenetic) occurs during growth at regions of separation, fusion, folding, bending, or cavitation (e.g. the posterior necrotic zone in the developing chick wing); the third (histogenetic), where tissues are remodelled and the final number of cells of different kinds adjusted after an initial period of excessive cell production.

There are two different developmental strategies that result in the death of neuronal precursors. The first is programmed cell death in which certain neurons in a developmental lineage are intrinsically programmed to die (this process has only been studied in invertebrates e.g. the nematode, C. *elegans* , in which the lineage of its few cells have all been traced in work by Sulston and Horvitz, 1977). The second strategy, and the one most widespread in histogenesis of the vertebrate nervous system is target-dependent neuron death: this does not involve lineage but results from competition between nerve cells at the level of the target they supply.

Histogenetic cell death is present at sites throughout the central nervous system (e.g. cerebral cortex, cerebellum, cranial motoneurons, spinal somatic motoneurons and retinal neurons) and the peripheral nervous system (for review see Jacobson, 1996), specifically in the superior cervical ganglion (mouse: Levi-Montalcini and Booker, 1960a; rat: Wright and Smolen, 1983, 1987; Chick embryo: Maderdrut et al., 1988) and parasympathetic

ciliary ganglia (Chick embryo: Landmesser and Pilar, 1978; Pilar et al . 1980; Wright, 1981) . The neuron death observed by the TUNEL method in the pelvic ganglion of newborn rats of both sexes in this thesis is probably another example of histogenetic cell death.

Although the numbers of neurons in the pelvic ganglion identified as apoptotic by TUNEL staining was small, this low incidence could be due to the staining technique employed, which like any histochemical procedure, only demonstrates a 'snapshot' in the time course of the total process of neuronal number regulation. Evidence (reviewed in Bursch et al., 1990) suggests that from the onset of the disintegration of the nucleolemma, through the degradation of the chromatin, and finally to the phagocytosis of the apoptotic cell fragments, the entire process of cell death and removal takes an estimated 3 hours. It has been estimated that the combination of this 'snapshot' notion and the rate of cell elimination can result in approximately 25% reduction in a cell population per day when as little as 2-4% of the cells in the preparation are observed as apoptotic.

As with many aspects of autonomic development, the superior cervical ganglion (SCG) has been selected to investigate how neuronal populations in the autonomic nervous system are regulated in order to innervate developing targets. In the SCG, during the first two postnatal weeks immature synaptic contacts (both pre-ganglionic/post-ganglionic and post-ganglionic/target) made initially in the embryo become mature (for review see Wright, 1995). The first postnatal week is when developmental neuron death occurs in the SCG, resulting in the loss of 30-40% of the neurons present at birth (Hendry and Campbell, 1976; Wright et al., 1983), the cell death reaching its peak on postnatal day 5 (Wright et al., 1983). Interestingly in the pelvic ganglion there is also an elevation in cell loss during the first week of life, but this increase appears to be restricted to the female; as Wright and co-workers (1983) do not state the gender of rats used, it is impossible to say whether neuron reduction in the SCG of this magnitude is a general developmental characteristic or one specific to the development of sexual dimorphism (see section 7.5.2).

Whereas Le Douarin (1986), through her neuron lineage studies in the chick embryo, has described the death of immature neurons in precursor neural crest cells (probably programmed cell death) or in very young ganglia, the neuron death reported in autonomic

ganglia occurs in more differentiated neurons (for reviews see Oppenheim, 1989, 1991). The developmental death of autonomic neurons often occurs at a later stage of maturation, when many neuronal phenotypic characteristics, including axonal projection to post-synaptic targets, are already present (e.g. SCG neurons that project to the middle cerebellar artery die in the post-natal period; O'Connor and van der Kooy, 1989). Whereas in some structures developmental neuron death provides the removal of cells that have formed unwanted target connections (e.g. retinal ganglion cells; O'Leary et al, 1986) this does not seem to be the case in the SCG where few errors in projection to sympathetic tissues are reported (Rubin, 1985c).

The mechanism behind the reduction in neurons described above is thought to be an active killing process, one initiated by the expression of specific genes that encode for the transcription of new gene products (Umansky, 1982, Martin et al, 1988; Oppenheim et al., 1990; Scott and Davies, 1990) that in turn lead to the death of the cell. To counter the action of the gene or gene products, trophic factors are thought to intervene and halt the process of death. It follows that the expression of cell death genes would be permitted in the absence of trophic agents, leading to the production of lethal proteins and ultimately cell deletion. Nerve Growth Factor (NGF) is postulated to be one of the agents responsible for maintaining cell integrity. The previous section describes how regulation of nerve cell morphology is dependent on NGF, and much evidence also suggests a similar role for NGF in the process of cell death. Most of the evidence is gained from SCG sympathetic neurons, although Tuttle and colleagues (1994) did show that NGF also increases the survival of pelvic ganglion neurons in culture.

A Role for Target -Derived NGF

Much evidence supports the notion that NGF produced by target tissues is responsible for the survival of sympathetic neurons in the superior cervical ganglion. Firstly, for survival of sympathetic neurons during the first post-natal week, target tissues which are known to contain NGF (e.g. the submandibular gland, Korsching and Thoenen, 1983), must be present (Dibner et al., 1977). Further compelling evidence arises from experiments in which exogenous NGF was administered which show that the protein prevents normal developmental neuron death, and also experiments involving target ablation or neuronal

axotomy that induce increases in neuron death (Levi-Montalcini and Booker, 1960b; Levi-Montalcini 1964; Hendry and Campbell, 1976; Banks and Walter, 1977; Goedert et al., 1978). Additional evidence supporting an influence of NGF (which is known to be retrogradely transported by neurons from target tissues; Korsching and Thoenen, 1988) in neuron survival was supplied by Gorin and Johnson (1979) who showed that if neuronal procurement of the protein ceases due to the removal of NGF via ant-NGF antibodies, then sympathetic neurons die.

NGF is first detected in the mouse SCG at about the same time, E12 and 13, that sympathetic fibres innervate target tissues; NGF levels continue to rise during this perinatal period before reaching adult levels in the third week after birth (Korsching and Thoenen, 1988). This evidence, combined with an observed correlation between the extent of innervation and NGF mRNA levels in target tissues (Goedert et al., 1986) suggests that the density of sympathetic axonal branching in peripheral tissues is dependent on the availability of NGF. What cells actually produce NGF, and by what exact mechanism this production is controlled are not known, although experiments involving cultured rat iris suggest a calcium-independent mechanism (Barth et al., 1984).

Competition for Neurotrophic Support

In the control of cell numbers, the basic concept of neurotrophic theory (described in section 7.4.3 in the control of cell morphology) is the same: neurons are critically dependent upon limited quantities of trophic molecules, those failing to acquire sufficient amounts fail to survive (Purves et al., 1988; Oppenheim, 1989). Evidence obtained from work with motoneurons has suggested that the determining factor is not the amount of neurotrophic factor but the limited opportunity for synaptic contact with the target; it follows that motoneurons with axons that have more branches or synaptic contacts gain larger trophic support and thus survive (Oppenheim, 1989). In sympathetic neurons, as already discussed, NGF also increases dendrite number and dendritic arborisation (Purves et al., 1988; Voyvodic, 1987), axonal branching in target tissues (Black and Mytilineou, 1976) and ganglionic synapses (Schafer et al, 1983), which suggests that a similar mechanism to that reported in motoneurons also exists in autonomic neurons.

Evidence provided by Hendry (1977) showing that later-born sympathetic neurons are more likely to die than older (earlier differentiated) neurons suggests that temporal factors may influence survival. Furthermore, observations that innervation from the SCG arrives at different times in different tissues (Black and Mytilineou, 1976; de Champlain et al., 1970) and that levels of NGF also differ between different targets (Wright et al., 1987; Korsching and Thoenen, 1988) lend support to the possibility of time related differences in the extent of neuronal death in sympathetic neurons supplying different tissues.

Other Sources Supporting Survival

There is evidence that trophic factors are not only derived from target tissues but that afferent connections, extracellular matrix and glial cells are also a source of such substances (Lipton, 1986; Johnson et al., 1988; Walicke, 1989).

Separate to support of neuronal survival from trophic substances is regulation supplied by preganglionic innervation. Control of this nature has been investigated in the SCG by experimental transection of the sympathetic cervical trunk in the neonatal rat which results in 20-25% fewer surviving neurons (Wright, 1987). Administering of ganglion blocking agents in chick embryos results in elevated neuron death in both sympathetic ganglia (Maderdrut et al., 1988) and the ciliary ganglion (Wright, 1981). However, it is not clear whether preganglionic support of neuronal survival is accounted for by trophic molecules released at terminals or whether it is an inherent characteristic of such connections.

7.4.4.2 Neuron Lineage

Another possibility that could account for the changes in neuronal number observed in the pelvic ganglion is interconversion between different cell types. The neural crest, a transient structure present during embryonic development, gives rise to several kinds of adrenergic cell types (Le Douarin, 1986; Landis and Patterson, 1981), that include principal neurons and small, intensely fluorescent cells (found in sympathetic ganglia and the 'mixed' pelvic ganglion), and also adrenal chromaffin cells (parasympathetic, enteric and sensory neurons as well as glial cells are also derived from the neural crest). The different adrenergic cell types have contrasting anatomical locations and cytological expression of particular biogenic amines. The SCG of the rat is reported to contain approximately 30,000 noradrenergic principal neurons and 600 dopaminergic SIF cells

(Björklund et al., 1970; Davies, 1978; Eränkö and Soinila, 1981; Smolen et al., 1983), but the proportions of SIF cells, although numerous, are not known in the pelvic ganglion (Kanerva and Teräväinen, 1972; Dail et al., 1975; Baker et al, 1977). Similar embryonic precursors found in ganglionic and adrenal primordia are thought to develop into sympathetic neurons, SIF cells and chromaffin cells (Landis and Patterson, 1981; Anderson and Axel, 1986; Anderson, 1989) and the direction of development is determined by environmental cues (Doupe et al., 1985a). Studies in vitro and in vivo indicate that glucocorticoids induce and maintain the SIF phenotype (Doupe et al., 1985b) while NGF promotes the survival of principal neurons (Levi-Montalcini and Angeletti, 1963; Chun and Patterson, 1977; Coughlin and Collins, 1985); interconversion of these end phenotypes occurs in culture (Doupe et al., 1985b). However, what determines SIF and principal neuron differentiation in vivo is less clear although Doupe and colleagues (1985b) did suggest that neuronal precursors resemble mature SIF cells and as such are possibly neuron precursors. In addition to cells with distinct neuronal and SIF cell characteristics in newborn pelvic ganglion, there were occasional cells described in this thesis that contained nuclei that resembled neurons and large dense core vesicles reminiscent of SIF cells. The lack of a clear phenotypic distinction at this stage could possibly represent the conversion of neurons to SIF cells. In the SCG most neurons at birth are post-mitotic (Hendry, 1977; Landis and Damboise, 1986) and examination shows that mature SIF cells are first observed after most neurons are fully differentiated (Hall and Landis, 1991) and so it appears that phenotypic development of SIF cells and principal is regulated by different developmental cues. If events in the pelvic ganglion resemble those in the SCG then it seems unlikely that interconversion occurs to an extent that would account for the extensive change in neuron numbers recorded.

7.5 Comparative (Sexual) Development and Castration

7.5.1 Ganglion Anatomy and Volume

There are marked anatomical variations in the pelvic ganglion between the sexes, and these differences develop during the early weeks of life. At three weeks of age (pre-pubertal) the anatomy of the ganglion is much the same as in adult animals i.e. shows

obvious sexual dimorphism. In contrast, in the newborn this gender difference is mush less apparent and, although there are anatomical differences in post-ganglionic nerves related to topography, the substantial differences in ganglion dimension and shape, is not seen.

The anatomical observations of sexual dimorphism are confirmed by morphometric measurement; the proportion to which the ganglion volume increases in comparison to the animals body weight varies between the sexes. In rats of both sexes, as the animal grows and increases in body weight, ganglion volume also increases. From the newborn animal to the pre-pubertal animal, there is an approximate 12-13 fold increase in body weight. In male rats this early increase in body weight is accompanied by a 4 fold increase in ganglion volume, while in the female this increase is only twice that recorded in the neonate; this sex difference is maintained into adulthood.

Castration of three week male animals exerts little effect on the gross anatomy of the ganglion, despite bringing about a significant reduction in pelvic visceral weight. All the major nerve connections observed in the intact animal are present and there are no detectable changes in ganglion volume as compared to unoperated animals.

At this level of investigation, it is clear that the pelvic ganglion develops in harmony with the organs that it innervates. The reproductive organs particular to each sex receive innervation and it is this physical anatomical difference itself that, by its very nature, requires nerves of differing topography. Separate to this is the appearance of the main ganglion body, that differs little in shape in neonates, but is vastly sexually dimorphic in pre-pubertal and adult animals. The volume of the main ganglion body is similar in the newborn, but differs significantly between the sexes in pre-pubertal and adult animals. What gross anatomical investigation cannot answer is whether these differences in ganglion volume observed during development are due to increases (mitoses) or reductions (cell death or migration) in neurons, changes in neuronal size, changes in other ganglion constituents (e.g. fibres in transit, glial cells and blood vessels) or a combination of these factors?

7.5.2 Neuron Number

Significant gender differences are present in the number of neurons present in the pelvic ganglion of the adult rats, male animals having roughly twice as many as females; this observation reaffirms that of Greenwood and co-workers (1985). Similar sex differences have been reported in the rat hypogastric ganglia (in this work termed the accessory ganglia that predominantly innervate the prostate, seminal vesicles and vas deferens) (Melvin and Hamill, 1989), the hypogastric ganglion (term used in that work to describe the mouse analogue of the pelvic ganglia) of the mouse (Suzuki and Arai, 1986) and also the rat SCG (Wright and Smolen, 1983a). A hypothesis that is widely made is that this sexual dimorphism is induced by actions of circulating testosterone, a sex steroid that occurs in high levels in males and much lower levels in females; whether testosterone exerts its effect via direct or indirect mechanisms is unknown.

7.5.2.1 Influence of Gonadal Steroids

During the period of three days before birth and a week after birth, the central nervous system is known to be sensitive to the effects of gonadal steroids (MacLusky and Naftolin, 1981). At this time there is a significant rise in the level of the circulating androgen, testosterone, in the male (Lieberburg et al, 1979; Weisz and Ward, 1980). Testosterone can exert its influence at cytoplasmic androgen receptors directly (Lieberburg and McEwen, 1977), or indirectly by conversion to 5-alpha-dihydrotestosterone (Martin, 1976). It has also been shown that testosterone can be aromatised to oestradiol within some neurons (Naftolin et al, 1975; Lieberburg and McEwen, 1977; Selmanoff et al, 1977) and it is presumably by this process that testosterone acts at oestrogen receptors (Toran-Allerand, 1976; Lieberburg and McEwen, 1977; Naftolin and Brawer, 1978; Toran-Allerand et al., 1980; McEwen, 1981). Whereas oestrogens do not enter the rat brain due to associations made with alpha-fetoprotein (MacLusky and Naftolin, 1981), this alpha-globulin does not bind testosterone and thus leaves the androgen free to exert its effects in the central nervous system, and presumably also in peripheral nervous system.

Sex organs sensitive to gonadal hormones (Wakade et al., 1975), are innervated by the pelvic ganglion, along with other non sex related structures such as the bladder and rectum

(Langworthy, 1965; Purinton, 1973; Baljet and Drukker, 1980). Work with biochemical markers has indicated that adrenergic neurons are sensitive to their hormonal environment; post-natal castration at day 10-11 leads to a significant reduction in tyrosine hydroxylase activity (Black and Green, 1973), DOPA decarboxylase activity and choline acetyltransferase activity (Melvin and Hamill, 1987) which is completely reversed by testosterone replacement. Furthermore, testosterone administration in post-natal animals leads to an increase in cell size and catecholamine histofluorescence in the male but not in female pelvic ganglion (Hervonen et al., 1972; Partanen and Hervonen, 1979a). Partanen and Hervonen (1979b) also show that pre-pubertal orchidectomy leads to a reduction in neuron size and catecholamine histofluorescence in neurons of accessory (hypogastric) ganglia, which is reversed by testosterone replacement. Melvin and Hamill (1989a) termed these transient effects of testosterone as "activational" and, due to the fact that androgen receptors are present in the accessory (hypogastric) ganglia (Melvin and Hamill, 1989b) and that the target tissues themselves are sexually dimorphic, may result from androgen action indirectly at the target tissue, directly on ganglion cells or a combination of the two.

Organisational/Activational Hypothesis

In contrast to adult animals, there is no difference in neuronal number in the pelvic ganglia of neonates. It has been suggested that systems subject to influence from sex hormones undergo permanent "organisational" changes due to these steroids acting in this critical period of development (Melvin and Hamill, 1987, 1989a). The critical periods of development where these permanent "organisational" changes in sexual differentiation take place, are characterised by well documented fluctuations in plasma testosterone levels. Weisz and Ward (1980) have shown that during the last week of embryonic life, systemic testosterone levels in male rats are significantly higher than those in females, this accompanied on embryonic days 18 and 19 by a major surge in the androgen in males. A further rise in testosterone occurs at birth, and throughout the first week of life androgen levels in the male exceed those in the female (Weisz and Ward, 1980). After the first week of life plasma testosterone levels in the male decline, and apart from surges of testosterone observed at puberty (Döhler and Wuttke, 1975), it is not until around 40-50 days of age when sexual behaviour emerges (Resco et al., 1968) that levels return to those of the

perinatal period. There is therefore the possibility that the elevated plasma testosterone in this perinatal period is responsible for inducing the difference of neuron numbers observed in older animals (Fig. 57), and this conclusion was also reached in both work in the superior cervical ganglion (Wright and Smolen, 1983a, b) and the pelvic accessory (hypogastric) ganglia (Melvin and Hamill 1989b) which experienced a large reduction in neuron number following neonatal castration (Melvin et al., 1988 and 1989). Furthermore, Suzuki and colleagues (1983) have also shown that neuron numbers are sensitive to perinatal testosterone, where prenatal exposure of male mice to the steroid induces a significant increase in neuronal number in the hypogastric ganglion; Suzuki and Arai (1986) later supplied evidence of sex difference in the volume of the hypogastric ganglion which they attributed to differences in neuron number that are controlled by androgens (Suzuki and Arai, 1985).

In pre-pubertal animals, gender difference in neuron number in the rat pelvic ganglion is observed, and pre-pubertal orchidectomy carried out in this thesis results in no reduction in the number of neurons in pelvic ganglion of the adult male, although does induce reduction in average neuronal size. This suggests that at about three weeks of age, control of the development of neuronal cell populations in the ganglion is complete, and that the surges of testosterone at puberty have no further effect. "Organisational" effects of testosterone in the pelvic ganglion have been reported to be dependent on both the time of exposure and dose of the steroid. Melvin and Hamill (major pelvic ganglion: 1989a; and hypogastric (accessory) ganglia: 1989b) showed that tyrosine hydroxylase activities and choline acetyltransferase activities were both restored to normal levels with testosterone replacement after neonatal castration; oestrogen replacement only restored choline acetyltransferase activities. A pre-natal androgen critical period was described after chemical 'castration' with the anti-androgen flutamide (Neri et al, 1972) induced an altered ontogeny such that both tyrosine hydroxylase activities and choline acetyltransferase activities were not restored with neonatal testosterone replacement (Melvin and Hamill, 1989a). This evidence suggests that alterations in the level of circulating testosterone have no organisational effect unless they occurs in this perinatal critical period.

However, the many neurons that must be undergoing cell death in the neonatal animals in order for the population to reduce to that observed in the pre-pubertal and adult, were not observed in electron microscopic preparations. This is surprising as, although in the male only a small adjustment in cell number must occur, in the female the reduction, assuming the difference in estimated cell number is solely due to cell death, is approximately 40%: surely these numerous cell deletions would be evident in histological section? One explanation is that the tissue employed in the electron microscope work was newborn preparations and as the results show, instances of cell death highlighted by TUNEL appeared more abundant in ganglia from 7 day old animals; this observation agrees with the peak period of cell death reported in the SCG (Wright et al., 1983). A second explanation for the absence of observed "dying" in ganglia viewed in the electron microscope can partly be explained tiny sample a field of view at high magnification affords and, this combined with the reported rapidity of the removal of apoptotic cells and cell debris (Bursch et al, 1990) would result in only a very small chance of viewing an apoptotic cell. Blood borne cells (macrophages) were viewed in the ganglionic neuropil and this lends support to the suggestion of rapid phagocytic removal.

7.5.3 Neuron Size

Neuronal sizes in the pelvic ganglion of adult animals are sexually dimorphic, with those from the male having a wider range and a larger (by approximately 1.5x) average size (cross sectional area) than those from the female. Although there is a slight difference recorded in average cell size in pre-pubertal male and female animals, this difference is not significant and size range is also more comparable. Neurons from the ganglia of newborn rats are remarkably similar in average size and range.

Testosterone treatment in newborn animals increases neuron cell size in the ganglion of the male but not in the female (Hervonen et al, 1972; Partanen and Hervonen, 1979a) and castration in the pre-pubertal animal leads to a decrease in cell size in accessory (hypogastric) ganglia that is reversed with administration of testosterone (Partanen and Hervonen, 1979b). The data produced in this thesis from the castration of three week old male rats shows no reduction of ganglion volume but induces a reduction in the average

neuronal cell size to a value slightly less than that of female rats; these observations are also similar to those described by Partanen and Hervonen (1979b). The overall histology of the pelvic ganglion is unaffected by this procedure.

These observations suggest that in pre-pubertal animals ganglion neurons are not fully mature and these immature ganglia of both sexes closely resemble one another in all but neuron number. At some time between this three week old stage and the adult stage, changes occur in certain neurons that result in sexually dimorphic average neuronal sizes. Surges of testosterone occur at puberty (Döhler and Wuttke, 1975; Corpechot et al, 1981) and it is possible that these cause the increase in average cell size. The range of neuronal sizes recorded increases in the adult male as compared to that of the pre-pubertal, while there is less of an increase of the range in adult female animals. This suggests that only certain neuronal populations undergo this hypertrophy, while others are influenced to a lesser degree.

Whether testosterone acts directly or indirectly on the sensitive neuronal populations is unknown. This question may be answered by taking into account the parallel events recorded in the pelvic viscera. In castrated animals, the significant reduction in organ weight indicates a direct action of pubertal testosterone on these structures, as these structures are substantially larger in control animals with normal steroid levels. The work by Wakade and colleagues (1975) also showed evidence of atrophy and added that the lack of testosterone had the effect of directly reducing the size of smooth muscle cells in these organs. It appears that neurons in the intact male that supply these androgen sensitive organs also undergo hypertrophy which is probably induced by increased amounts of acquired target-derived neurotrophic factors (e.g. NGF) rather than from a direct action of testosterone via neuronal receptors (Fig. 57). NGF synthesis in the sympathetically innervated mouse submaxillary gland is sensitive to testosterone (Ishii and Shooter, 1975) and similarly it is possible that NGF production in tissues supplied by the pelvic ganglion is also stimulated by the androgen.

Figure 57: ONTOGENY OF GENDER DIFFERENCE IN THE MAJOR PELVIC GANGLION.

The pelvic ganglion in male and female newborn rats (**1a** and **1b**) is homogeneous in structure. At birth the neuronal population is roughly the same in male and female animals as are the neuronal cell sizes.

In the pre-pubertal animal (**3a** and **3b**), the neuron number in the female (**3b**) has reduced, this value remaining into adulthood (**4b**). Perinatal exposure to testosterone (**T**) is a possible control for this ontogeny, the androgen supporting neurons in the male, the lack of the hormone in the female allowing increased neuron death (dying neurons show a stippled appearance- **1b**).

Further adjustment of the neuron number also occurs in development. As neurons find their target organs, those making contact gain adequate quantities of trophic substances (e.g. **NGF**) and survive (**2a** and **3a**, **2b** and **3b**), while those that fail to make effector contact die, possibly due to lack of trophic support (dying neurons show a stippled appearance- **2a** and **2b**). (For simplicity neurons in **1a** and **1b** have been depicted as having no axons when in fact these nerve processes are present in post-ganglionic nerves viewed in newborn preparations).

Neurons in ganglia from both sexes undergo developmental increases in perikaryonic size (from **3a** and **3b** to **4a** and **4b**). The innervated tissue influences the neuron growth, the main mechanism involved being based on the availability of trophic substances (e.g. **NGF**) for nerve cells.

Neuron sizes in pre-pubertal animals show no gender difference (**3a** and **3b**) but do so in the adult (**4a** and **4b**). Testosterone (T_2) again is a strong candidate for exerting this control, its elevated levels in the pubertal male inducing marked hypertrophy in the reproductive organs. Neurons innervating these stimulated organs would thus receive larger amounts of NGF and increase in their somal size (**4a**).

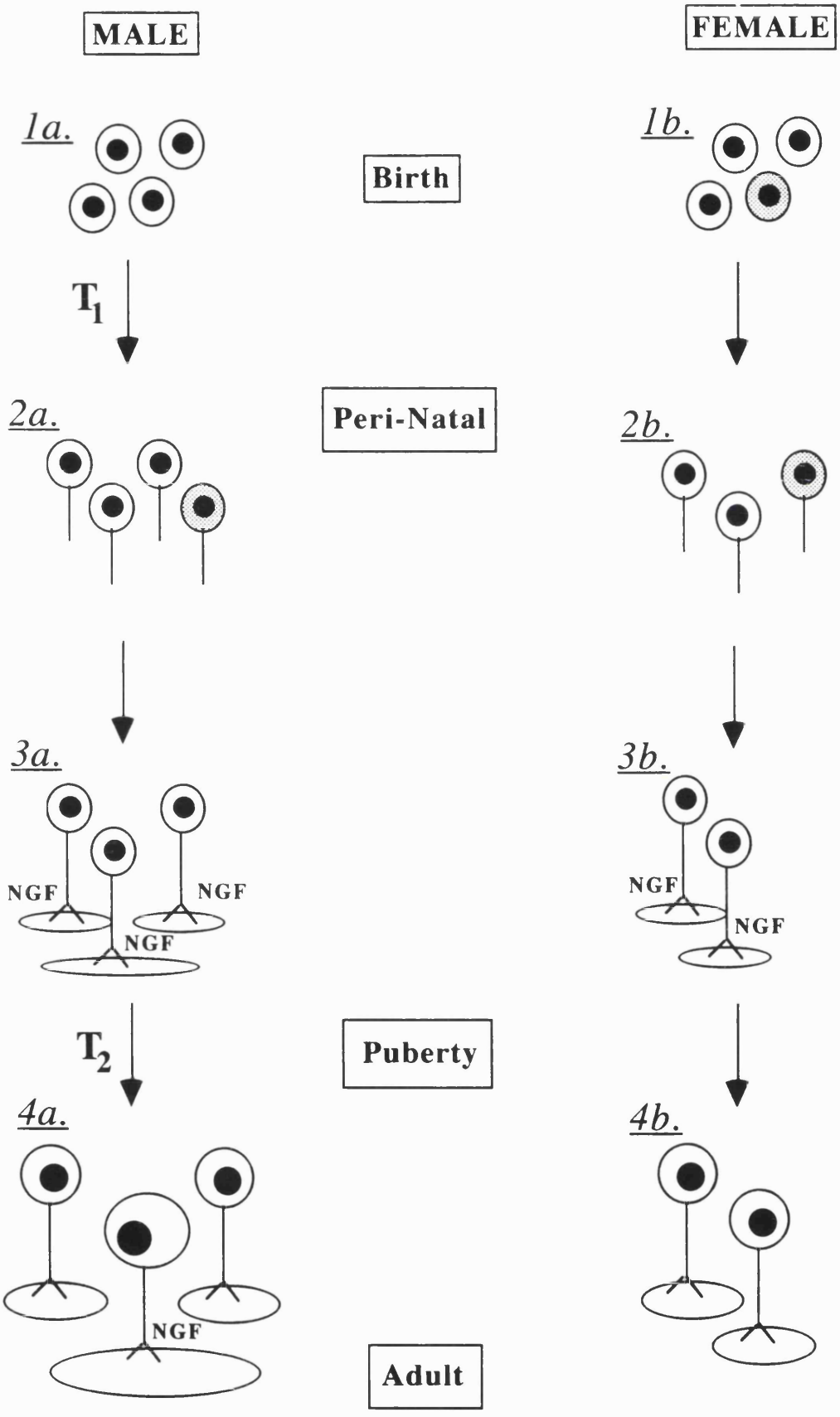
MALE
FEMALE
1a.
1b.
Birth
T1
2a.
Peri-Natal
2b.
3a.
NGF
NGF
NGF
3b.
NGF
NGF
T2
Puberty
4a.
4b.
NGF
Adult

7.5.4 Functional Specificity and Topographical Representation

In the pre-pubertal animal, as in the adult, the same sex difference in the viscerotopic spread of NADPH-d positive cells is observed, the characteristic density of NADPH-d positive cells at the emergence of the genital nerve is present in male rats but not in females. This is presumably a result of sexually specific development, where a population of nitrergic neurons project via the genital nerve to penis in the male, and it is therefore interesting that it is also present in sexually immature pre-pubertal rats. In the pre-pubertal animal, neurons that express certain cytochemicals that are specifically involved in the control of male external genitalia (Burnett et al., 1992) are already of the adult phenotype and distribution, although the animal is not yet sexually mature.

The increasing levels of circulating testosterone present in the male at puberty (Döhler and Wuttke, 1975) that induce sexual maturity in the animal, produce no further change in expression of neuronal NADPH-diaphorase/NOS. The control of these cytochemical characteristics must take place earlier in development (possibly in the perinatal period) and not being sensitive to changes in androgen levels at puberty is probably what might be termed an 'organisational' effect.

Distribution of tyrosine hydroxylase, vasoactive intestinal polypeptide, substance P and neuropeptide Y, and their co-localisation with NADPH-diaphorase (and therefore the ability to synthesise nitric oxide) were unaltered in ganglia from adult rats castrated just prior to puberty as compared to ganglia from intact adult male rats. Although no absolute quantitation was undertaken, the overall distribution and extent of these cytological markers remained constant in castrated as compared to control animals.

Co-localisation of tyrosine hydroxylase and NADPH-diaphorase staining was not observed in neurons from either intact or castrated rats, and fluorescence for tyrosine hydroxylase was generally in cells at the larger end of the size scale. This evidence suggests that sympathetic, adrenergic neurons do not express NADPH-diaphorase, which is restricted to parasympathetic neurons (Papka et al. 1995, Warburton and Santer, 1993).

The reduction of catecholamine fluorescence in accessory (hypogastric) ganglia following pre-pubertal castration (Partanen and Hervonen, 1979b) was not observed in

this thesis; whether they recorded a reduction in catecholamine per se, or whether the observation was simply due to an apparent reduction in fluorescence resulting from the smaller neuronal sizes after pre-pubertal castration (also noted in this thesis) is questionable, but no reduction in the intensity of TH immunoreactivity after orchidectomy was observed in this thesis.

Vasoactive intestinal polypeptide is extensively co-localised with NADPH-diaphorase in the perikarya of neurons from intact adult and orchidectomised adult male rats. The intensity of immunofluorescence was lower in comparison to the appearance of some preparations in the literature but this was probably due to masking, as the tissue section is first incubated NADPH-diaphorase and the subsequent formazan product could effect the immunoreactivity of the neuron. VIP is known to be widely distributed throughout the pelvic ganglion with an estimated one-third to one-half of the total ganglion neurons expressing the polypeptide (Dail et al., 1983; Gu et al., 1984; Keast and de Groat, 1989). AChE staining has been reported to be extensively co-localised with VIP (Dail et al, 1983) in neurons of the pelvic ganglion. Keast and de Groat report an absence of VIPergic neurons that also express noradrenaline, and that VIPergic neurons in the male rat are smaller than noradrenergic cells. The extensive co-localisation of NADPH-diaphorase activity and VIP reported in this thesis appears in smaller neurons and this cumulative evidence suggests that VIP is restricted to parasympathetic neurons. VIP is believed to assist nitric oxide in eliciting the erectile response in the penis, so it is presumably these NADPH-diaphorase positive, penile projecting neurons that are immunofluorescent for VIP. Therefore, it seems that neuropeptides involved in penile function are not effected by reduction in levels of circulating testosterone.

Immunoreactivity to neuropeptide Y was predominantly, although not exclusively in neurons that were unstained with the NADPH-diaphorase reaction product in both intact and castrated animals. If NADPH-diaphorase staining is regarded as a parasympathetic marker, then as reported in the literature, NPY is predominant in adrenergic neurons. Hamill and Schroeder (1990) reported a reduction in biochemically measured NPY after adult castration accompanied also by a decrease in noradrenaline and tyrosine hydroxylase activity; no quantitation of NPY immunoreactivity was undertaken in this thesis and so it

is difficult to judge whether NPY expression was lower in castrated animals. Expression of substance P in axons traversing the ganglion (presumably sensory fibres) were in evidence in both intact and castrated animals.

During normal development studies have shown that some sympathetic neurons are capable of changing the type of neurotransmitter they express (Patterson and Chun, 1974; Kessler, 1985). Landis and Keefe (1983) demonstrated that noradrenergic sympathetic fibres (projecting from neurons of the SCG) that innervate the sweat glands change during development to cholinergic fibres with VIP-immunoreactivity. Target-derived factors control normal sympathetic transmitter and peptide expression (Fukada, 1980; Garcia-Arraras et al., 1986) as well as the conversion between transmitters (Landis, 1990). The reduction of normal testosterone levels after castration have little effect on transmitter expression in neurons (both sympathetic and parasympathetic) of the pelvic ganglion and therefore it appears the androgen is incapable of inducing transmitter conversion of this type.

While pre-pubertal castration seems to have little effect (or effects too small to be highlighted by immunocytochemistry) on the overall neurochemistry of the pelvic ganglion, castration in the older animal has more effect on biochemical demonstration of neurochemicals in sympathetic neurons of accessory (hypogastric) ganglia (Hamill and Schroeder, 1990). However, generally this lesser effect of pre-pubertal castration is supported by the literature which reports a greater reaction to perinatal castration. Taken as a whole, the results in this thesis demonstrate a pre-pubertal ganglion that is remarkably resistant to the influence of androgen on the expression of neurochemicals. It appears that the pre-pubertal pelvic ganglion has already attained neurochemistry consistent with the adult, and that the surge of testosterone at puberty has little effect on this chemical architecture. Overall the effects of pre-pubertal castration on neurochemical expression is therefore consistent with the activational/organisational role of testosterone and it would seem that, while possibly exerting an activational effect (influencing TH and NPY expression) on the constituent neurons, the major control governing the synthesis of different neurotransmitters occurs earlier in development, possibly in the perinatal period.

CHAPTER 8

SUMMARY AND CONCLUSION

The pelvic ganglion, the main component of the pelvic plexus, supplies post-ganglionic innervation to the reproductive, lower intestinal and urinary tracts. Observations in this thesis demonstrate that the pelvic ganglion of the adult rat displays marked gender differences in ganglion volume, number of neurons and average size of neurons, as well as in the neuronal expression of NADPH-diaphorase and the topographical spread of these cells. The findings concur with, and expand those already described in the literature. Morphometric study of the ganglion volume reveal sexual dimorphism in adult and pre-pubertal animals, values in the male rats approximately 1.5x and 2x that of the female, respectively. While average nerve cell size in the adult male was 1.5x that of the female, in pre-pubertal animals there was no significant gender difference in this value, although neuronal expression of NADPH-diaphorase and the topographical distribution of these cells was sexually dimorphic as observed in the adult. Stereological analysis (with the disector method) revealed a large sex difference in neuronal number in the pelvic ganglion in both pre-pubertal and adult rats, estimates in the male approximately 2x that of the female.

In contrast, these sex differences were not evident in the newborn rats where ganglion volume, nerve cell size and estimated nerve cell numbers were very similar in male and female individuals. The neuron number in ganglia from newborn rats of both sexes were similar to the neuron number in those from pre-pubertal and adult male rats. In light of this evidence it appears that the ganglion develops from a structure that is sexually indistinct at birth, to one that has become markedly sexually disparate in pre-pubertal and adult rats.

Common with studies investigating sexual dimorphism certain pertinent factors were subsequently investigated. Castration of pre-pubertal rats was employed to investigate the possible role of pubertal testosterone in the development of the ganglion, and to see if any of the recorded sex differences present in the adult were induced by the androgen in the pubertal period. The results showed that the absence of pubertal testosterone spurt had no effect on total adult neuronal cell populations or on the presence of a range of neurotransmitter substances (NADPH-diaphorase and its co-localisation with VIP, TH, NPY and SP). However, the absence of pubertal testosterone arrested the development of sex difference in average neuronal cell size in the ganglion and also induced significant atrophy of reproductive organs (penis, seminal vesicles and prostate gland). The results hint at the possibility of an androgenic influence occurring at different extents at different times in development, a dual mechanism (described as either organisational or activational) that has previously been suggested in the literature.

Next, an attempt was made to investigate the nature of the cellular processes altered by exposure to the steroid (e.g. cell division, migration, cell death). The TUNEL method was employed, this technique specifically labelling cells that have recently undergone developmental cell death. TUNEL provided positive evidence that histogenetic cell death was occurring in ganglion neurons in newborn and week old rats, and it appeared that a disparate amount of neuronal apoptosis was taking place in ganglia from week old female rats as compared to males of the same age. These observations lead to the hypothesis that the sexually distinct quantities of neuronal cell death was influenced by the elevated perinatal testosterone levels in the male, the presence of which sustained certain neurons in the male, its absence resulting in increased cell death in the female.

In conclusion it appears that the pelvic ganglion in male and female newborn rats is a relatively homogeneous structure, but as the animal develops becomes increasing sexually dimorphic; the main features of gender difference become established after birth and before puberty. At birth the neuronal population is roughly the same in male and female animals as is the average neuronal cell size. In the pre-pubertal animal, the neuron number in the female has approximately halved, this value remaining into adulthood. A strong candidate for the control of this ontogeny is perinatal testosterone, the androgen staving off cell death in the

male, the lack of the hormone in the female allowing an increased loss of neurons. Increasing testosterone levels in the early post-natal period probably influence the ontogeny of the pelvic ganglion, acting either directly on the neurons, or indirectly via trophic factors released from developing pelvic organs. Evidence suggests that target-derived factors, effected by hormone or not, play a role in neuronal survival and neuronal growth in the pelvic ganglion.

CHAPTER 9

REFERENCES

Abercrombie M (1946) Estimation of nuclear population from microtome sections. The Anatomical Record **94**, 239-247.

Alian M, Gabella G (1996) Decrease and disappearance of intramural neurons in the rat bladder during post-natal development. Neuroscience Letters **218**, 103-106.

Alm P, Uvelius B, Ekstrom J, Holmquist B, Larsson B, Andersson KE (1995) Nitric oxide synthase-containing neurons in rat parasympathetic, sympathetic and sensory ganglia: a comparative study. Histochemical Journal **27**, 819-831.

Altman J, Bayer S (1984) The development of the rat spinal cord. Advances in Anatomy, Embryology and Cell Biology **85**, 1-164.

Anderson DJ (1989) The neural crest cell lineage problem: neuropoiesis? Neuron **3**, 1-12.

Anderson DJ, Axel R (1986) A bipotential neuroendocrine precursor whose choice and cell fate is determined by NGF and glucocorticoids. Cell **47**, 1079-1090.

Arnold AP (1980) Sexual differences in the brain. Scientific American **68**, 165-73.

Arnold AP, Breedlove SM (1985) Organisational and activational effects of sex steroids on brain and behaviour: a re-analysis. Hormones and Behaviour **19**, 469-498.

Baker D, Santer R, Blaggen A (1989) Morphometric studies on the microvascular tree of pre- and paravertebral sympathetic ganglia in the adult and aged rat by light and electron microscopy. Journal of Neurocytology **18**, 647-660.

Baker HA, Burke JP, Bhatnagar RK, van Orden DE, van Orden LS, Hartman BK (1977) Histochemical and biochemical characterisation of the rat paracervical ganglion. Brain Research **132**, 393-405.

Baljet B, Drukker J (1980) The extrinsic innervation of the pelvic organs in the female rat. Acta Anatomica **107**, 241-267.

Baluk P, Fujiwara T, Matsuda S (1985) The fine structure of the ganglia of the guinea-pig trachea. Cell and Tissue Research **239**, 51-60.

Baluk P, Gabella G (1989) Innervation of the guinea pig trachea: quantitative morphological study of intrinsic neurons and extrinsic nerves. Journal of Comparative Neurology **285**, 117-132.

Banks BEC, Walter SJ (1977) The effects of postganglionic axotomy and nerve growth factor on the superior cervical ganglion of developing mice. Journal of Neurocytology **6**, 287-297.

Barth EM, Korsching S, Thoenen H (1984) Regulation of nerve growth factor synthesis and release in organ cultures of rat iris. Journal of Cell Biology **99**, 839-843.

Baum MJ, Carroll RS, Cherry JA, Tobet SA (1990) Steroidal control of behavioural, neuroendocrine and brain sexual differentiation: studies in a carnivore, the ferret. Journal of Neuroendocrinology **2**, 401-418.

Benes FM, Parks TN, Rubel EW (1977) Rapid dendritic atrophy following deafferentation: an EM morphometric analysis. Brain Research **122**, 1-13.

Berry M, Bradley P, Borges S (1978) Environmental and genetic determinants of connectivity in the central nervous system - An approach through dendritic field analysis. Progress in Brain Research **48**, 133-148.

Berthoud H-R, Carlson NR, Powley TL (1991) Topography of efferent vagal innervation of the rat gastrointestinal tract. American Journal of Physiology **260**, 200-207.

Berthoud H-R, Powley TL (1992) Vagal afferent innervation of the rat fundic stomach: morphological characterisation of the gastric tension receptor. Journal of Comparative Neurology **319**, 261-276.

Björklund A, Cegrell L, Falck B, Ritzen M, Rosengren E (1970) Dopamine containing cells in sympathetic ganglia. Acta Physiologica Scandinavica **78**, 334-338

Black IB, Green SC (1973) Trans-synaptic regulation of adrenergic neuron development: Inhibition by ganglion blockade. Brain Research **63**, 291-302.

Black IB, Mytilineou C (1976) The interaction of nerve growth factor and transsynaptic regulation in the development of target organ innervation by sympathetic neurons. Brain Research **108**, 199-204.

Bowers CW, Zigmond RE (1979) Localisation of neurons in the rat superior cervical ganglion that project into different post-ganglionic trunks. Journal of Comparative Neurology **185**, 381-392.

Bredt DS, Hwang PM, Snyder SH (1990) Localisation of nitric oxide synthase indicating a neuronal role for nitric oxide. Nature **347**, 768-770.

Bredt DS, Snyder SH (1992) Nitric oxide, a novel neuronal messenger. Neuron **8**, 3-11.

Breedlove SM (1986) Cellular analyses of hormone influence on motoneuronal development and function. Journal of Neurobiology **17**, 157-176.

Breedlove SM (1992) Sexual dimorphism in the vertebrate nervous system. Journal of Neurobiology **21**, 869-882.

Breedlove SM, Arnold AP (1980) Hormone accumulation in a sexually dimorphic motor nucleus of the rat spinal cord. Science **210**, 564-566.

Breedlove SM, Arnold AP (1983a) Hormonal control of the developing neuromuscular system: I. Complete demasculinisation of the spinal nucleus of the bulbocavernosus in male rats using the anti-androgen flutamide. Journal of Neuroscience **3**, 417-423.

Breedlove SM, Arnold AP (1983b) Hormonal control of the developing neuromuscular system: II. Sensitive periods for the androgen-induced masculinisation of the rat spinal nucleus of the bulbocavernosus. Journal of Neuroscience **3**, 424-432.

Brenowitz EA, Arnold AP, Levin RN (1985) Neural correlates of female song in tropical duetting birds. Brain Research **343**, 104-112.

Brooks-Fournier R, Coggeshall RE (1981) The ratio of preganglionic axons to postganglionic cells and the sympathetic nervous system of the rat. Journal of Comparative Neurology **197**, 207-216.

Broughton-Pipkin F (1984) Medical Statistics Made Easy. Churchill Livingstone: Edinburgh.

Burnett AL, Lowenstein CJ, Bredt DS, Chang TSK, Snyder SH (1992) Nitric oxide: a physiologic mediator of penile erection. Science **257**, 401-403.

Burnstock G (1970) Structure of smooth muscle and its innervation. In: Smooth Muscle. Edited by E Bülbring, AF Brading, AW Jones,T Tomita, pp. 1-99. London: Arnold.

Burnstock G (1990) Noradrenaline and ATP as cotransmitters in sympathetic nerves. Neurochemistry International **17**, 357-368.

Bursch W, Kleine L, Tenniswood M (1990) The biochemistry of cell death by apoptosis. Biochemistry and Cell Biology **68**, 1071-1074.

Bush PA, Aronson WJ, Buga GM, Rajfer J, Ignarro LJ (1992) Nitric oxide is a potent relaxant of human and rabbit corpus cavernosum. Journal of Urology **147**, 1650-1655.

Campenot RB (1977) Local control of neurite development by nerve growth factor. Proceedings. National Academy of Sciences (USA) **74**, 4516-4519.

Campenot RB (1982a) Development of sympathetic neurons in compartmentalised cultures. I. Local control of neurite growth by nerve growth factor. Developmental Biology **93**, 1-12.

Campenot RB (1982b) Development of sympathetic neurons in compartmentalised cultures. II. Local control of neurite survival by nerve growth factor. Developmental Biology **93**, 13-21.

Cauna N, Naik N (1963) The distribution of cholinesterase in sensory ganglia of man and mammals. Journal of Histochemistry and Cytochemistry **11**, 129-138.

Chun LLY, Patterson PH (1977) Role of nerve growth factor in the development of rat sympathetic neurons *in vitro*. I. Survival, growth and differentiation of catecholamine production. Journal of Cell Biology **75**, 694-704

Cihak R, Gutmann E, Hanzlikova V (1970) Involution and hormone-induced persistence of the muscle sphincter (levator) ani in female rats. Journal of Anatomy **106**, 93-110.

Coggeshall RE (1992) A consideration of neural counting methods. Trends in Neurosciences **15**, 9-13.

Coggeshall RE, La Forte R, Klein CM (1991) Calibration of methods for determining numbers of dorsal root ganglion cells. Journal of Neuroscience Methods **35**, 187-194.

Coggeshall RE, Lekan HA (1996) Methods for determining numbers of cells and synapses: a case for more uniform standards of review. Journal of Comparative Neurology **364**, 6-15.

Collins F, Dawson A (1983) An effect of nerve growth factor on parasympathetic neurite outgrowth. Proceedings. National Academy of Sciences (USA) **80**, 2091-2094.

Connors NA, Sullivan JM, Kubb KS (1983) An autoradiographic study of the distribution of fibres from the dorsal motor nucleus of the vagus to the digestive tube of the rat. Acta Anatomica **115**, 266-271.

Corpechot C, Baulieu E-E, Robel P (1981) Testosterone, dihydrotestosterone and androstanediols in plasma, testes and prostates of rats during development. Acta Endocrinologica **96**, 127-135.

Cottrell DF (1984) Conduction velocity and axonal diameter of alimentary C fibres. Quarterly Journal of Experimental Physiology **69**, 355-64.

Coughlin MD, Collins MB (1985) Nerve growth factor-independent development of embryonic mouse sympathetic neurons in dissociated cell culture. Developmental Biology **110**, 392-401.

Dahlstrom A, Haggendal J (1966) Some quantitative studies on the noradrenaline content in the cell bodies and terminals of a sympathetic neuron system. Acta Physiologica Scandinavica **67**, 271-277.

Dail WG, Barton S (1983) Structure and organisation of mammalian sympathetic ganglia. In: Autonomic Ganglia. Edited by L-G Elfvin, pp. 3-25. John Wiley: Chichester.

Dail WG, Dziurzynski R (1985) Substance P immunoreactivity in the major pelvic ganglion of the rat. The Anatomical Record **212**, 103-109.

Dail WG, Evan AP, Eason HR (1975) The major ganglion in the pelvic plexus of the male rat. Cell and Tissue Research **159**, 49-62.

Dail WG, Hamill RW (1989) Parasympathetic nerves in penile erectile tissue of the rat contain choline acetyltransferase. Brain Research **487**, 165-170.

Dail WG, Minorsky N, Moll MA, Manzanares K (1986) The hypogastric nerve pathway to penile erectile tissue: histochemical evidence supporting a vasodilator role. Journal of the Autonomic Nervous System **15**, 341-349.

Dail WG, Moll MA, Weber K (1983) Localisation of vasoactive intestinal polypeptide in penile erectile tissue and in the major pelvic ganglion of the rat. Neuroscience **10**, 1379-1386.

Dail WG, Trujillo D, de la Rosa D, Walton G (1989) Autonomic innervation of reproductive organs: analysis of the neurons whose axons project in the main penile nerve in the pelvic plexus of the rat. The Anatomical Record **224**, 94-101

Davies DC (1978) Neuronal cell numbers in the superior cervical ganglion of the neonatal rat. Journal of Anatomy **123**, 43-51.

Dawson TM, Bredt DS, Fotuhi M, Hwang PM, Snyder SH (1991) Nitric oxide synthase and neuronal NADPH diaphorase are identical in brain and peripheral tissues. Neurobiology **88**, 7797-7801.

de Champlain J, Malmfors T, Olson L, Sachs C (1970) Ontogenesis of peripheral adrenergic neurons in the rat: pre- and postnatal observations. Acta Physiologica Scandinavica **80**, 276-288.

DeVoogd T, Nottebohm F (1981) Gonadal hormones induce dendritic growth in the adult avian brain. Science **214**, 202-204.

Dibner MD, Mytilineou C, Black IB (1977) Target organ regulation of sympathetic neuron development. Brain Research **123**, 301-310.

Ding YQ, Wang YQ, Qin BZ, Li JS (1993) The major pelvic ganglion is the main source of nitric oxide synthase-containing nerve fibres in penile erectile tissue of the rat. Neuroscience Letters **164**, 187-90.

Döhler KD, Hines M, Coquelin A, Davis F, Shryne JE, Gorski RA (1982) Pre- and postnatal influence of diethylstilbestrol on differentiation of the sexually dimorphic nucleus in the preoptic area of the female rat brain. Neuroendocrinology Letters **4**, 361.

Döhler KD, Wuttke W (1975) Changes with age in levels of serum gonadotrophins, prolactin, and gonadal steroids in prepubertal male and female rats. Endocrinology **97**, 898-911.

Domoto T, Tsumori T (1994) Co-localisation of nitric oxide synthase and vasoactive intestinal peptide immunoreactivity in neurons of the major pelvic ganglion projecting to the rat rectum and penis. Cell and Tissue Research **278**, 273-278.

Doupe AJ, Landis SC, Patterson PH (1985a) Environmental influences in the development of neural crest derivatives: glucocorticoids, growth factors and chromaffin cell plasticity. Journal of Neuroscience **5**, 2119-2142.

Doupe AJ, Patterson PH, Landis SC (1985b) Small intensely fluorescent cells in culture: role of glucocorticoids and growth factors in their development and interconvertions with other neural crest derivatives. Journal of Neuroscience **5**, 2143-2160.

Ehinger B, Sundler F, Uddman R (1983) Functional morphology in two parasympathetic ganglia: the ciliary and the pterygopalatine. In: Autonomic Ganglia. Edited by L-G Elfvin, pp. 97-123. Chichester: John Wiley and Sons.

Elfvin L-G (1983) Autonomic Ganglia. Chichester: John Wiley and Sons.

Eränkö O, Soinila S (1981) Effect of early postnatal division of the postganglionic nerves on the development of principal cells and small intensely fluorescent cells in the rat superior cervical ganglion. Journal of Neurocytology **10**, 1-18.

Ernst M (1926) Uber Untergang von Zellen während der normalen Entwicklung bei Wirbeltieren. Zeitschrift für Anatomie und Entwicklungsgeschichte **79**, 228-262.

Fishman RB, Breedlove SM (1988) Neonatal androgen maintains sexually dimorphic perineal muscles in the absence of innervation. Muscle and Nerve **11**, 553-560.

Fishman RB, Chism L, Firestone GL, Breedlove SM (1990) Evidence for androgen receptors in sexually dimorphic perineal muscles of neonatal male rats. Absence of androgen accumulation by the perineal motoneurons. Journal of Neurobiology **21**, 694-705.

Floderus S (1944) Untersüchungenuber den bau der meschlichen hypophyse mit besonderer berücksichtigung der quantitativen mikromorphologischen verhältnisse. Acta Pathologica, Microbiologica et Immunologica Scandinavica **53**, 1.

Förstermann U, Schmidt HHHW, Pollock JS, Sheng H, Mitchell JA, Warner TD, Nakane M, Murad F (1991) Isoforms of nitric oxide synthase. Characterisation and purification from different cell types. Biochemistry and Pharmacology **42**, 1849-1857.

Fukada K (1980) Hormonal control of neurotransmitter choice in sympathetic neuron cultures. Nature **287**, 553-555.

Furchgott RF, Zawadski JV (1980) The obligatory role of endothelial cells in the relaxation of arterial smooth muscle by acetylcholine. Nature **288**, 373-376.

Furness JB, Costa M (1987) The Enteric Nervous System. Edinburgh: Churchill Livingstone.

Gabella G (1976) Structure of the Autonomic Nervous System. London: Chapman and Hall.

Gabella G (1987) Structure of muscle and nerves in the gastrointestinal tract. In: Physiology of the Gastrointestinal Tract. 2nd edition, edited by LR Johnson, pp. 335-381. New York: Raven.

Gabella G (1995) Autonomic Nervous System. In: The Rat Nervous System. Second edition, edited by G Paxinos, pp. 81-103. San Diego: Academic Press.

Gabella G, Trigg P (1984) Size of neurons and glial cells in the enteric ganglia of mice, guinea-pigs, rabbits and sheep. Journal of Neurocytology **13**, 49-71.

Gabella G, Trigg P, McPhail H (1988) Quantitative cytology of ganglion neurons and satellite glial cells in the superior cervical ganglion of the sheep. Relationship with ganglion neuron size. Journal of Neurocytology **17**, 753-769.

Gabella G, Berggren T, Uvelius B (1992) Hypertrophy and reversal of hypertrophy in rat pelvic ganglion neurons. Journal of Neurocytology **21**, 649-662.

Garcia-Arraras JE, Fauquet M, Chanconie M, Smith J (1986) Coexpression of somatostatin-like immunoreactivity and catecholaminergic properties in neural crest derivatives, comodulation of peptidergic and adrenergic differentiation in cultured neural crest. Developmental Biology **114**, 247-257.

Garthwaite J, Charles SL, Chess-Williams R (1988) Endothelium-derived relaxing factor release on activation of NMDA receptors suggests role as intercellular messenger in the brain. Nature **336**, 385-388.

Gavrielli Y, Sherman Y, Ben-Sasson SA (1992) Identification of programmed cell death in situ via specific labelling of nuclear DNA fragmentation. Journal of Cell Biology **119**, 493-501.

Gibbins IL (1990) Target-related patterns of co-existence of neuropeptide Y, vasoactive intestinal peptide, enkephalin and substance P in cranial parasympathetic neurons innervating the facial skin and exocrine glands of guinea-pigs. Neuroscience **38**, 541-560.

Gilpin CJ, Dixon JS, Gilpin SA, Gosling JA (1983) The fine structure of autonomic neurons in the wall of the human urinary bladder. Journal of Anatomy **137**, 705-713.

Glücksman A (1951) Cell deaths in normal vertebrate ontogeny. Biological Review **26**, 59-86.

Goedert M, Otten U, Thoenen H (1978) Biochemical effects of antibodies against NGF on developing and differentiated sympathetic ganglia. Brain Research **148**, 264-268.

Goedert M, Fine A, Hunt SP, Ullrich A (1986) Nerve growth factor mRNA in peripheral and central rat tissues and in the human central nervous system. Lesion effects in the rat brain and levels in Alzheimer's Disease. Molecular Brain Research **1**, 86-92.

Goldman S, Nottebohm F (1984) Neuronal production, migration and differentiation in a vocal control nucleus of the adult female canary brain. Proceedings. National Academy of Sciences (USA) **80**, 2390-2395.

Gordon-Weeks PM (1988) The ultrastructure of noradrenergic and cholinergic neurons in the autonomic nervous system. In: Handbook of Chemical Neuroanatomy. Volume 6: The Peripheral Nervous System. Edited by A Björklund, T Hökfelt, C Owman, pp. 117-142. Amsterdam: Elsevier.

Gorin PD, Johnson EM (1979) Experimental autoimmune model of nerve growth factor deprivation: effects on developing peripheral sympathetic and sensory neurons. Proceedings. National Academy of Science (USA) **76**, 5382-5386.

Gorski RA, Gordon JH, Shryne JE, Southam AM (1978) Evidence for a morphological sex difference within the medial preoptic area of the rat brain. Brain Research **148**, 333-346.

Greene EC (1963) Anatomy of the Rat. New York: Hafner.

Greenwood D, Coggeshall RE, Hulsebosch CL (1985) Sexual dimorphism in the numbers of neurons in the pelvic ganglia of adult rats. Brain Research **340**, 160-162.

Gu J, Polak JM, Su HC, Blank MA, Morrison JF, Bloom SR (1984) Demonstration of paracervical ganglion origin for the vasoactive intestinal peptide-containing nerves of the rat uterus using retrograde tracing techniques combined with immunocytochemistry and denervation procedures. Neuroscience Letters **51**, 377-382.

Gundersen HJG, Bendtsen TF, Korbo L, Marcussen N, Moller A, Nielson K, Nyengaard JR, Pakkenberg B, Sorenson FB, Vesterby A, West MJ (1988b) Some new, simple and efficient stereological methods and their use in pathological research and diagnosis. Acta Pathologica, Microbiologica et Immunologica Scandinavica **96**, 379-394.

Gundersen HJG, Bagger P, Bendtsen TF, Evans SM, Korbo L, Marcussen N, Moller A, Nielson K, Nyengaard JR, Pakkenberg B, Sorenson FB, Vesterby A, West MJ (1988a) The new stereological tools: disector, fractionator, nucleator and point sampled intercepts and their use in pathological research and diagnosis. Acta Pathologica, Microbiologica et Immunologica Scandinavica **96**, 857-881.

Gurney ME (1981) Hormonal control of cell form and number in the zebra finch song system. Journal of Neuroscience **1**, 658-673.

Gurney ME, Konishi M (1980) Hormone induced sexual differentiation of brain and behaviour in zebra finches. Science **208**, 1380-1382.

Hall AK, Landis SC (1991) Principal neurons and small intensely fluorescent (SIF) cells in the rat superior cervical ganglion have distinct developmental histories. The Journal of Neuroscience **11**, 472-484.

Hamburger V (1977) The developmental history of the motor neuron. Neuroscience Research Programme Bulletin **15** 3-37.

Hamill RW, Schroeder B (1990) Hormonal regulation of adult sympathetic neurons: the effects of castration on neuropeptide Y, norepinephrine, and tyrosine hydroxylase activity. Journal of Neurobiology **21**, 731-742.

Hart BL, Leedy MG (1985) Neurological bases of sexual behaviour. A comparative analysis. In: Handbook of Behavioural Neurobiology, Volume 7. Edited by N Adler, D Pfaff, RW Goy, pp. 373-422. New York: Plenum.

Hayes KJ (1965) The so-called levator ani of the rat. Acta Endocrinologica (Copenhagen) **48**, 337-347.

Hedger J, Webber R (1976) Anatomical study of the cervical sympathetic trunk and ganglia in the albino rat (*Mus norvegicus albinus*). Acta Anatomica **96**, 206-217.

Hendry IA (1976) A method to correct adequately for the change in neuronal size when estimating neuronal numbers after nerve growth factor treatment. Journal of Neurocytology **5**, 337-349.

Hendry IA (1977) Cell division in the developing sympathetic nervous system. Journal of Neurocytology **6**, 299-309.

Hendry IA, Campbell J (1976) Morphometric analysis of rat superior cervical ganglion after axotomy and nerve growth factor treatment. Journal of Neurocytology **5**, 351-360.

Henneman E, Clamann HP, Gillies JD, Skinner RD (1974) Rank order of motoneurons within a pool: law of combination. Journal of Neurophysiology **37**, 1338-1349.

Henneman E, Somjen G, Carpenter DO (1965) Functional significance of cell size in spinal motoneurons. Journal of Neurophysiology **28**, 560-80.

Herrmann K, Arnold AP (1991) Lesions of HVc block the developmental masculinising effects of estradiol in the female zebra finch. Journal of Neurobiology **22**, 29-39.

Hervonen A, Kanerva L, Lietzen R, Partanen S (1972) Effects of steroid hormones on differentiation of the catecholamine storing cells of the paracervical ganglion of the rat uterus. Zeitschrift für Zellforschung **134**, 519-527.

Hibbs JB, Jr., Taintor RR, Vavrin Z (1987) Macrophage cytotoxicity: role for L-arginine deiminase and imino nitrogen oxidation to nitrite. Science **235**, 473-476.

Hökfelt T, Elfvin LG, Elde R, Schultzburg M, Goldstein M, Luft R (1977a) Occurrence of somatostatin-like immunoreactivity in some peripheral sympathetic noradrenergic neurons. Proceedings. National Academy of Sciences (USA) **74**, 3587-3591.

Hökfelt T, Elfvin LG, Schultzburg M, Fuxe K, Said SI, Mutt V, Goldstein M (1977b) Immunohistochemical evidence of vasoactive intestinal polypeptide-containing neurons and nerve fibres in sympathetic ganglia. Neuroscience **2**, 885-896.

Hökfelt T, Elfvin LG, Schultzburg M, Goldstein M, Nilsson G (1977c) On the occurrence of substance P-containing fibres in sympathetic ganglia: Immunohistochemical evidence. Brain Research **132**, 29-41.

Holmquist F, Helund H, Anderson KE (1992) Characterisation of inhibitory neurotransmission in the isolated corpus cavernosum from rabbit and man. Journal of Physiology **449**, 295-311.

Holmquist F, Stief CG, Jonas U, Anderson KE (1991) Effect of the nitric oxide synthase inhibitor Ng-nitro-L-arginine on the erectile response to cavernous nerve stimulation in the rabbit. Acta Physiologica Scandinavica **143**, 299-304.

Hondeau E, Prud'homme M-J, Rousseau A, Rousseau JP (1995) Distribution of noradrenergic neurons in the female rat pelvic plexus and involvement in the genital tract innervation. Journal of the Autonomic Nervous System **54**, 113-125.

Hope BT, Michael GJ, Knigge KM, Vincent SR (1991) Neuronal NADPH-diaphorase is a nitric oxide synthase. Proceedings. National Academy of Sciences (USA) **88**, 2811-2814.

Hulsebosch CE, Coggeshall RE (1982) An analysis of the axon populations in the nerves to the pelvic viscera in the rat. Journal of Comparative Neurology **211**, 1-10.

Ignarro LJ, Bush PA, Buga G, Wood KS, Fukuto JM, Rajfer J (1990) Nitric oxide and cyclic GMP formation upon electrical field stimulation cause relaxation of corpus cavernosum smooth muscle. Biochemical and Biophysical Research Communications **170**, 843-850.

Inyama CO, Hacker GW, Gu J, Dahl D, Bloom SR, Polak JM (1985) Cytochemical relationships in the paracervical ganglion (Frankenhäuser) of rat studied by immunocytochemistry. Neuroscience Letters **55**, 311-316.

Inyama CO, Wharton J, Su HC, Polak JM (1986) CGRP-immunoreactive nerves in the genitalia of the female rat originate from dorsal root ganglia T11-L3 and L6-S1: a combined immunocytochemical and retrograde tracing study. Neuroscience Letters **69**, 13-18.

Ishii DN, Shooter EM (1975) Regulation of nerve growth factor synthesis in mouse submaxillary glands by testosterone. Journal of Neurochemistry **25**, 843-851.

Jacobson CD, Gorski RA (1981) Neurogenesis of the sexually dimorphic nucleus of the preoptic area in the rat. Journal of Comparative Neurology **196**, 519-529.

Jacobson M (1996) Developmental Neurobiology: Third Edition. New York and London: Plenum Press.

Jänig W (1988) Pre- and postganglionic vasoconstrictor neurons: differentiation, types, and discharge properties. Annual Review of Physiology **50**, 525-39.

Johnson EM, Taniuchi M, Distefano PS (1988) Expression and possible function of nerve growth factor receptors on Schwann cell. Trends in Neurosciences **11**, 289-304.

Jordan CL, Breedlove SM, Arnold AP (1991) Ontogeny of steroid accumulation in spinal lumbar motoneurons of the rat: implications for androgen's site of action during synapse elimination. Journal of Comparative Neurology **312**, 1-8.

Jordan CL, Letinsky MS, Arnold AP (1989) The role of gonadal hormones in neuromuscular synapse elimination in rats. I. Androgen delays the loss of multiple innervation in the levator ani muscle. Journal of Neuroscience **9**, 229-238.

Jordan CL, Pawson PA, Arnold AP, Grinell AD (1992) Hormonal regulation of motor unit size and synaptic strength during synapse elimination in the rat levator ani muscle. Journal of Neuroscience **12**, 4447-4459.

Kanerva L, Lietzen R, Teräväinen H (1972) Catecholamines and cholinesterases in the paracervical (Frankenhäuser) ganglion of normal and pregnant rats. Acta Physiologica Scandinavica **86**, 271-277.

Kanerva L, Teräväinen H (1972) Electron microscopy of the paracervical (Frankenhäuser) ganglion of the adult rat. Zeitschrift für Zellforschung und Mikroskopische Anatomie. **129**, 161-77.

Karnovsky MJ, Roots L (1964) A 'direct-colouring' thiocholine method for cholinesterase. Journal of Histochemistry and Cytochemistry **12**, 219-221.

Keast JR (1991) Patterns of co-existence of peptides and differences of nerve fibre types associated with noradrenergic and non-noradrenergic (putative cholinergic) neurons in the major pelvic ganglion of the male rat. Cell and Tissue Research **266**, 405-415.

Keast JR (1992) A possible source of nitric oxide in the rat penis. Neuroscience Letters **143**, 69-73.

Keast JR (1995) Pelvic Ganglia. In: Autonomic Ganglia, edited by EM McLachlan, pp. 445-479. Luxembourg: Harwood Academic.

Keast JR, Chiam HC (1994) Selective association of nerve fibres immunoreactive for substance P or bombesin with putative cholinergic neurons of the male rat major pelvic ganglion. Cell and Tissue Research **278**, 589-594.

Keast JR, de Groat WC (1989) Immunohistochemical characterisation of pelvic neurons which project to the bladder, colon, or penis in rats. Journal of Comparative Neurology **288**, 387-400.

Keast JR, Booth AM, de Groat WC (1989) Distribution of neurons in the major pelvic ganglion of the rat which supply the bladder, colon or penis. Cell and Tissue Research **256**, 105-112.

Kelley DB (1988) Sexually dimorphic behaviour. Annual Review in Neuroscience **11**, 225-251.

Kelley DB, Dennison J (1990) The vocal motor neurons of Xenopus laevis: development of sex differences in axon number. Journal of Neurobiology **21**, 869-882.

Kepper M, Keast J (1995) Immunohistochemical properties and spinal connections of pelvic autonomic neurons that innervate the rat prostate gland. Cell and Tissue Research **281**, 533-42.

Kessler JA (1985) Parasympathetic, sympathetic and sensory interactions in the iris: nerve growth factor regulates cholinergic ciliary ganglion innervation *in vivo*. Journal of Neuroscience **5**, 2719-2725.

Kim N, Azadzoi KM, Goldstein I, Saenz de Tejada I (1991) A nitric oxide-like factor mediates nonadrenergic-noncholinergic neurogenic relaxation of penile corpus cavernosum smooth muscle. Journal of Clinical Investigation **88**, 112-118.

Kluck P (1980) The autonomic innervation of the human urinary bladder, bladder neck and urethra: a histochemical study. The Anatomical Record **198**, 439-447.

Konigsmark BW (1970) Methods for the counting of neurons. In: Contemporary research methods in neuroanatomy. Edited by WJH Nauta and SOE Ebbesson, pp. 315-338. Heidleberg: Springer.

Konishi M (1989) Birdsong for neurobiologists. Neuron **3**, 541-549.

Konishi M, Akutagawa E (1985) Neuronal growth, atrophy and death in a sexually dimorphic song nucleus in the zebra finch brain. Nature **315**, 145-147.

Korsching S, Thoenen H (1983) Nerve growth factor in sympathetic ganglia and corresponding target organs of the rat: Correlation with density of sympathetic innervation. Proceedings. National Academy of Sciences (USA) **80**, 3513-3516.

Korsching S, Thoenen H (1988) Developmental changes of nerve growth factor levels in sympathetic ganglia and their target organs. Developmental Biology **26**, 40-46.

Landis SC (1990) Target regulation of neurotransmitter phenotype. Trends in Neurosciences **13**, 344-350.

Landis SC, Damboise S (1986) Neuron birthdays in the paravertebral sympathetic chain of the rat. The Anatomical Record **214**, 71A.....

Landis SC, Fredieu JR (1986) Coexistence of calcitonin gene-related peptide and vasoactive intestinal polypeptide in cholinergic innervation of rat sweat glands. Brain Research **377**, 177-18.

Landis SC, Keefe D (1983) Evidence for neurotransmitter plasticity *in vivo*. Developmental changes in properties of cholinergic sympathetic neurons. Developmental Biology **98**, 349-372.

Landis SC, Patterson PH (1981) Neural crest cell lineages. Trends in Neurosciences **4**, 172-175.

Landmesser L, Pilar G (1978) Interactions between neurons and their targets during *in vivo* synaptogenesis. Federation Proceedings **37**, 2016-2022.

Langley JN (1921) The Autonomic Nervous System, Part 1. Cambridge: W Heffer and Sons.

Langley JN, Anderson HK (1895a) On the innervation of the pelvic and adjoining viscera. I. The lower portion of the intestine. Journal of Physiology **18**, 67-105.

Langley JN, Anderson HK (1895b) The innervation of the pelvic and surrounding viscera. II. The bladder. Journal of Physiology **19**, 71-84.

Langley JN, Anderson HK (1896) The innervation of the pelvic and surrounding viscera. VII. Anatomical observation. Journal of Physiology **20**, 372-406.

Langworthy OR (1965) Innervation of the pelvic organs of rat. Investigative Urology **2**, 372-406.

Langworthy OR, Rosenberg SJ (1939) Control by the central nervous system of rectal smooth muscle. Journal of Neurophysiology **2**, 356-360.

Lawrence JM, Black IB, Mytilineou C, Field PM, Raisman G (1979) Decentralisation of the superior cervical ganglion in neonates impairs the development of the innervation of the iris. A quantitative ultrastrutural study. Brain Research **168**, 13-19.

Le Douarin NM (1986) Cell line segregation during peripheral nervous system ontogeny. Science **231**, 1515-1522.

Lehmann HJ, Stange HH (1953) Über das Vorkommen vakuolenhaltiger Ganglienzellen im Ganglion Cervicale Uteri trächtiger und nichtträchtiger Rattan. Zeitschrift für Zellforschung und Mikroskopische Anatomie **38**, 230-236.

Levi G (1925) Wachstum und Körpergrösse. Die strukturelle Grundlage der Körpergrösse bei Vollausgebildeten und im wachstum begriffen Tieren. Ergebnisse der Anatomie und Entwicklungs-Geschichte **26**, 187-342.

Levi-Montalcini R (1949) The development of the acoustico-vestibular centres in the chick embryo in the absence of afferent root fibre and of descending fibre tracts. Journal of Comparative Neurology **91**, 209-241.

Levi-Montalcini R (1964) Growth control of nerve cells by protein factor and its antiserum. Science **145**, 105-110.

Levi-Montalcini R (1987) The nerve growth factor: Thirty-five years later. European Molecular Biology Organisation Journal **6**, 1145-1154.

Levi-Montalcini R, Angeletti P (1963) Essential growth of the nerve growth factor in the survival and maintenance of dissociated sympathetic neurons *in vitro*. Developmental Biology **7**, 653-689.

Levi-Montalcini R, Booker B (1960a) Excessive growth of sympathetic ganglia evoked by a protein isolated from mouse salivary glands. Proceedings. National Academy of Sciences (USA) **46**, 373-384.

Levi-Montalcini R, Booker B (1960b) Destruction of sympathetic ganglia in mammals by an antiserum to the nerve-growth promoting factor. Proceedings. National Academy of Sciences (USA) **42**, 384-391.

Levi-Montalcini R, Calissano P (1966) The nerve growth factor. Scientific American. **240**, 68-77.

Lichtman JW (1977) The reorganisation of synaptic connexions in the rat submandibular ganglion during post-natal development. Journal of Physiology **273**, 155-177.

Lichtman JW, Purves D (1980) The elimination of redundant preganglionic innervation to hamster sympathetic ganglion cells in early postnatal life. Journal of Physiology **301**, 213-228.

Lieberburg I, Krey LC, McEwen BS (1979) Sex differences in serum testosterone and in exchangeable brain cell nuclear estradiol during the neonatal period in rats. Brain Research **178**, 104-212.

Lieberburg LC, McEwen BS (1977) Brain cell nuclear retention of testosterone metabolites, 5-alpha-dihydrotestosterone and estradiol-17-beta, in adult rats. Endocrinology **100**, 588-597.

Lieberman AR (1971) The axon reaction: a review of the principal features of perikaryal responses to axon injury. International Review of Neurobiology **14**, 49-124.

Lipton SA (1986) Blockade of electrical activity promotes the death of mammalian retinal ganglion cells in culture. Proceedings. National Academy of Sciences (USA) **8**, 974-977.

MacLusky NJ, Naftolin F (1981) Sexual differentiation of the Central Nervous System. Science **211**, 1294-1303.

Madeira MD, Lieberman AR (1995) Sexual dimorphism in the mammalian limbic system. Progress in Neurobiology **45**, 275-333.

Maderdrut JL, Oppenheim RW, Prevette D (1988) Enhancement of naturally occurring cell death in the sympathetic and parasympathetic ganglia of chicken embryo following blockade of ganglionic transmission. Brain Research **444**, 189-194.

Martin DP, Schmidt RE, Distefano PS, Lowry OH, Carter JG, Johnson EM Jr. (1988) Inhibitors of protein synthesis and RNA synthesis prevent neuronal death caused by nerve growth factor deprivation. Journal of Cell Biology **106**, 829-844.

Matthews MR (1973) An ultrastructural study of axonal changes following constriction of postganglionic branches of the superior cervical ganglion in the rat. Philosophical Transactions. Royal Society London (B) **264**, 479-505.

Matthews MR, Cuello AC (1982) Substance P-immunoreactive peripheral branches of sensory neurons innervate guinea pig sympathetic neurons. Proceedings. National Academy of Sciences (USA) **79**, 1668-1672.

Matthews MR, Nelson VH (1975) Detachment of structurally intact nerve endings from chromatolytic neurones of rat superior cervical ganglion during the depression of synaptic transmission induced by post-ganglionic axotomy. Journal of Physiology **245**, 91-135.

Matthews MR, Raisman G (1972) A light and electron microscopic study of the cellular response to axonal injury in the superior cervical ganglion of the rat. Proceedings. Royal Society of London (B) **181**, 43-79.

Mayhew TM (1992) A review of recent advances in stereology for quantifying neural structure. Journal of Neurocytology **21**, 313-328.

McEwen BS (1981) Neural gonadal steroid action. Science **211**, 1303-1311.

McLachlan EM (1974) The formation of synapses in mammalian sympathetic ganglia re-innervated with preganglionic or somatic nerves. Journal of Physiology **237**, 217-242.

McNeill DL, Papka RE, Harris CH (1992a) CGRP Immunoreactivity and NADPH-diaphorase in afferent nerves of the rat penis. Peptides **13**, 1239-1246.

McNeill DL, Traugh Jr. NE, Vaidya AM, Hua HT, Papka RE (1992b) Origin and distribution of NADPH-diaphorase-positive neurons and fibres innervating the urinary bladder of the rat. Neuroscience Letters **147**, 33-36.

McPhedran AM, Wuerker RB, Henneman E (1964) Properties of motor units in a homogeneous red muscle (soleus) of the cat. Journal of Neurophysiology **28**, 71-84.

Melvin JE, Hamill RW (1986) Gonadal hormone regulation of neurotransmitter synthesising enzymes in the developing hypogastric ganglion. Brain Research **383**, 38-46.

Melvin JE, Hamill RW (1987) The major pelvic ganglion: Androgen control of postnatal development. Journal of Neuroscience **7**, 1607-1612.

Melvin JE, Hamill RW (1989a) Androgen-specific critical periods for the organisation of the major pelvic ganglion. Journal of Neuroscience **9**, 736-742.

Melvin JE, Hamill RW (1989b) Hypogastric ganglion perinatal development: evidence for androgen specificity via androgen receptors. Brain Research **485**, 11-19.

Melvin JE, McNeill TH, Hamill RW (1988) Biochemical and morphological effects of castration on the post organisational development of the hypogastric ganglion. Developmental Brain Research **38**, 131-139.

Melvin JE, Hervonen A, McNeill TH, Hamill RW (1989) Organisational role of testosterone on the biochemical and morphological development of the hypogastric ganglion. Brain Research **485**, 1-10.

Mendell LM, Munson JB, Scott JG (1976) Alterations of synapses on axotomized motoneurons. Journal of Physiology **255**, 67-79.

Moncada S, Palmer RMJ, Higgs EA (1991) Nitric oxide: physiology, pathophysiology, and pharmacology. Pharmacological Review **43**, 109-142.

Naftolin F, Brawer JR (1978) The effect of estrogens on hypothalamic structure and function. American Journal of Obstetrics and Gynecology **132**, 758-765.

Naftolin F, MacLusky N (1984) Aromatisation hypothesis revisited. In : Differentiation: Basic and Clinical Aspects. Edited by M Serio pp. 169-180. New York: Raven.

Naftolin F, Ryan KJ, Davies IJ, Reddy VV, Flores F, Petro Z (1975) The formation of estrogens by central neuroendocrine tissues. Progress in Hormone Research **31**, 295-319.

Neri R, Florance K, Koziol P, VanCleave S (1972) A biological profile of a nonsteroidal antiandrogen, SCH13521 (4'-nitro-3'-tri-fluoromethylisobutyranilde). Endocrinology **91**, 427-437.

Neuhuber WL (1987) Sensory vagal innervation of the rat oesophagus and cardia: a light and electron microscopic anterograde tracing study. Journal of the Autonomic Nervous System **20**, 243-255.

Nordeen EJ, Nordeen KW (1989) Estrogen stimulates the incorporation of new neurons into avian song nuclei during adolescence. Developmental Brain Research **49**, 27-32.

Nordeen EJ, Nordeen KW, Sengelaub DR, Arnold AP (1985) Androgens prevent normally occurring cell death in a sexually dimorphic spinal nucleus. Science **229**, 671-673.

Nottebohm F (1981) A brain for all seasons: cyclical anatomical changes in song control nuclei of the canary brain. Science **214**, 1368-1370.

Nottebohm F, Arnold AP (1976) Sexual dimorphism in vocal control areas of the songbird brain. Science **194**, 211-213.

Nottebohm F, Stokes TM, Leonard CM (1976) Central control of song in the canary Serinus canarius. Journal of Comparative Neurology **165**, 457-486.

Nottebohm F, Alvarez-Buylla A, Cynx J, Kirn J, Ling CY, Nottebohm M, Suter R, Tolles A, Williams H (1990) Song learning in birds: the relation between perception and production. Philosophical Transactions of the Royal Society (B) **29**, 115-124.

O'Connor TP, van der Kooy D (1989) Co-operation and competition during development: neonatal lesioning of the superior cervical ganglion induces cell death of trigeminal neurons innervating the cerebral blood vessels but prevents the loss of axon collaterals from the neurons that survive. Journal of Neuroscience **9**, 1490-1501.

O'Leary DD, Fawcett JW, Cowan WM (1986) Topographic targeting errors in the retinocollicular projection and their elimination by selective ganglion cell death. Journal of Neuroscience **6**, 3692-3705.

Oppenheim RW (1981) Cell death of motoneurons in the chick embryo spinal cord. V. Evidence on the role of cell death and neuromuscular function in the formation of specific peripheral connections. Journal of Neuroscience **1**, 141-151.

Oppenheim RW (1989) The neurotrophic theory and naturally occurring motoneuron death. Trends in Neurosciences **12**, 252-255.

Oppenheim RW, Prevette D, Tytell M, Homma S (1990) Naturally occurring cell death in the chick embryo *in vivo* requires protein and RNA synthesis: evidence for the role of cell death genes. Developmental Biology **138**, 104-113.

Pakkenberg B, Gundersen HJG (1988) New stereological method for obtaining unbiased and efficient estimates of total nerve cell number in human brain areas. Acta Pathologica, Microbiologica et Immunologica Scandinavica **97**, 677-681.

Palmer RMJ, Ashton DS, Moncada S (1988) Vascular endothelial cells synthesise nitric oxide from L-arginine. Nature **333**, 664-666.

Palmer RMJ, Ferrige AG, Moncada S (1987) Nitric oxide release accounts for the biological activity of endothelium-derived relaxing factor. Nature **327**, 524-526.

Papka RE (1990) Some nerve endings in the rat pelvic paracervical autonomic ganglia and varicosities contain calcitonin gene-related peptide and originate from dorsal root ganglia. Neuroscience **39**, 459-470.

Papka RE, McNeill DL (1992) Distribution of NADPH-diaphorase-positive nerves in the uterine cervix and neurons in dorsal root and paracervical ganglia of the female rat. Neuroscience Letters **147**, 224-228.

Papka RE, McNeill DL (1993) Light- and electron-microscopic study of synaptic connections in the paracervical ganglion of the female rat: special reference to calcitonin gene-related peptide-, galanin- and tachykinin (substance P and neurokinin A)- immunoreactive nerve fibres and terminals. Cell and Tissue Research **271**, 417-428.

Papka RE, Cotton JP, Traurig HH (1985) Comparative distribution of neuropeptide tyrosine, vasoactive intestinal polypeptide-, substance P-IR, acetylcholinesterase-positive and noradrenergic nerves in the reproductive tract of the female rat. Cell and Tissue Research **242**, 475-490.

Papka RE, Traurig HH, Klenn P (1987) Paracervical ganglia of the female rat: histochemistry and immunohistochemistry of neurons, SIF cells and nerve terminals. American Journal of Anatomy **179**, 243-257.

Papka RE, McNeill DL, Thompson D, Schmidt HHHW (1995) Nitric oxide nerves in the uterus are parasympathetic, sensory, and contain neuropeptides. Cell and Tissue Research **279**, 339-349.

Partanen M, Hervonen A (1979a) The formaldehyde induced fluorescence of the developing hypogastric (main pelvic) ganglion of the rat. Histochemistry **62**, 239-248.

Partanen M, Hervonen A (1979b) The effects of long-term castration on the histochemically demonstrable catecholamines in the hypogastric ganglion of the rat. Journal of the Autonomic Nervous System **1**, 139-147.

Partanen M, Hervonen A, Vaalasti A, Kanerva L, Hervonen H (1979) Vacuolated neurons in the hypogastric ganglion of the rat. Cell and Tissue Research **199**, 373-386.

Patterson PH, Chun LLY (1974) The influence of non-neuronal cells on catecholamine and acetylcholine synthesis and accumulation in cultures of dissociated sympathetic neurons. Proceedings. National Academy of Sciences (USA) **71**, 3607-3610.

Pfaff DW (1966) Morphological changes in the brains of adult male rats after neonatal castration. Journal of Endocrinology **36**, 415-416.

Phoenix CH, Goy RW, Gerall AA, Young WC (1959) Organising action of prenatally administered testosterone propionate on the tissues mediating mating behaviour in the female guinea-pig. Endocrinology **65**, 369-382.

Pilar G, Landmesser L (1972) Axotomy mimicked by localised colchicine application. Science **177**, 1116-1118.

Pilar G, Landmesser L, Burstein L (1980) Competition for survival among developing ciliary ganglion cells. Journal of Neurophysiology **43**, 233- 254.

Pover CM, Coggeshall RE (1991) Verification of the disector method for counting neurons, with comments on the empirical method. The Anatomical Record **231**, 573-578.

Prechtl JC, Powley TL (1990) The fibre composition of the abdominal vagus of the rat. Anatomy and Embryology **181**, 101-115.

Purinton PT, Fletcher TF, Bradley WE (1971) Sensory perikarya in autonomic ganglia. Nature New Biology **231**, 63-64.

Purinton PT, Fletcher TF, Bradley WE (1973) Gross and light microscopic features of the pelvic plexus in the rat. The Anatomical Record **175**, 697-706.

Purves D (1975) Functional and structural changes in mammalian sympathetic neurones following interruption of their axons. Journal of Physiology **252**, 429-463.

Purves D, Lichtman JW (1985a) Geometrical differences among homologous neurons in mammals. Science **228**, 298-302.

Purves D, Lichtman JW (1985b) Principals of neural development. Sunderland, Massachusetts: Sinauer Associates.

Purves D, Rubin E, Snider WD, Lichtman J (1986) Relation of animal size to convergence, divergence and neuronal number in peripheral sympathetic pathways. The Journal of Neuroscience **6**, 158-163.

Purves D, Snider WD, Voyvodic JT (1988) Trophic regulation of nerve cell morphology and innervation in the autonomic nervous system. Nature **336**, 123-128.

Raisman G, Field PM (1973) Sexual dimorphism in the neuropil of the preoptic area of the rat and its dependence on neonatal androgen. Brain Research **54**, 1-20.

Rakic P (1974) Neurons in rhesus monkey visual cortex: Systematic relation between time of origin and eventual disposition. Science **183**, 425-427.

Rand MJ (1992) Nitrergic transmission: nitric oxide as a mediator of non-adrenergic, non-cholinergic neuro-effector transmission. Clinical and Experimental Pharmacology and Physiology **19**, 147-169.

Rand RM, Breedlove SM (1987) Ontogeny of functional innervation of bulbocavernosus muscles in male and female rats. Developmental Brain Research **33**, 150-152.

Rando T, Bowers C, Zigmond R (1981) Localisation of neurons in the rat spinal cord which project to the superior cervical ganglion. Journal of Comparative Neurology **196**, 73-83.

Resco JA, Feder HH, Goy RW (1968) Androgen concentrations in plasma and testis of developing rats. Journal of Endocrinology **40**, 485-491.

Rubin E (1985a) Development of the rat superior cervical ganglion: Ganglion cell maturation. Journal of Neuroscience **5**, 673-684.

Rubin E (1985b) Development of the rat superior cervical ganglion: Ingrowth of preganglionic axons. Journal of Neuroscience **5**, 685-696.

Rubin E (1985c) Development of the rat superior cervical ganglion: Initial stages of synapse formation. Journal of Neuroscience **5**, 697-704.

Ruit KG, Osborne PA, Schmidt RE, Johnson EM, Snider WD (1990) Nerve growth factor regulates sympathetic ganglion cell morphology and survival in adult mouse. Journal of Neuroscience **10**, 2412-2419.

Rushton WAH (1951) A theory of the effect of fibre size in medullated nerve. Journal of Physiology **115**, 101-122.

Saffrey MJ, Hassall CJS, Moules EW, Burnstock G (1994) NADPH diaphorase and nitric oxide synthase are expressed by the majority of intramural neurons in the neonatal guinea pig urinary bladder. Journal of Anatomy **185**, 487-495.

Sanders KM, Ward SM (1992) Nitric oxide as a mediator of nonadrenergic noncholinergic neurotransmission. American Journal Physiology **262**, G379-392.

Santer RM, Symons D (1993) Distribution of NADPH-diaphorase activity in rat paravertebral, prevertebral and pelvic sympathetic ganglia. Cell and Tissue Research **271**, 115-121.

Sassoon DA, Segil N, Kelley DB (1986) Androgen-induced myogenesis and chondrogenesis in the larynx of Xenopus laevis. Developmental Biology **113**, 135-140.

Schafer T, Schwab ME, Thoenen H (1983) Increased formation of preganglionic synapses and axons due to retrograde trans-synaptic action of nerve growth factor in the rat sympathetic nervous system. Journal of Neuroscience **3**, 1501-1510.

Schirar A, Giuliano F, Rampin O, Rousseau JP (1994) A large proportion of pelvic neurons innervating the corpora cavernosa of the rat penis exhibit the NADPH-diaphorase activity. Cell and Tissue Research **278**, 517-525.

Schmidt HHHW, Gagne GD, Nakane M, Pollock JS, Miller MF, Murad F (1992) Mapping of neural nitric oxide synthase in the rat suggests frequent colocalisation with NADPH diaphorase but not with soluble guanyl cyclase, and novel paraneural functions for nitrinergic signal transduction. Journal of Histochemistry and Cytochemistry **40**, 1439-1456.

Scott SA, Davies AM (1990) Inhibition of protein synthesis prevents cell death in sensory and parasympathetic neurons deprived of neurotrophic factor *in vitro*. Journal of Neurobiology **21**, 630-638.

Selmanoff MK, Brodkin LD, Weiner LD, Siteri PK (1977) Aromatization and 5-alpha-reduction of androgens in discrete hypothalamic and limbic regions of the male and female rat. Endocrinology **101**, 841-848.

Sengelaub DR, Arnold AP (1986) Development and loss of early projections in a sexually dimorphic rat spinal nucleus. Journal of Neuroscience **6**, 1613-1620.

Sjöstrand NO (1965) The adrenergic innervation of the vas deferens and the accessory male genital glands. Acta Physiologica Scandinavica **65**, 1-82.

Smolen AJ, Beaston-Wimmer P (1986) Dendritic development in the rat superior cervical ganglion. Developmental Brain Research **29**, 245-252.

Smolen AJ, Beaston-Wimmer P, Wright LL, Lindley T, Cader C (1985) Neurotransmitter synthesis, storage, and turnover in neonatally deafferented sympathetic neurons. Developmental Brain Research **23**, 211-218.

Smolen AJ, Raisman G (1980) Synapse formation in the rat superior cervical ganglion during normal development and after neonatal deafferentation. Brain Research **181**, 315-323.

Smolen AJ, Wright LL, Cunningham TJ (1983) Neuron numbers in the superior cervical ganglion of the rat. A critical comparison of methods for cell counting. Journal of Neurocytology **12**, 739-750.

Sneddon P, Graham A (1992) Role of nitric oxide in the autonomic innervation of smooth muscle. Journal of Autonomic Pharmacology **12**, 445-456.

Snider WD (1986) Rostrocaudal differences in dendritic growth and synaptogenesis in rat sympathetic chain ganglia. Journal of Comparative Neurology **244**, 245-253.

Snider WD (1987) The dendritic complexity and innervation of submandibular neurons in five species of mammals. Journal of Neuroscience **7**, 1760-1768.

Snider WD (1988) Nerve growth factor enhances dendritic arborization of sympathetic ganglion cells in developing mammals. Journal of Neuroscience **8**, 2628-2634.

Steers WD, Tuttle JB, Creedon DJ (1989) Neurotrophic influence of the bladder following outlet obstruction: implications for the unstable detrusor. Neurourology and Urodynamics **8**, 395-396.

Steers WD, Ciambotti J, Erdman S, de Groat WC (1990) Morphological plasticity in efferent pathways to the urinary bladder of the rat following urethral obstruction. Journal of Neuroscience **10**, 1943-1951.

Sterio DC (1984) The unbiased estimation of number and sizes of arbitrary particles using the disector. Journal of Microscopy **134**, 127-136.

Sulston-JE; Horvitz-HR (1977) Post-embryonic cell lineages of the nematode, *Caenorhabditis elegans*. Developmental Biology **56**, 110-156.

Suzuki N, Hardebo JE (1991) The pathway of parasympathetic nerve fibres to cerebral vessels from the otic ganglion in the rat. Journal of the Autonomic Nervous System **36**, 39-46.

Suzuki N, Hardebo JE, Owman C (1988) Origins and pathways of cerebrovascular vasoactive intestinal polypeptide-positive nerves in the rat. Journal of Cerebral Blood Flow and Metabolism **8**, 697-712.

Suzuki Y, Arai Y (1985) Androgen regulation of neuron number in the developing hypogastric ganglion of mice. Zoological Science **2**, 807-809.

Suzuki Y, Arai Y (1986) Laterality associated with sexual dimorphism in the volume of the mouse hypogastric ganglion. Experimental Neurology **94**, 241-245.

Suzuki Y, Ishii H, Arai Y (1983) Prenatal exposure of male mice to androgen increases neuron number in the hypogastric ganglion. Developmental Brain Research **10**, 151-154.

Tabatabai M, Booth AM, de Groat WC (1986) Morphological and electrophysiological properties of pelvic ganglion cells in the rat. Brain Research **382**, 61-70.

Thoenen H, Barde YA (1980) Physiology of nerve growth factor. Physiological Review **60**, 1284-1335.

Thomas A, Pearse AGE (1964) The solitary active cells. Histochemical demonstration of damage-resistant nerve cells with a TPN-diaphorase reaction. Acta Neuropathologica **3**, 238-249.

Tobin C, Joubert Y (1991) Testosterone-induced development of the rat levator ani muscle. Developmental Biology **146**, 131-138.

Toran-Allerand CD (1976) Sex steroids and the development of the newborn mouse hypothalamus and preoptic area *in vitro*. Implications for sexual differentiation. Brain Research **106**, 407-412.

Toran-Allerand CD, Gerlach JL, McEwen BS (1980) Autoradiographic localisation of 3H-estradiol related to steroid responsiveness in cultures of the newborn mouse hypothalamus and preoptic area. Brain Research **14**, 517-522.

Tuttle JB, Mackey T, Steers WD (1994) NGF, bFGF and CNTF increase survival of major pelvic ganglion neurons cultured from the adult rat. Neuroscience Letters **173**, 94-8.

Umansky SR (1982) The genetic programme of cell death. Hypothesis and some applications: transformation, carcinogenesis, ageing. Journal of Theoretical Biology **97**, 591-602.

Vincent SR, Hope BT (1992) Neurons that say NO. Trends in Neurosciences **15**, 108-113.

Vizzard MA, Erdman SL, Förstermann U, de Groat WC (1994) Differential distribution of nitric oxide synthase in neural pathways to the urogenital organs (urethra, penis, urinary bladder) of the rat. Brain Research. **646**, 279-291.

Voyvodic JT (1987) Development and regulation of dendrites in the rat superior cervical ganglion. Journal of Neuroscience **7**, 904-912.

Voyvodic JT (1989a) Peripheral target regulation of dendritic geometry in the rat superior cervical ganglion. Journal of Neuroscience **9**, 1997-2010.

Voyvodic JT (1989b) Target size regulates calibre and myelination of sympathetic axons. Nature **342**, 430-433.

Wakade AR, Garcia AG, Kirpekar SM (1975) Effect of castration on the smooth muscle cells of the internal sex organs of the rat: influence of the smooth muscle on the sympathetic neurons innervating the vas deferens, seminal vesicle and coagulating gland. Journal of Pharmacology and Experimental Therapeutics **193**, 424-434.

Walicke PA (1989) Novel neurotrophic factors, receptors and oncogenes. Annual Review of Neuroscience **12**, 103-126.

Wang BR, Senba E, Tohyama M (1990) Met 5-enkephalin-Arg 6-Gly 7-Leu 8-like immunoreactivity in the pelvic ganglion of the male rat: a light and electron microscopic study. Journal of Comparative Neurology **293**, 26-38.

Warburton AL, Santer RM (1993) Localisation of NADPH-diaphorase and acetyl cholinesterase activities and of tyrosine hydroxylase and neuropeptide-Y immunoreactivity in neurons of the hypogastric ganglion of young adult and aged rats. Journal of the Autonomic Nervous System **45**, 155-163.

Warren DW, Haltmeyer GC, Eik-Nes KB (1973) Testosterone in the fetal rat testis. Biology of Reproduction **8**, 560-565.

Wechsler HL, Fisher ER (1968) Eccrine glands of the rat. Archives of Dermatology **97**, 189-201.

Weisz J, Ward IL (1980) Plasma testosterone and progesterone titers of pregnant rats, their male and female fetuses, and neonatal offspring. Endocrinology **106**, 306-315.

West MJ (1993) New stereological methods for counting neurons. Neurobiology of Ageing **14**, 275-285.

West MJ, Slomianka L, Gundersen HJG (1991) Unbiased stereological estimation of the total number of neurons in the subdivisions of the rat hippocampus using the optical fractionator. The Anatomical Record **231**, 482-497.

Wilson JD, George FW, Griffin JE (1981) The hormonal control of sexual development. Science **211**, 1278-1284.

Womble MD, Roper S (1987) Retrograde effects of target atrophy on submandibular ganglion neurons. Journal of Neurophysiology **58**, 276-287.

Wozniak W, Skowronska U (1967) Comparative anatomy of pelvic plexus in cat, dog, rabbit, macaque and man. Anatomische Anzeiger **120**, 457-473.

Wright LL (1981) Cell survival in chick embryo ciliary ganglion is reduced by chronic ganglionic blockade. Developmental Brain Research **1**, 283-286.

Wright LL (1987) Development of sex difference in neuron numbers of the superior cervical ganglion: effects of transection of the cervical sympathetic trunk. Journal of Comparative Neurology **263**, 259-264.

Wright LL (1995) Development and Sexual Differentiation of Sympathetic Ganglia. In: Autonomic Ganglia, edited by EM McLachlan pp. 481-508. Harwood Academic

Wright LL, Smolen AJ (1983) Neonatal testosterone treatment increases neuron and synapse numbers in male rat superior cervical ganglion. Developmental Brain Research **8**, 145-153.

Wright LL, Smolen AJ (1987) The role of neuron cell death in the development of the gender difference in the number of neurons in the rat superior cervical ganglion. International Journal of Developmental Neuroscience **5**, 305-311.

Wright LL, Cunningham TJ, Smolen AJ (1983) Developmental neuron death in the rat superior cervical sympathetic ganglion: cell counts and ultrastructure. Journal of Neurocytology **12**, 727-738.

Wright LL, Beck C, Perez-Polo JR (1987) Sex differences in nerve growth factor levels in superior cervical ganglia and pineal. International Journal of Developmental Neuroscience **5**, 383-390.

Yamamoto K, Senba E, Matsunga T, Tahyama M (1989) Calcitonin gene-related peptide containing sympathetic preganglionic and sensory neurons projecting to the superior cervical ganglion of the rat. Brain Research **487**, 158-16.

Yamauchi A, Lever JD (1971) Correlations between formol fluorescence and acetylcholinesterase (AChE) staining in the superior cervical ganglion of normal rat, pig and sheep. Journal of Anatomy **110**, 435-443.

Yawo H (1987) Changes in the dendritic geometry of mouse superior cervical ganglion cells following postganglionic axotomy. Journal of Neuroscience **7**, 3703-3711.

Yokota R, Burnstock G (1983) Synaptic organisation of the pelvic ganglion of the guinea-pig. Cell and Tissue Research **232**, 379-397.

ACKNOWLEDGEMENTS

This thesis is dedicated to my parents who have supplied endless support, understanding and encouragement throughout its duration. Much appreciation also goes to Sarah Bale for her kind support in the latter stages of the project.

I give my warmest thanks to my supervisor, Professor Giorgio Gabella, who has throughout my period of study tirelessly supplied critical analysis, academic incisiveness and direction to my research. I have gained so much during my time spent with Giorgio, qualities that will always stand me in good stead.

For excellent, and selfless technical support I must thank Christine Davis (for amiable lab supervision and anaesthetics), Peter Trigg (for darkroom wizardry) and Mike Corder (for sectioning advise, and computer support); without their infatiguable contributions I'm sure that many problems would not have been overcome.

I have been lucky to have studied alongside many stimulating people to whom I owe my thanks: Christos Balaskas (who supplied invaluable input regarding chicken, galopoula and immunostaining), Derek Kayanja (for assistance with neuronal counting and fuel injection systems) and Masoud Alian (for bladder dissection and political analysis).

The work in this thesis was funded by a Medical Research Council scholarship (PhD studentship) and research grants from the Welcome Trust (G. Gabella).

Appendix 1 - Sample Disector Calculation

Employing the following disector method, cell numbers in each ganglion were calculated

$$N \text{ (No. of ganglion cells)} = V(ref) \bullet N_V$$

where:

V(ref) = Volume of ganglion.

N_V = Estimated numerical density of disector.

$$V(ref) = a \bullet t \bullet s$$

where:

a = Average cross-sectional area of ganglion.

t = Thickness of section.

s = Total number of sections taken.

$$N_V = \Sigma Q- / \Sigma V(dis)$$

where:

$\Sigma Q-$ = Sum of number of tops [profile that appears in reference, but not look up].

$\Sigma V(dis)$ = Sum of disector volumes.

$$V(dis) = a(ref) \bullet h$$

a(ref) = Area of reference section.

h = Height of disector.

The following is an example calculation taken from the data:

$t = 2\mu m$ $a = 232155.3\ \mu m^2$ $s = 600$

$V(ref) = 232155.3 \bullet 2 \bullet 600$

$= 278586360 \mu m^3$

ΣQ-= 597

$\Sigma V(dis) = 13929318\ \mu m^3$

[a(ref) = 232155.3 μm^2 h = 6 μm

no. of dis = 10]

$N_V = 597 / 13929318$

$= 42.9 \times 10^{-6}$

$N = 278586360 \cdot 42.9 \times 10^{-6}$

$= \underline{\mathbf{11951}}$

Appendix 2 - Sample Student T-Test Calculation

Employing the following students t-test, the statistical significance between data from male and female animals (and control and experimental) was calculated throughout this thesis: the following example is ganglion volume data from newborn animals.

	Population (n)	Average Volume (x) ($10^6 \mu m^3$)	Standard Deviation (s)
$Newborn_1$ Male	3	66	16
$Newborn_2$ Female	3	59	9

The aim is to concur with or reject the Null Hypothesis (H_O), which states that the two average values are the same.

An F test is first applied to the data in order to confirm that the samples come from the same population, and that consequently a t-test is an appropriate analysis.

$$F = \frac{16^2}{9^2} = 3.16$$

Data tables show that the variance ratio is not significant, therefore a t-test is appropriate.

To calculate the t-test value

$$t = \frac{\bar{x}_1 - \bar{x}_2}{S_c \sqrt{\frac{1}{n_1} + \frac{1}{n_2}}}$$

the combine variance (S_C) must fist be calculated

$$S_c^2 = \frac{\left[s_1^2 \times (n_1 - 1)\right] + \left[s_2^2 \times (n_2 - 1)\right]}{(n_1 + n_2 - 2)}$$

In this example

$$S_c^2 = \frac{\left[16^2 \times 2\right] + \left[9^2 \times 2\right]}{(3 + 3 - 2)} = 168.5$$

$$S_c = \sqrt{168.5} = 12.98$$

Substituting the newborn ganglion volume data

$$t = \frac{66 - 59}{12.98\sqrt{\frac{1}{3} + \frac{1}{3}}} = 0.66$$

With referral to statistical tables (Medical Statistics Made Easy. Broughton-Pipkin F, 1984) where, t has a value of 0.66 ($P>0.1$) the Null Hypothesis is not rejected, so there is no statistical difference between the average ganglion volume from the two animal groups.

Appendix 3 - Table of Disector Data of Ganglion VOLUME

	Ganglion Volume Data			
	Thickness (μm) (t)	Sections (s)	Av. Area (a)	Vol. (μm^3)
adult M	2	600	232155.3	278586360
adult M	2	540	280280.2	302702616
adult M	2	490	313681.7	307408066
adult F	2	670	155191.8	207957012
adult F	2	840	103169.3	173324424
adult F	2	488	165216.9	161251694
pre-p M	2	665	170247.3	226428909
pre-p M	2	490	277671.4	272117972
pre-p M	2	610	210261.6	256519152
pre-p F	2	555	105116.4	116679204
pre-p F	2	555	133733.5	148444185
pre-p F	2	600	102305.1	122766120
n-b M	2	210	114121.1	47930879
n-b M	2	330	109589.9	72329341
n-b M	2	240	160126.3	76860600
n-b F	2	270	122001.8	65880961
n-b F	2	270	90174.8	48694381
n-b F	2	330	93632.6	61797483
castr M	2	550	191847.7	211032421
castr M	2	555	233796.3	259513893
castr M	2	550	251496.7	276646370

Appendix 4 - Table of Disector Data of Neuron NUMBER ESTIMATES

	Dissector Data				
	Σ Areas	Σ Vdis	Σ Tops	Nv (10^{-6})	N
adult M	2321553	13929318	597	42.9	11951
adult M	2522522	15135132	616	40.7	12320
adult M	2823135	16938810	730	43.1	13247
adult F	1862301	11173806	406	36.3	7540
adult F	1444370	8666220	369	42.6	7386
adult F	1486952	8921712	334	37.4	6031
pre-p M	2213215	13279290	704	53.0	12003
pre-p M	2499043	14994258	763	50.9	13862
pre-p M	2312878	13877268	809	58.3	14951
pre-p F	1156280	6937680	347	50.0	5792
pre-p F	1471068	8826408	423	48.0	7121
pre-p F	1023051	6138306	339	55.2	6776
n-b M	429647	2577882	591	229.3	10989
n-b M	556886	3341316	614	183.8	13291
n-b M	633380	3800280	669	176.0	13531
n-b F	583894	3503364	632	180.4	11885
n-b F	411426	2468556	540	218.8	10652
n-b F	498152	2988912	599	200.4	12384
castr M	1918477	11510862	702	61.0	12873
castr M	2337963	14027778	735	52.4	13599
castr M	2514967	15089802	784	52.0	14386

Appendix 5 - Statistical Tables

	Ganglion Volume						
	Mean (x) $x10^6 \mu m^3$	Standard Deviation (s)	Number of Rats (n)	Variance Ratio (F)	Combined Variance (s_c)	't'-test Value (t)	Signif.
n-b M	66	±16	3				
n-b F	59	±9	3	3.16	12.98	0.66	P>0.1
pre-p M	251	±23	3				
pre-p F	129	±17	3	1.83	20.22	7.34	P<0.002
adult M	296	±15	3				
adult F	181	±24	3	2.56	20.01	0.68	P<0.01
castr M	249	±34	3				
adult M	296	±15	3	5.14	26.28	-2.18	P<0.10

	Average Neuronal Cross Sectional Area.						
	Mean (x) μm^2	Standard Deviation (s)	Number of Rats (n)	Variance Ratio (F)	Combined Variance (S_c)	't'-test Value (t)	Signif.
n-b M	81	±2	3				
n-b F	80	±3	3	2.25	2.55	0.48	P>0.1
pre-p M	338	±68	3				
pre-p F	237	±34	3	4	53.8	1.01	P>0.1
adult M	501	±13	3				
adult F	328	±16	3	1.51	14.6	6.48	P<0.01
castr M	252	±37	3				
adult M	501	±13	3	8.1	27.7	10.96	P<0.001

	Neuron Number

	Mean (x)	Standard Deviation (s)	Number of Rats (n)	Variance Ratio (F)	Combined Variance (s_C)	't'-test Value (t)	Signif.
n-b M	12604	±1403	3				
n-b F	11640	±892	3	2.47	1176	1.00	P>0.1
pre-p M	13605	±1490	3				
pre-p F	6563	±689	3	4.68	1161	7.40	P<0.001
adult M	12506	±668	3				
adult F	6845	±717	3	1.15	693	9.97	P<0.001
castr M	13619	±616	3				
adult M	12506	±668	3	1.18	643	-2.11	P>0.1

	NADPH-d +ve Neurons/unit volume						
	Mean (x)	Standard Deviation (s)	Number of Rats (n)	Variance Ratio (F)	Combined Variance (s_C)	't'-test Value (t)	Significance
adult M	35	±5	3				
adult F	17	±4	3	1.56	4.53	4.86	P<0.01
pre-p M	33	±6	3				
pre-p F	18	±5	3	1.44	5.52	3.33	P<0.05

	Pelvic Visceral Weights (g)						
	Mean (x)	Standard Deviation (s)	Number of Rats (n)	Variance Ratio (F)	Combined Variance (s_C)	't'-test Value (t)	Significance
Body							
adult M	188.5	±3.5	3				
castr M	174.0	±5.2	3	2.21	4.43	3.20	P<0.05
Bladder							
adult M	0.14	±0.01	3				
castr M	0.09	±0.00	3	0	0.007	8.71	P<0.001
Sem.Ves.							
adult M	0.13	±0.01	3				
castr M	0.03	±0.01	3	1	0.01	12.20	P<0.001
Prostate							
adult M	0.20	±0.01	3				
castr M	0.04	±0.01	3	1	0.01	19.51	P<0.001
Penis							
adult M	0.25	±0.01	3				
castr M	0.10	±0.01	3	1	0.01	18.30	P<0.001